THE INFLUENCE OF ACETYL AND PYRUVIC ACID SUBSTITUENTS ON THE SOLUTION AND INTERACTION PROPERTIES OF XANTHAN

Karolyn P. Shatwell

Thesis Presented for the Degree
Doctor of Philosophy

Department of Microbiology
University of Edinburgh

March, 1989

To my parents

ACKNOWLEDGEMENTS

I wish to express my gratitude to my supervisors Drs I.W. Sutherland and I.C.M. Dea for their guidance, encouragement and interest throughout the course of this project. I would also like to thank Dr S.B Ross-Murphy for acting in a supervisory capacity and for his sound advice and friendship. I am particularly indebted to him for his help with the computing and for allowing me to use his light scattering data in this thesis.

I gratefully acknowledge the receipt of an AFRC CASE studentship in conjunction with Unilever Research, Colworth Laboratory.

At Edinburgh my thanks are due to Dr A.F.D. Kennedy for his help with the HPLC and Mr C. Kierulf for many useful discussions.

At Colworth I would like to thank in particular Mr H. McEvoy, Mr B. James, Mr R.K. Richardson, Mr A.N. Cutler and Mr P.M. Hart for their excellent advice and technical assistance. To Mr C.R.T. Brown my appreciation for tolerating so cheerfully the invasion of his bench space, and to Dr A.H. Clark again my thanks for a number of helpful discussions.

Last but not least I would like to thank my parents for their encouragement and financial assistance in the preparation of this thesis, and the many friends and colleagues who have made my time at Edinburgh and at Colworth so enjoyable.

ABSTRACT

A range of xanthans (Na^+ salt form) with varying levels of acetyl and pyruvate substitution were prepared by culturing different strains of *Xanthomonas campestris*, and by chemical deacetylation and depyruvylation. The polymers were characterized chemically using a number of colorimetric and chromatographic methods; the molecular weights were determined by light scattering and from intrinsic viscosity data. A range of physical techniques were used to study the solution and interaction properties of the materials, concentrating on four in particular. These were ps.646 (4.5% acetyl, 4.4% pyruvate), ps.1128 (7.7%, 1.7%), ps.PXO_{61} (14.3%, 0.3%) and ps.556 (1.6%, 6.0%).

Optical rotation (OR) was used to characterize the helix-coil transition behaviour of the polymers. In deionized water there was a strong correlation between T_m and the levels of acetyl and pyruvate substitution. The degree of conformational order and the thermal stability of the polysaccharides increased with the ionic strength. Sample ps.556 exhibited an unusual two-phase OR transition in the presence of NaCl.

The flexibility of ps.646, ps.1128, ps.PXO_{61} and ps.556 were compared, using the Smidsrød and Haug B-value method and static light scattering. According to the B-value method the polymers with high pyruvate and low acetyl showed the greatest flexibility. However, the Kuhn segment lengths measured by light scattering in 0.1M KCl did not vary significantly.

The effect of salt on specific viscosity (η_{sp0}) was studied using the same four materials. Addition of salt to a 0.2% solution of xanthan produced an initial sharp fall in viscosity attributed to the decrease in hydrodynamic volume resulting from charge shielding. This was followed by a gradual increase in viscosity believed to be due to enhanced macromolecular association. Viscosity data for ps.556 determined over a range of polysaccharide concentrations and ionic strengths ($\leqslant$20mM NaCl), together with limited data for ps.646 and ps.PXO_{61}, were shown to fit a master curve of η_{sp0} versus $c[\eta]$. The data for ps.1128 however, did not superpose apparently because of the formation of stable high molecular weight aggregates upon freeze drying.

Mechanical spectrometry was used to study the solution and interaction properties of xanthan, locust bean gum, guar gum and konjac mannan. Solutions (2.0%) of xanthan in aqueous NaCl showed typical weak gel network behaviour but in deionized water the behaviour resembled that of an entanglement system. The gluco- and galactomannan solutions (1.0%) all showed entanglement behaviour both in deionized water and salt solution. The majority of xanthans (0.5%) interacted with locust bean gum and konjac mannan (1.0%) in deionized water to form a strong, thermoreversible gel network. The xanthan/konjac mannan gels had

significantly higher melting and setting temperatures than the xanthan/locust bean gum gels, and the transition from the liquid to the gel state on cooling was much sharper. The xanthan/locust bean gum mixed systems formed gels down to a much lower total polysaccharide concentration. Mixtures of xanthan and guar gum did not gel but instead showed entanglement behaviour. Acetyl substitution appeared to inhibit gelation with both locust bean gum and konjac mannan and addition of NaCl also produced a significant reduction in gel strength. A correlation was found between T_m and gel strength for the xanthan/locust bean gum systems only and denaturation of the xanthan helix was shown to be unnecessary for the interaction with both locust bean gum and konjac mannan.

Limited studies on ps.BD9A, a mutant polymer believed to lack the terminal mannose residue from the trisacharide side-chain, indicated that the terminal sugar residue plays an important role both in stabilizing the ordered helical conformation of xanthan and in the gelling interaction with locust bean gum.

ABBREVIATIONS

Ac	Acetyl
CD	Circular dichroism
DA	Deacetylated
DAP	Deacetylated and depyruvylated
DP	Depyruvylated
EOR	Enhanced oil recovery
EPS	Exocellular polysaccharide
G	α-L-guluronic acid
Gal	Galactose
GG	Guar gum
Glc	Glucose
GLC	Gas liquid chromatography
GlcA	Glucuronic acid
GM	Galactomannan
HPLC	High performance liquid chromatography
KM	Konjac mannan
LBG	Locust bean gum
LL	Galactomannan from *Leucaena leucocephala*
M	β-D-mannuronic acid
Man	Mannose
NMR	Nuclear magnetic resonance
NRRL	Northern Regional Research Laboratory
NTG	N-methyl-N-'nitro-N-nitrosoguanidine
OR	Optical rotation
Pyr	Pyruvate
Rha	Rhamnose
Rib	Ribose
rt	Retention time
TFA	Trifluoroacetic acid
X/Xan	Xanthan

GLOSSARY OF SYMBOLS

a	Persistence length
B	Intercept of $[\eta]$ versus $I^{-1/2}$ plot
c	Concentration
c^*/c^{**}	Critical concentrations
$c[\eta]$	Coil overlap parameter
G'	Elastic (storage) modulus
G''	Viscous (loss) modulus
G^*	Complex modulus
I	Ionic strength
K	Mark-Houwink parameter (prefactor)
K'	Huggins constant
K''	Kraemer constant
L	Contour length
l_K	Kuhn segment length
M/M_w	Molecular weight
M_L	Linear mass density
N_K	Number of Kuhn segment lengths per chain
R_g	z-average root mean square radius of gyration
S	Slope of $[\eta]$ versus $I^{-1/2}$ plot
$\tan \delta$	Tangent of the phase angle
T_m	Helix-coil transition midpoint temperature
α	Mark-Houwink parameter (exponential factor)
$[\alpha]_{365}$	Specific optical rotation at 365 nm
η	Viscosity
η'	Oscillatory shear viscosity
η^*	Dynamic viscosity
$[\eta]$	Intrinsic viscosity
η_{red}	Reduced viscosity
η_{rel}	Relative viscosity
η_s	Viscosity of solvent
η_{sp}	Specific viscosity
η_{sp0}	"Zero shear" specific viscosity
$\dot{\gamma}$	Shear rate
ω	Oscillatory frequency

CONTENTS

CHAPTER 1
GENERAL INTRODUCTION

1.1 History

In the mid 1950's scientists at the Northern Regional Research Laboratory (NRRL), Peoria, Illinois, undertook a survey of their large microbial collection with a view to discovering new, potentially useful biopolymers. Among those studied was one, PS B-1459, an exocellular polysaccharide slime from *Xanthomonas campestris*, later given the generic name xanthan gum. This material, which was produced in copious amounts in batch culture, had a number of unusual rheological properties (Jeanes *et al*, 1961). It produced at relatively low concentrations, highly viscous solutions with excellent shear-thinning properties that could be maintained over a broad range of temperature, pH and ionic strength. In respect of these features xanthan appeared superior to any of the existing commercially available plant hydrocolloids and industry was quick to realize its potential. A number of companies embarked upon intensive application and fermentation studies but of these only one, the Kelco Division of Merck and Co. Inc., San Diego, California, went on to achieve significant large scale production. It introduced the first industrial grade gum - trade named Kelzan - onto the market in 1961 and substantial commercial production began in 1964 (McNeely and Kang, 1973).

To enable the use of xanthan in food products extensive toxicological and safety testing was required. A range of long and short term feeding experiments and reproductive studies were carried out during the 1960's (Booth *et al*, 1963; Robbins *et al*, 1964; Woodard *et al*, 1973; McNeely and Kovacs, 1975; Kovacs and Kang, 1977). They showed it to be non-irritant, non-sensitizing and to possess no toxic, carcinogenic or growth inhibiting properties. In 1969, therefore, the United States Federal Food and Drug Administration issued a food additive regulation permitting the use of xanthan by the food industry (Anon., 1969). In the same year the Kelco Company produced the first food grade gum, known as Keltrol. Since then other countries including Canada, Mexico, New Zealand and the EEC member states (European Economic Community, 1974) have followed suit and allowed the use of xanthan as a food additive.

Commercial applications for xanthan proved numerous and demand for the product grew rapidly. In 1977 the Kelco Division began production of both Kelzan and Keltrol at a new facility in Okmulgee, Oklahoma, constructed at a cost of nearly 40 million dollars to support its existing plant in San Diego (Cottrell and Kang, 1978). Other companies too began marketing the product. By 1978 world production had reached 19,000 tons and it continues to grow. Projected figures for 1990 indicate a further increase to 30,000 tons. The commercial success of xanthan is unquestionable and, in 1974, the Institute of Food Technologists recognized this by presenting the Food Technology Industrial Achievement Award for outstanding advances in the application of food technology to food production jointly to the Kelco Division and the NRRL (Anon., 1974).

1.2 Microbial Production of Xanthan in the Natural Environment

Microbial Origin and Pathogenicity

Although commercial xanthan is synthesized by *X. campestris*, other bacteria of the genus *Xanthomonas* produce an extracellular polysaccharide (EPS) of similar composition and nature. (Sutherland, 1981a). The members of this group are gram negative, aerobic, non-sporing bacilli which are normally pigmented and are pathogenic for a range of host plants. Within the genus only four distinct species are recognized. The remainder are regarded as subspecies of the *X. campestris* group, distinguishable only by their host specificity (Wernham, 1948; Dye and Lelliot, 1974). Hence *X. phaseoli*, for example, should, strictly speaking, be referred to as *X. campestris* pv. *phaseoli*. For convenience though the abbreviated nomenclature will be adopted here. Table 1.1 shows a number of the *X. campestris* subspecies and the diseases for which they are the causative agents. The types of disease fall into three broad groups, vascular wilts, spots and blights, and cankers. Many of the diseases are of world-wide distribution and affect important crop plants. They are therefore of considerable economic significance.

X. campestris itself causes black rot disease of crucifers, a serious problem in tropical and subtropical regions of the world (Sutton and Williams, 1970a; Williams, 1980). Infection occurs via the hydathodes at the leaf margin, the stomata and wounds and the bacteria multiply and spread along the veins by way of the xylem. EPS produced by the organism, together with plant pectins and wound gums, causes occlusion of the vessel and this results in a blockage of water flowing through the system, and hence a localized water shortage, although not generalized wilting of the plant. Disorganization of the surrounding tissue follows. First the xylem, then the xylem parenchyma, phloem and bundle sheaths degenerate and as this occurs the first visible signs of the disease become apparent. Four to five days after infection the veins are seen to blacken due to the laying down of melanin among the collapsed vessels and this is followed, one to two days later, by progressive chlorosis and local desiccation. As the xylem vessels collapse, the bacteria escape into the surrounding tissues infecting adjacent vessels. This results in the development of a characteristic V-shaped lesion as the vein blackening, chlorosis and local wilting follow the path of the bacterium along the infected vessel. Finally the diseased area is invaded by the soft rotting bacteria *Erwinia caratovora* or *Pseudomonas marginalis*.

X. campestris produces no resting state and there are no authenticated reports of the organism being found outside of the host plant. However, spread is believed to occur through the dissemination of the organism from the leaf surfaces by wind, rain and insect and animal vectors. The organism can overwinter in plant debris, infected seeds (Williams, 1980) and cruciferous weeds (Schaad and Dianese, 1981) which

then act as a reservoir of infection for future crops. Control has focused upon seed treatment and the development of resistant plant strains (Humaydan *et al*, 1980; Williams, 1980; Garrett, 1982).

Functions of Xanthan

Sutton and Williams (1970b) demonstrated by compositional analysis and immunological cross-reactivity that the xanthan produced by *X. campestris* in artificial culture and the EPS produced by the microorganism in the infected plant are one and the same. This begs the question - what function is served by the polymer in the natural environment? The large amount of genetic material necessarily given over to the biosynthesis of such a complex polysaccharide (see section 1.5) suggests some fundamentally important role in the survival of the organism. A number of possibilities have been suggested and it seems likely that xanthan is in fact multifunctional.

In the disease process occlusion of the xylem vessels by polymer, leading to a localized water shortage, appears to be an important factor in the subsequent development of the lesion. Evidence for this comes from Leach and coworkers (1957) who showed that when excised tomato, sunflower and bean seedlings were placed in solutions of EPS from *X. phaseoli* the polymer caused non-specific occlusion of the vessels leading to wilting. Corey and Starr (1957) also described the development of small lesions on the leaves of bean seedlings inoculated with a mixture of silicon carbide and, either heat-killed mucoid cells of *X. phaseoli*, or a 0.1% solution of the polysaccharide. Sutton and Williams (1970a) demonstrated that when infected vessels became plugged with polymer, passage of eosine and radiolabelled $^{32}PO_4^{3-}$ within the xylem was prevented, implying also the inhibition of water flow, and explaining the subsequent development of water stress in the surrounding tissues. They showed, too, that if water loss from cabbage leaves infected with *X. campestris* was prevented by a high atmospheric humidity, secondary symptoms such as chlorosis, loss of turgor and electrolyte imbalance failed to develop. The precise mechanism of pathogenicity, however, is unknown.

The polymer may protect the bacterium from inhibitory substances produced by the host plant or, alternatively, could prevent the organism from eliciting a host defence response by blocking any interaction between the bacterium and receptors on the host cell surface. The latter is indicated by an experiment in which cabbage leaves were inoculated with a combination of a virulent strain of *X. campestris* and a weakly virulent, non-mucoid variant which alone showed only a limited capacity to spread through the host (Sutton and Williams, 1970a). When the two strains were inoculated in equal proportions, the non-mucoid strain multiplied and spread as well as the pathogen, suggesting that the EPS produced by the virulent strain inhibited the host "immune response" against both. If, however, the weakly virulent and virulent types were inoculated in proportions of 99:1, multiplication and spread of both strains was

severely restricted. This implies that a strong response against the weakly virulent strain, unprotected by EPS, was also effective against the small population of virulent organisms.

Another possible role in the disease process is suggested by the observation that xanthan will interact synergistically with some β-(1→4)-linked glycans of the plant cell wall (Dea *et al*, 1977; Morris *et al*, 1977a). These include certain gluco- and galactomannans and even cellulose itself, when first solubilized by derivatization. Such an interaction could be important in the initial adhesion and colonization of the host and in vascular occlusion. It has even been suggested that differences in the polysaccharide content of various plant cell walls could account for the selective binding of the organism to specific cell types and plant hosts (Morris *et al*, 1977a).

Besides shielding the organism from the host's defense mechanisms the polymer may serve other protective functions. *X. phaseoli*, when stored in exudate under conditions of low relative humidity, has been shown to survive for periods in excess of three years and this suggests that the polymer may prevent dehydration (Leach *et al*, 1957). Protection from bacteriophage attack is another possibility (Pettitt, 1979) and the finding that xanthan will absorb ultraviolet light to a significant degree (Leach *et al*, 1957) implies that it could help to prevent damage caused to the organism by the ultraviolet in natural daylight.

Production of the polymer as a storage material seems improbable since copious amounts of xanthan are produced in culture even under conditions of severe carbon limitation (Davidson, 1978) and because there is no direct evidence for its degradation by *X. campestris*.

1.3 Industrial Production and Usage of Xanthan

Fermentation and Recovery

Xanthan is produced commercially from *X. campestris* grown in batch culture. The conditions used were largely defined in two early studies by Lilly and coworkers (1958) and Rogovin *et al* (1961) and although details of the fermentation and recovery procedures do vary slightly from one company to another, broadly speaking, they are as follows (Godet, 1973; McNeely and Kang, 1973; Kovacs and Kang, 1977; Cottrell and Kang, 1978; Pettitt, 1979): The carbohydrate substrate is normally glucose, sucrose or hydrolysed starch at a concentration of 1-5%. Other substrates have however been suggested including, interestingly, acid whey, a by-product from the manufacture of cottage cheese (Charles and Radjai, 1977). Acid whey contains high levels of lactose which can be enzymically hydrolysed to glucose and galactose, both excellent substrates for xanthan biosynthesis. Charles and Radjai showed that the use of acid whey gave xanthan yields comparable with those of other substrates, making it economically viable and, in addition, had the advantage of simultaneously

removing a high B.O.D. waste product, the disposal of which is normally extremely expensive. Nitrogen is provided in both inorganic and organic form, the latter generally as a protein supplement, and magnesium, sulphur and phosphorous salts are also included in the medium. Trace minerals may be added but these are usually already available in the water supply. A temperature of 28-31°C is typical and the pH is maintained at between 6.0-7.5 by addition of sodium hydroxide. Careful control of aeration is necessary since, as the culture becomes more viscous, aeration becomes increasingly difficult. It is usual to limit the amount of carbohydrate substrate to ensure that the maximum viscosity attained by the culture will still permit the diffusion of oxygen.

The possibility of using continuous culture in place of batch culture has received considerable attention (Patton and Lindblom, 1962; Lipps, 1966; Silman and Rogovin, 1972; Davidson, 1978; Evans *et al*, 1979; Patton and Dugar, 1981) and on the face of it would be a desirable step forward since higher yields of the polymer could be achieved. However, continuous culture of *X. campestris* has two inherent problems, namely culture contamination and culture deterioration. *X. campestris* produces no antibiotics to inhibit the growth of other microorganisms and the culture conditions used are also non-inhibitory to the majority of other species. Hence contamination is a frequent and serious problem (Patton and Dugar, 1981). Culture deterioration generally occurs after between six and nine turnovers; a less productive colonial variant appears (Silman and Rogovin, 1972; Evans *et al*, 1979) and this results in a reduction in the yield of polysaccharide. Although evidence suggests that by adjusting the composition of the medium it may be possible to overcome this problem, (Evans *et al*, 1979) for the moment at least, continuous culture is regarded as a high risk enterprise.

The polysaccharide is harvested after 60-70 hours fermentation. Pasteurization of the culture, using a continuous heat exchanger, destroys the bacteria and the cells may then be partially removed by diluting the fermentation broth and filtering. This is usual for high quality food grade products. A low molecular weight alcohol such as methanol, ethanol, propanol or butanol is used to precipitate the polymer and the material is removed by filtration. Recovery of the alcohol is essential to the economics of the process (Godet, 1973). Finally the polymer is dried in a hot air drier, milled, tested and blended to the required specifications.

A number of alternative procedures have been suggested for recovery of xanthan from the fermentation broth but none have so far proved sufficiently advantageous for adoption by the industry. Methods for the precipitation of xanthan using long-chain quaternary ammonium salts have been described by Rogovin and Albrecht (1964) and Kennedy *et al* (1981a). Such methods are unsuitable, however, because the expense of the salts makes their complete recovery essential for the process to be economically viable and because the use of ammonium salts is likely to be unacceptable for food-grade products. Precipitation methods using calcium salts at a pH

of above 10, and aluminium salts at a pH of 3-5, have been patented by McNeely and O'Connell (1966)and Towle (1977) respectively, and Kennedy and coworkers (1981b) have also described a procedure for the recovery of xanthan using the polymeric cation $PHMB^{+}Cl^{-}$ - poly(hexamethylenebiguanide hydrochloride). Drum drying or spray drying of the fermentation broth (Rogovin *et al*, 1965) are also possibilities, but both yield a very crude grade polysaccharide product and with drum drying difficulties are encountered because of the tenacious adherence of the polymer to the metal drying surfaces.

Food Uses

Since its initial acceptance for food use by the United States Federal Food and Drug Administration in 1969 (Anon., 1969) xanthan, because of its exceptional rheological and safety properties, has become an invaluable asset to the food industry. Its multifarious uses in food products have been the subject of a number of reviews (Rocks, 1971; Kovacs, 1973; McNeely and Kang, 1973; Andrew, 1977; Kovacs and Kang, 1977; Cottrell and Kang, 1978; Pettitt, 1979).

Xanthan dissolves readily in both hot and cold water to produce high viscosity solutions at relatively low concentrations (figure 1.1). Because of the high viscosity, solutions of xanthan have excellent particle suspending and emulsion stabilizing properties and the polymer has therefore found use as a thickener, emulsifier and stabilizer in products such as french dressings, fruit beverages, ice creams, milk shakes and processed cheeses. The high viscosity is maintained over a broad range of temperature, pH and ionic strengths, making xanthan a suitable additive in a wide range of food environments.

Figure 1.2 shows the effect of electrolyte concentration upon viscosity. The influence of salt is dependent upon the concentration of the polysaccharide itself. At a concentration of 0.1%, addition of salt results in a slight drop in the viscosity but at higher concentrations the viscosity increases. This is in marked contrast to the behaviour of other anionic polysaccharides which, typically, show a large fall in viscosity across the entire concentration range. Xanthan is therefore particularly suitable for processed foods which contain high levels of added salt.

In the absence of salt, differences in pH affect the viscosity of xanthan solutions only slightly (Rocks, 1971), and addition of even a small amount of electrolyte diminishes the effect still further. Figure 1.3 shows that in the presence of 0.1% sodium chloride, the viscosity of a 1% solution of xanthan gum shows no appreciable change over the pH range 1.5-13. Xanthan can therefore be used in very acid products such as pickled foods and relishes.

The polymer is remarkably resistant to thermal degradation and in the presence of salt will retain its viscosity at high temperatures for prolonged periods. This is useful in canned foods which must be heat

sterilized and in products such as gravies and sauces which may be kept hot for several hours on a steam table. At low temperatures the viscosity and stabilizing properties of xanthan are unaltered and hence the polymer contributes excellent freeze-thaw stability to a variety of frozen foods including frozen starch-based puddings and pie fillings, which would otherwise show considerable retrodegradation and syneresis upon thawing.

Although xanthan remains viscous up to very high temperatures (figure 1.4), at the retort temperature of 120°C, 98% of the viscosity is lost. 80% is subsequently recovered on cooling. This thickener which is thin at the retort temperature, facilitates good heat transfer, thus reducing the processing time and production cost. It is also valuable for food materials that are adversely affected by prolonged heating.

The thickening and stabilizing properties of xanthan in solution are not the only textural characteristics conferred by the polymer. In cakes it improves the sponge structure by foam/air cell stabilization and by giving better moisture retention. It has also been suggested as a binding agent in gluten-free starch bread (Christianson *et al*, 1974) since it gives the desired loaf volume, crumb texture and crust quality. Control of syneresis is important in instant starch puddings and in bakery products where the polymer prevents the filling from being absorbed into the pastry or doughnut. It reduces drainage in relishes such as pickle relish and confers good clinging properties in sauces and salad dressings.

One of the most valuable characteristics of xanthan solutions is their pseudoplasticity (figure 1.5); that is to say, shear-thinning followed by immediate recovery of the viscosity once the shear-stress is removed. Because of this, even the most viscous xanthan-containing systems have good pouring and spreading characteristics. Pseudoplasticity is important in conferring good organoleptic properties on food. Because xanthan loses its viscosity at relatively low shear rates, the minimal shear effect of mastication is enough to temporarily break the viscosity of the solution and this gives good flavour release and very little hang up in the mouth. Shear-thinning is also of value where thickened systems must be pumped within a food plant.

Xanthan is compatible with almost all other chemicals used in foods. It is highly tolerant of acids and bases, as already indicated, and will dissolve directly in solutions of 5% acetic acid, 10% hydrochloric acid and 5% sodium hydroxide. It is also compatible with the vast majority of salts and with most other hydrocolloids. Exceptions include certain specific dextrins, with which it interacts, and highly concentrated gum arabic solutions at a pH of below 5. It is insoluble in organic solvents but will tolerate up to 50% water-ethanol mixes.

Although xanthan does not interact with the majority of other polysaccharides, it does show a definite reactivity with the plant galactomannans, most notably guar gum, tara gum and locust bean gum (Kovacs, 1973; Dea *et al*, 1977). The interaction with guar gum is

manifested as a detectable increase in viscosity over and above that predicted on the basis of the viscosity of the individual components. The same is true for xanthan/tara gum and xanthan/locust bean gum mixtures at low total polysaccharide concentrations. Figure 1.6 shows the tremendous synergistic effect between xanthan and locust bean gum. At a total colloid concentration of 0.1%, the viscosity of the xanthan/locust bean gum solution is approximately 2000 cP, markedly higher than that of both xanthan (approximately 50 cP) and locust bean gum (approximately 9 cP) alone and higher too than that of other industrially used hydrocolloids. At greater concentrations still, xanthan interacts synergistically with tara gum and locust bean gum to form firm, rubbery, thermoreversible gel networks. Such gelling interactions are used in a variety of foods including gelled milk-puddings, gelled salads and desserts, and gelled meat products. Xanthan is also used in combination with galactomannans and other hydrocolloids to achieve desirable textural and other properties, besides gelling.

A study by Booth and coworkers, published in 1963, showed that virtually all of the xanthan fed to animals could be recovered in the stools. They concluded from this that xanthan is not digestible. Later radioactive tracer experiments (Gumbmann, 1964 - unpublished report), however, showed that 15% of xanthan is in fact digested, probably by non-enzymic hydrolysis in the acid conditions of the stomach. The approximate calorific value based upon this study was 0.5 kcal/g. Because of its low calorific content xanthan is used a great deal in low calorie foods.

Non-Food Uses

The rheological properties described above are as valuable to other industries as they are to food manufacturers (McNeely and Kang, 1973; Jeanes, 1974; Andrew, 1977; Sandford *et al*, 1983). Xanthan is used as a stabilizer in a range of agricultural products including flowable pesticides, suspension fertilizers, calf milk replacers and cattle feed supplements. In paints and adhesives it is used as a thickener and to improve the flow and film-forming properties of the product, and in ceramic glazes it acts, not only as a suspending agent, but also promotes grinding, improves wet adhesion and controls drying. The cosmetic and pharmaceutical industries use it as an emulsifier and bodying agent in toothpaste and ointments, and in the textile industry xanthan is used as a stabilizer in various formulations for the printing of fabrics, carpets and upholstery. It has also found limited application as a sizing agent. The chemical inertia and stability to strong acids and alkalis, make it a suitable stabilizer for use in industrial cleaners, rust removers and metal pickling baths, and its ability to cross-link with certain multivalent metal ions suggests a use as a flocculant in water clarification and in the paper industry. It has also been patented as a possible thickener or gelling agent for use in explosives. The largest single potential market for xanthan, however, is the oil industry where research has indicated a valuable role for the polymer both in enhanced oil recovery (EOR) and in drilling muds.

In terms of EOR, xanthan appears to be a suitable candidate for use in polymer and polymer-surfactant flooding (Sandvik and Maerker, 1977; Gabriel, 1979). Injection of water into an oil reservoir displaces the oil towards the producing well and increases the yield. However, because of its high mobility, water tends to "finger" rapidly through regions of high permeability but bypass the less porous regions, where oil remains trapped by capillary forces. Addition of a high molecular weight polymer to the injection water raises the viscosity and lowers the mobility, giving better displacement of oil (figure 1.7) and inhibiting fingering of the drive fluid through the oil bank. Xanthan, unlike its major competitor, the polyacrylamides, is not prone to shear degradation and retains its viscosity at high salt concentrations. Because of this, it should be particularly suitable for use in less porous reservoirs and where the salinity is very high (eg. North Sea reservoirs).

Significant amounts of xanthan are already used in drilling muds. These are thickened fluids which are pumped down the drill pipe and exit through a nozzle in the bit at the drill face. The mud acts as a lubricant and also picks up the cuttings generated by the rotating bit and returns them to the surface. Xanthan is suitable for this type of function because of its pseudoplasticity. At the drill face, where there is a high shear rate, the polymer solution has only a low viscosity but, away from the drill face, the viscosity increases giving the good suspension properties necessary to carry the cuttings to the surface. Resistance to high temperatures and shear degradation are also important here (McNeely and Kang, 1973).

Xanthan Derivatives

A number of xanthan derivatives have been reported and patented (McNeely and Kang, 1973; Jeanes, 1974). These include xanthan sulphate which has been proposed as a thickening agent for glues, the carboxymethyl ether, a possible replacement for carboxymethylcellulose as a thickener in the paper and textile industries, and the propylene glycol ester, which could be used to enhance the viscosity of food products and cosmetics. Few of these derivatives, though, are suitable for commercial production. The reason for this is that for production to be economically viable, an inexpensive manufacturing process compatible with the main production process would need to be developed. The derivative would also need to possess unique properties not available in other commercial polymers. Hardly any of the xanthan derivatives fit this description. Deacetylated xanthan, however, does and a partially deacetylated polymer with unusual film-forming properties and a greatly enhanced viscosity in the presence of salts (Jeanes and Sloneker, 1962) is now commercially available.

1.4 Primary Structure and Conformation

Although xanthan was discovered in the 1950's and extensively used and studied thereafter, the true structure remained a mystery until some two decades later.

The first tentative model for the primary structure was proposed by Sloneker and coworkers in 1964, on the basis of results from partial hydrolysis (Sloneker and Jeanes, 1962) and Smith degradation (Sloneker and Orentas, 1962b; Sloneker *et al*, 1964) studies. The structure they suggested had a 16 residue repeat unit (figure 1.8) comprising a D-glucose, D-mannose and D-glucuronic acid backbone with single residue D-mannose side-chains linked at intervals along its length. O-acetyl groups were believed to be attached at the C6 position of the backbone mannose residues, whilst pyruvic acid substituents were thought to be 4,6-linked, probably to a terminal D-glucose side chain (Sloneker and Orentas, 1962b; Gorin *et al*, 1967). A similar model with a 14 residue repeat unit was suggested three years later by Siddiqui (1967) after a structural study using methylation analysis. Both models were regarded with some scepticism. Evidence from past studies had indicated that a repeat unit of no more than six sugar residues was typical for bacterial polysaccharides, and the tremendous biosynthetic complexity that such a large repeat unit would require also cast doubt upon the credibility of these models.

In the 1970's, therefore, Jansson and coworkers reinvestigated the primary structure of xanthan using what were by this time greatly improved methods of methylation analysis, in combination with an elegant series of stepwise degradation procedures. From their results they were able to construct a new model with a much simplified pentasaccharide repeat unit (Jansson *et al*, 1975). This structure is illustrated in figures 1.9 and 1.10. It consists of a β-(1$\rightarrow$4)-D-glucose backbone with trisaccharide side-chains β-(1$\rightarrow$3)-linked to alternate backbone residues. The side-chains are β-D-mannose-(1$\rightarrow$4)-β-D-glucuronic acid-(1$\rightarrow$2)-α-D-mannose. O-acetyl groups are linked stoichiometrically to the C6 of the inner mannose residue, whilst roughly half of the side-chains carry a pyruvic acid substituent 4,6-linked to the terminal mannose. Further data from partial hydrolysis (Melton *et al*, 1976) and partial acetolysis (Lawson and Symes, 1977a,b) studies as well as ^{1}H and ^{13}C NMR (Garegg *et al*, 1980; Rinaudo *et al*, 1983; Horton *et al*, 1985) have confirmed this structure as correct. Indeed the data from the earlier studies by Sloneker and Siddiqui also broadly agrees with this structure but anomalous results, arising probably from incomplete reactions or analytical difficulties, were not recognized as such and were instead interpreted as minor structural features, thus necessitating the longer repeating sequences of the earlier models.

The level of acetyl and pyruvate substitution has been found to vary with both the producing strain (Orentas *et al*, 1963; Cadmus *et al*, 1976; Sutherland, 1981a) and the conditions under which the organism is cultured (Cadmus *et al*, 1978; Davidson, 1978). Values of up to 5.0% acetyl and 8.1% pyruvate are theoretically possible, assuming one acyl group per side-chain. However, on analysis the amount of acetyl is often found to be higher and strains of *X. oryzae* are known which produce polymer with as much as 14% acetyl substitution (Parry, 1985). This implies the presence

of additional acetyl groups at some point on the side-chain. Little is known about the distribution of the acyl groups on the molecule but preliminary evidence (Dell and Sutherland - unpublished results) suggests multiple acetylation of the internal mannose residue.

There is some evidence to suggest that the distribution of trisaccharide side-chains may not be quite as regular as the model of Jansson and coworkers implies. The consistent finding of more glucose than mannose on chemical analysis - a 1:1 ratio would be expected for a completely regularly substituted polymer - and the apparent existence of preferential sites of cleavage for fungal cellulases on the xanthan backbone (Sutherland, 1984) suggests that side-chains may be absent from some regions of the molecule.

The molecular weight (relative molecular mass) of xanthan is uncertain. Estimates ranging from 1.1 - 62 x 10^6 (see table 5.1) have been published and the value seems to vary considerably according to the method of measurement. Recently, however, the consensus of opinion has settled at about 2 x 10^6 with the higher values obtained experimentally believed to be the result of molecular aggregation.

Interpretation of information derived from X-ray fibre diffraction studies (Moorhouse *et al*, 1977a,b) has indicated that the xanthan molecule in solution adopts a right-handed helical conformation, with five-fold symmetry and a helix pitch of 4.7 nm. This view is supported by data from Sato *et al* (1984a,b,c) which shows that the contour length per main chain glucose residue for xanthan in 0.1M aqueous sodium chloride is 0.47 nm. The orientation of the side-chains has still to be determined unequivocally. From the X-ray diffraction data it appears that the branches may fold back onto the polymer backbone, the whole structure being stabilized by non-covalent interactions. However, a recent attempt at molecular modelling using potential energy calculations (Pérez and Vergelati, 1987) has indicated that the side-chains are capable of adopting any of a number of possible conformations and show no particular tendency to fold backwards. Figure 1.11 shows the preferred 5/1 helical conformation of xanthan proposed by Moorhouse *et al* (1977b). In this particular model the branches are folded back onto the cellulosic backbone. Okuyama *et al* (1980) have put forward alternative models for both a parallel and an antiparallel xanthan double helix, based upon the 5/1 helical conformation.

Whether xanthan exists in solution as a single-stranded or a double-stranded structure has been the subject of much controversy. The main evidence for a single-stranded molecule is the first-order kinetics of the salt-induced disorder-order transition (Norton *et al*, 1980, 1984). Other evidence includes the lack of concentration dependence of the transition (Morris *et al*, 1977a), the negligible change in the molecular weight, monitored by light scattering, over the temperature course of the disorder-order transition (Milas and Rinaudo, 1979; Norton *et al*,1984) and

the apparent increase in the level of cation binding upon helix formation. Norton and coworkers (1984) compared the increase in cation binding, derived from the salt dependence of the helix-coil transition midpoint (see Chapter 4), with values calculated for both single and double helical molecules using the Manning polyelectrolyte theory. The experimental value obtained was in reasonable agreement with that for the single helix transition. Interestingly, though, a study by Paoletti *et al* (1983), also employing the Manning polyelectrolyte theory, favoured a double-stranded structure in preference to a single helix.

Evidence for a double-stranded structure includes the following: both Paradossi and Brant (1982) and Coviello and coworkers (1986), in their light scattering studies, obtained a linear mass density in the region of 2000 daltons/nm for native xanthan, whilst a value of 1900 daltons/nm was reported by Holzwarth (1978) on the basis of a hydrodynamic analysis of ultrasonically degraded xanthan samples. The theoretical linear mass density for a single-stranded xanthan helix would be only half this value - close to 1000 daltons/nm. In the electron microscopy studies of Holzwarth and Prestridge (1977) the native xanthan molecules were observed to be 4 nm thick, whilst the thickness of the denatured xanthan molecules was only 2 nm. Furthermore, the renatured molecules, which were also 4 nm thick, showed so-called "hockles", that is, regions in which the native assembly appeared to be partly unravelled. This indicated that the native structure comprised two strands arranged in a right-handed twist. Sato *et al* (1984b) studied a series of sonicated xanthan fragments in 0.1M aqueous sodium chloride and in cadoxen using static light scattering and observed that the molecular weight in the salt solution was invariably twice that of the molecular weight in cadoxen, a solvent system in which xanthan has been shown to dissolve as single-stranded flexible chains.

Most of the evidence currently available appears to favour a double-stranded structure but it is not yet clear whether this structure is a double helix, as Liu and coworkers (1987; Liu and Norisuye, 1988) have suggested, or a dimer formed by the association of two single helical molecules, as has been suggested by Paoletti *et al* (1983). Much of the evidence is contradictory.

It is possible that xanthan may adopt different structures in solution depending upon the source of the polymer (ie. the bacterial strain by which it was produced and the fermentation conditions), any treatments to which it may have been subjected (eg. heating and chemical modification) and the prevailing environmental conditions (eg. the temperature and ionic strength). Coviello *et al* (1986), for example, obtained a ratio of experimental to theoretical mass per unit length of close to 2 for both native and deacetylated xanthan, indicating a double-stranded structure, but the ratio for depyruvylated xanthan was only about 1.5, suggesting the presence of a significant number of single strands. Stokke and coworkers (1986) demonstrated, using electron microscopy, that

in 2mM ammonium acetate the polymer from *X. oryzae* strain PXO_{61} existed predominantly in the single-stranded state whilst a solution of Keltrol contained both single and double-stranded molecules, as well as partially dissociated double strands. Increasing the concentration of salt, in both cases, promoted the formation of double strands.

1.5 Biosynthesis

To date, very little research has been carried out on the mechanism of xanthan biosynthesis and this is perhaps surprising considering the huge commercial importance of the polymer. However, from the data that is available, together with evidence from other species, it is possible to construct a crude picture of the synthetic process.

Glucose is the usual carbohydrate substrate for *X. campestris* in artificial culture and a study by Horton and coworkers (1985) using ^{13}C NMR has shown that the monosaccharide acts as a precursor for all the subunits of the polysaccharide repeat structure, including the acetyl and pyruvate substituents.

The process by which glucose, or occasionally another carbohydrate substrate, is taken up into the cell is uncertain. For bacteria in general Saier (1985) has defined five distinct mechanisms for nutrient uptake. The first - facilitated diffusion - requires no input of free energy and involves transport of the substrate across the membrane via a hydrophilic, proteinaceous pore. This is the usual mechanism by which materials cross the outer membrane and in *Escherichia coli*, a number of these so-called outer membrane "porins" have been characterized. Examples include the *omp*F and *omp*C porins which are fairly non-specific with respect to their substrate requirements, and *pho*E and *lam*B which show a high degree of substrate specificity. The *pho*E porin carries inorganic phosphate and phosphorylated carbohydrates, whilst *lam*B transports maltodextrins. Transportation across the cytoplasmic membrane is rarely by facilitated diffusion, the only notable exception being the glycerol permease system. The second type of mechanism, which does require free energy, is the substrate-protein symport. The best characterized system of this type is the lactose permease system in *E. coli*. Here the lactose substrate is transported across the cytoplasmic membrane by another molecule, known as a symport, which carries protons down a concentration gradient at the same time. The proton gradient is maintained by a flow of protons from proton donors such as NADH, through the respiratory chain. The third type of mechanism is analogous to this but involves the simultaneous transport of sodium ions instead of protons. The melibiose permease system in *Salmonella typhimurium* is an example of this type of process. The maltose permease system in *E. coli* represents the fourth type of mechanism - a protein dependent active transport system. Here four distinct proteins, E, F, G and K, act as a unit to drive the uptake of maltose and its higher homologues across the periplasm and cytoplasmic membrane. The precise functions of these four proteins, have still to be established but there

is evidence to suggest that they act by a channel rather than a carrier-type mechanism. There is also little information available about the energy source which drives this active transport mechanism. The fifth and final process, referred to as group translocation, involves the simultaneous phosphorylation and transportation of the substrate across the inner cell membrane. The phosphoenoltransferase system of *E. coli* illustrates this type of mechanism. Again it consists of four proteins, enzymes I, II and III, and HPr, a small heat stable molecule. The phosphoryl group from phosphoenolpyruvate is passed sequentially from enzyme I to HPr to enzyme III. Enzyme II, which is the actual membrane channel, then catalyses the transfer of the phosphoryl group from enzyme III to the sugar, which is simultaneously transported across the membrane to the inside of the cell. The phosphoenoltransferase system is responsible for the uptake of a range of different sugars. Enzyme I and HPr appear to be general for all of these transport systems, but enzyme II and enzyme III are specific for particular sugar residues.

Which of these five systems of carbohydrate uptake operate in *X. campestris* has still to be established. Attempts by Whitfield (1979) to stimulate a phosphoenoltransferase system in *X. campestris* membrane vesicles proved unsuccessful, appearing to preclude a group translocation mechanism. However, an active transport mechanism may well exist. In *Pseudomonas aeruginosa*, which is closely related to the *Xanthomonads* (Dye and Lelliot, 1974), when excess glucose is present, an oxidative pathway in the periplasm generates gluconate and 2-oxo-gluconate from glucose. These are then taken up across the cytoplasmic membrane via specific transport systems (Midgley and Dawes, 1973; Roberts *et al*, 1973; Whiting *et al*, 1976) and fed into an intracellular phosphorylative pathway. During glucose-limited growth, this extracellular oxidative system is repressed (Whiting *et al*, 1976) and glucose is taken up directly via a high-affinity transport system involving a periplasmic glucose-binding protein (Stinson *et al*, 1977). The close similarity between the glucose metabolizing systems in *P. aeruginosa* and *X. campestris*, as demonstrated by Whitfield *et al* (1982), suggests that similar mechanisms may operate in *X. campestris*. Whitfield and coworkers examined wild-type *X. campestris* and a range of mutant strains for the presence of enzymes involved in both the periplasmic oxidative pathway and the intracellular phosphorylative pathway. They found that crenated mutants of *X. campestris* carried the enzymes necessary for both pathways but that the wild-type and non-mucoid mutants lacked glucose dehydrogenase activity, making the oxidative pathway inoperable.

In *X. campestris* the phosphorylated products of the intracellular pathway are further metabolized via the Entner-Doudoroff pathway and tricarboxylic acid cycle. Some pentose phosphate activity also occurs (Zagallo and Wang, 1967). Intermediary metabolites thus generated provide the precursors for xanthan biosynthesis as illustrated in figure 1.12. The sugar nucleotides, UDP-glucose, GDP-mannose and UDP-glucuronic acid, which

are synthesized from glucose-6-phosphate are the precursors for the pentasaccharide repeat unit, whilst acetyl CoA and phosphoenolpyruvate are used to generate the acetyl and pyruvic acid substituents respectively.

Construction of the pentasaccharide repeat unit involves a carrier lipid, an isoprenoid alcohol phosphate, located in the cytoplasmic membrane. This has been clearly demonstrated by Ielpi, Couso and Dankert (1981a) who, using EDTA-treated cells, studied the in vitro incorporation of radiolabelled glucose from UDP-(^{14}C)-glucose into a chloroform / methanol / water extractable material - the "1203" extract - and into the polysaccharide. When the cells were incubated in the presence of UDP-(^{14}C)-glucose alone, radioactivity was detected in the 1203 extract only and was shown to be located in a solvent soluble lipid-pyrophosphate-cellobiose structure. Addition of GDP-mannose to the incubation mixture resulted in a lipid-bound trisaccharide, identified as mannosyl-cellobiose, and only when all three sugar nucleotide precursors, UDP-(^{14}C)-glucose, GDP-mannose and UDP-glucuronic acid were present was any radiolabelled xanthan synthesized. This was coincident with a drop in the radioactivity detected in the 1203 extract and the structure of the lipid-bound oligosaccharide was tentatively identified as the pentasaccharide repeat unit.

From this data Ielpi and coworkers concluded that the xanthan repeat unit is assembled by sequential addition of sugars from the sugar nucleotide precursors onto the carrier lipid. Glucose is added first and is linked to the carrier via a pyrophosphate bridge. Glucose, mannose, glucuronic acid and a further mannose residue are then added in turn and the pentasaccharide is finally polymerized onto xanthan gum. This type of synthetic process is common to many other repeat unit-containing glycan polymers and the same carrier lipid is believed to be involved in the synthesis of lipopolysaccharide, peptidoglycan, teichoic acid and EPS (Sutherland, 1977).

Subsequent investigations, using the same type of approach, showed that (^{14}C)-acetyl (Ielpi *et al*, 1983) and (^{14}C)-pyruvic acid residues (Ielpi *et al*, 1981b) were incorporated into the lipid-bound material prior to polymerization, and proved conclusively that the acyl donors were as expected acetyl CoA and phosphoenolpyruvate.

Little is known about the way in which polymerization of the pentasaccharide repeat unit occurs. An acceptor molecule may be required but none has so far been identified. How the chain length is controlled is also a mystery and likewise how the polymer is transferred from its site of synthesis at the cytoplasmic membrane to the outside of the cell. A clue to the method of secretion may be found in freeze-etch electron micrographs of other species. *Acetobacter xylinum* synthesizes cellulose and Zaar (1979) has described the presence of pores in the outer membrane through which the completed cellulose microfibrils may pass. Similarly in temperature-sensitive mutants of *E. coli* points of adhesion between the

cell wall and outer membrane have been visualized (Bayer and Thurow, 1977) and these appear to correspond to sites of export for the capsular polysaccharide material. It is possible, therefore, that *X. campestris* EPS is transferred to the cell surface via similar outer membrane pores.

The mechanisms involved in regulating xanthan biosynthesis have not been investigated but control is likely to occur at a number of levels including substrate uptake, precursor synthesis and polymer formation.

Feedback inhibition of enzymes is a possible control mechanism at any of these stages. Such a mechanism could govern the rate of synthesis within a given metabolic pathway or could limit the entry of a substrate into the pathway. Kornfeld and Ginsburg (1966) have demonstrated this type of mechanism in species of bacteria synthesizing polymers comprising D-mannose, L-fucose and mixtures of the two. In each case enzymes involved in the synthesis of the sugar nucleotide precursors have been shown to be under the control of the sugar nucleotide products themselves. For example in strains of bacteria synthesizing poly-D-mannose, the GDP-mannose pyrophosphorylase enzyme was found to be subject to feedback inhibition by GDP-mannose.

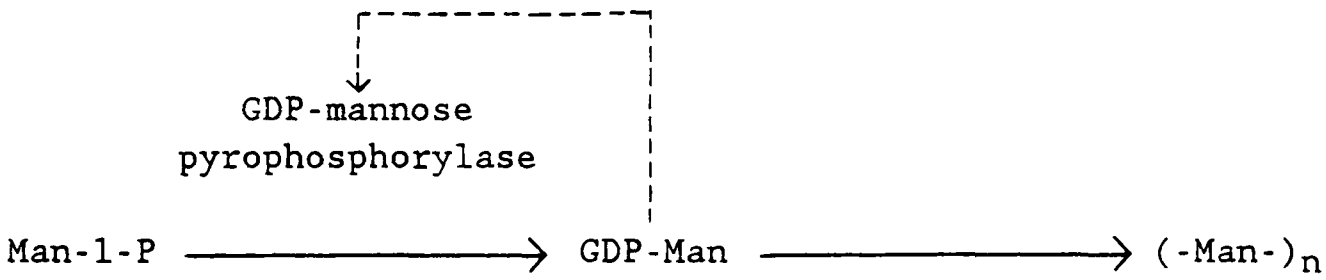

Regulation may also occur at the genetic level as it does in the synthesis of colanic acid by members of the *Enterobacteriaceae*. Markovitz (1977) investigated the regulation of colanic acid synthesis in *E. coli* K12 and he identified three genes, *cap*R, *cap*S and *cap*T, which controlled the synthesis of a number of enzymes involved in colanic acid production.

Substrate and lipid carrier availability do not appear to be important limiting factors in xanthan biosynthesis since the polymer is synthesized in batch culture throughout the growth cycle (Moraine and Rogovin, 1966). However, Tait *et al* (1986) have shown that material produced during the exponential phase of growth has a lower acyl content than that produced at a later stage. This is probably due to the reduced availability of the acetyl CoA and phosphoenolpyruvate precursors when the cells are growing rapidly.

Remarkably little research has so far been carried out on the genetics of xanthan biosynthesis. The biosynthetic pathway is complex, involving a multitude of enzymes. At least eight of these (five specific transferases, acetylase, ketal transferase and a polymerase) will be involved in polymer synthesis. Another may be necessary to liberate the completed polysaccharide from the lipid carrier and then there are the possible regulatory proteins. The genetics of xanthan biosynthesis is therefore likely to be equally complicated.

Recently two groups of workers, Barrère *et al* (1986) and Harding *et al* (1987) have succeeded in cloning genes involved in xanthan biosynthesis from a genomic library of *X. campestris* DNA into broad-host-range cloning vectors. The resultant plasmids were capable of restoring xanthan biosynthesis to non-mucoid mutants of the bacterium and in some cases increased the level of synthesis to over and above that of the wild-type strain. This was probably due to gene dosage effects. Harding and coworkers also identified the existence of a gene involved in pyruvylation, which enhanced the extent of side-chain acylation by 45%. Subcloning and transposon mutagenesis with subsequent analysis of genetic complementation in the non-mucoid mutants have been used to roughly characterize those regions of the DNA involved in xanthan biosynthesis and it appears that the *xps* genes are clustered together. However, the individual genes and their functions have not so far been identified.

1.6 Aim and Outline of Thesis

At the time at which this project was initiated, the relationship between the chemical structure of xanthan, the ordered conformation and the solution and interaction properties was only poorly understood. Xanthan was believed to exist in solution in the ordered helical conformation and the acetyl and pyruvate substituents had been shown to play a major role in determining the stability of the ordered form (Holzwarth and Ogletree, 1979; Smith *et al*, 1981; Rinaudo *et al*, 1983; Dentini *et al*, 1984). There was some evidence to suggest that pyruvate promotes increased viscosity through enhanced macromolecular association (Sandford *et al*, 1977; Smith *et al*, 1981) and the converse appeared to be true for the acetyl group, since deacetylation seemed to lead to an increase in viscosity (Jeanes *et al*, 1961; Tako and Nakamura, 1984). Locust bean gum was believed to interact with xanthan in the helical state (Dea *et al*, 1977) and data from one group of workers (Tako *et al*, 1984) indicated direct involvement of the xanthan side-chains in the xanthan-galactomannan interaction. There was also some evidence to suggest that the acetyl group has an inhibitory effect upon the interaction between xanthan and locust bean gum (Dea *et al*, 1977; Tako *et al*, 1984). However, the molecular basis for these observations had still to be completely established.

The aim of this project was to gain a better understanding of the relationship between the primary structure of xanthan and its behaviour in solution, both alone and in combination with other polysaccharides. The role of the trisaccharide side-chain together with its two acyl substituents was the main area of interest. The idea was to generate a range of xanthan-type polysaccharides with minor structural differences, to study the solution and interaction properties of these materials using a range of physical techniques, and to try to relate any differences in behaviour to differences in the chemical composition. The helix-coil transition behaviour of the polysaccharides and the solution viscosity were areas of particular interest, as was the interaction with the galactomannans, locust bean gum and guar gum, and the glucomannan konjac mannan.

Chapter 3 of this thesis deals with the production and chemical characterization of the materials used in this study. Xanthan-type polysaccharides were produced by growing different strains and subspecies of the *X. campestris* group under a range of cultural conditions and by chemical deacetylation and/or depyruvylation. Some commercial materials were also used. A selection of colorimetric and chromatographic techniques, together with elemental analyses, were used to determine the chemical composition of the polymers and to assess their purity.

As it transpired, the vast majority of the materials differed only in the levels of acetyl and pyruvate substitution, and the role of the acyl substituents therefore became the main focus of this study. Two polymers with a reduced mannose content were identified and one of these (ps.BD9A) was studied in an attempt to determine the role of the terminal side-chain residue in the solution and interaction behaviour. However, the chemical composition of materials from the so-called "crenated mutants" of *X. campestris* indicated a structure very different to that of xanthan and these polymers were not therefore the subject of further investigation.

In Chapter 4 the order-disorder transition of xanthan is considered. The influence of different levels of acetyl and pyruvate substitution on the helix-coil transition behaviour of a range of polymers was studied using optical rotation and the results were analysed statistically. The effects of salt upon the helix-coil transition behaviour were also examined, as was the behaviour of ps.BD9A.

Molecular weight and chain flexibility are the subjects of Chapter 5. In the absence of a more direct technique, the molecular weight of the materials was estimated from intrinsic viscosity measurements using published data. The intrinsic viscosity of four materials with different levels of acetyl and pyruvic acid substitution was determined over a range of ionic strengths in an attempt to compare the relative flexibility of the polymers using the Smidsrød and Haug B-value method. Data for the same four polymers, produced subsequently by static light scattering, enabled a more critical evaluation of the intrinsic viscosity data.

Chapter 6 details a study of the effects of polysaccharide concentration and ionic strength upon the viscosity of two materials in particular, one high acetyl, low pyruvate xanthan and another low acetyl, high pyruvate polymer.

The aim of Chapter 7 was to characterize, in rheological terms, the interaction between xanthan and the gluco- and galactomannans, and to examine the effects of acetyl and pyruvate substitution on the strength of the interaction with locust bean gum and konjac mannan. The role of the terminal mannose residue in the interaction with locust bean gum was also considered. Using both steady and oscillatory shear measurements solutions of xanthan, locust bean gum, guar gum and konjac mannan were characterized individually, both in the presence and absence of added salt. The

behaviour of the mixed systems in deionized water was studied using polarimetry, falling ball experiments, oscillatory shear measurements and by estimation of the minimum gelling concentrations. A range of xanthans with very different levels of acetyl and pyruvate substitution were tested and the data from the oscillatory shear measurements was analysed statistically to search for correlations between gel strength, the levels of acetyl and pyruvate substitution, intrinsic viscosity and the helix-coil transition midpoint. Attempts to study the behaviour of the mixed systems in the presence of sodium chloride were restricted by instrumental problems. The assertion by Cairns *et al* (1986a; 1987) and Brownsey *et al* (1988) that denaturation of the xanthan helix is necessary for the interaction with locust bean gum and konjac mannan was also tested.

Chapter 8 gives a summary of the main findings of this project and discusses to what extent the initial aim of the study, outlined here, was achieved.

Finally although most of this project was concerned with the solution and interaction properties of xanthan, neither aspect has been dealt with in any depth in this General Introduction. Instead Chapters 3-7 each have their own introduction dealing specifically with those aspects of the production, solution properties and interaction behaviour of xanthan, which are directly relevant.

Table 1.1: Some plant diseases caused by members of the *X. campestris* group (Dye and Lelliott, 1974; Agrios, 1978).

Organism	Disease
	1. Vascular Wilts
X. campestris	Black rot of crucifers
X. vascularum	Gumming disease of sugar cane
	2. Spots and Blights
X. begoniae	Begonia leaf spot
X. juglandis	Walnut blight
X. minihotis	Blight of cassava
X. oryzae	Leaf blight of rice
X. phaseoli	Common blight of beans
	Bacterial pustule of soya bean
X. pruni	Spot of stone fruits
X. rubrilineans	Red stripe and top rot of sugar cane
X. translucens	Blight or stripe of cereals
	3. Cankers
X. citri	Bacterial canker of *Citrus* spp.
X. ampelina	Canker of grapevine

Table 1.2: In vitro biosynthesis of xanthan gum. Results from a series of studies by Ielpi, Couso and Dankert.

a) Incorporation of (^{14}C)-glucose into the 1203[1] extract and polysaccharide (Ielpi *et al*, 1981a).

Additions	(^{14}C)-Glc incorporated (pmol)		Tentative structure of lipid-bound oligosaccharide
	polysaccharide	1203 extract	
1. None	0.8	153	Cellobiose
2. GDP-Man	8.0	120	Man-cellobiose
3. UDP-GlcA	0.8	121	Cellobiose
4. GDP-Man + UDP-GlcA	41.5	51	Pentasaccharide

b) Incorporation of (^{14}C)-pyruvate (from phosphoenolpyruvate) into the 1203 extract and polysaccharide (Ielpi *et al*, 1981b).

Additions	(^{14}C)-pyruvate incorporated (pmol)	
	polysaccharide	1203 extract
1. None	N	21
2. UDP-Glc	N	28
3. GDP-Man	N	24
4. UDP-GlcA	N	22
5. UDP-Glc + GDP-Man	N	24
6. UDP-Glc + UDP-GlcA	N	21
7. GDP-Man + UDP-GlcA	N	21
8. UDP-Glc + GDP-Man + UDP-GlcA	N	67
9. Native xanthan	0	1
10. Pyruvate-free xanthan	0	0

c) **Incorporation of (^{14}C)-acetyl (from acetyl CoA) into the 1203 extract and polysaccharide (Ielpi *et al*, 1983).**

Additions	(^{14}C)-acetyl incorporated (pmol)	
	polysaccharide	1203 extract
1. None	1	2
2. UDP-Glc	1	1
3. GDP-Man	1	2
4. UDP-Glc + GDP-Man	2	62
5. UDP-Glc + GDP-Man + UDP-GlcA	34	33
6. Native xanthan	4	4
7. Acetyl-free xanthan	4	4

1 The 1203 extract (chloroform/methanol/water; 1:2:0.3) contains the polyprenyl phosphosugars.

N No data is given in the paper.

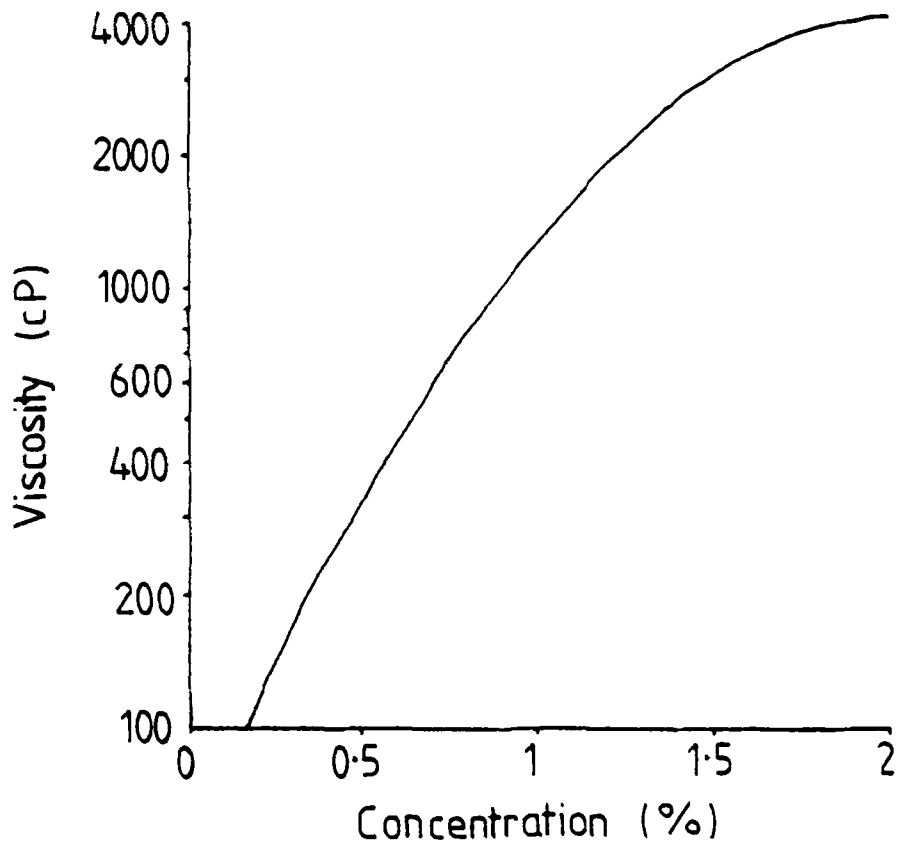

Fig. 1·1 Effect of concentration on the viscosity of xanthan gum (Kovacs and Kang, 1977).

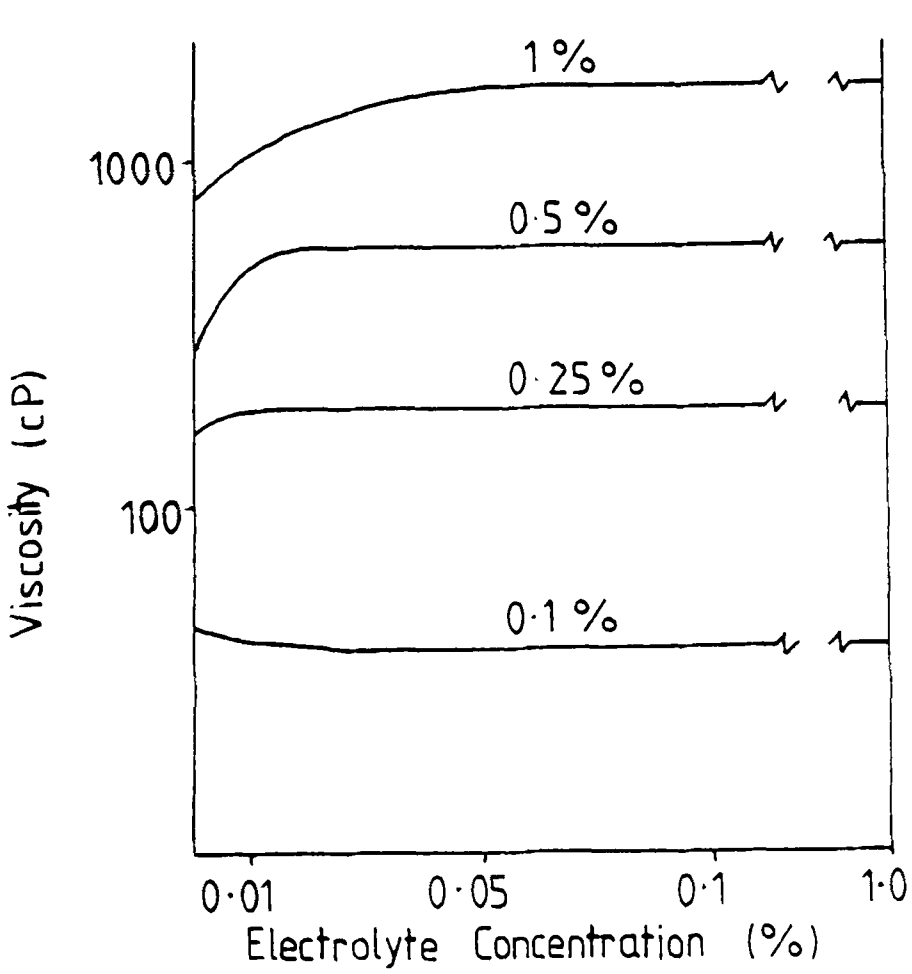

Fig. 1·2 Effect of electrolyte concentration on the viscosity of xanthan gum (Kovacs and Kang, 1977).

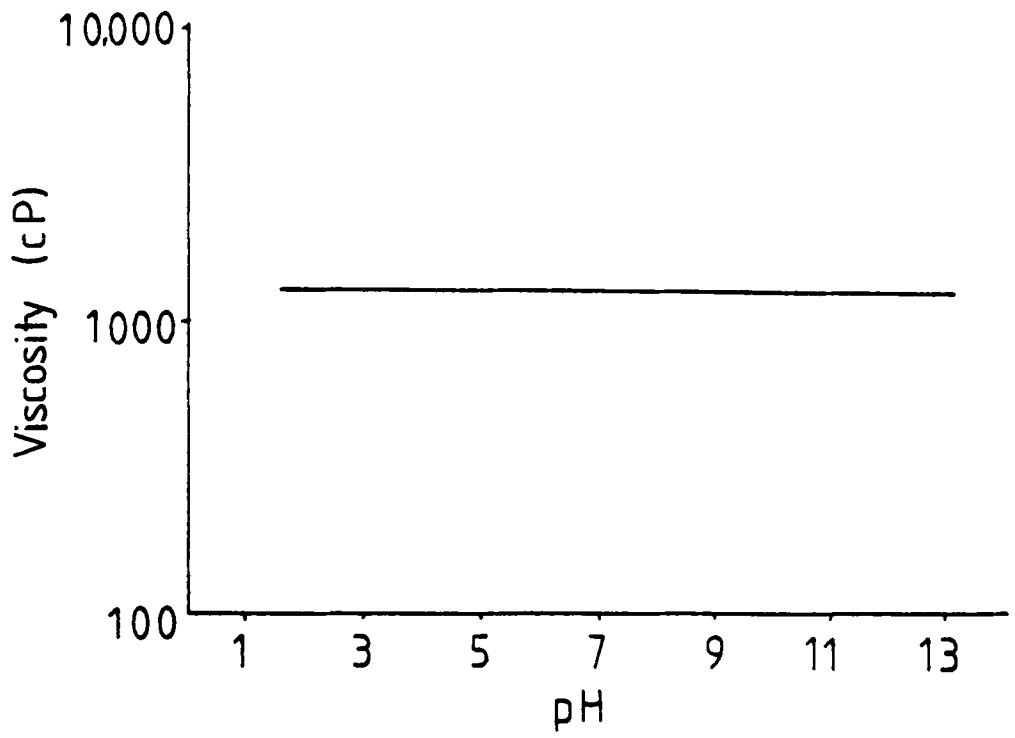

Fig. 1·3 Effect of pH on the viscosity of a 1% solution of xanthan gum in 0·1% NaCl (Kovacs and Kang, 1977).

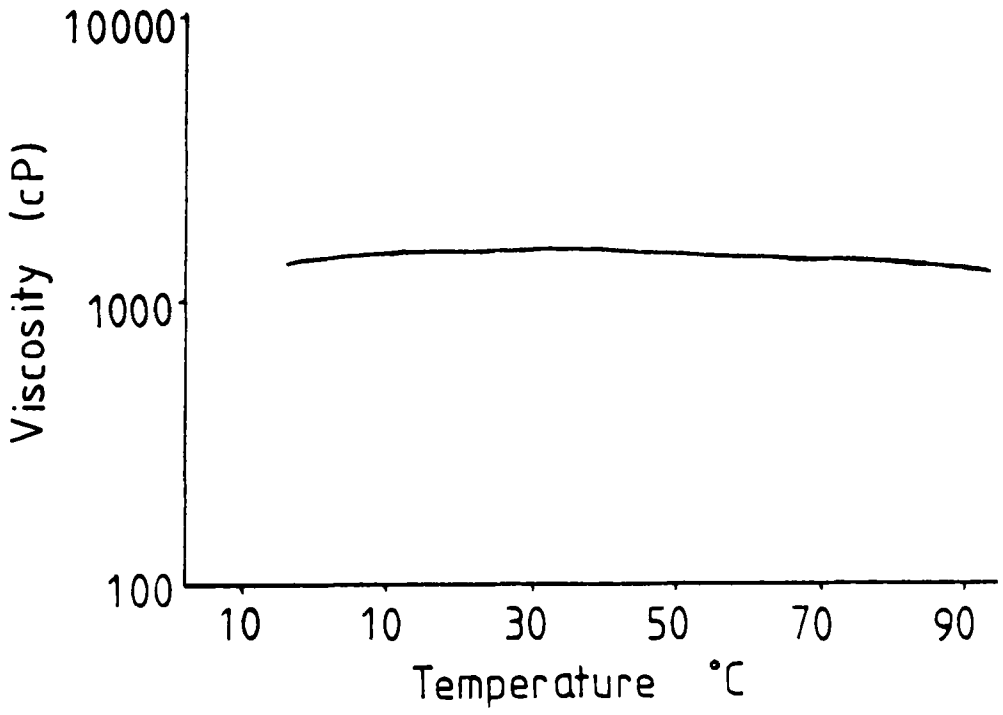

Fig. 1·4 Effect of temperature on the viscosity of a 1% solution of xanthan gum in 0·1% NaCl (Kovacs and Kang, 1977)

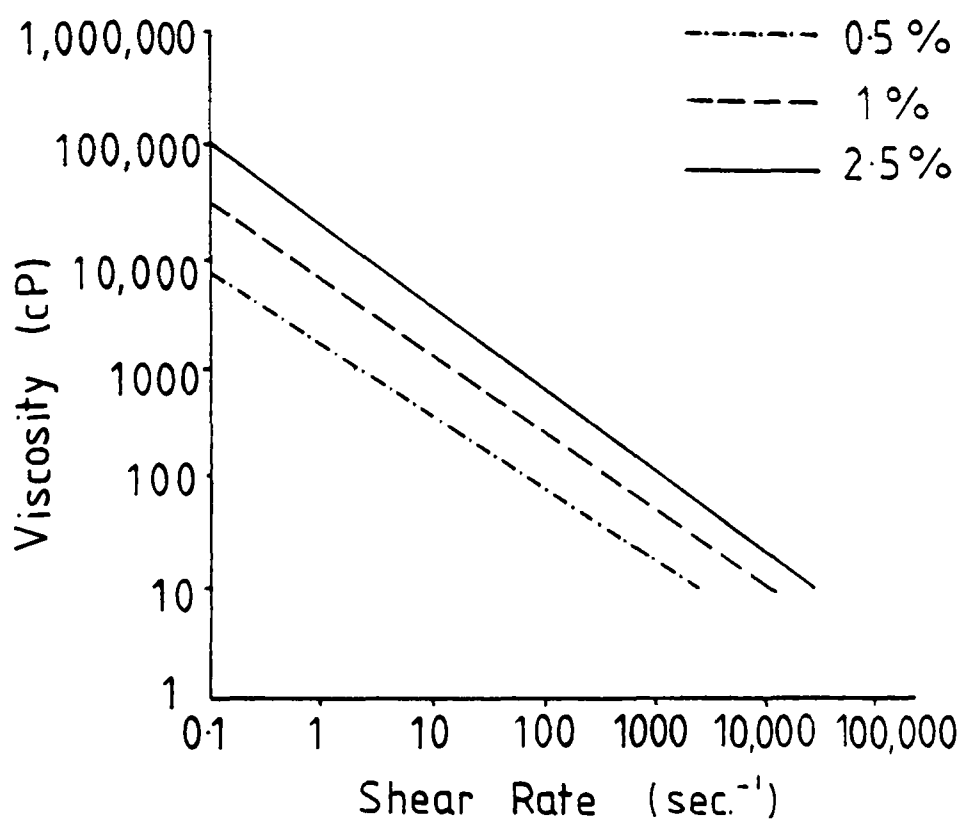

Fig. 1·5 Effect of shear rate on the viscosity of xanthan gum (Kovacs and Kang, 1977).

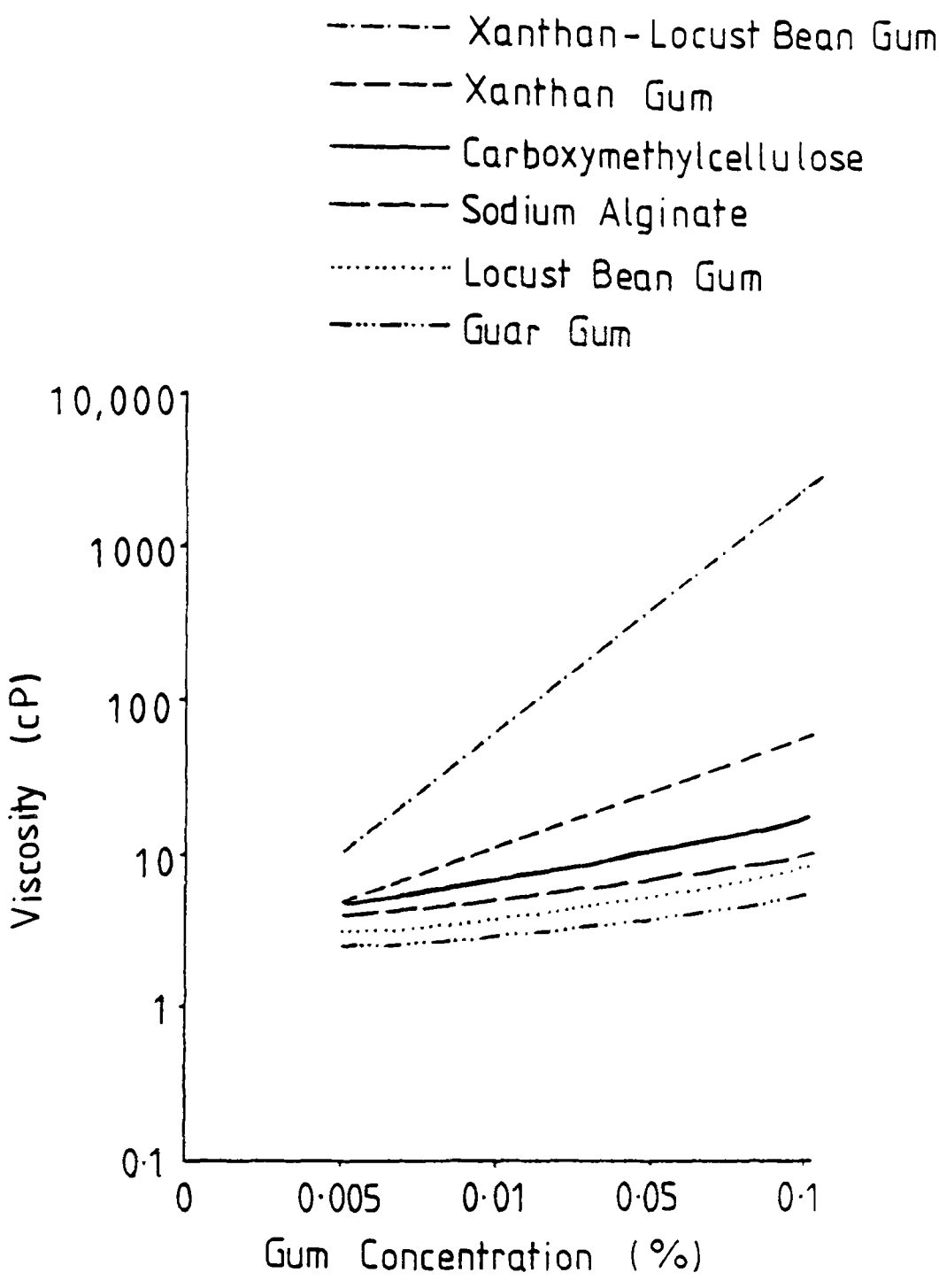

Fig. 1·6 Effect of concentration on the viscosity of low concentration colloid solutions (Kovacs and Kang, 1977).

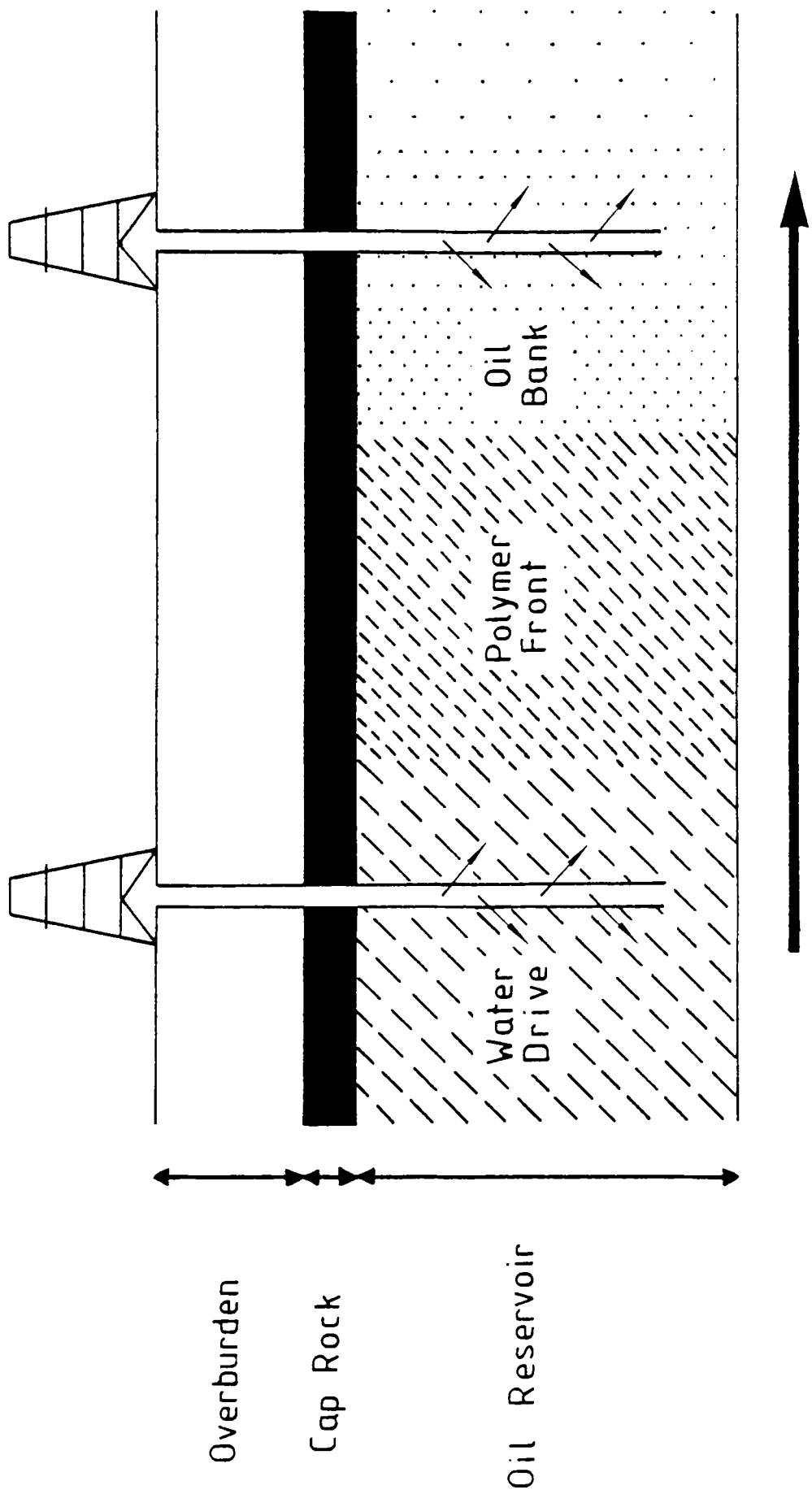

Fig. 1·7 Enhanced Oil Recovery by Polymer Flooding

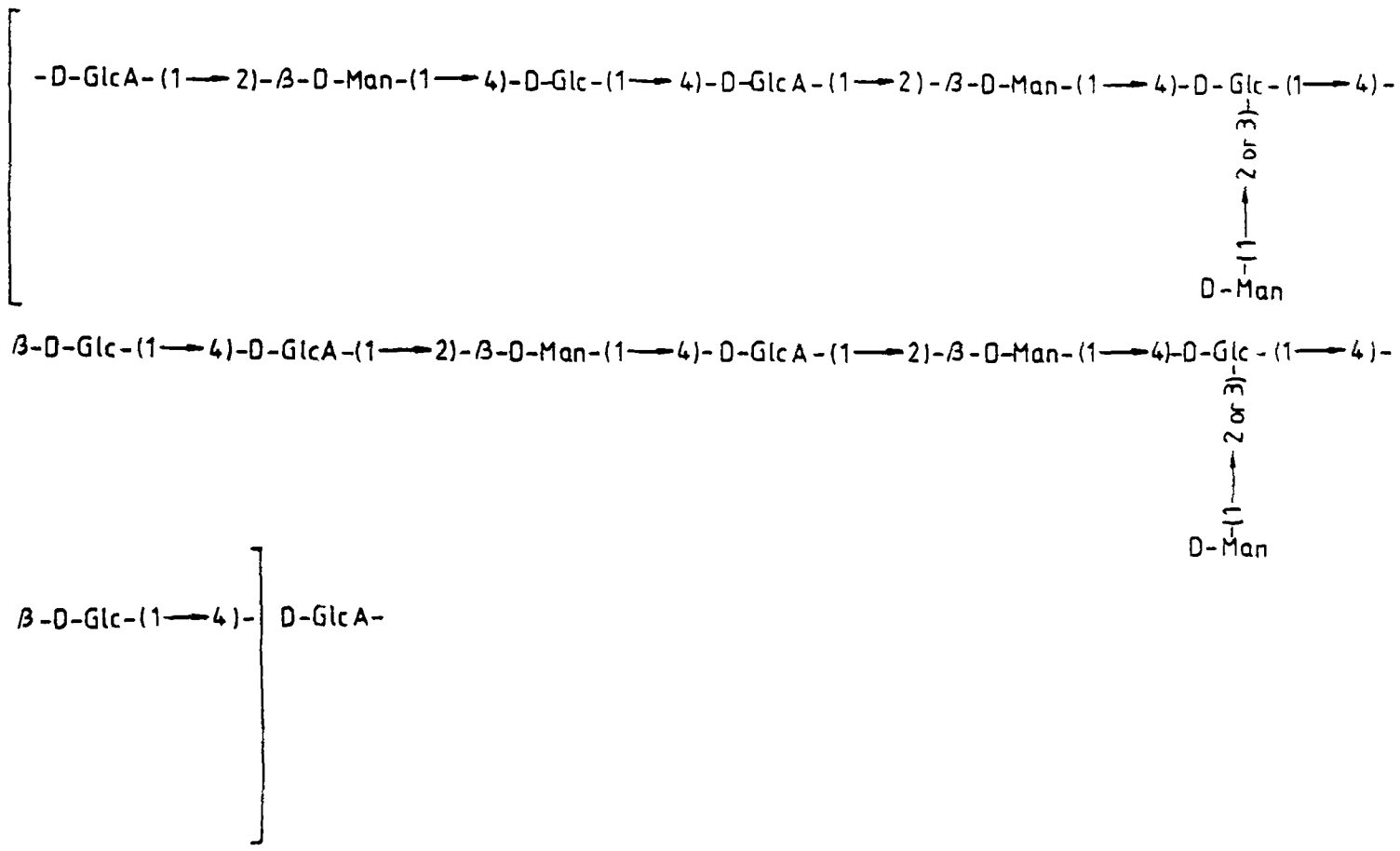

Fig 1·8 16 Residue repeat unit structure of xanthan proposed by Sloneker et al, (1964). The location of the acetyl and pyruvate substituents is not shown.

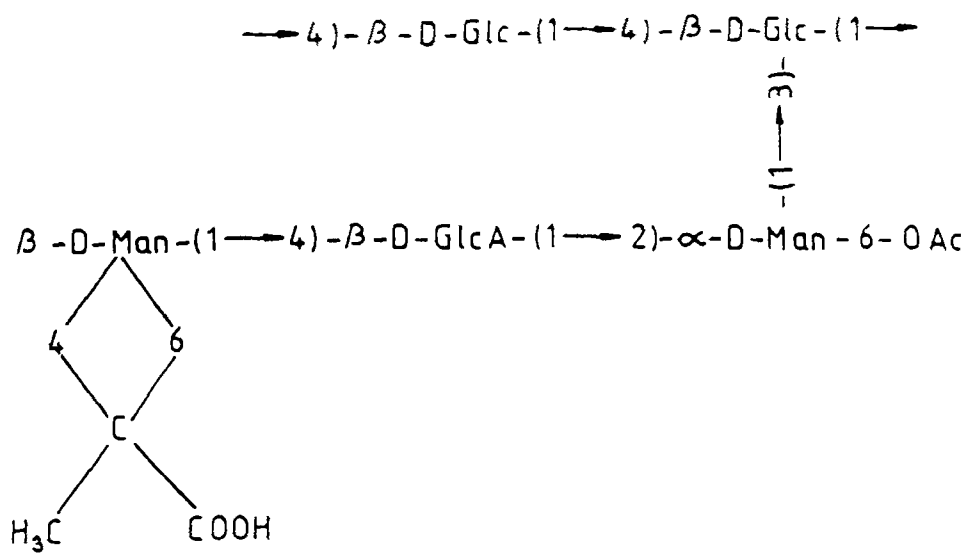

Fig. 1·9 Pentasaccharide repeat unit structure of xanthan proposed by Jansson et al, (1975)

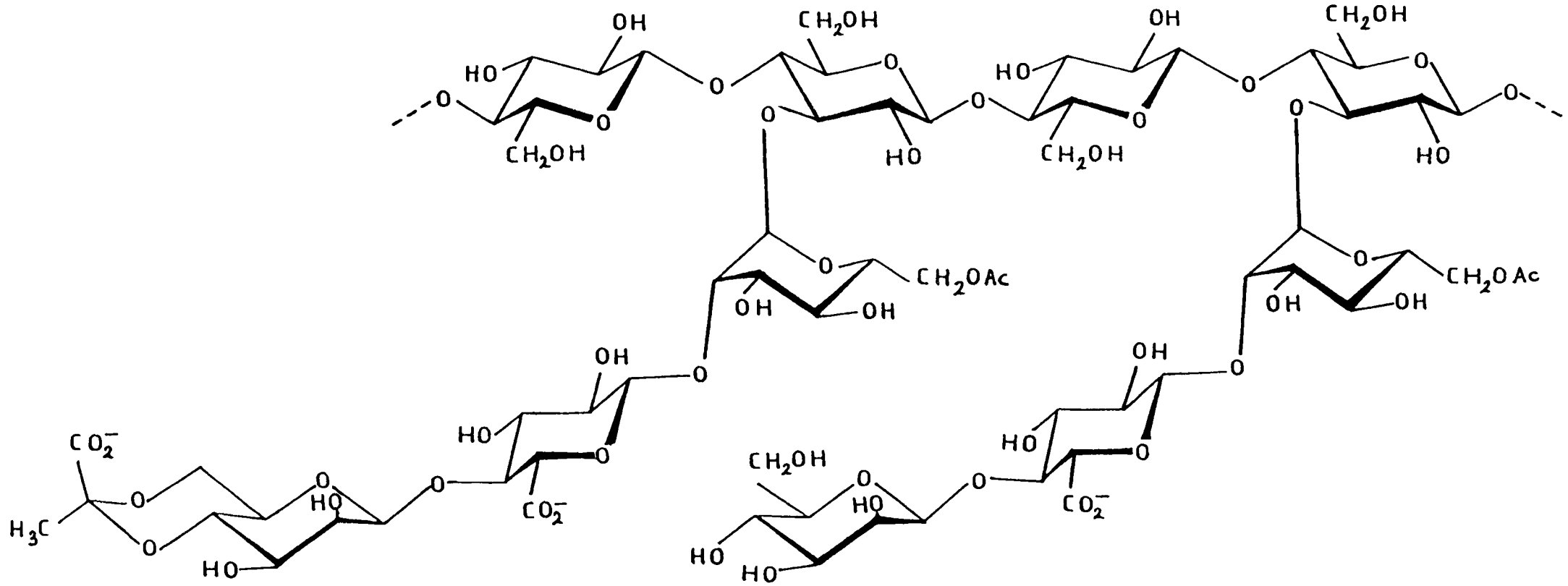

Fig. 1·10 Primary structure of xanthan

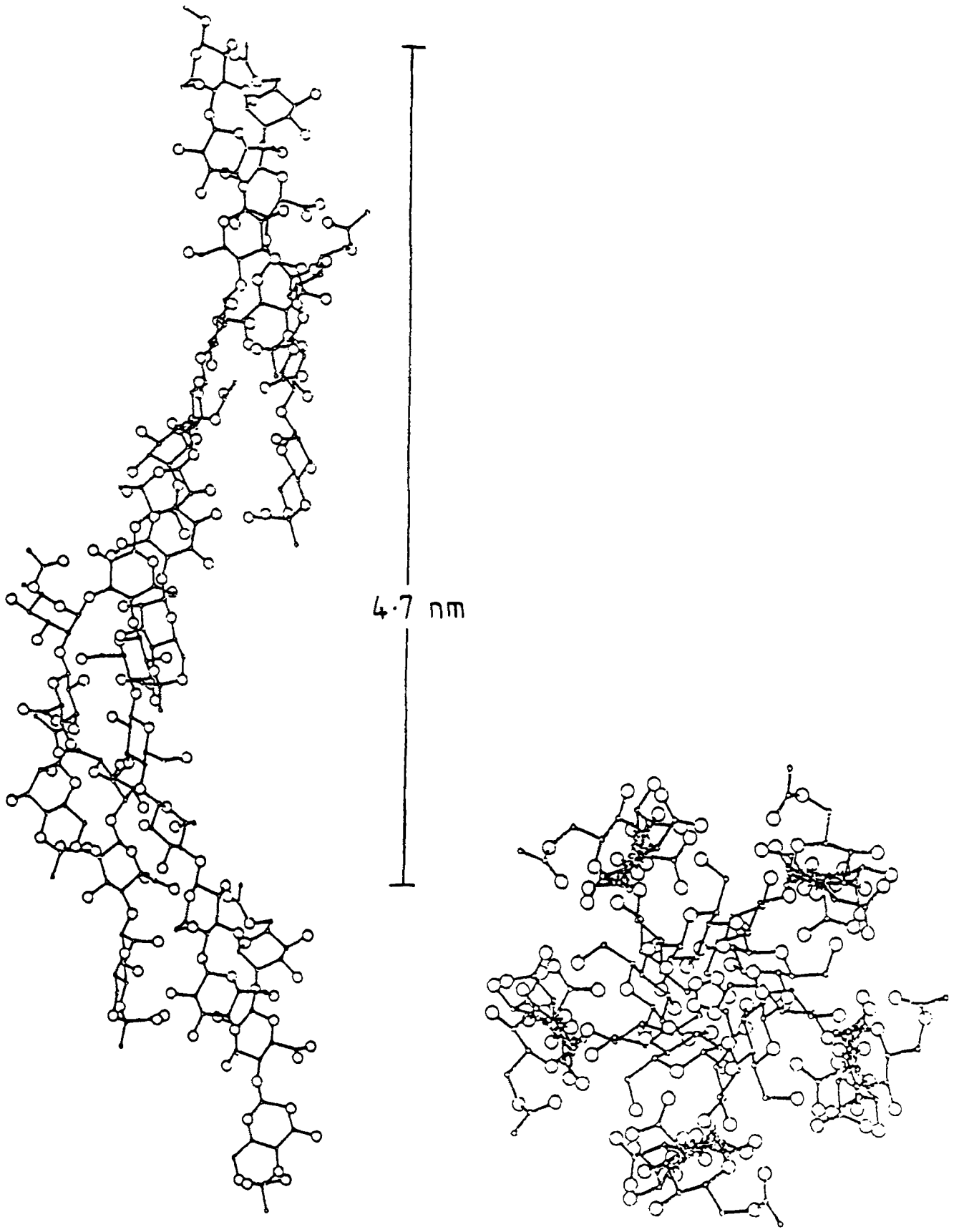

Fig. 1·11 Packed 5/1 helical model of xanthan viewed (a) perpendicular to and (b) down the helix axis (Moorhouse *et al*, 1977 b)

Fig. 1-12 Glucose uptake and metabolism by X. campestris in relation to xanthan biosynthesis (Tait, 1984).

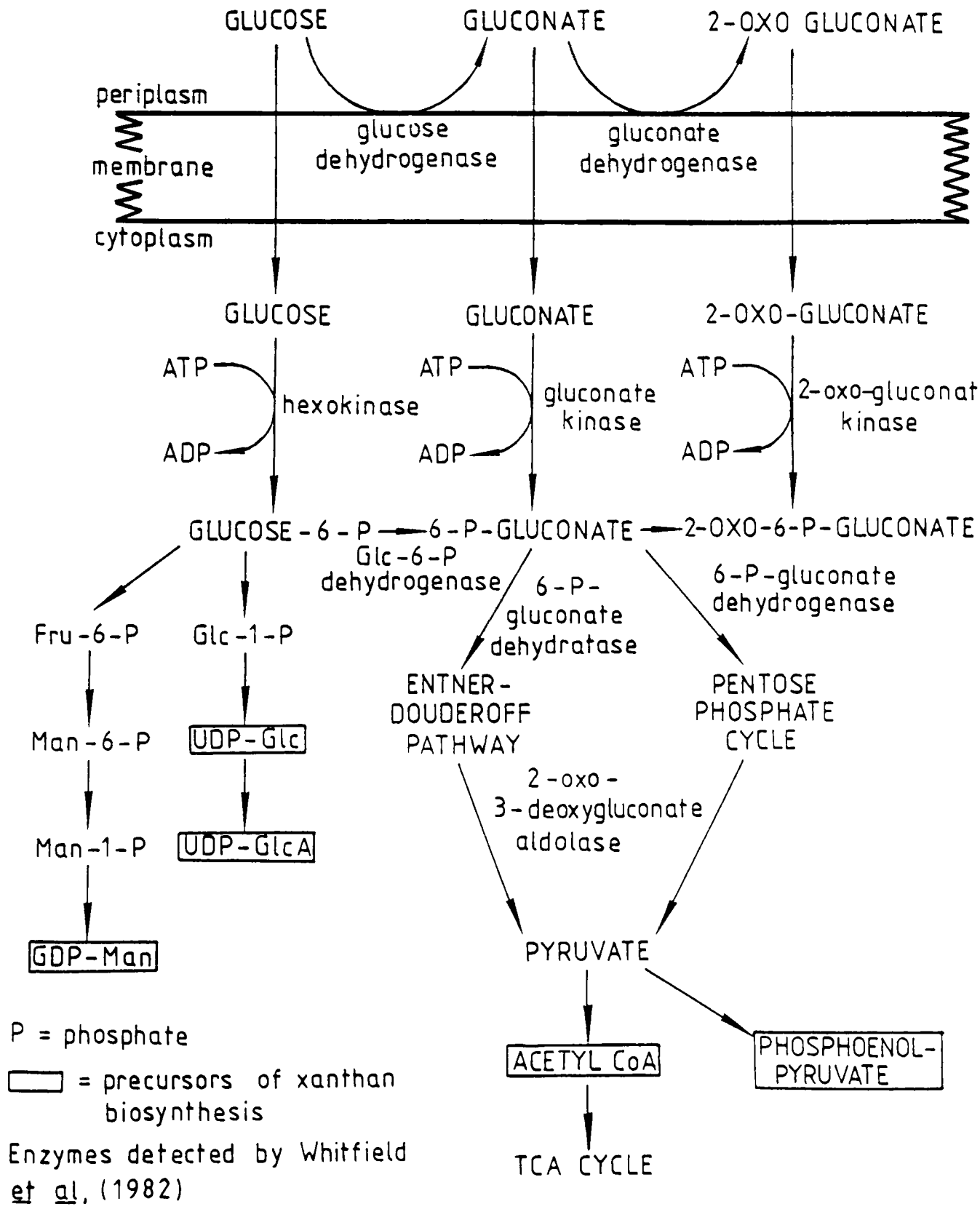

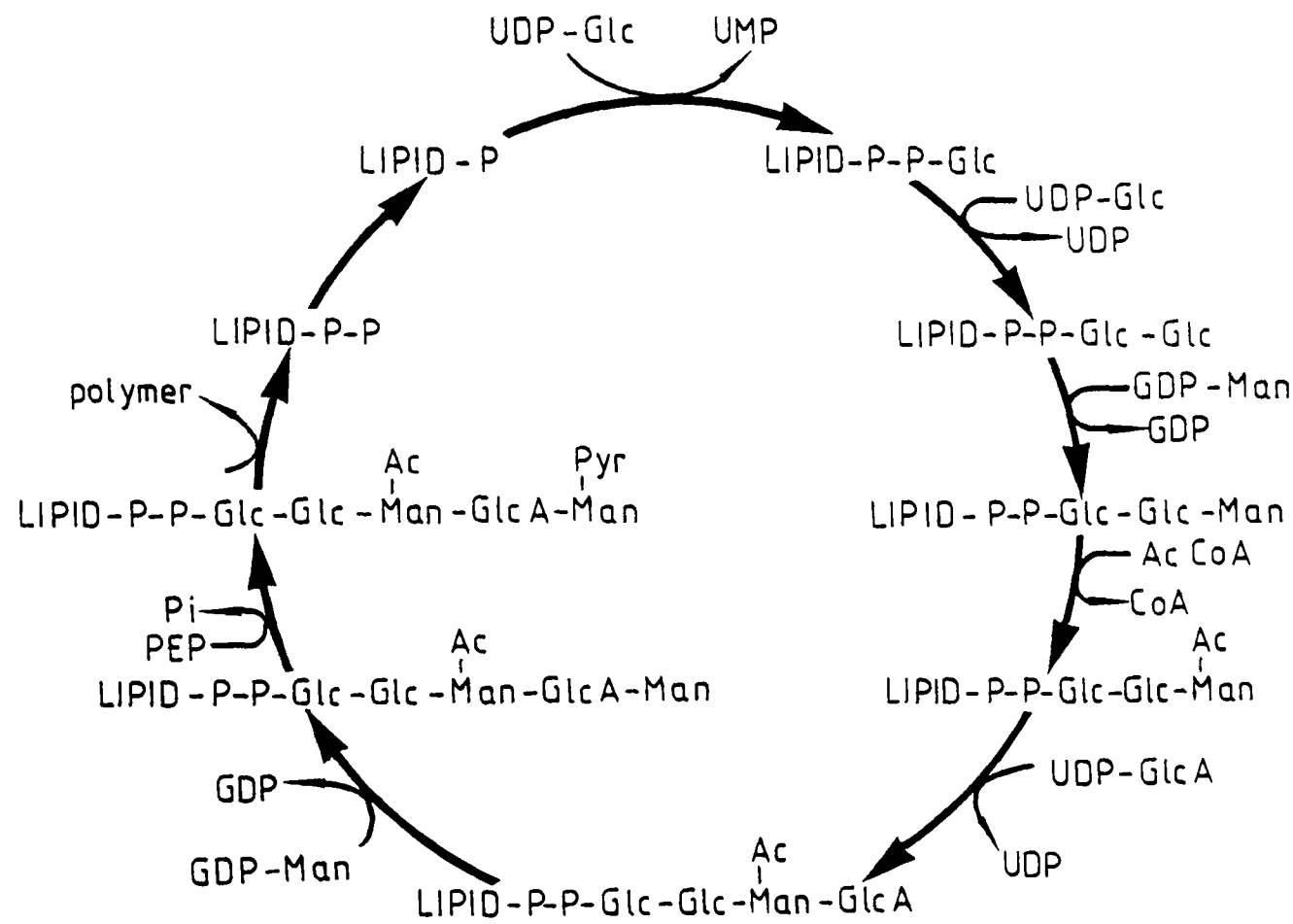

Fig. 1·13 Biosynthesis of xanthan gum (Ielpi, Couso and Dankert, 1981a, 1981b, 1983).

CHAPTER 2

MATERIALS AND METHODS

Microorganisms

Strains of *Xanthomonas campestris* and subspecies of the *X. campestris* group were cultured for the production of exopolysaccharide. These organisms are listed in table 2.1.

Batch Culture

All strains with the exception of PXO_{61} were grown in batch culture using the sulphate deficient medium defined by Davidson (1978; table 2.2a). The medium was dispensed in 1 l amounts into 2 l Erlenmeyer flasks and cultures were incubated for 4-5 days at 30°C on an orbital shaker.

Strain PXO_{61} was grown in yeast extract medium (table 2.2b) supplemented with 0.25% glutamic acid in an L.H. Engineering Fermenter (20 l nominal volume, 15 l operating volume). The culture was maintained for 96 hours at 30°C and pH 7.0, with a stirring rate of 200 rpm.

Strains 556 and 646 were, in addition, grown in the presence of reduced levels of magnesium, potassium and phosphate. The media used were based upon that of Davidson but with the modifications listed in table 2.2c. The cultures (50 ml) were grown in 250 ml conical flasks and were incubated for 4-6 days at 30°C on an orbital shaker.

To assess whether or not the reduced nutrient conditions were growth limiting, the dry weights of the cells were determined. The cells were recovered by centrifugation at 10,000 g for 30 minutes. They were then washed in distilled water, recentrifuged, lyophilized and weighed. In addition the optical densities of duplicate cultures were determined at 520 nm in the stationary phase. The media were then supplemented with an additional 0.08 g/l $MgSO_4.7H_2O$, 0.12 g/l KCl or 0.8 g/l NaH_2PO_4 and the optical density was measured again after 48 hours.

Continuous Culture

Strains 556 and 646 were grown in continuous culture (Bioengineering A.G. Baby Fermenter, KLF 2000) under the nutrient conditions listed in table 2.2d. Cultures were maintained at 30°C and pH 7.0, and samples were collected at the dilution rates listed in the table.

Isolation and Purification of Xanthan

Cells were removed by centrifuging the culture for 30 minutes at 10,000 g and the supernatant was then concentrated using a Pellicon cassette system (Millipore) with a polysulfone PTHK cassette of porosity 100,000 molecular weight. The concentrate was treated with two volumes of cold acetone to precipitate the polymer and the material was then redissolved in distilled water and precipitated once again. After resuspending for the second time, the polymer solution was ultracentrifuged for

75 minutes at 100,000 g to remove subcellular debris, and dialysed against distilled water for 48 hours at 4°C. Conversion to the sodium form was achieved by passing the material through sodium (Amberlite, IR-120) and chloride (Amberlite, IRA-410) ion exchange resins. The polymer solution was then finally redialysed against distilled water to remove the sodium azide used as a preservative, and lyophilized.

The commercial materials used in this study, Flocon 4800C (Pfizer Ltd., Sandwich) and Kelzan (Kelco Co. Inc., San Diego, California) were resuspended in distilled water and purified in exactly the same manner, starting at the ultracentrifugation step.

Purification of Material by Phenol Extraction

Ultracentrifugation of exopolysaccharide from strain 646KR gave rise to both an aqueous and an insoluble gel-like fraction. The aqueous fraction was treated as described for xanthan, whilst the gel-like material was freeze-dried directly. Later, however, the lyophilized gel was further purified by phenol extraction, in order to remove contaminating proteinaceous material. The procedure adopted was as follows: the polymer was resuspended in distilled water and combined at 60°C with a 90% $^{w}/_{v}$ solution of phenol. The mixture was stirred for 10 minutes and then centrifuged for 20 minutes at 10,000 g. Thereafter, the lower phenol layer containing any protein was drawn off and the upper aqueous phase with the polysaccharide, was dialysed exhaustively against distilled water and freeze dried.

Purification of Galactomannans

Purified guar gum (Hercules Ltd., London) and locust bean gum were prepared from commercial flours using a modification of the method previously described by McCleary *et al* (1983). Crude galactomannan (15 g) was treated with 200 ml of boiling aqueous 80% ethanol for 10 minutes. The slurry was collected on sintered glass and washed successively with ethanol, acetone and ether. This material was added to 1 l of hot water and allowed some time to hydrate before standing for 30 minutes in a boiling water bath. It was then homogenized using a food blender and centrifuged at 10,000 g for 30 minutes. The pellet was resuspended in 300 ml of hot water and the extraction procedure was repeated until no further polysaccharide was detectable in the supernatant (usually twice). The extracts were then pooled and precipitated in two volumes of cold acetone. After redissolving in hot water, the polymer solution was ultracentrifuged at 100,000 g and 40°C for 90 minutes and reprecipitated in two volumes of ethanol. The precipitate was collected on sintered glass and washed with ethanol, acetone and ether before freeze drying.

Purification of Konjac Mannan

Konjac mannan was prepared by purification of a commercial food grade flour using the method of Dea *et al* (1977).

Chemical Modification of Polymers

Deacetylation of xanthan was achieved by treating a 0.25% solution of the purified polymer with 0.1M NH_4OH at 60°C for 1 hour. The solution was then dialysed against running tap water overnight and for a further 48 hours against distilled water at 4°C. Conversion to the sodium form was by passage through sodium (Amberlite, IR-120) and chloride (Amberlite, IRA-410) ion exchange resins and the material was then redialysed and lyophilized.

Depyruvylation was by treatment of a 0.5% polysaccharide solution with 5mM trifluoroacetic acid (TFA) at 100°C for 90 minutes (Bradshaw *et al*, 1983). The solution was subsequently dialysed, passed through ion exchange resins and lyophilized as for the deacetylated material.

To ascertain whether any depolymerization was likely to have occurred during chemical modification, 100 ml of the deacetylated material and 50 ml of the depyruvylated material (both equivalent to 0.25 g of the native xanthan) after reaction, were dialysed repeatedly against small volumes of distilled water at 4°C. The dialysates were then pooled and dried under vacuum. Any residual material was resuspended in 750 µl of distilled water and the sample was analysed by descending paper chromatography for the presence of low molecular weight material indicative of chemical degradation. A small aliquot (20 µl) of the preparation was spotted onto Whatman no. 1 paper and run against a range of mono- and oligosaccharide standards, using a mobile phase comprising butan-1-ol / pyridine / water (6:4:3 by volume; 30 hour run). Chromatograms were developed in alkaline silver nitrate reagent (Trevelyan *et al*, 1950).

Colorimetric Assays

The levels of acetyl and pyruvate substitution were determined by the hydroxamic acid (Hestrin, 1949) and 2,4-dinitrophenylhydrazine (Sloneker and Orentas, 1962a) methods respectively. D-glucuronic acid was assayed using both the meta-hydroxydiphenyl (Blumenkrantz and Asboe-Hansen, 1973) and carbazole (Bitter and Muir, 1962) methods. The glucose content of some samples was determined using glucose oxidase (Boehringer, Mannheim), peroxidase and 2,2'-azino-di-(3-ethylbenzthiazoline sulfonic acid) as described by Brivonese (1985). All assays were performed at least in triplicate and the results are expressed as a percentage of the total carbohydrate, as determined by the phenol-sulphuric acid assay (Dubois *et al*, 1956).

Paper Chromatography

Hydrolysates were prepared by heating 1.0 ml of 0.5% polysaccharide in 0.5M TFA, to 100°C, for 16 hours, in sealed glass tubes. The acid was then evaporated off and the residue resuspended in 400 µl of distilled

water. The water was evaporated off and the procedure repeated one more time. Finally the hydrolysed material was resuspended in 500 µl of distilled water. Hydrolysates were analysed by descending paper chromatography using Whatman no. 1 paper and the mobile phase described above. Chromatograms were developed in alkaline silver nitrate reagent.

High Performance Liquid Chromatography (HPLC)

HPLC was used to determine the neutral sugar content of the materials used in this study. Hydrolysates were prepared by heating 20 ml of 0.2% polysaccharide with 0.25M sulphuric acid for 18 hours at 100°C. The sample was then neutralized and the D-glucuronic acid removed by treating overnight with Amberlite IRA-410 resin in the bicarbonate form. After filtering, the neutralized solution was dried under vacuum and the residue resuspended in 200 µl of distilled water. It was then passed through a 0.45 µm Millipore sample filter. Materials were analysed on a Gilson HPLC system with a Rheodyne 7125 syringe injection valve. They were separated at 85°C on a Brownlee Polypore PB analytical cartridge (4.6 mm I.D. x 22 cm; Anachem Ltd., Luton) preceded by Polypore H and Polypore PB guard cartridges (4.6 mm I.D. x 3 cm). The mobile phase was deionized water and the flow rate 0.2 ml/min. Detection of sugars was by means of a Knauer differential refractometer.

The bicarbonate resin used to neutralize the hydrolysates was prepared from Amberlite IRA-410 (chloride form) by the following procedure: it was first treated for 30 minutes with 1M HCl and then washed repeatedly in distilled water until the pH had returned to neutral. This was followed by 30 minutes in 1M NaOH and further repeated washings. Finally the material was allowed to stand overnight in 10% $NaHCO_3$, washed as before and then dried.

Ion Exchange Chromatography

Ion exchange chromatography was used in an attempt to separate material from *X. campestris* strain 556 into two fractions with differing levels of pyruvic acid. Approximately 10 mg of the polysaccharide in solution was applied to a column (22 cm x 2 cm ID) packed with DEAE-microgranular cellulose (Whatman DE52), and the material was separated using a gradient of 0-2M NaCl in phosphate buffer (pH, 7.0). The flow rate was about 10 ml/hr and fractions, roughly 3 ml in volume, were collected.

Each fraction was tested for the presence of carbohydrate using essentially the same method as for the phenol-sulphuric acid assay (Dubois *et al*, 1956). Aliquots of 5% phenol (200 µl) and concentrated sulphuric acid (1 ml) were added in turn to 200 µl of the test fraction with vigorous mixing, and the reaction mixture was then allowed to stand for 15 minutes at ambient temperature. The absorbance was determined spectrophotometrically at 490 nm against a reagent blank prepared with phosphate buffer.

Fractions containing carbohydrate were pooled using the elution profile as a guide. The pooled fractions were dialysed exhaustively against distilled water at 4°C to remove salts, and were then reduced in volume using a rotary evaporator and freeze dried. The resultant materials were analysed for pyruvic acid.

Elemental Analysis

The carbon, hydrogen and nitrogen content of the polymers was determined by elemental analysis. Na^+, K^+ and Ca^{++} levels were measured by flame photometry and ion chromatography (Butterworth Laboratories Ltd., Teddington, Middlesex).

Polarimetry

Optical rotation measurements were made in a Perkin-Elmer 241 polarimeter, using 10 cm quartz thermostatted cells, at a wavelength of 365 nm (mercury emission line). The cell temperature was controlled by a Haake F3 refrigerated water bath and the sample temperature was measured with a chromel-alumel thermocouple.

Xanthan solutions (0.3% $^{w}/_{w}$) were used in this study. Salt-free solutions were prepared by dissolving the freeze dried polymer in deionized water at the required concentration (dissolution by prolonged stirring and standing for 1 hour in a 90°C water bath) and then filtering through a series of Millipore filters down to a minimum pore size of 0.45 μm. Where measurements were made in the presence of salt the xanthan solution was prepared and filtered at double the concentration (ie 0.6% $^{w}/_{w}$) and then combined by weight with equal quantities of a pre-filtered NaCl solution, also at double the required concentration. Mixtures were stirred hot to ensure homogeneity.

A standard procedure was adopted for sample handling. Cells were filled with the sample solution at 90°C and after degassing the temperature was dropped to 10°C (bath cooling rate approximately 1°C per min). The sample was maintained at this temperature overnight (16 hours). The optical rotation course of the helix-coil transition was then monitored. Measurements were made over a temperature range of 10-91°C. The temperature was raised in 3°C increments, allowing 10 minutes at each step for the sample to equilibrate before taking the reading. For cooling sweeps the time increments were the same, but measurements could be made directly after degassing.

Intrinsic Viscosity Measurements

A 0.1% $^{w}/_{w}$ solution of xanthan or a 0.2% $^{w}/_{w}$ solution of the gluco- or galactomannan was prepared (dissolution by stirring and standing for 1 hour in a 90°C water bath) and dialysed exhaustively against aqueous NaCl. The polymer solution and dialysate were then filtered through a

1.2 μm Millipore filter. Using these as stock solutions, a series of 5 dilutions with relative viscosities ($\eta_r = \eta / \eta_s$, where η is the viscosity of the solution and η_s that of the solvent) in the range 1.2-2.0, were prepared by weight. The relative viscosity of each solution was determined at 25°C using a Contraves Low Shear (LS30) couette viscometer. A voltage ramp was supplied to the external drive input (shear rate proportional to voltage) of the viscometer using the analogue output of a DEC MINC 11/23 laboratory computer. The range of shear rates applied was typically 1-30/sec, and the fluid torque response (also proportional to voltage) was collected as an analogue signal and converted to digital data by the computer. The relative viscosity is then equal to the ratio of the response voltage to the applied voltage for the solution and the solvent, respectively. From this data the zero-shear intrinsic viscosity was determined using the Huggins and Kraemer extrapolations (section 5.3). The absolute concentration of the stock solution was determined from the dry weight after freeze drying, and the carbon content was determined by elemental analysis. The intrinsic viscosity was adjusted accordingly (Appendix 2).

Viscosity Measurements at Higher Polysaccharide Concentrations

Viscosity measurements on xanthan solutions of concentrations up to 0.5% $^{w}/_{w}$ were made, at 25°C, using the Contraves Low Shear (LS30) couette viscometer. Solutions were prepared on a weight/weight basis by dissolving the polymer in deionized water, at a concentration higher than the maximum required for the study. The polymer was dissolved by stirring for 1 hour, heating for a further hour in a 90°C water bath and then stirring overnight. The solution was filtered through a 1.2 μm Millipore filter. Finally it was combined by weight with quantities of prefiltered NaCl solution and deionized water, to give the required polymer and salt concentrations. Samples were homogenized using a vortex mixer and air bubbles were removed on standing or, if the solution was particularly viscous, were drawn off under vacuum.

Measurements on polysaccharide solutions of still higher concentrations (1.0-2.0% $^{w}/_{w}$) were made in conjunction with the oscillatory shear measurements. Details are given in the section on mechanical spectrometry.

Light Scattering

Static light scattering measurements were carried out by Dr S.B. Ross-Murphy at the Institut für Makromolekulare Chemie, University of Freiburg, West Germany, using an ALV-Laser 3000 System with a servo-controlled SP-81 Goniometer.

Stock xanthan solutions at a concentration of $<3 \times 10^{-4}$ g/ml (ie. below the overlap concentration, defined by $c^* = 1/[\eta]$) were prepared by dissolving the polymer in 0.1M KCl and then autoclaving at 116°C for

approximately 30 minutes. This was necessary to disrupt supramolecular aggregates (Coviello *et al*, 1986). The samples were then dialysed against aqueous 0.1M KCl for 5 days and dilutions - typically five, in the range 1×10^{-5}-1×10^{-4} g/ml - were prepared and autoclaved for a further 10 minutes. They were then filtered through 0.22 μm Millipore sterilized one-way filters directly into the precision cylindrical quartz scattering cells.

Static light scattering measurements were carried out over the angular range 20-145° and at a temperature of 20°C, using the blue line of a Spectra Physics 2020 Ar ion laser. The turning arm of the goniometer was under computer control and the scattered intensity was measured with a Thorn EMI Model 2735 photon counting tube. The signal from this was fed to the ALV 3000 correlator system and the summed signal, relative to two constantly monitored light diode arrays, passed to a Sirius AT compatible microcomputer. The absolute scattering was calculated relative to a toluene standard and the sample dialysate (solvent). The value of the specific refractive index increment was taken to be 0.144 ml/g (Paradossi and Brant, 1982).

Following Coviello *et al* (1986) a Zimm/Holtzer analysis of the angular dependence of the zero concentration scattered light was used to calculate the following:

1. Weight average molecular weight.
2. Z-average root mean square radius of gyration.
3. Linear mass density.
4. Number of Kuhn segment lengths per chain.
5. Chain contour length.
6. Kuhn segment length.

Estimation of Minimum Gelling Concentrations

Gels comprising 0.5% $^{w}/_{w}$ xanthan and 1.0% $^{w}/_{w}$ gluco- or galactomannan were prepared as follows: the constituent polymers were weighed into a screw-top universal bottle, together with distilled water or NaCl solution (total weight, 15.0 g), and the materials were allowed to stand overnight so that the polymers became well hydrated. This facilitated easy dispersion. They were then heated to 80°C in a water bath and sheared vigorously for 5 minutes at high speed using a top-drive Atomix. Air bubbles were removed by centrifuging for 2 minutes at 20,000 rpm in a bench centrifuge and the mixture was reheated to 80°C. Serial 1/2 dilutions were made by dispensing 5.0 ml quantities of the melted gel system into preheated 5.0 ml aliquots of water or salt solution and homogenizing with a vortex mixer. Dilutions down to 1/64 (ie approximately 0.008% xanthan and 0.016% gluco-/galactomannan) were prepared and these were allowed to age for 24 hours at room temperature before being examined for gel formation.

The extent of gelation was assessed visually and the samples were grouped into one of four categories using the criteria listed in table 2.3.

Falling Ball Experiments

The apparatus used for the falling-ball experiments was essentially that described by Richardson and Ross-Murphy (1981) and is illustrated in figure 2.1. It comprises an inner glass tube containing the gel and a small lead sphere approximately 2 mm in diameter. Surrounding this is an outer tube connected to a Haake F3 refrigerated water bath and this acts as a water jacket controlling the temperature of the gel.

The gel mixture was prepared exactly as described for the minimum gelling concentration experiments as far as the centrifugation step. Thereafter, the gel was remelted and dispensed from a hot glass syringe, through a plastic pipe, into the inner tube of the apparatus. The gel cooled and as it was about to set, the small lead sphere was dropped in and pushed below the surface. Care was taken to ensure that it was in contact with neither the meniscus of the gel nor the side of the tube. Either would have introduced additional stresses which could have affected the point at which the ball began to move. The gel was then allowed to age for 24 hours at ambient temperature.

The melting temperature of the gel was determined by increasing the temperature at a rate of 0.5°C/min from ambient and observing the lead sphere continuously through a travelling microscope. The temperature at which it began to drop constantly through the gel was taken as the melting point.

Mechanical Spectrometry

The response of mixed gel systems to oscillatory shear was measured using the Rheometrics Mechanical Spectrometer RMS-605 with automatic computation and plotting of results. 50 mm diameter parallel plates were used (with a gap of 1 mm) in combination with the normal (TC-2000) transducer.

Samples comprising 0.5% $^{w}/_{w}$ xanthan and 1.0% $^{w}/_{w}$ gluco- or galacto-mannan were prepared by dissolving the freeze-dried materials in deionized water or NaCl solution (total weight, 15.0 g) in screw-top universal bottles. Dissolution was achieved by first allowing the polymers to become hydrated overnight, then heating to 85°C in a water bath and shearing for 5 minutes at high speed using a top-drive Atomix. The samples were pressure cooked for 5 minutes at 110°C and sheared again for 5 minutes at maximum speed. Air bubbles were removed by centrifuging at 20,000 rpm for 2 minutes in a bench centrifuge and the gel was remelted and loaded onto the instrument. Samples were routinely loaded at 85°C and the gap around the periphery of the sample was sealed with a light silicon oil (Dow

Corning 200/10cs) to prevent water loss. The temperature was adjusted to 75°C, held for 5 minutes and then reduced, under computer control, at a rate of 1°C/min until 25°C was reached. The system was then allowed to age for a further 30 minutes before any additional measurements were made.

Steady and oscillatory shear measurements on solutions of xanthan (2.0% $^{w}/_{w}$) and the gluco- and galactomannans (1.0 $^{w}/_{w}$) were made using the 72 mm cone and plate assembly with the normal (TC-2000) transducer. The samples were prepared exactly as for the mixed systems but were loaded, and the measurements made, at ambient temperature (24 +/- 1°C).

Table 2.1: Strains of the *X. campestris* group cultured for exopolysaccharide production.

Strain	Microorganism
646	Wild-type *X. campestris* pv. *campestris* obtained originally from the American Type Culture Collection (Rockville, Maryland), ATCC 13951.
556	Wild-type *X. campestris* pv. *phaseoli* obtained from the National Collection of Plant Pathogenic Bacteria, Harpenden.
1128	Wild-type *X. campestris* pv. *phaseoli* obtained from the National Collection of Plant Pathogenic Bacteria, Harpenden.
PXO_{61}	*X. campestris* pv. *oryzae* obtained from T.W. Mew of the International Rice Research Institute, Manilla.
XA46	Non-pigmented mutant of *X. campestris* pv. *campestris* obtained from Pfizer Ltd., Sandwich.
2BD	Mutant strain of *X. campestris* pv. *campestris* S459 (a streptomycin resistant variant prepared from strain 646) isolated after treatment with N-methyl-N-'nitro-N-nitrosoguanidine - NTG (Tait, 1984).
BD9A	Mutant strain of *X. campestris* pv. *campestris* S459 isolated after treatment with NTG (Tait, 1984).
646E	Crenated mutant of *X. campestris* pv. *campestris* 646 isolated after treatment with ethyl methane sulphonate (Whitfield, 1979).
646KR	Crenated mutant of *X. campestris* pv. *campestris* 646 isolated after treatment with γ-radiation (Whitfield, 1979).
MT16.8	Crenated mutant of *X. campestris* pv. *campestris* 646.

Table 2.2: Media used for the cultivation of *X. campestris*.

a) Basic medium defined by Davidson (1978).

Component	Concentration (g/l)
Glucose	20.0
NH_4Cl	5.0
$NaSO_4.10H_2O$	1.5*
KH_2SO_4	5.0
$Mg_2SO_4.7H_2O$	0.2
Citric acid	2.1
$CaCO_3$	0.02
ZnO	0.004
$FeCl_3.6H_2O$	0.0024
PH, 6.8	

* Sulphate deficient medium used for most batch cultures contained 0.3 g/l $Na_2SO_4.10H_2O$.

b) Yeast extract medium.

Component	Concentration (g/l)
Glucose	30.0
Na_2HPO_4	10.0
NaCl	1.0
KH_2PO_4	3.0
$MgSO_4.7H_2O$	0.2
K_2SO_4	1.0
$CaCl_2$	0.01
$FeSO_4$	0.001
Casamino acids	1.0
Yeast Extract	1.0
pH, 7.0-7.2	

c) **Media used for the growth of strains 556 and 646 in batch culture under nutrient deficient conditions.**

Nutrient Conditions	Medium
Non-nutrient limiting	Complete medium as defined by Davidson (1978)
Reduced magnesium	Various concentrations of $MgSO_4.7H_2O$: 0.02 g/l, 0.04 g/l, 0.06 g/l
Reduced potassium	NaH_2PO_4 was substituted for KH_2PO_4 and KCl was added at concentrations of 0.03 g/l, 0.06 g/l, 0.09 g/l
Reduced phosphate	KCl was substituted for KH_2PO_4 and NaH_2PO_4 was added at concentrations of 0.2 g/l, 0.4 g/l, 0.6 g/l

d) **Nutrient conditions and dilution rates used for the growth of strains 556 and 646 in continuous culture.**

Strain	Medium	Dilution rate
556	Complete medium as defined by Davidson (1978), supplemented with 3 g/l glutamic acid	0.024/hr 0.090/hr
556	Carbon limited medium (Davidson, 1978); 5 g/l glucose	0.051/hr
646	Potassium limited medium (Davidson, 1978); 0.07 g/l KCl	0.024/hr 0.120/hr

Table 2.3: Visual assessment of gel strength, as used in experiments to determine the approximate minimum gelling concentration of xanthan-glucomannan and xanthan-galactomannan systems.

Gel Strength	Criteria
++	Strong gel; maintained its shape unsupported and was firm to the touch
+	Weak gel; incapable of supporting its own weight and yielded readily to compression
+/-	Structured solution
-	Flowed readily. No sign of "cross-linking".

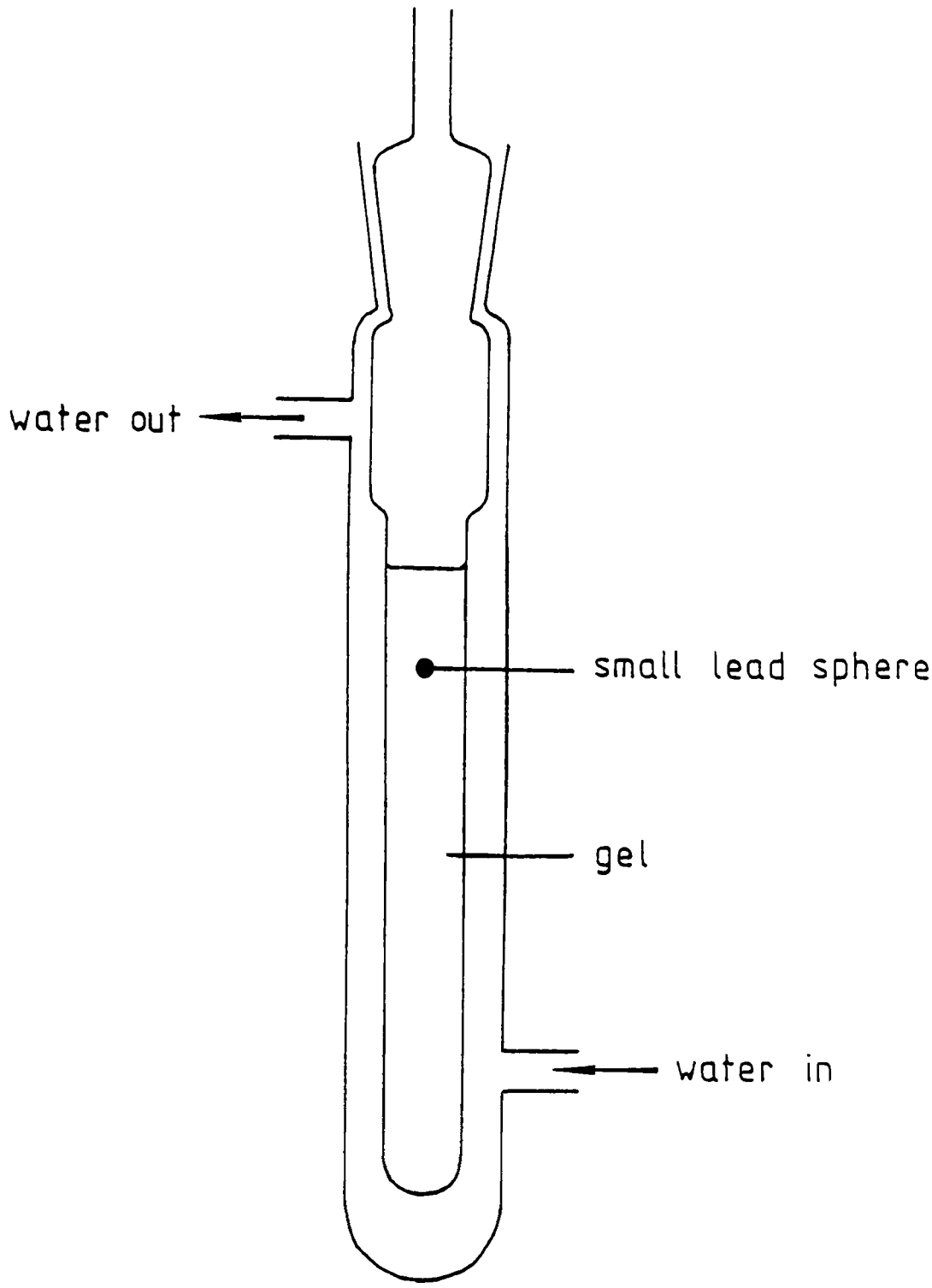

Fig. 2·1 Apparatus used for the falling ball experiments

CHAPTER 3

PRODUCTION AND CHEMICAL CHARACTERIZATION OF POLYMERS

Introduction

3.1 Xanthan Production in Artificial Culture

X. campestris produces profuse quantities of xanthan gum in artificial culture. This is manifested as the development of large, mucoid colonies on nutrient agar (figure 3.1a) and by the production of highly viscous broths in submerged culture.

Although Dye and Lelliot, in Bergey's Manual of Determinative Bacteriology (1974), have stated that the nutrient requirements of the *Xanthomonads* are complex, the majority of species will grow quite readily in a simple, chemically defined medium of glucose, ammonium chloride and salts (Starr, 1946). Growth occurs over a broad range of temperature and pH, but the optima seem to lie in the region of 24-28^{o}C (Moraine and Rogovin, 1966) and pH 7.0. Adequate aeration is essential since *X. campestris* is a strict aerobe.

Figure 3.2 shows the changes that occur during the course of a typical batch fermentation (Moraine and Rogovin, 1966). In this instance, 450 ml of a *X. campestris* seed culture was inoculated into an 8 l fermenter. The medium consisted of D-glucose (2%), an extract of Distillers dried solubles (8%) and salts, at a starting pH of 7.0. The culture was incubated at 28^{o}C. Sterile air was introduced at a flow rate of 1 v/v/min and the medium was agitated by means of two 6.5 cm turbine-type propellers rotating at a rate of 1000 rpm. Cell growth, as indicated by the optical density, occurred predominantly over the first 20 hour period and levelled off after this. The same was true for nitrogen utilization. Glucose uptake occurred throughout fermentation but was more rapid during the early stages of growth. Polymer production, and hence the increase in viscosity, showed essentially the same pattern. Xanthan biosynthesis does not therefore appear to be growth associated. The yield of xanthan, based on glucose consumption, remained almost constant (between 70-80%) throughout the course of fermentation, and this indicates that only a relatively small proportion of the sugar taken up by the cell is used for active growth. Over the first 10 hours, the pH of the culture increased from 7.0 to 7.2 as the by-products of nitrogen metabolism accumulated in the medium. Thereafter, increasing quantities of the polymer with its free carboxylic acid groups and other acidic products of sugar metabolism caused a steady fall in the pH of the medium.

The amount of xanthan synthesized in batch culture is heavily influenced by the environmental conditions and, in particular, the nutrient composition of the medium, the pH, the temperature and the level of aeration. The amount of carbon available is a principal determining factor. With glucose as the sole carbon source, the quantity of material produced increases with the sugar concentration up to a maximum of 4% (Rogovin *et al*, 1961; Souw and Demain, 1979). However, the greatest percentage yield from glucose (up to 90%) is achieved at a concentration

of only 1% sugar (Lilly *et al*, 1958; Rogovin *et al*, 1961). Glucose and sucrose appear to be the best carbon sources, but maltose and soluble starch products also give satisfactory polymer yields. Other hexoses (eg. galactose) and disaccharides (eg. cellibiose, lactose, mellibiose) tend to give poor yields, as do cellulose and the polyols (eg. mannitol, sorbitol). The pentose sugar, D-fructose, supports no polysaccharide production at all (Leach *et al*, 1957; Lilly *et al*, 1958; Souw and Demain, 1979). The quantity and form of the nitrogen source also affects the polysaccharide yield. Souw and Demain (1979) demonstrated that certain amino acids (eg. glutamate) and nitrate salts at moderate concentrations were superior, in terms of xanthan productivity, to ammonium salts but that at higher concentrations they had a marked inhibitory effect. Kennedy *et al* (1982) tested a range of organic nitrogen sources and showed that of these, at equivalent nitrogen concentrations, corn steep liquor and peptone gave the highest xanthan yields whilst Distillers dried solubles gave the lowest. Furthermore, they showed that whilst increasing the amount of organic nitrogen in the medium increased the polymer yield, it reduced the quality of the product in terms of purity and solution rheology. Addition of low levels of certain organic acids (eg. succinate, pyruvate, α-ketoglutarate) has also been shown to stimulate EPS production (Souw and Demain, 1979). Tait and coworkers, (1986) studied the influence of a range of nutrient limiting conditions on xanthan biosynthesis in batch culture and showed that different nutrient deficiencies resulted in markedly different polymer yields. EPS production was greatest in ammonium deficient medium, lower in sulphur and magnesium deficient media, lower still in phosphorous and iron deficient media and least of all under conditions of carbon limitation. The pH optimum for xanthan biosynthesis is broad. Anywhere between 6.5-8.5 will give a good yield (Rogovin *et al*, 1961) but either side of this the amount falls rapidly. The drop is particularly sharp if the starting pH is low since fermentation is, itself, acidogenic. Maintaining a constant pH within the optimum range by steady addition of alkali has been shown to significantly increase the yield (Cadmus *et al*, 1978). The optimum temperature for biosynthesis is 28°C (Moraine and Rogovin, 1966) and the amount of xanthan produced is roughly proportional to the level of aeration (Lilly *et al*, 1958).

The patterns of change occurring during a typical single-stage continuous fermentation are illustrated in figure 3.3 (Silman and Rogovin, 1970, 1972). The conditions used in this experiment, with respect to the composition of the medium, temperature, pH and aeration, were very similar to those described above. The culture was run initially, for 17 hours, as a batch fermentation and then for a further 120 hours as a continuous fermentation. The medium was introduced at a dilution rate of 0.054/hr. and nitrogen was the limiting factor. Each of the variables measured changed gradually over the first 40 hour period until steady state conditions were reached. The optical density increased from just above zero to 10.5. The xanthan concentration rose to 1.22% and the viscosity increased to 5200 cP. The glucose concentration, in contrast, decreased

from 2% to 0.75%, whilst the pH dropped from 7.1 to 6.3. The xanthan production rate was 0.66 g/hr/kg and the yield, based on glucose consumption, was 82%.

Many of the factors influencing xanthan production in continuous culture are the same as those outlined for batch fermentations. For example, Davidson (1978) studied the effect of nutrient limitation on xanthan production by *X. campestris* in continuous culture and found that the pattern was essentially the same as that observed by Tait *et al* (1986). Ammonium limitation produced the highest yield, followed in turn by sulphur, magnesium, potassium, phosphorous and carbon limitation. Similar studies by Evans and coworkers (1979) on *X. juglandis*, a subspecies of the *X. campestris* group which produces two distinct polysaccharides (xanthan and a second polymer consisting of glucose and rhamnose) gave slightly different results. Here potassium and magnesium limitation were found to suppress polysaccharide production whilst phosphorous and sulphur limitation appeared to enhance it. The effects of pH, temperature and aeration remain largely unstudied but they too are likely to resemble those under batch conditions. Silman and Rogovin (1970) demonstrated the inhibitory effects of low pH on xanthan productivity. By raising the pH of the feed from 7.1 to 7.5, they were able to increase the steady state pH and this, in turn, lead to an increase in glucose consumption and polymer production. The effects of dilution rate are by no means clear cut. In a simple chemically defined medium, the yield from *X. campestris* appeared to be largely unaffected at dilution rates of between 0.03-0.07/hr (Tait *et al*, 1986) and the same was true for *X. juglandis* at rates of 0.03-0.05/hr (Evans *et al*, 1979). At higher dilution rates, however, the amount of material produced fell dramatically in both cases. In a more complex medium Silman and Rogovin (1972) observed a different pattern. Their experiments showed a persistent decrease in xanthan yield over the entire range of dilution rates from 0.0233-0.196/hr.

Many of the *Xanthomonas* group show an inherent lack of stability in continuous culture. The development of a less productive colonial variant often occurs after between 6.5-8.7 turnovers (Silman and Rogovin, 1972; Evans *et al*, 1979) and this results in a fall in the culture viscosity and the establishment of a new steady state. Culture deterioration can severely restrict the amount of xanthan produced, but evidence from Evans and coworkers (1979) suggests that the use of appropriate nutrient conditions will increase the stability of the culture. In their studies both sulphur and inorganic nitrogen limitation appeared to eliminate culture variation among strains of *X. juglandis*.

3.2 Structural Variation Among Polymers Produced by the *Xanthomonas* Group

The majority of members of the *X. campestris* group, together with *X. axonopodis* (a separate species), produce an EPS with the same composition as xanthan gum (Gorin and Spencer, 1963; Orentas *et al*, 1963; Sutherland, 1981a; Fett and Osman, 1985). Exceptions, however, include

X. vesicatoria (Orentas *et al*, 1963) and *X. stewartii* (Gorin and Spencer, 1961) which produce a polymer containing galactose instead of mannose, and *X. albilineans* and *X. fragaria* (both separate species) which synthesize a polymer consisting of galactose in addition to the normal proportions of glucose, mannose and glucuronic acid (Sutherland. 1981a). *X. juglandis*, as noted earlier, produces a second distinct polymer composed of glucose and rhamnose (Evans *et al*, 1979). Chowdhury *et al* (1987) have recently elucidated the repeat unit structure of the polysaccharide S-657 elaborated by *Xanthomonas* ATCC 53159. It is a branched hexasaccharide comprising three glucose and three rhamnose residues. Among the xanthan-type materials, the only major difference appears to be in the degree of acetyl and pyruvate substitution (Sutherland, 1981a). Pyruvic acid may be present in any amount up to the equivalent of one acyl group per side-chain (~8.1%) whilst the acetyl groups, though frequently stoichiometric (~5.0%), can be present in larger amounts. The polymer from *X. gummisudans* has been shown to contain about 10% acetyl (Sutherland, 1981a) whilst strains of *X. oryzae* are known which produce materials with in excess of 14% acetyl substitution (Parry, 1985).

Differences in the level of acetyl and pyruvic acid substitution can be found within a single subspecies. For example, members of the *X. campestris* group have been shown to give rise to small colonial variants under conditions of routine maintenance and propagation (Kidby *et al*, 1977; Cadmus *et al*, 1978) and in continuous culture (Silman and Rogovin, 1972; Evans *et al*, 1979). Analysis of the polymer from such variant strains has indicated that they carry a lower level of pyruvic acid, as well as differing somewhat in their solution properties (Cadmus *et al*, 1976, 1978; Sandford *et al*, 1977).

The composition of the polymer produced by a given strain can also vary with the conditions under which the organism is grown. Using a complex medium, Cadmus and coworkers (1978) studied the effects of various culture conditions on the pyruvic acid content of xanthan gum produced by *X. campestris* NRRL B-1459 and its substrains in batch culture. They found that a whole range of factors influenced the degree of pyruvic acid substitution. Low nitrogen, low aeration and high temperatures tended to promote reduced levels of the acyl substituent, whilst the converse conditions promoted higher levels of pyruvic acid. In one particular substrain, the type of nitrogen source appeared to be important. With diammonium phosphate a relatively high pyruvate gum was produced but with sodium nitrate, Distillers dried solubles or Brewers yeast autolyzate as the nitrogen source, the level of pyruvic acid was much lower. Even the type of fermenter and the method used to sterilize the medium appeared to have an impact. The problem with this study, of course, was the sheer complexity of the medium and the number of bacterial strains used. It is extremely difficult to discern precisely what the important determining factors were and which were unique to a particular strain. The data from chemically defined, synthetic media is generally easier to interpret. Tait *et al* (1986), as a result of their studies on nutrient limitation in batch

culture, claimed that nutrient exhaustion influenced the composition of the polymer. This appears to be true in the case of the ammonium deficient medium where the level of acetyl substitution was a little higher and the pyruvic acid content a little lower than normal. However, under the other nutrient limiting conditions tested, very little difference was observed. Slightly raised pyruvic acid levels in the polymers from the magnesium, carbon and iron limited cultures were probably due to the use of a different analytical technique.

Studies by Sutherland (1981a), also in batch culture, showed that when *X. campestris* was grown in the presence of alanine as the sole carbon source, the pyruvic acid content fell, but that when the alanine was replaced by pyruvate, the level of the substituent rose dramatically to 10.6%. This is somewhat surprising since there are hardly any other reports of pyruvic acid being present in more than stoichiometric amounts. Also pyruvate is not itself the acyl donor and it is therefore difficult to see why, in its presence, such unusually high levels of pyruvic acid substitution should occur.

In continuous culture growth of *X. campestris* under magnesium and phosphorus limiting conditions (Davidson, 1978) produced a reduction in the amount of pyruvic acid. Increasing the dilution rate had the same effect, whilst simultaneously raising the acetyl content (Tait *et al*, 1986), but the change was not marked.

When *Bacillus subtilis* is grown under phosphate limiting conditions the organism synthesizes teichuronic acid in place of normal cell wall teichoic acid (Ellwood and Tempest, 1972). Such a gross change in polysaccharide composition has never been observed for the *Xanthomonads*. Indeed, among the xanthan-producing strains there are hardly any reports of a change in sugar composition in response to environmental factors. However, *X. juglandis* is an exception to the rule (Evans *et al*, 1979). The relative proportions of the two exopolysaccharides synthesized by this particular subspecies changed with the nutrient conditions. In continuous culture, under carbon limitation, a high proportion of the second polysaccharide was formed, but in phosphorus or sulphur deficient media the product was almost exclusively xanthan. When the medium was potassium limited, the material synthesized contained 75% glucose with low levels of mannose, glucuronic acid and rhamnose. After precipitation in acetone, this product was poorly soluble in water and this led Evans and coworkers to speculate that the polymer might consist largely of cellulosic material (in effect the xanthan backbone with a high proportion of the side-chains missing). Their was also some evidence to suggest that the material synthesized in the carbon limited medium might be structurally different, since the culture broth had an exceptionally low viscosity for the amount of xanthan that it was subsequently found to contain.

There is evidence to suggest that the degree of acyl substitution varies during the course of a batch fermentation. Lower levels of both acetyl (Sutherland, 1981a; Tait *et al*, 1986) and pyruvate (Cadmus *et al*,

1978) substituents have been detected for *X. campestris* during the early logarithmic phase of growth and similar patterns have also been observed in other organisms, notably *Rhizobium trifolii* and *R. leguminosarum* (Cadmus *et al*, 1982a). This can be explained by the reduced availability of the acetyl CoA and phosphoenolpyruvate precursors (section 1.5) when the cells are growing rapidly. Since molecules with varying amounts of substituents are produced at different stages in the fermentation process and since neither the acetyl nor the pyruvic acid groups can be added onto the polymer extracellularly (Ielpi *et al*, 1981, 1983), it is likely that the population of xanthan molecules produced in batch culture is fairly heterogeneous. More direct evidence for this comes from Sandford and coworkers (1978) who, by means of serial precipitation in alcohol, were able to separate a batch of normal xanthan into a number of fractions ranging widely in pyruvic acid content. Sutherland (1981b) was also able to divide xanthans from different sources into high and low pyruvate fractions using an affinity chromatography method in which antibodies directed against the pyruvic acid group were bound to the column packing material. If the level of substitution varies as the conditions in the batch fermenter change, then it is reasonable to assume that in continuous culture, where the environmental conditions and growth rate remain stable, the polymer produced will be very much more homogeneous.

The distribution of substituents within the xanthan molecule is unknown. Regular or random arrangements appear equally feasible and no evidence is currently available to favour one above the other. The location of the additional acyl groups in materials carrying more than the stoichiometric amount of acetyl has also still to be determined unequivocally. Preliminary evidence obtained by fast atom bombardment spectroscopy studies on enzymically degraded fragments of the polymer from *X. oryzae* PXO_{61}, suggests that the internal mannose residue is multiply acetylated (Dell and Sutherland - unpublished results) but this may not be true in every case.

3.3 Chemical Characterization of Xanthan

Since the chemical composition of xanthan and, in particular, the level of acetyl and pyruvic acid can vary from one material to another, and since evidence is available to suggest that this can have a profound effect upon the solution and interaction behaviour of the polymer, it is important when undertaking any kind of study to ensure that the material being used has been thoroughly characterized. Over the years a wide range of analytical techniques have been employed to this end.

Sloneker and Jeanes (1962) were the first people to try to determine the sugar composition of xanthan. Their approach was to hydrolyse the polysaccharide, separate the component sugars by paper chromatography, elute the fractions from the paper and then determine the quantity of carbohydrate in each fraction by the phenol-sulphuric acid assay of Dubois *et al* (1956). The sugar ratios they obtained were far from accurate.

Nowadays the neutral sugar components in a xanthan hydrolysate are usually quantitated by GLC of their volatile alditol acetate (Sawardeker *et al*, 1965; Sandford *et al*, 1977; Evans *et al*, 1979; Bradshaw *et al*, 1983) or peracetylated aldonitrile (Whitfield *et al*, 1981; Cadmus *et al*, 1982b) derivatives. The advantages of this type of technique are the high sensitivity afforded by the detectors (eg. flame ionization detector, mass spectrometer) and the accuracy of the integrators used to measure the peak height or peak area. The disadvantages lie principally in the hydrolysis and derivatization steps. These are time consuming and some loss of the component sugars may occur in the process.

To eliminate the need for derivatization, HPLC methods have been developed which can be carried out directly on the neutralized sugar hydrolysate (Tait, 1984; Tait *et al*, 1986; Sutherland and Kennedy, 1986). Though fast and sensitive, such techniques still suffer the limitations on accuracy imposed by incomplete hydrolysis, or the degradation and epimerization of sugars that can occur in the presence of hot acid. Tait (1984) attempted to overcome this problem. He analysed samples of xanthan hydrolysed over a wide range of acid concentrations and time periods, and from the results determined the optimum conditions for release of both glucose and mannose. He then fed the data into a computer regression program and, thereafter, was able to mathematically normalize the results obtained under optimum conditions to 100% recovery.

The glucuronic acid content of the polymer is usually measured separately, either by the carbazole assay of Bitter and Muir (1962) or by the meta-hydroxydiphenyl method of Blumenkrantz and Asboe-Hansen (1973). Lehrfield (1981), however, has described an integrated GLC method for the simultaneous determination of hexoses and uronic acids. In this process the hydrolysed sample is divided into two portions. One of these is analysed by the conventional aldonitrile method which destroys the uronic acids or converts them to compounds that do not co-chromatograph with the neutral sugar derivatives. The second is analysed by a modified alditol acetate procedure. By the normal alditol acetate method, if the glucuronic acid is not first removed by neutralizing the hydrolysate then, on reduction with sodium borohydride, it may be non-quantitatively converted, via the lactone, to the corresponding sugar alditol. This increases the apparent concentration of glucose in the sample. In the modified method the reduction step is repeated three times instead of just once and this quantitatively converts the uronic acid to the alditol. GLC analysis, therefore, reflects the sum of the monosaccharide plus its corresponding uronic acid. The difference between the values obtained by the aldonitrile acetate and the modified alditol acetate methods is a measure of the glucuronic acid present in the polysaccharide.

Like glucuronic acid, the acetyl and pyruvate components of the polymer are usually determined colorimetrically. The hydroxamic acid assay (Hestrin, 1949) is most frequently used to measure the amount of acetyl, whilst for pyruvate the 2,4-dinitrophenylhydrazine (Sloneker and Orentas,

1962a) or the lactate dehydrogenase methods (Duckworth and Yaphe, 1970; Jeanes *et al*, 1976) may be employed. The popularity of such assays lies in their relative simplicity. No expensive apparatus and few costly chemicals are required. However, colorimetric methods do tend to lack sensitivity and specificity. The carbazole assay, for example, suffers from interference by hexoses and by the furfural derivatives of both hexoses and uronic acids which may be formed on acid hydrolysis. Differences in the temperature and pH, as well as other procedural changes, also tend to affect the results.

Other methods, used in the past, for acetyl determination include back titration with acid after the release of acetate under alkaline conditions (Jeanes *et al*, 1961), and a GLC method developed by Turner and Cherniak (1981) for the quantitation of O-acetyl groups as their benzyl acetate derivative. Tait (1984) has described a satisfactory method for measuring the pyruvic acid content by HPLC, and Cheetham and Punruckvong (1985) were able to develop a method for the chemical release of both acyl groups from the polysaccharide and their simultaneous determination by HPLC using a cation exchange resin. Finally ^{1}H-nuclear magnetic resonance has been used on a number of occasions in the past to determine the degree of acylation. The methyl groups of both the acetyl and pyruvic acid substituents give well resolved peaks at δ2.1 ppm and δ1.5 ppm respectively, and these can therefore be used to measure the amount of each component relative to a suitable integration standard. Smith and coworkers (1981) were the first to use ^{1}H-NMR in this context and they did so in conjunction with a wet method. The pyruvate content was first determined using the lactate dehydrogenase assay and this value was then used as an integration standard to determine the amount of O-acetate ester, by comparing the integrals of the two peaks in the ^{1}H-NMR spectrum. Rinaudo *et al* (1983) described a method for the simultaneous determination of both groups using xanthan, partially depolymerized with cellulase to reduce the viscosity and then exchanged several times in deuterium oxide, prior to the recording of the spectrum. This procedure was necessary to observe the anomeric proton of the internal mannose residue which was used as the integration standard in this case. Kennedy *et al* (1984) have used a simpler method in which the levels of acetate and pyruvate were determined relative to an internal quinol integration standard, and which required no preliminary treatment of the xanthan other than dissolution.

3.4 Materials Produced for Use in this Study

As outlined in the General Introduction (section 1.6), the principal aim of this study was to examine the effect of chemical composition, and in particular the degree of acetyl and pyruvate substitution, on the solution behaviour of xanthan, both alone and in combination with polysaccharides of the gluco- and galactomannan type. This chapter deals with the production and purification of the materials used in this study and their characterization by an assortment of analytical techniques.

To generate xanthans of differing chemical structure, a number of approaches are potentially available. The use of a variety of bacterial strains is one possibility, and another is to grow the organisms under a range of different cultural conditions, as illustrated in section 3.2. Alternatively, one could attempt to modify the polymer post-synthetically by the use of chemical or enzymic manipulations. Of these four broad possibilities, three have been adopted here. Firstly a selection of *X. campestris* strains and subspecies, many of which had been studied in the past (eg. Sutherland 1981a) and were known to synthesize quite different materials, were cultured in the laboratory for the production of the xanthan biopolymer. Secondly, of these strains, two were selected for growth under a narrow range of nutrient limiting conditions to test for further alterations in composition. Thirdly, a proportion of the native polymers were treated chemically to deacetylate and/or depyruvylate them.

The vast majority of the materials were produced in batch culture using a simple chemically defined medium of glucose, ammonium chloride and salts (Davidson, 1978). The medium chosen was deficient in sulphur since this had been shown to promote relatively high levels of polysaccharide production both in batch (Tait *et al*, 1986) and continuous culture (Davidson, 1978; Evans *et al*, 1979) and because, in continuous culture at least, there is evidence to suggest that sulphur limitation gives greater cultural stability (Evans *et al*, 1979). A small number of polymers were produced by continuous fermentation, using a similar medium and growth conditions, and two commercial polymers were also included for use in this study.

All of the xanthans were subjected to a rigorous regime of purification. The bulk of the cells were removed by centrifugation and the polymers were then precipitated, at least twice, in cold acetone. In the case of the material from strain 556, as many as five precipitation steps were necessary since this organism produces exceptionally large amounts of carotenoid pigments which tend to discolour the product. Ultracentrifugation was used to remove subcellular debris and the materials were dialysed exhaustively against distilled water to extract low molecular weight contaminants. The polymers were then converted to the sodium form by passage through ion exchange resins, and lyophilized. Initially a proportion of the materials were prepared in the non-salt form using a mixed bed resin (Amberlite MB-1). However, after freeze drying many of these xanthans failed to redissolve satisfactorily in water, even after prolonged heating, and this was therefore abandoned. The gluco- and galactomannans were purified by conventional procedures which included extraction, precipitation, centrifugation and dialysis steps.

The choice of analytical techniques was dictated predominantly by the available apparatus and chemicals. The levels of acetyl and pyruvate substitution were determined by colorimetric assay and the same was true for the glucuronic acid content of the polymers. For the neutral sugar ratio a modification of the HPLC technique of Sutherland and Kennedy

(1986) was used. A neutralized hydrolysate of the polymer was separated on a Gilson HPLC system, using a Brownlee Polypore PB analytical cartridge and a mobile phase of deionized water. The packing material for this cartridge comprises a cross-linked polystyrene base substituted with Pb^{++} ions. Separation involves ligand exchange of the polyol $R(OH)_n$ (ie. the sugar residue) with water molecules in the hydration sphere of the lead cation. The stability of the complex formed with Pb^{++} changes in relation to the availability of favourably oriented -OH groups for co-ordination.

Paper chromatography was used as an indication of purity. The presence of rhamnose and galactose, in amounts too small to be detected by HPLC, can indicate low levels of lipopolysaccharide contamination in the xanthan, whilst ribose in the chromatogram suggests the presence of nucleic acids. Elemental analysis was also used as a purity check. The detection of nitrogen indicates protein and nucleic acid contamination, whilst a high hydrogen to carbon ratio implies the presence of residual water in the freeze dried polymer. Ion measurements were made to ascertain the extent to which the xanthan had been converted to the sodium salt form.

Results and Discussion

3.5 Analysis of Commercial Xanthans, Materials Produced by Different Strains of *X. campestris*, and the Chemically Modified Derivatives of Both Groups.

The three categories of material listed below were prepared in sufficiently large amounts to be used in later physico-chemical studies:

1. The commercial materials Kelzan and Flocon 4800C. Kelzan is an industrial grade gum produced in powdered form by Kelco Co. Inc. (San Diego, California). Flocon 4800C is ostensibly a high pyruvate xanthan, produced by Pfizer Ltd. (Sandwich) as a concentrated broth for use in the oil industry. Both polymers were purified prior to analysis.

2. Polymers produced in the laboratory by batch fermentation of a series of *X. campestris* strains and subspecies, and by continuous fermentation of strain 556.

3. Chemically deacetylated and depyruvylated derivatives of both of the above groups.

All of the materials are listed in table 3.1, together with their chemical composition as determined by colorimetry and HPLC (note that where appropriate, the polymer is referred to by the number of its producing strain preceded by "ps."). The acetyl and pyruvic acid contents

were determined by the hydroxamic acid and 2,4-dinitrophenylhydrazine methods respectively, and the results are expressed as a percentage of the total carbohydrate (phenol-sulphuric acid assay) plus acetyl and pyruvate. The neutral sugar ratio was determined by the HPLC method outlined in section 3.4. The sugars were detected using a differential refractometer and an example of the trace obtained for a typical xanthan is shown in figure 3.4a. The ratio of glucose (rt = 14.57 mins) to mannose (rt = 17.47 mins) was determined from the relative peak heights, taking into account the difference in the refractive index monitored for each sugar. The glucuronic acid content of the polymer was determined by the carbazole assay and is expressed as a percentage of the total carbohydrate only. (It has been related to the level of glucose and mannose by the method outlined in Appendix 1). The carbazole assay was used in preference to the meta-hydroxydiphenyl method despite the fact that the latter is reputedly more specific and therefore more accurate. The reason was that the meta-hydroxydiphenyl method, although it has been used successfully in the past (eg. Bradshaw *et al*, 1983), gave percentage glucuronic acid values that were repeatedly lower than those anticipated on the basis of the known pentasaccharide repeat unit structure. Results in the region of 10% were typical, whereas 20% would be expected. The reason for the persistent underestimate is unknown, but some unidentified defect in the experimental procedure seems the most likely explanation.

The only major difference between the polymers in table 3.1 was in the level of acetyl and pyruvic acid substituents that they carried. Consider the materials produced in the laboratory by batch fermentation. The polymer from wild-type *X. campestris* strain 646 appeared to be the archetypal xanthan molecule - that is, the molecule described by Jansson and coworkers (1975) which carries one acetyl group per side-chain and approximately one pyruvic acid for every other side-chain branch. *X. phaseoli* strain 556, in contrast, produced a low acetyl, high pyruvate polymer with roughly three out of every four side-chains substituted with pyruvic acid. High acetyl and low pyruvate polysaccharides were synthesized by *X. phaseoli* 1128, *X. campestris* XA46 and *X. oryzae* PXO_{61}. The latter is one of a series of strains of *X. oryzae* known to produce xanthans with exceptionally high levels of acetyl substitution (Parry, 1985). The distribution of the acetyl groups within this molecule has been discussed in section 3.2.

The polymers produced by strain 556 in continuous culture carried a similar amount of acetyl and pyruvate to that produced by batch fermentation but it is interesting to note that, at the higher of the two dilution rates studied, the amount of acetyl increased slightly whilst the level of pyruvic acid dropped. A similar phenomenon was described by Tait *et al* (1986).

The composition of commercial Kelzan gum was similar to that of the polymer from strain 646 but with slightly more acetyl. This similarity is not surprising since both materials are purportedly derived from the same

bacterial strain. Studies on Flocon 4800 by the parent company (Philips *et al*, 1982) have shown that the polymer can carry as much as 7.8% pyruvic acid - almost complete side-chain substitution. However repeated analysis of the particular batch used in this research project, indicated a rather more modest 4.9% pyruvylation. With the exception of Flocon 4800C, however, the analytical results obtained for all of the xanthans agreed well with past estimates, both published and unpublished.

Chemical deacetylation and depyruvylation successfully removed most of the acyl groups from the polymers, although in the majority of cases a small proportion still remained.

Knowing the xanthan repeat unit structure, one can anticipate a carbohydrate composition of close to 40% glucose, 40% mannose and 20% glucuronic acid ie. a molar sugar ratio of 2:2:1. All of the materials listed in table 3.1 had essentially these proportions of component sugars. The amount of glucose ranged from 37.7-44.5%, the amount of mannose from 35.9-40.0% and the glucuronic acid content from 17.5-24.7%, but all of the polymers did appear to be of the conventional xanthan type.

It is interesting to note that in the vast majority of cases, a significant excess of glucose over mannose was detected. This phenomenon has been observed in the past (eg. Davidson, 1978; Evans *et al*, 1979; Sutherland, 1981a; Whitfield *et al*, 1981), but the reason for it is unknown. The unsatisfactory nature of the hydrolysis step prior to HPLC analysis may provide an explanation. The conditions used to treat the polymer (0.25M sulphuric acid at 100°C, for 18 hours) were selected to give good acid hydrolysis without producing significant degradation, but they had never actually been optimized. Indeed, even if they had been, there is no guarantee that the optimum for one polymer would be the same as for another. It is possible, therefore, that incomplete hydrolysis or, alternatively, degradation of the component sugars after hydrolysis could account for the excess of glucose. The α-(1$\rightarrow$2)-linkage between the internal mannose residue and the anomeric carbon of the glucuronic acid is known to be particularly resistant to acid hydrolysis and it is possible that some aldobiuronic acid remained undegraded within the sample. This may have manifested itself as one of the smaller peaks of unidentified material observed occasionally in the HPLC chromatograms. In the presence of hot acid, hexoses can undergo a whole series of different degradation reactions, many of which have still to be identified. Any preferential degradation of mannose relative to glucose has not been demonstrated but the yellowing of the xanthan samples upon heating provides irrefutable evidence that some degradation did occur. Tait (1984) has also suggested that epimerization of mannose to glucose could be a minor contributing factor. Of course one cannot discount the possibility that the glucose to mannose ratio is a genuine reflection of some structural non-uniformity within the molecule. Sutherland (1984) suggested that this might be the case after studying the degradation of disordered xanthan by fungal cellulases. He found that upon treatment with enzyme, the xanthan was

broken down into a series of fragments of different sizes - D-glucose, cellobiose and a variety of oligosaccharides. The range of products, he suggested, was due to the presence of preferential sites of cleavage for the cellulase along the xanthan backbone, and he further proposed that these sites could be regions of the polysaccharide chain from which one or more of the side-branches was missing.

3.6 Chemical Modification of Xanthans

The problem with comparing polymers from different bacterial strains or, for that matter, from the same bacterial strain but produced under different cultural conditions, is that the assayable differences in composition, that is the sugar ratio and the levels of acetyl and pyruvate substitution, may not be the only ones to occur. Alterations in the fine structure and in the molecular weight could also arise, and whilst these are not readily detectable by standard analytical techniques, they could have a marked affect upon the solution behaviour of the polymer. In principal, therefore, it is preferable to compare materials that have been derived from a single bacterial source by chemical modification. Chemically modified polymers should be identical to the parent material in all other respects. For this reason a series of deacetylated and depyruvylated xanthans were prepared (Tables 3.1 and 3.5). Deacetylation was achieved by treating a 0.25% solution of the polysaccharide with 0.1M ammonium hydroxide at 60°C for 1 hour. Depyruvylation was by hydrolysis of a 0.5% polymer solution with 5mM TFA at 100°C for 90 minutes (Bradshaw *et al*, 1983). The conditions for both types of chemical modification were fairly harsh and although no evidence has been produced in the past to suggest the occurrence of unwanted secondary reactions, and in particular depolymerization, it was deemed necessary to try to establish this unequivocally before attempting to compare "like with like". To assess whether any degradation had occurred, three types of approach were used. The first was to compare the sugar ratio of the derivative with that of the native polymer. Table 3.5 shows no significant change in any of the xanthans after treatment, with the possible exception of the material from strain 556. Depyruvylated ps.556 had slightly less mannose than its parent polymer and it may therefore conceivably have lost a small proportion of the terminal side-chain residues. The second approach, which will be discussed in Chapter 5, was to compare the intrinsic viscosity of polymers under conditions of uniform ionic strength. This should indicate any marked changes in molecular weight. The third was to look for the production of dialysable low molecular weight materials, detectable by paper chromatography. Deacetylated and depyruvylated ps.646 and Flocon 4800C were tested in this manner. Aliquots of the reaction mixture were dialysed repeatedly against small volumes of distilled water and the dialysates were then pooled, concentrated and analysed by descending paper chromatography. The dialysates from both of the deacetylated polymers gave an almost clean chromatogram. An intense spot with an R_{glc} value of 1.47 will have been the acetate group released from the polymer or, less probably, acetylated mannose. Very faint traces of material at R_{glc} values

of 0.14 and 0.27 were the only possible degradation products and may have been aldobiuronic acid or oligosaccharides of some sort. In contrast, the dialysates from the depyruvylation reaction mixtures provided quite strong evidence for degradation. No monosaccharides were detected and an intense spot at R_{glc}, 1.45 will almost certainly have been pyruvate or pyruvylated mannose. However, unidentified spots of reasonable intensity were detected at R_{glc} values of 0.25, 0.63, 0.76 and 1.05. The 0.25 spot was probably aldobiuronic acid and the spots at 0.63 and 0.76 may have been disaccharides of some sort; one will probably have been cellobiose. This evidence suggests that the deacetylation reaction produced relatively little degradation, whilst depyruvylation produced quite a lot. It is worth bearing in mind though, that one break in the cellulosic backbone is sufficient to reduce the average molecular weight of a polymer by half, but in the process no low molecular weight product need have been generated.

As well as deacetylating and depyruvylating the polymers, an attempt was made to raise the acetyl content by random acetylation of the hydroxyl groups in ps.1128. The polymer was treated with glacial acetic acid, acetic anhydride and perchloric acid according to the method of Schweiger (1962). This method had been used successfully in the past to acetylate alginic acid. However, with xanthan it gave a totally insoluble and therefore unusable product.

3.7 Production of Xanthan Under Nutrient Limiting Conditions

It is clear from the studies outlined in section 3.2, that growth of *X. campestris* and its subspecies under nutrient limiting conditions can, in some cases, have a profound effect upon the composition of the EPS produced. The same is true in both batch and continuous culture. In the early days of this research project, therefore, the use of nutrient limiting cultural conditions was considered a potentially promising way of synthesizing structurally variant xanthan types. Davidson (1978) had demonstrated that growth of *X. campestris* in continuous culture, using a magnesium or phosphate deficient medium, lead to a decrease in the pyruvic acid content of the polymer and Evans and coworkers (1979), on culturing *X. juglandis* in a potassium limited environment, had obtained a polymer with apparently significantly fewer side-chains. An attempt was therefore made to study the effects of magnesium, phosphate and potassium limitation on the composition of xanthan produced by strains of *X. campestris* and *X. phaseoli* in batch culture instead. In addition, X.*campestris* was grown under potassium limiting conditions in continuous culture and *X. phaseoli* was grown in a low carbon medium. Evans *et al* had demonstrated that *X. juglandis* when grown under conditions of carbon limitation produced a polymer with an exceptionally low viscosity.

Batch Fermentation Experiment

X. campestris strain 646 and *X. phaseoli* strain 556 were grown in 50 ml batch cultures under a range of nutrient conditions. The complete medium as defined by Davidson (table 2.2) was used as a control and a series of other media containing reduced levels of magnesium, potassium and phosphate salts were also employed (see table 2.2c). The cultures were grown in 250 ml conical flasks and were incubated for 4-6 days, at 30°C, on an orbital shaker. The xanthan was harvested from the culture supernatant by precipitation in cold acetone. Purification was by ultracentrifugation and dialysis, and the material was then lyophilized prior to analysis.

Before drawing any conclusions about the effects of nutrient limitation on the xanthans produced by batch fermentation, it was important to ascertain that the cultures were indeed growth limited. This was done in two ways. Firstly, cells harvested from the culture in the stationary phase were freeze dried and weighed so that the yields from the nutrient deficient media could be compared with that of the control. Secondly, the effect on growth of adding more of the "limiting" nutrient to the stationary phase culture was assessed. The optical density of duplicate cultures was measured at 520 nm and more of the magnesium, potassium or phosphate salt was then added. After a further two days incubation the optical density was determined again. An increase in absorbance was taken to mean that at the original stationary phase, growth was restricted by exhaustion of the particular test nutrient. The dry weights of the cells and the optical density measurements are shown in table 3.2. For those cultures grown in the presence of reduced levels of magnesium, both the dry weight and the optical density values were comparable with those of the control experiments and there was no significant increase in optical density after the addition of more magnesium sulphate. Magnesium did not therefore appear to be the limiting factor. In contrast, in both the potassium and phosphate deficient cultures, the dry weight and the optical density were very much lower than those of the control, and addition of more of the potassium or phosphate salt caused a marked increase in the absorbance reading. Hence these cultures were quite clearly nutrient limited. Strain 556 appeared to be inhibited rather more than strain 646 by the nutrient limiting conditions since the dry weight and optical density readings were lower.

Although in absolute terms a reduction in cell growth was observed in all of the potassium and phosphate limited cultures, there was no apparent graduation in the amount of growth as the concentration of the limiting nutrient in the original medium increased. This is both surprising and difficult to explain. One contributing factor may have been the lack of homogeneity of the culture. This would undoubtedly have affected the optical density reading, if not the dry weight, and would explain why, for example, the addition of more magnesium sulphate produced

a slight fall in the optical density of two of the cultures. It would also explain why addition of equal amounts of a given nutrient did not produce a similar increase in the optical density.

The low cell yields from the potassium and phosphate limited cultures were reflected in a similarly low yield of xanthan, typically in the region of 20-90 mg. In most cases, therefore, insufficient material was available for HPLC analysis. Thus, whilst the amounts of acetyl, pyruvate and glucuronic acid were determined by the usual colorimetric techniques, the glucose content was measured using the glucose oxidase assay instead of HPLC. The amount of mannose was not determined. Table 3.3 shows the results.

If one compares the amounts of glucose and glucuronic acid measured for these polymers with the results in tables 3.1 and 3.5, their unsatisfactory nature becomes immediately obvious. The glucose content was generally well below the anticipated value of 40% (as much as 18% lower for one particular sample) whilst, in most cases, the amount of glucuronic acid was higher than the 20% expected. In molar terms this is equivalent to a glucose to glucuronic acid ratio ranging from 2.00:1.26 to as high as 2.00:2.04. These results can hardly be genuine. It is almost inconceivable that polymers produced by the same strain of *Xanthomonas*, under almost identical cultural conditions, could show so much more variability than materials produced by a range of different bacterial strains. Their was also no consistent pattern between the change in the sugar ratio and the nutrient composition of the medium, and the amount of glucuronic acid relative to glucose was significantly higher than that for the same native materials produced under similar cultural conditions, in the larger scale batch fermentations. In fact, the ratios of glucuronic acid to glucose were higher for the samples of ps.646 and ps.556 produced in this experiment than for any other material prepared in this study.

The reasons for the anomalous results lie probably in the analytical procedures. In the case of the glucose oxidase assay, assuming that the enzyme reactions were allowed to run to completion and there is no reason to believe that they were not, the low glucose values were probably the result of incomplete acid hydrolysis. Prior to analysis, 0.5% solutions of the polysaccharide were treated with 0.5M TFA at 100°C, for 16 hours, in sealed glass ampoules, in order to release the free sugar. A small amount of precipitate was observed in the tubes after heating and it is possible that this was insoluble cellulosic backbone material which had precipitated out after removal of the trisaccharide side-chains. A variable amount of precipitation would explain why the results were both low and erratic. With the glucuronic acid assay, the tendency to overestimate the amount of sugar may have been due to interference by other materials. The carbazole assay is known to be particularly prone to interference and the polymers prepared in this experiment were purified less rigorously than those produced in the larger scale batch and continuous cultures. A higher level of contamination was therefore likely.

This was indicated by the cream rather than white colouration of the materials and by the presence of traces of rhamnose and ribose in the paper chromatograms, suggesting lipopolysaccharide and nucleic acid contamination. Residual cell debris may therefore have been responsible for raising the apparent uronic acid content of the materials. Interference with the phenol-sulphuric acid assay against which the percentage of sugars was determined, is also a possibility.

Looking again at table 3.3, one can see that the acetyl and pyruvate contents of the polymers, like the sugar ratios, varied a lot but, at least here, the values fell within acceptable limits. In the case of ps.556 no acetyl was detected and the amount of pyruvic acid appeared to vary from 4.5-8.2%, as against the 6.0% measured for the normal native batch culture material. With ps.646 both the acetyl and pyruvate values were higher than those recorded previously for the native polymer. Again there was no discernible correlation between the degree of acyl substitution and the nutrient composition of the media.

It is quite clear that the results obtained in this experiment, for whatever reason, are wholly unreliable and that no real conclusions can be drawn from them about the effects of nutrient limitation on the structure of xanthan produced in batch culture. It is also likely that had this experiment been repeated, the results would have been entirely different and there was, therefore, no justification for producing either material on a larger scale under any of the nutrient conditions tested. Since this experiment was performed Tait and coworkers (1986) have published data showing no change in the composition of xanthan produced by a streptomycin resistant variant of *X. campestris* grown in magnesium and phosphate limited batch cultures. This supports the view that many of the differences recorded here were simply artifacts of the experimental procedures used.

Continuous Fermentation Experiments

Xanthans were produced in continuous culture under both potassium and carbon limiting conditions. Strain 646 was grown in the potassium limited medium at two different dilution rates, 0.024/hr and 0.12/hr, whilst strain 556 was grown in the carbon limited medium at a dilution rate of 0.051/hr. The materials were harvested, purified and analysed in the usual manner. The composition of the polymers is given in table 3.4. None of the polysaccharides showed any significant deviation from the norm in terms of sugar ratio and there was certainly no indication of the loss of side-chains observed by Evans and coworkers in their studies on *X. juglandis*. The acetyl content of the ps.646 samples was rather higher than that of the same material produced in batch culture but the pyruvate content was much the same. Interestingly, as noted earlier for ps.556 produced in continuous culture and by Tait *et al* in 1986, more acetyl and less pyruvate was present in the material produced at the higher dilution rate. Sample ps.556 from the carbon limited medium contained slightly more

acetyl and slightly less pyruvic acid than its batch equivalent and had a similar composition to the polymers produced formerly by strain 556 in continuous culture (table 3.1). There was no sign of the reduced viscosity reported by Evans for *X. juglandis*.

None of the materials produced in this rather limited investigation of the effects of nutrient deficiency on the composition of the xanthan polymer showed any major and reliable differences. What the study did show, however, was that as an approach, the use of different cultural conditions could be highly labour intensive and at the end of the day might yield little in the way of useful materials. Since, therefore, the main aim of this research project was to look at the effects of structure upon solution behaviour and not the effects of nutrient limitation upon structure, and as there were clearly more efficient ways of generating the range of materials required, this type of experiment was abandoned.

3.8 Analysis of EPS Produced by Mutant Strains of *X. campestris*

All of the *Xanthomonads* studied so far have produced EPS with essentially the same composition as the xanthan biopolymer. However, mutant strains of bacteria are known which synthesize polysaccharide of a radically different type, and a number of these strains were also cultured in the laboratory. The organisms grown were all derived originally from wild-type *X. campestris* strain 646, either by chemical mutagenesis or by treatment with γ-radiation (see table 2.1). They were grown in batch culture and the materials produced were recovered, purified and analysed by the usual range of colorimetric and chromatographic techniques. The results are shown in tables 3.6a and 3.6b.

The strains tested may be divided into two broad groups. *X. campestris* 2BD and BD9A were morphologically similar to the wild-type strain but synthesized what appeared to be an incomplete xanthan-type polymer. Strains 646E, 646KR and MT16.8, which are referred to collectively as crenated mutants, had an altered colonial morphology as illustrated in figure 3.1 and synthesized EPS with a quite different composition.

Looking at tables 3.5 and 3.6, one can see that the materials from strains 2BD and BD9A consisted of the same three sugar residues as the xanthan polymer, but that the ratios of glucose:mannose:glucuronic acid were closer to 2:1:1 than to the conventional 2:2:1. This, combined with the very low pyruvic acid content of the polymers, suggests that they were structurally similar to xanthan but had lost the terminal mannose residue from the majority of trisaccharide side-chains. The mutation, therefore, was most probably located in the gene for the specific transferase adding the terminal mannose to the repeat unit whilst still attached to the carrier lipid (section 1.5). Alternatively, it could have been a regulatory mutation facilitating polymerization of the repeat unit prior to the addition of the terminal sugar residue.

That the EPS from the crenated mutants was substantially different to conventional xanthan became obvious as soon as the culture supernatant was precipitated in acetone. Material from the wild-type strain precipitated in the organic solvent as a thick gel which could be wound around a stirring rod. The polymer from the crenated mutants, however, formed a fine, almost granular precipitate which could not be recovered by centrifugation and had instead to be allowed to settle overnight, before syphoning off the water-acetone mixture.

The EPS yield from the crenated mutants was very much lower than for the wild-type strain and, in the case of ps.646KR, the polymer on ultracentrifugation separated into both a soluble and an insoluble gel-like fraction. The former was purified by conventional procedures, the latter by phenol-extraction, and the two were analysed separately.

Analysis by paper chromatography, colorimetry and HPLC showed that in addition to glucose, mannose and glucuronic acid, ps.646E carried considerable quantities of galactose and rhamnose, whilst ps.MT16.8 contained a lot of galactose but only trace amounts of the rhamnose sugar. The soluble fraction from strain 646KR consisted of glucose, galactose and glucuronic acid but contained no mannose or rhamnose. Acetyl and pyruvic acid substituents were detected in varying amounts in all of the polymers.

The results obtained by HPLC agreed well with those from paper chromatography except with respect to the rhamnose content of ps.646E and ps.MT16.8. Rhamnose appeared to be present in the paper chromatograms but was not detected in the HPLC traces. The reason for this becomes obvious when one examines the HPLC chromatogram for ps.646E. For normal xanthan (figure 3.4a) the resolution of the glucose and mannose peaks was quite good, enabling the sugars to be quantitated accurately. However, the retention times for both galactose and rhamnose lay between those of the glucose and mannose peaks, so that when three or more sugars were present in the hydrolysate, separation was really very poor. Consequently, any rhamnose present in the samples may have been swamped by the other sugars and did not register as a separate peak. The poor resolution meant that the sugar contents of ps.646E and ps.MT16.8 could not be calculated from the peak heights and for ps.646KR (soluble fraction; figure 3.4c) they could only be determined approximately. Because of the lack of solubility, the insoluble fraction from strain 646KR could not be analysed by any of the usual quantitative techniques. Nevertheless, partial acid hydrolysis followed by paper chromatography suggested that it consisted of glucose, galactose and glucuronic acid, like the soluble fraction, but contained, in addition, trace amounts of rhamnose.

The exocellular polysaccharides from strains 646E and 646KR have been analysed in the past by Whitfield and coworkers (1981) using GLC of their peracetylated aldonitrile derivatives. The information gained by these authors indicated that both of the polymers consisted predominantly of glucose and galactose, with lesser amounts of mannose, rhamnose and

uronic acid (table 3.7a). It also suggested, however, that the composition varied from one batch to another even when the strain and cultural conditions were identical. There was no evidence for a separate soluble and insoluble fraction for ps.646KR.

Interpretation of this data is difficult, particularly in light of the apparent random variation in composition described by Whitfield *et al* and implied by the difference in results between their study and this. One relevant factor which should be taken into account is the difference in the lipopolysaccharide constitution also observed in the crenated mutants (table 3.7b). Whitfield *et al* (1981) noted that the carbohydrate component of the lipopolysaccharide in the wild-type strain consisted largely of glucose with only tiny amounts of galactose and rhamnose present, but in the crenated mutants galactose and rhamnose formed the major components. Sutherland and Kennedy (1986) found a higher level of galactose and rhamnose in the wild-type lipopolysaccharide but noted a similar increase in the amount of both sugars in the mutant strain *X. campestris* 6D. The biosynthetic pathways for xanthan and for the carbohydrate component of the lipopolysaccharide share a number of features in common. The repeat unit for both is built up from sugar nucleotide precursors by sequential transfer of sugar residues from the nucleotides to a common carrier lipid located in the cytoplasmic membrane. The repeat unit is then added onto the growing polysaccharide chain by some as yet unidentified mechanism. The alteration of both polymers implies that the mutation must affect some part of the biosynthetic mechanism common to both products. It also seems likely that the mutation lies within a gene involved in regulating the biosynthetic pathways, since the variation observed between batches could be the result of some loss of control over the incorporation of sugars into the polysaccharides.

3.9 Analysis of Gluco- and Galactomannans

The compositions of the gluco- and galactomannans used in this study were determined by HPLC, using the same procedure as for the bacterial polysaccharides. The results are given in table 3.8, and HPLC chromatograms for guar gum and konjac mannan are shown in figures 3.4d and 3.4e respectively.

As one would anticipate, the galactomannans consisted solely of galactose and mannose. The galactose content of the guar gum was 35.7%. This compares well with values of 36-40% attained by McCleary *et al* (1985), using both an enzymic assay and GLC of the alditol acetate derivatives, and 33% achieved by Tako and Nakamura (1985) using an HPLC method. The locust bean gum contained 19% galactose. Again, this is in reasonable agreement with the 21-23% range reported by McCleary *et al* (1985) and 18.5% given by Tako and Nakamura (1984). Locust bean gum consists of both a hot water and a cold water soluble fraction, the latter carrying more galactose side-chains than the former (eg. McCleary *et al*, 1985). The sample prepared in this study was extracted in hot water and

should therefore have contained both fractions. However, during the purification process the polymer was ultracentrifuged for 90 minutes at only 40°C and it is possible that some of the hot water soluble fraction precipitated out.

The konjac mannan comprised 39.3% glucose and 60.7% mannose - a mannose to glucose ratio of 1.54:1.00. A similar result was reported by Shimahara *et al* (1975a) who, after acid hydrolysis and paper chromatography, assayed the mannose and glucose content of the polymer and obtained a molar ratio of 1.60:1.00. A value of 4.2% acetyl, determined by the hydroxamic acid assay, compares favourably with published values of 3.7% (Dea *et al*, 1977), 3.94% and 4.09% (Cheetham and Punruckvong, 1985).

3.10 Elemental Analysis and Paper Chromatography Studies

Although all of the polymers used in the course of this research project were subjected to a rigorous regime of purification, it is possible that some contamination still remained. The most likely contaminants for a material synthesized in bacterial culture would be other cell products, particularly proteins, nucleic acids and lipopolysaccharide, but some water may also have remained bound to the hygroscopic xanthan molecule, even after exhaustive freeze drying. Two approaches, therefore, were used to assess the purity of the xanthan polysaccharides. The first was elemental analysis. The second was paper chromatography.

Nitrogen was measured as an indication of the level of protein and nucleic acid contamination. In each case (table 3.9) the amount was found to be on or below the limit of resolution of the instrument ie. 0.2%. Assuming 16% nitrogen in protein (Tait *et al*, 1986) and assuming also that the nitrogen in the samples was derived mainly from cell surface and extracellular proteins (eg. cellulases and other enzymes secreted from the cell), 0.2% nitrogen would be equivalent to 1.2% contaminating protein. Hence, the amount of protein and nucleic acid present in the samples was very low. This was confirmed by paper chromatography. The presence of nucleic acids would be indicated by the appearance of ribose in the paper chromatogram. In a proportion of the polymers faint traces of a material with an R_{glc} value of 1.25 were detected, but although this may have been ribose, the amount was small enough to preclude any significant degree of contamination. Flocon 4800C and the materials produced by strains 646 and 556 in continuous culture, contained trace amounts of rhamnose, detectable by paper chromatography but not by HPLC. This suggests a very low level of lipopolysaccharide contamination in these samples.

Theoretically the sodium salt of xanthan should contain 42.22-43.24% carbon and 5.10-5.55% hydrogen, depending on the number of side-chain substituents carried (see table 3.10). Elemental analysis of the materials (table 3.9), in contrast, gave values of 35.06-39.82% carbon and 5.48-6.21% hydrogen. The low carbon values and excess hydrogen can

probably be attributed to the presence of residual water in the freeze dried materials. It is quite usual for polymers to retain some water after lyophilization and values of 10%, by weight, are considered typical. However, even assuming that all of the extra hydrogen were present in water, the amount in these samples would still be well below 10%.

Interestingly the quantities of carbon and hydrogen measured for the gluco- and galactomannans were both below the values anticipated on the basis of the known structure (see table 3.11). This suggests some sort of contamination, but it is difficult to envisage quite what the impurity might be. There was no excess of hydrogen to indicate bound water and too little nitrogen to suggest the presence of other organic materials such as proteins and nucleic acids. A high salt content also seems unlikely since these polymers carry no charged groups.

The xanthans were converted to the sodium form by passage through ion exchange resins. To determine whether or not all of the charged groups on the polymers had picked up a sodium ion, the sodium contents were measured and compared with the anticipated values (table 3.10). In every case the actual value was found to be well below the amount predicted. For example, the sodium salt of a polymer with no pyruvic acid should still carry one sodium ion per repeat unit, bound to the carboxyl group of the glucuronic acid residue. This is equivalent to 2.59-2.72% of the total weight, depending on the amount of acetyl also present. All of the low pyruvate polymers tested (eg. ps.1128, depyruvylated ps.646, depyruvylated ps.556, depyruvylated Flocon 4800C) carried significantly less sodium than this. A typical wild-type xanthan carrying one acetyl group per repeat unit and one pyruvic acid residue for every two repeat units, should contain theoretically 3.69% sodium. Sample ps.646, however, which carried close to the standard complement of acetyl and pyruvate, was found to carry only 2.99% sodium, whilst Kelzan which was similar in structure, contained only 2.41%. A drop in the sodium content was observed on depyruvylation, as one would expect, but this was not in proportion to the fall in pyruvic acid substitution. No marked change would be expected on deacetylation but with ps.1128 the amount of sodium fell dramatically. In other words, whilst the polymers were converted to predominantly the sodium form, a proportion of the charged groups, which varied from one material to another, either remained unsubstituted or carried a metal ion other than sodium.

To indicate whether or not other ions were present in substantial amounts, the levels of potassium and calcium in the samples were determined. Small quantities of each ion were found to be present but the amounts did not vary in relation to the level of charge. This was to be expected since the assay used was only accurate at concentrations of greater than 0.3% and for all but one of the samples tested, the results were below the limit of resolution.

Why the polymers were not converted completely to the sodium salt form is uncertain. Experimentally, overloading the column or running the polymer solutions through too rapidly could have accounted for the incomplete ion exchange, but neither seems likely to have occurred. Incomplete ion exchange would explain the presence of potassium and calcium ions in the samples since some ions still present from the culture medium will not have been removed. However, in addition, ions may have been contributed by the resin itself, which was not of the purest grade available, or may have come from the distilled water, against which the polymers were dialysed prior to lyophilization.

In conclusion, therefore, it appears that the xanthan samples prepared for use in this study were extremely pure but that conversion to the sodium form was only partially successful, leaving a small proportion of other ions still bound to the polymer.

Table 3.1: Chemical composition of (a) the commercial materials used in this study, (b) xanthans produced by a range of different strains of *X. campestris* and (c) chemically modified derivatives of groups (a) and (b).

Polymer	% Glc	% Man	% GlcA	% Ac	%Pyr
Flocon 4800C	41.7	37.1	21.2	2.0	4.9
DA Flocon 4800C	41.4	36.7	21.9	0	4.9
DP Flocon 4800C	42.8	36.8	20.4	2.7	1.0
DAP Flocon 4800C	44.5	38.0	17.5	0	0.9
Kelzan	40.8	36.4	22.8	6.6	4.8
ps.646	40.2	36.0	23.8	4.5	4.4
DA ps.646	38.3	37.6	24.1	1.3	3.6
DP ps.646	39.6	36.3	24.1	4.4	0.6
DAP ps.646	39.2	36.1	24.7	1.0	0.6
ps.556	40.5	38.7	20.8	1.6	6.0
ps.556^{a1}	39.4	35.9	24.7	1.3	5.2
ps.556^{a2}	40.0	36.9	23.1	2.2	4.9
DP ps.556	43.8	36.1	20.1	1.1	1.0
ps.XA46	38.3	40.0	21.7	4.6	0.3
ps.1128	40.3	36.7	23.0	7.7	1.7
DA ps.1128 (Batch 1)	37.4	39.2	23.4	1.6	1.3
DA ps.1128 (Batch 2)	37.8	39.1	23.1	1.5	1.3
ps.PXO$_{61}$	40.6	37.7	21.7	14.3	0.3
DA ps.PXO$_{61}$	37.7	39.8	22.5	2.3	0.8

DA Deacetylated material.
DP Depyruvylated material.
DAP Deacetylated and depyruvylated material.
a1 Polymer produced by strain 556 in continuous culture at a dilution rate of 0.024/hr.
a2 Polymer produced by strain 556 in continuous culture at a dilution rate of 0.09/hr.

Table 3.2: Effect of nutrient deficient conditions on the growth of *X. campestris* strain 646 and *X. phaseoli* strain 556 in batch culture.

Nutrient Conditions	Strain 646			Strain 556		
	Dry Wt	OD_{520}	OD_{520}[a]	Dry Wt	OD_{520}	OD_{520}[a]
Complete medium	0.146	>	>	0.187	>	>
Magnesium Limitation $MgSO_4.7H_2O$:						
0.02 g/l	0.148	1.946	2.026	0.189	2.038	>
0.04 g/l	0.149	2.040	2.070	0.173	>	>
0.06 g/l	0.140	2.075	2.062	0.190	2.051	2.038
Potassium Limitation KCl:						
0.03 g/l	0.026	0.930	1.108	0.012	0.432	0.574
0.06 g/l	0.024	0.818	1.136	0.010	0.300	0.511
0.09 g/l	0.023	0.884	1.159	0.007	0.381	0.610
Phosphate Limitation NaH_2PO_4:						
0.2 g/l	0.026	0.996	1.333	0.002	0.110	0.291
0.4 g/l	0.027	1.176	1.511	0.004	0.174	0.509
0.6 g/l	0.028	1.124	1.358	0.004	0.180	0.420

a After addition of a further 0.08 g/l $MgSO_4.7H_2O$, 0.12 g/l KCl or 0.8 g/l NaH_2PO_4 and 48 hours incubation.

> OD is greater than the limit of resolution of the spectrophotometer.

Table 3.3: Chemical composition of materials produced by strains 646 and 556 in batch culture under nutrient deficient conditions.

Strain	Nutrient Conditions	% Glc	% GlcA	Molar Ratio Glc : GlcA	% Ac	% Pyr
646	Complete Medium	30.8	27.1	2.00 : 1.63	5.6	5.2
	Magnesium Limitation $MgSO_4.7H_2O$:					
	0.02 g/l	30.6	27.4	2.00 : 1.66	6.4	4.7
	0.04 g/l	34.0	30.8	2.00 : 1.66	6.1	6.0
	0.06 g/l	30.1	33.1	2.00 : 2.04	5.8	7.6
	Potassium Limitation KCl:					
	0.03 g/l	36.1	31.6	2.00 : 1.62	5.9	5.0
	0.06 g/l	38.0	29.4	2.00 : 1.44	7.3	5.8
	0.09 g/l	28.3	27.0	2.00 : 1.77	5.8	5.0
	Phosphate Limitation NaH_2PO_4:					
	0.2 g/l	32.3	27.4	2.00 : 1.57	5.7	5.1
	0.4 g/l	28.3	27.6	2.00 : 1.81	5.7	4.5
	0.6 g/l	28.7	25.4	2.00 : 1.64	6.3	4.9
556	Complete Medium	35.6	29.2	2.00 : 1.52	0	8.2
	Magnesium Limitation $MgSO_4.7H_2O$:					
	0.02 g/l	33.7	29.7	2.00 : 1.64	0	7.4
	0.04 g/l	25.6	20.4	2.00 : 1.48	0	5.6
	0.06 g/l	34.5	25.9	2.00 : 1.39	0	7.8

Table 3.3: continued.

Strain	Nutrient Conditions	% Glc	% GlcA	Molar Ratio Glc : GlcA	% Ac	% Pyr
556	Potassium Limitation KCl:					
	0.03 g/l	22.3	18.5	2.00 : 1.54	0	4.5
	0.06 g/l	31.4	21.3	2.00 : 1.26	0	5.1
	0.09 g/l	32.7	25.3	2.00 : 1.44	0	6.0
	Phosphate Limitation NaH_2PO_4:					
	0.2 g/l	28.9	22.7	2.00 : 1.46	0	4.8
	0.4 g/l	35.5	25.2	2.00 : 1.32	0	5.9
	0.6 g/l	33.7	30.6	2.00 : 1.68	0	6.6

Table 3.4: Chemical composition of materials produced by strains 646 and 556 in continuous culture under nutrient limiting conditions.

Producing Strain and Cultural Conditions	% Glc	% Man	% GlcA	% Ac	%Pyr
Strain 646 Potassium Limitation Dilution Rate:					
0.024/hr	39.6	35.9	24.5	6.4	4.6
0.120/hr	39.8	35.7	24.5	7.4	3.6
Strain 556 Carbon Limitation Dilution Rate:					
0.051/hr	39.6	38.7	21.7	2.1	5.6

Table 3.5: Molar sugar ratios of polymers.

Polymer	Molar Sugar Ratio		
	Glc	Man	GlcA
Flocon 4800C	2.00	1.77	0.94
DA Flocon 4800C	2.00	1.77	0.98
DP Flocon 4800C	2.00	1.71	0.88
DAP Flocon 4800C	2.00	1.71	0.73
Kelzan	2.00	1.78	1.03
ps.646	2.00	1.80	1.10
DA ps.646	2.00	1.96	1.17
DP ps.646	2.00	1.82	1.13
DAP ps.646	2.00	1.84	1.17
ps.646[b1]	2.00	1.81	1.15
ps.646[b2]	2.00	1.79	1.14
ps.556	2.00	1.91	0.95
ps.556[a1]	2.00	1.82	1.16
ps.556[a2]	2.00	1.85	1.07
DP ps.556	2.00	1.65	0.85
ps.556[a3]	2.00	1.95	1.02
ps.XA46	2.00	2.09	1.05
ps.1128	2.00	1.82	1.06
DA ps.1128 (Batch 1)	2.00	2.10	1.17
DA ps.1128 (Batch 2)	2.00	2.07	1.13
ps.PXO_{61}	2.00	1.86	0.99
DA ps.PXO_{61}	2.00	2.11	1.11
ps.BD9A	2.00	0.80	0.77
ps.2BD	2.00	1.32	1.09

a1 As for table 3.1.
a2 As for table 3.1.
a3 Polymer produced by strain 556 in continuous culture under carbon limiting conditions and at a dilution rate of 0.051/hr.
b1 Polymer produced by strain 646 in continuous culture under conditions of potassium limitation and at a dilution rate of 0.024/hr.
b2 Polymer produced by strain 646 in continuous culture under conditions of potassium limitation and at a dilution rate of 0.120/hr.

Table 3.6: Chemical composition of materials produced by mutant strains of *X. campestris*.

a) Analysis by paper chromatography

EPS from Strain:	Glc	Man	GlcA	Gal	Rha
ps.BD9A	+	+	+	Ft	-
ps.2BD	+	+	+	-	-
ps.646E	+	+	Ft	+	+
ps.646KR (soluble)	+	-	Ft	+	-
ps.646KR (insoluble)	+	-	+	+	Ft
ps.MT16.8	+	+	Ft	+	Ft

Ft Faint traces of the sugar were detectable.

b) Analysis by HPLC and colorimetric assays

EPS from Strain:	% Glc	% Man	% GlcA	% Gal	% Rha	% Ac	%Pyr
ps.BD9A	55.1	22.0	22.9	ND	ND	2.3	2.0
ps.2BD	44.4	29.4	26.2	ND	ND	6.5	1.6
ps.646E	++	++	17.7	++	ND	5.1	3.1
ps.646KR (soluble)	~35.2	ND	27.2	~37.6	ND	3.5	5.4
ps.646KR (insoluble)	UD	UD	UD	UD	UD	UD	UD
ps.MT16.8	++	++	22.8	+	ND	1.2	1.6

ND None detected.
UD Undetermined.

Table 3.7: Composition of polymers from wild-type *X. campestris* 646 and its crenated mutants (Whitfield *et al*, 1981).

a) Exopolysaccharide

Strain	Percentage Sugar Composition				
	Glc	Man	Uronic Acid	Gal	Rha
646	42	38	20	0	0
646E	37	12	9	28	14
646KR	29	21	11	27	12

b) Lipopolysaccharide

Strain	Percentage Sugar Composition				
	Glc	Man	Gal	Rha	Rib
646	94.6	0	3.9	1.6	Trace
646E	8.3	0	29.6	53.5	3.2
646E (soluble)*	8.9	4.7	27.7	53.4	1.6
646KR	8.3	Trace	29.6	53.5	3.2
	5.3	Trace	31.4	52.2	0.9

* Low molecular weight polysaccharide not sedimented by centrifuging an aqueous phenol extract for 4 hours at 100,000 g.

Table 3.8: Chemical composition of gluco- and galactomannans.

Polymer	% Glc	% Man	% Gal	Molar Ratio	%Ac
Konjac Mannan	39.3	60.7	-	Man, 1.54 : Glc, 1.00	4.2
Locust Bean Gum	-	81.0	19.0	Man, 4.26 : Gal, 1.00	-
Guar Gum	-	64.3	35.7	Man, 1.80 : Gal, 1.00	-

Table 3.9: Elemental analysis of polymers (Butterworth Laboratories Ltd.)

Polymer	% C	% H	% N	% Na^+	% K^+	%Ca^{++}
ps.646	39.36	5.70	<0.2	2.99	0.190	0.13
DA ps.646	38.01	5.91	<0.2	2.84	0.230	0.19
DP ps.646	38.59	5.74	<0.2	1.47	0.220	0.08
DAP ps.646	38.71	5.93	<0.2	1.97	0.050	0.55
ps.646[b1]	35.06	-	-	-	-	-
ps.646[b2]	37.39	5.49	<0.2	2.61	0.074	0.25
Kelzan	37.71	5.48	<0.2	2.41	0.070	0.14
Flocon 4800C	36.76	5.68	<0.2	2.76	0.096	0.07
DP Flocon 4800C	37.20	5.88	<0.2	1.98	0.110	0.09
ps.556	39.03	5.80	<0.2	1.93	0.097	0.21
DP ps.556	39.25	6.21	<0.2	1.39	0.240	0.20
ps.1128	38.31	5.88	<0.2	1.95	0.097	0.09
DA ps.1128 (Batch 1)	37.13	-	-	-	-	-
DA ps.1128 (Batch 2)	39.82	6.21	<0.2	1.13	0.062	0.17
ps.PXO_{61}	38.15	6.14	<0.2	1.75	0.031	0.13
DA ps.PXO_{61}	38.99	5.67	<0.2	1.58	0.110	0.09
ps.BD9A	37.60	5.94	<0.2	2.43	0.037	0.28
Konjac Mannan	39.62	5.85	<0.2	-	-	-
Locust Bean Gum	39.11	5.75	<0.2	-	-	-
Guar Gum	39.98	5.64	<0.2	-	-	-

b1, b2 As for table 3.5

Table 3.10: Theoretical elemental composition of xanthan in the sodium salt form, based upon the pentasaccharide repeat unit structure of Jansson *et al* (1975).

Acyl substitution	Theoretical Elemental Composition			
	%C	%H	%O	$\%Na^+$
0% Acetyl, 0% Pyruvate	42.55	5.55	49.17	2.72
100% Acetyl, 0% Pyruvate	43.24	5.52	48.65	2.59
0% Acetyl, 100% Pyruvate	42.22	5.12	47.76	4.90
100% Acetyl, 100% Pyruvate	42.86	5.10	47.35	4.69

Table 3.11: Theoretical elemental composition of gluco- and galactomannans, based upon the chemical constitution determined in this study.

Polymer	Theoretical Elemental Composition		
	%C	%H	%O
Konjac Mannan	44.28	6.12	49.60
Locust Bean Gum	44.44	6.17	49.39
Guar Gum	44.44	6.17	49.39

Fig. 3·1 Colonies of X. campestris pv. campestris on yeast extract nutrient agar: a) Strain 646 (wild-type), b) strain 646E and c) strain MT16·8 (crenated mutants of strain 646).

a)

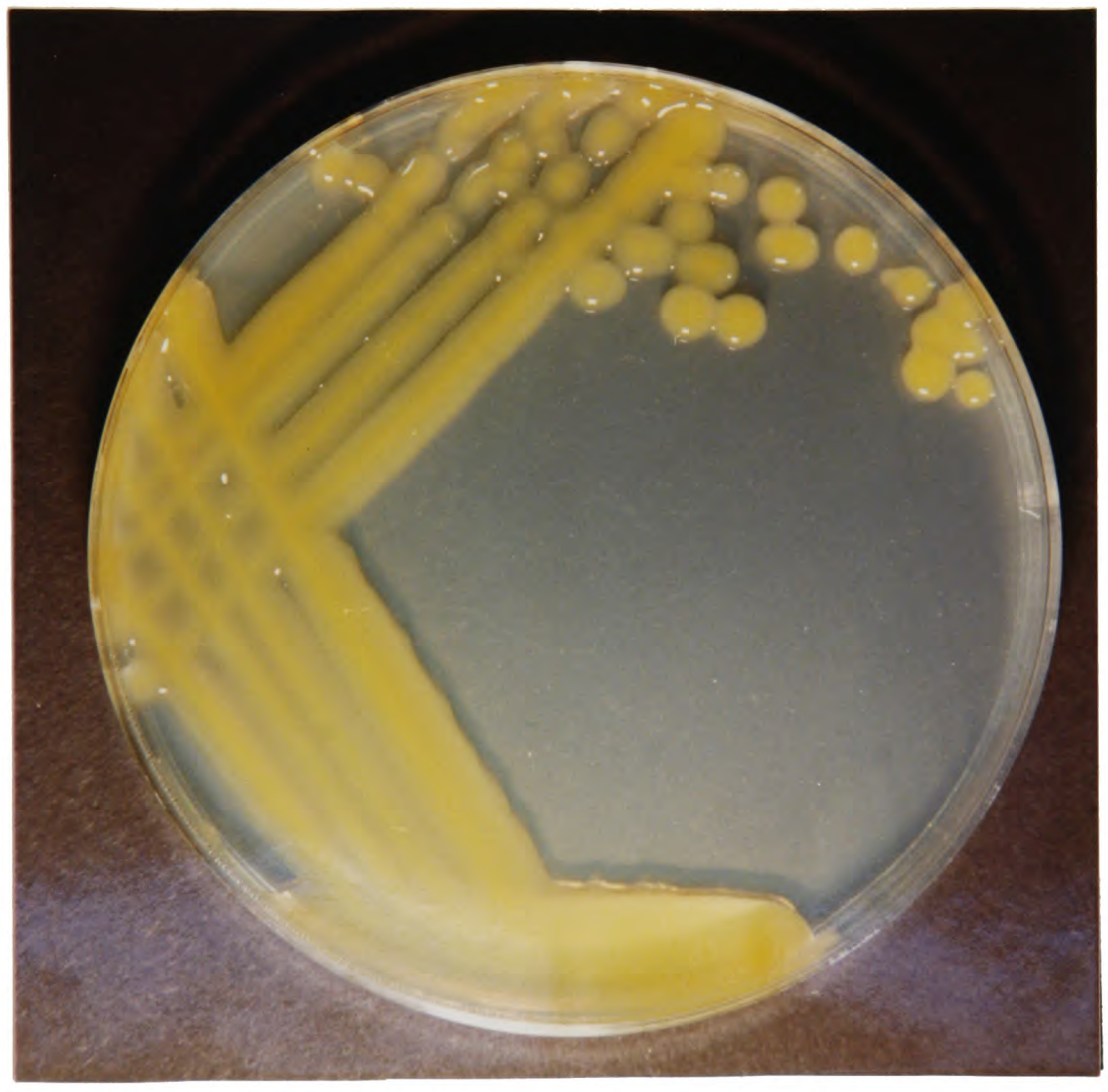

b)

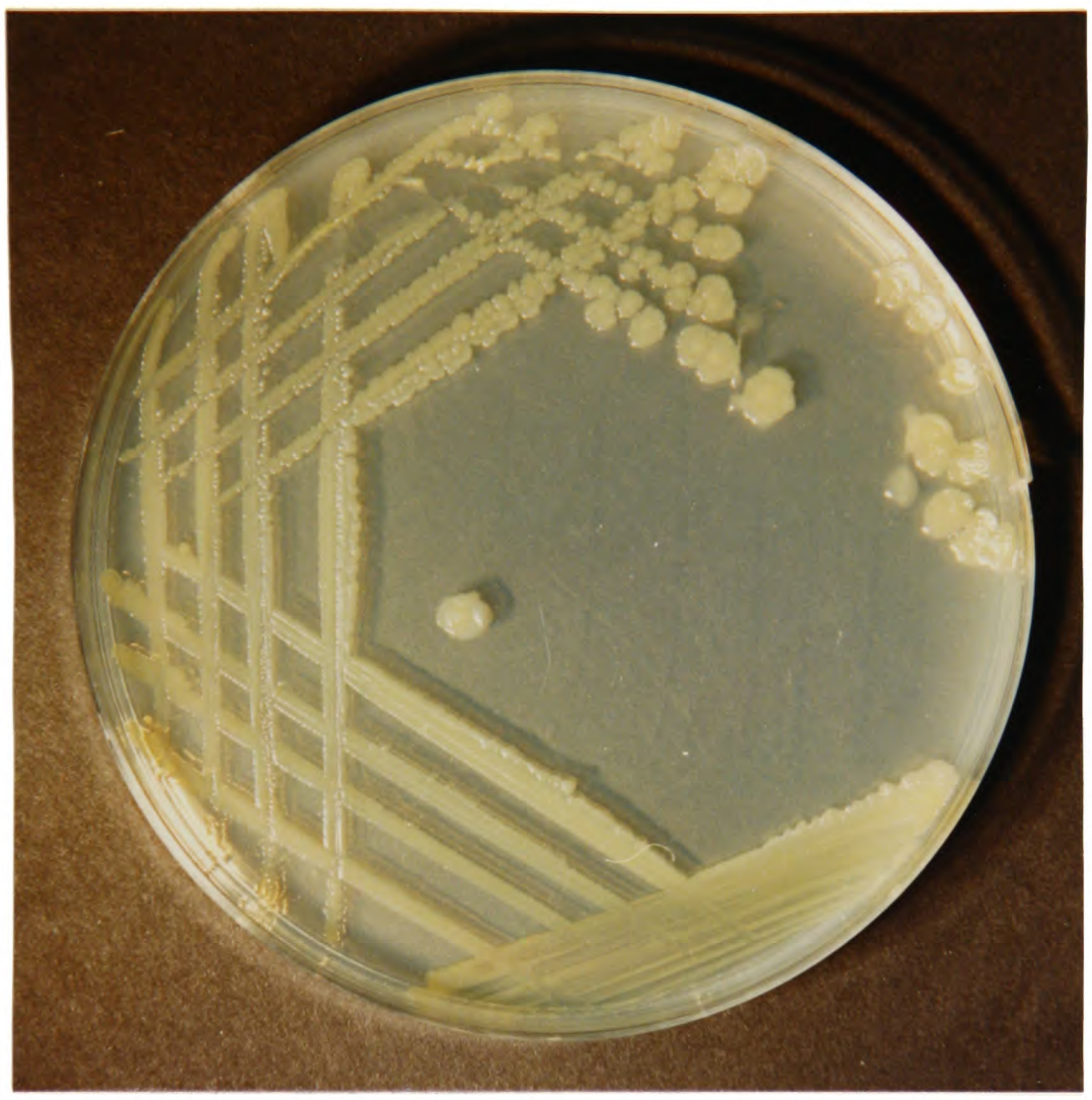

c)

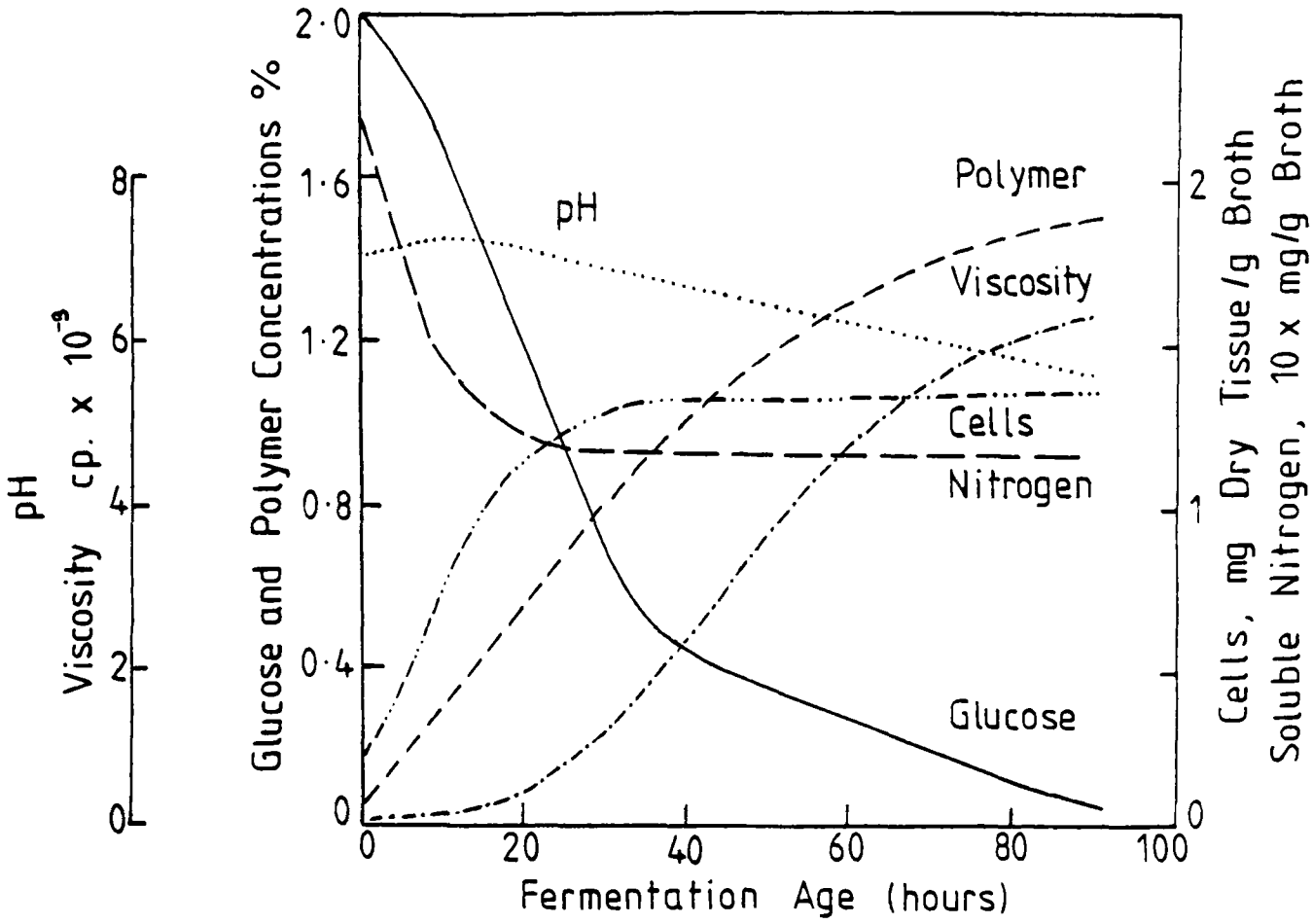

Fig. 3·2 Course of a typical X. campestris batch fermentation (Moraine and Rogovin, 1972).

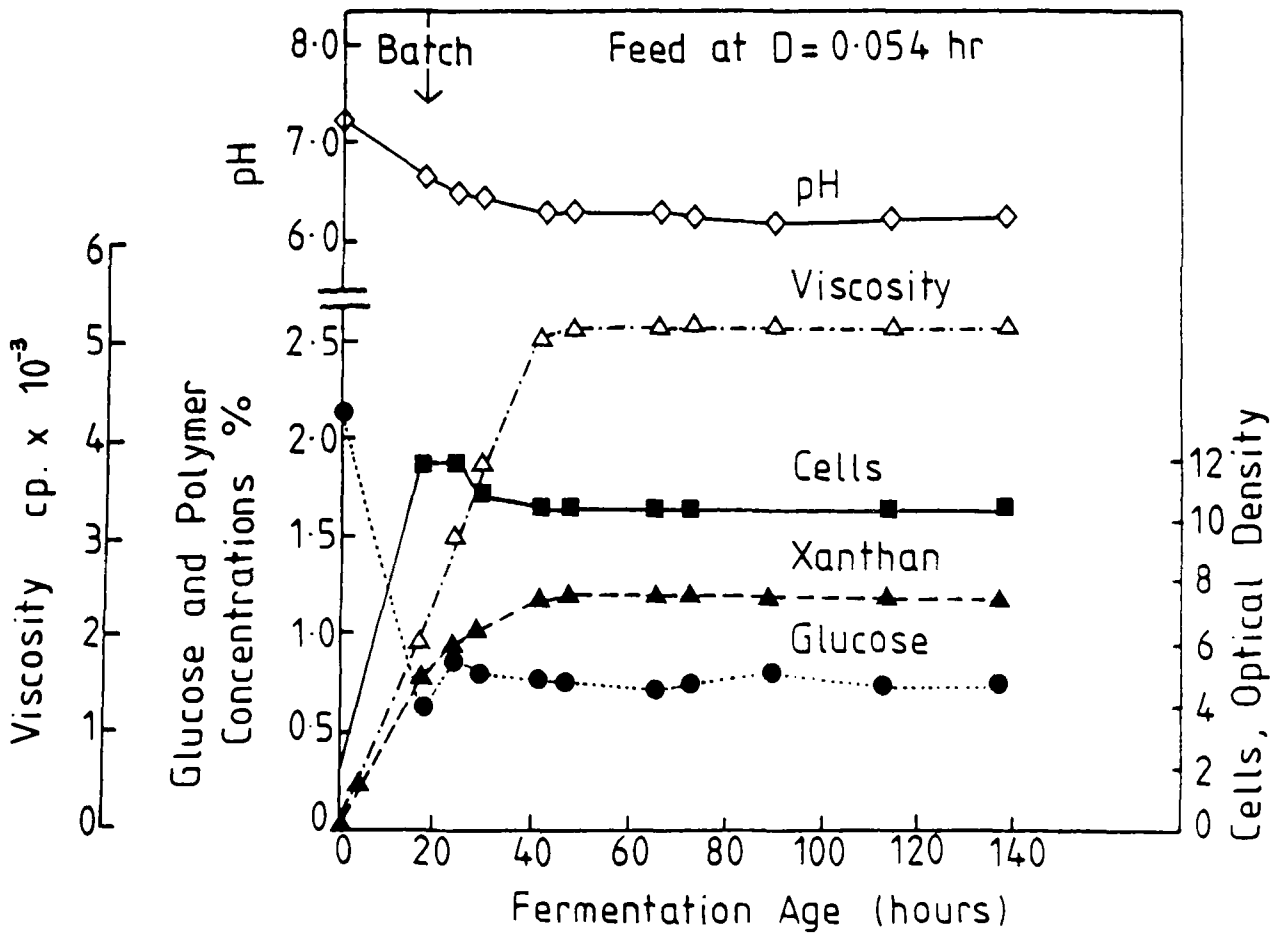

Fig. 3·3 Course of a typical X. campestris single-stage continuous fermentation (Silman and Rogovin, 1972).

Fig. 3·4 HPLC chromatograms

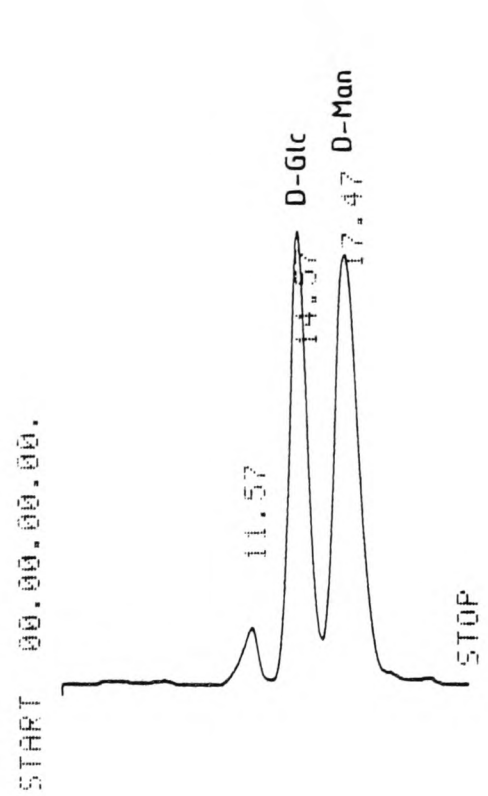

a) Deacetylated ps.1128 (batch 1)

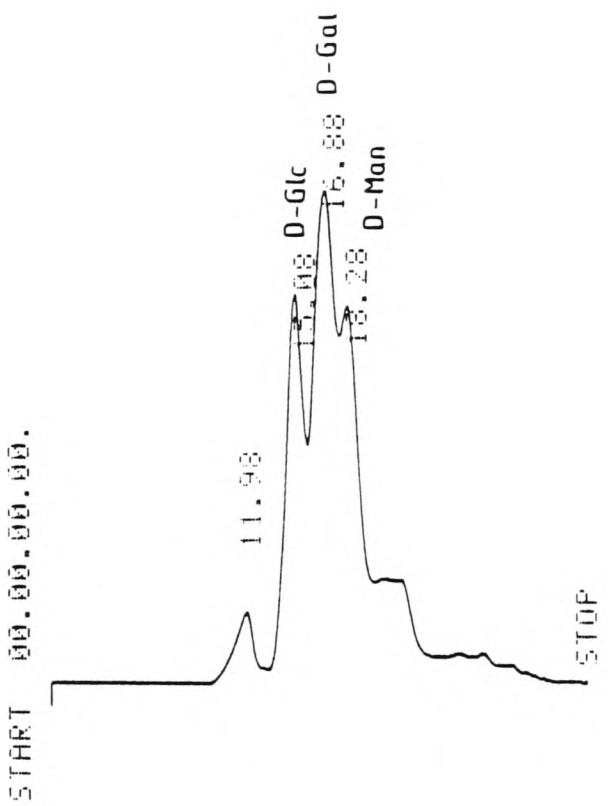

b) ps. 646E

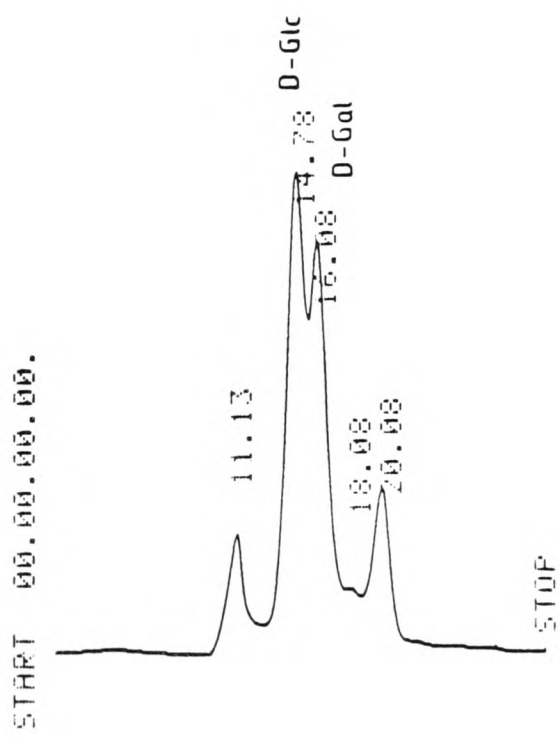

c) ps. 646KR (soluble fraction)

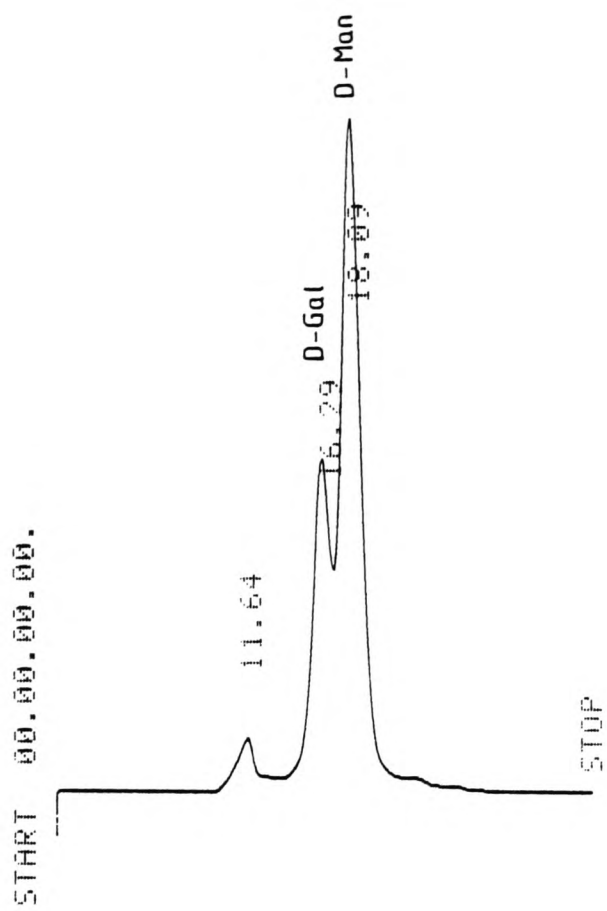

d) Guar gum

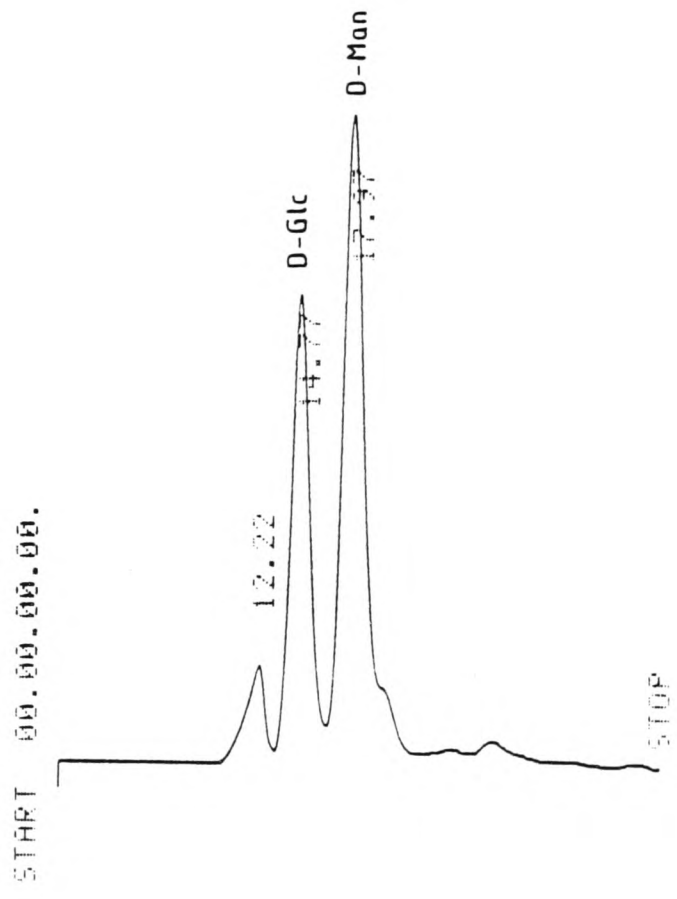

e) Konjac mannan

CHAPTER 4

PHYSICAL CHARACTERIZATION I: POLARIMETRY

Introduction

4.1 The Helix-Coil Transition

On heating, the xanthan molecule undergoes a (normally reversible) conformational transition from the ordered helical structure believed to exist in solution, to a more flexible, disordered state, generally referred to as a random coil. The earliest evidence for such a transition was obtained by Jeanes and coworkers (1961). They observed that in the absence of salt and at high shear rates the polysaccharide underwent an anomalous sigmoidal increase in viscosity upon heating (figure 4.1). This increase, which was subsequently demonstrated by other authors (Holzwarth, 1976; Morris, 1977; Morris *et al*, 1977a; Southwick *et al*, 1979), was attributed to the formation of non-specific molecular entanglements as the polymer underwent some sort of conformational change. Further evidence was obtained by optical rotation (OR), circular dichroism (CD) and relaxation nuclear magnetic resonance (NMR) studies (Morris, 1977; Morris *et al*, 1977a). As the temperature increased xanthan was found to undergo a large sigmoidal change in optical rotation (figure 4.5b) which coincided exactly with the increase in viscosity, and the amplitude of the peaks in the CD spectrum (figure 4.5a) was also observed to change. The molecular basis for these events will be discussed in section 4.2. The linewidth signals in the high resolution proton magnetic resonance spectrum were found to decrease with increasing temperature, indicating the adoption of a more flexible conformation.

Nuclear spin is a fundamental property of all atomic nuclei. When nuclei (except those with an even mass and even atomic number) are placed in a magnetic field, they behave like tiny bar magnets and become aligned with the applied field. Subsequent decay of the induced magnetization, or relaxation as it is known, occurs by loss of phase of the individual precessing nuclei as energy is exchanged between neighbouring atoms. The rate of relaxation can be measured directly as the time constant for the exponential decay of magnetization, T_2, or indirectly from the linewidth of the signals in the high resolution NMR spectrum. The linewidth is inversely related to the rate of decay. Thermal motions interfere with the exchange of energy between nuclei and hence small free-moving molecules such as mono- and oligosaccharides, have a relatively high T_2 value (in the order of hundreds of milliseconds) and give sharp, narrow spectral lines. Random coil polymers, in contrast, have a lower T_2 value (approximately 50 msec) and although the peaks are still clearly discernible the linewidths are much broader. A polymer with a rigid ordered conformation, for example the carrageenan double helix, has a T_2 of only about 50 μsec and the linewidths are so great that the peaks have become flattened into the baseline. Figure 4.2 shows the high resolution NMR spectrum for the methyl protons of the acetyl and pyruvic acid substituents of xanthan, at a range of temperatures. The peaks diminish in size as the temperature falls and disappear completely below 60°C (Morris

et al, 1977a). The collapse of the spectrum illustrates quite clearly the transition from a flexible random coil to a more rigid ordered conformation.

Although the existence of a thermally induced conformational change has been long established, its precise nature remains uncertain. A wide variety of techniques including, for example, light scattering, intrinsic viscosity measurements and stopped-flow polarimetry, have been used to try to gain a better understanding of the molecular events taking place in the course of the transition. These methods, together with the principal publications in the area, are listed in table 4.1. Many of these studies will be discussed in more detail in the course of this introduction.

4.2 Theory and Application of Chiroptical Techniques

Optical rotation and circular dichroism, which are (together with optical rotatory dispersion) referred to collectively as the chiroptical techniques, are well established probes of polysaccharide conformation. They have been used in the past to study the thermally induced conformational transition of a range of polysaccharides including iota and kappa-carrageenan, agarose and agarose sulphate, furcellaran, the extracellular bacterial polysaccharide from *Arthrobacter* species and of course xanthan (Morris *et al*, 1977b; Morris and Frangou, 1981). The chiroptical methods and in particular OR, are by far the most widely used techniques for monitoring the xanthan conformational transition, and OR was the method of choice in this study. For this reason it is worth considering in more detail the theory behind these measurements and their application to the study of xanthan.

Waves of electromagnetic radiation are characterized by the amplitude and orientation of their component electric and magnetic fields. In circularly polarized light the electric and magnetic field vectors are of constant intensity but rotate around the axis of propagation in a clockwise (right-handed) or anticlockwise (left-handed) fashion (see figure 4.3). Rotation is at a constant frequency (ν) which is related to the wavelength (λ) and the speed of light (c) by the equation:

$$\nu = c/\lambda$$

Plane polarized light can be resolved into two circularly polarized waves of equal but opposite sense.

Molecules will absorb electromagnetic radiation in the ultraviolet or visible region of the spectrum if the frequency of the light matches the energy requirements for the promotion of electrons from the normal ground state to an excited higher energy level. The absorbing group is known as a chromophore. Carbohydrates, in common with many other materials of biological origin, are disymmetric. That is to say, they cannot be superimposed on their own mirror image. In disymmetric molecules one

handedness of the electron displacement is favoured and thus one type of circularly polarized light may be preferentially absorbed by the chromophore. (Obviously the mirror image molecule will show the same preference for the opposite sense of polarization.) The difference in the absorption of left and right circularly polarized light is known as circular dichroism (Morris and Frangou, 1981).

Where the wavelength of the radiation supplied does not satisfy the energy requirements for complete absorption, some exchange of energy may still occur between the electronic orbitals of the sample and the electric field of the light wave. However, there is no net loss of energy. Energy absorbed in one part of the electromagnetic cycle is simply re-emitted at a later part, the effect being to reduce the rate of propagation of light through the medium. The extent to which light is delayed on passage through a sample is expressed by its refractive index (ie. the ratio of the speed of light in a vacuum to the speed of light on passage through the sample). When plane polarized light interacts with a disymmetric molecule, the right and left circularly polarized components may not be retarded to the same extent. As a result, the plane of the emergent light is rotated relative to the incident light, a phenomenon known as optical rotation (Morris and Frangou, 1981). The angle through which the plane of polarized light is rotated (α) depends upon the nature of the substance, the path length through the sample (d) and the concentration of the optically active material in the sample (c). Thus:

$$\alpha = [\alpha]dc$$

where $[\alpha]$ is the specific rotation. By convention c is measured in grams per millilitre and d in decimetres.

CD and OR are both manifestations of the same underlying behaviour and the relationship between the two is expressed by a series of equations known as the Kronig-Kramer relations.

A simple, semi-empirical relationship has been demonstrated between the change in OR and the change in the glycosidic bond angles of adjacent carbohydrate residues (Rees, 1970). Rees introduced the concept of linkage rotation $[\Lambda]$ which in the case of a disaccharide containing a non-reducing (N) and a reducing (R) sugar residue is defined by the following equation:

$$[\Lambda] = [M_{NR}] - \{[M_{MeN}] + [M_R]\}$$

$[M_{NR}]$ is the D-line molar rotation of the disaccharide, $[M_R]$, the molar rotation of the reducing residue and $[M_{MeN}]$, the molar rotation of the methyl glycoside of the non-reducing residue in the anomeric configuration. The relative orientation of adjacent sugar residues is defined by the two dihedral angles Φ and ψ (see figure 4.4). Thus according to Rees, the conformation of the carbohydrate and the linkage rotation are related as follows:

For α-linkages: $[\Lambda] = -120\ (\sin\Phi + \sin\psi) - 105$

and for β-linkages: $[\Lambda] = -120\ (\sin\Phi + \sin\psi) + 105$

A typical OR scan for the xanthan helix-coil transition is shown in figure 4.5b (Morris *et al*, 1977a) . A low temperature plateau region, which corresponds to the ordered helical conformation, is separated from the high temperature random coil plateau by a sharp shift in the optical rotation to less negative values. The midpoint temperature of the transition is referred to as the melting temperature or T_m. The slight slope observed in the low temperature region corresponds probably to a gradual loosening of the native structure prior to the onset of the transition proper (Holzwarth, 1976).

CD spectra for xanthan measured at a range of temperatures over the course of the transition are shown in figure 4.5a (Morris *et al*, 1977a). At room temperature the spectrum shows two main bands, a peak at around 205 nm which is attributed largely to the carboxylate groups of the glucuronic acid residue and the pyruvic acid substituent, and a trough at around 220 nm which is believed to be due principally to the O-acetyl ester, since its size decreases markedly when the polymer is deacetylated. The amplitude of both bands changes on heating. The peak diminishes linearly in height whilst the trough increases sigmoidally in magnitude. Two smaller bands are observed at higher wavelengths. Their assignment is uncertain, and the size and even their occurrence varies from one sample to another. Isodichroic points at 225 and 255 nm suggest the interconversion of two distinct conformations which have the same ellipticity at the wavelengths in question.

The chromophores in the xanthan molecule are located on the side chains, implying that side chain movements dominate the CD spectrum. Because the overall change in ellipticity is negative, its contribution to the OR shift in the higher wavelength regions of the spectrum, inaccessible to CD, must also be negative. The OR shift, however, is to less negative values and this indicates, therefore, that the OR behaviour is dominated by electronic transitions in the backbone regions of the polymer.

4.3 Factors Influencing the Transition

The transition behaviour of xanthan is heavily influenced by environmental factors and in particular the ionic strength and pH of the medium. Salt represses the transition and the melting temperature therefore goes up as the ionic strength increases (Holzwarth, 1976; Morris *et al*, 1977a; Holzwarth and Ogletree, 1979; Milas *et al*, 1979; Norton *et al*, 1984; Milas and Rinaudo, 1986; Liu *et al*, 1987). Quantitatively there is a linear relationship between the melting temperature and the log of the ionic strength (Holzwarth, 1976; Milas and Rinaudo, 1979) or, expressed differently, between the reciprocal of the melting temperature

in Kelvin and the natural log of the salt concentration (Norton *et al*, 1984). The explanation for the increase in melting temperature is simple. Xanthan is a polyanion with negatively charged carboxylate groups located on the side chain residues. Under conditions of low ionic strength the charged groups tend to repel one another, destabilizing the whole structure, but if salt is added the cations have a charge shielding effect and therefore stabilize the ordered conformation against disruption on heating. As one might, expect divalent cations such as calcium are very much more effective at stabilizing the ordered structure than monovalent ions like sodium (Holzwarth, 1976). Calcium ions also appear to reduce the range of temperature over which the transition occurs, whilst sodium ions do not (Holzwarth, 1976). Reducing the pH has the same effect upon melting temperature as increasing the ionic strength. Holzwarth (1976) demonstrated that in 0.01M sodium chloride the melting temperature of xanthan increased by 15°C as the pH was lowered from 7 to 4. A further reduction in pH to 3.4 produced a rise of more than 40°C. Urea also has the effect of stabilizing the ordered conformation and forcing up the melting temperature (Frangou *et al*, 1982). The reason for this is unknown but by modifying the dielectric constant of the medium it may promote apolar interactions within the molecule.

The degree of acyl substitution has been shown to dramatically affect the stability of the helix. A number of authors have compared the transition midpoint for native xanthan with that of its chemically deacetylated and/or depyruvylated derivatives (Holzwarth and Ogletree, 1979; Rinaudo *et al*, 1983; Dentini *et al*, 1984; Callet *et al*, 1987) and in every case, the removal of the acetyl groups was found to produce a fall in the melting temperature, whilst removal of pyruvic acid caused it to increase. Smith and coworkers (1981) compared the melting temperature for six native polymers, five of which were from commercial sources and one which was produced by bacterial fermentation in the laboratory. They demonstrated that the melting temperature was dependent upon the ratio of pyruvate to acetyl substitution and that the ordered conformation became more stable as the proportion of acetyl groups increased or as the pyruvic acid content fell. The destabilizing effect of pyruvate can be explained by the increase in internal repulsion between the charged side chains. However, the reason for the stabilizing influence of the acetyl groups is less obvious. Smith *et al* have suggested that apolar interactions between the methyl groups of the acetyl residues could be responsible. Alternatively the polar oxygen atom of the acetyl substituents could act as a hydrogen bond acceptor, stabilizing the molecule in this way (Dentini *et al*, 1984).

It is interesting, at this point, to note certain similarities between the behaviour of xanthan and the exocellular polysaccharide from *Arthrobacter viscosus*. The latter is an O-acetylated polymer believed to be based upon a linear, →4)-β-D-mannuronic acid-(1→4)-β-D-glucose-(1→4)-β-D-galactose-(1→ repeat unit. Like xanthan, it adopts a rigid ordered conformation which can be melted out at high temperatures and is

stabilized by the presence of salt. However, deacetylation of the *A. viscosus* polysaccharide destabilizes the molecule to the point where the ordered structure can no longer be detected at room temperature (Darke *et al*, 1978). Hence the stabilizing influence of the acetyl group is even greater in this polymer.

Besides affecting the melting temperature, Holzwarth and Ogletree (1979) have suggested that the distribution of acetyl and pyruvic acid groups within a population of xanthan molecules could affect the range of temperature over which the transition occurs. They observed that the removal of pyruvic acid residues from native xanthan caused a significant sharpening of the helix-coil transition, whereas removal of the acetyl groups did not. The pyruvate content of the xanthan molecules within a population has been shown to vary significantly (Cadmus *et al*, 1978; Sandford *et al*, 1978; Sutherland *et al*, 1981b), and Holzwarth and Ogletree attributed the narrowing of the transition upon depyruvylation to the switch from a heterogeneous population of molecules, in which the pyruvic acid content and therefore the melting temperature varied enormously, to a more homogeneous, non-pyruvylated population. Deacetylation had no effect, they said, because the distribution of acetyl groups within the native polymer was stoichiometric.

At constant ionic strength the melting temperature of xanthan is unaffected by the polysaccharide concentration (Morris, 1977; Morris *et al*, 1977a; Milas and Rinaudo, 1979) but the molecular weight does appear to have some influence. The data available in this area is contradictory. Liu and Norisuye (1988), using a series of different molecular weight fractions generated by sonication, have recently produced evidence to suggest that above 3×10^5 the helix-coil transition as monitored by OR at 300 nm is, to all intents and purposes, unaffected by differences in molecular weight. Below 2×10^5 , however, $[\alpha]_{300}$ shows a profound molecular weight dependence, as illustrated in figure 4.6. As the molecular weight decreases, so does the melting temperature, and the OR in the low temperature plateau region of the curve becomes less negative, suggesting a reduction in the amount of order. Less rigorous evidence from Paradossi and Brant (1982) agrees with these findings insofar as the specific OR at 302 nm and 25°C, for a series of fractions generated by sonication, showed no correlation with molecular weight. All of the xanthans used in this study had a molecular weight of 2.4×10^5 or above. Milas and Rinaudo (1981), however, using xanthan fractions produced by partial enzymic hydrolysis with cellulase, showed that the melting temperature decreased with molecular weight for three samples of 3.2×10^6, 7×10^5 and 2×10^5 . Two of these samples are above the molecular weight threshold proposed by Liu and Norisuye, and no obvious explanation is available for the discrepancy.

From the reports in the literature it is unclear whether or not solutions of xanthan show thermal hysteresis. Milas and Rinaudo (1979) studied the helix-coil transition by OR at a series of different sodium

chloride concentrations and found no hysteresis at any concentration of salt or in its absence. Frangou and coworkers (1982) who studied the transition in the presence of urea also showed that it was perfectly reversible. In contrast, however, Liu *et al* (1987) noted that in 0.01M sodium chloride there was a significant amount of thermal hysteresis but that if the concentration of salt was increased, the amount of hysteresis diminished. In a subsequent paper Liu and Norisuye (1988) stated that for any given temperature, solutions of xanthan quickly reached an equilibrium state. Holzwarth (1976) observed that if, in the absence of salt, a xanthan solution was heated and then cooled quickly it would retain the OR of the denatured state. Even after 45 days storage at 5°C the OR was found to have returned only halfway towards that of the native conformation. The conflicting nature of these reports suggests that the behaviour of xanthan with respect to thermal hysteresis is heavily influenced by environmental conditions and a possible unifying explanation is discussed in section 4.11.

4.4 The Nature of the Conformational Change

The precise molecular basis of the thermally induced conformational transition is unknown, although a number of authors have been led to speculate on the subject. To date two principal models exist. The first of these was proposed by Morris and coworkers (1977a) who envisaged an intramolecular transition. The native ordered conformation is, they suggested, a single-stranded helix with the side-arms folded back along the backbone. The whole structure is stabilized by non-covalent interactions and these are broken down upon heating to give a disordered random coil (figure 4.7). Their hypothesis was based originally on rather flimsy evidence - the X-ray fibre diffraction data of Moorhouse *et al* (1977a,b) and the observation that the conformational transition is concentration independent. Subsequently, however, more evidence was produced to support the model. Norton and coworkers (1980, 1984) studied the dynamics of the order-disorder transition by stopped-flow polarimetry, using a rapid increase in ionic strength (salt-jump) to induce the switch to the ordered state. They found that the reaction was, over more than 90% of its course, first order, strongly indicating an intramolecular transition (although a highly co-operative intermolecular interaction, as is seen in DNA, could not be completely ruled out). The apparent molecular weight of the molecule was measured using low-angle laser light scattering and did not change over the temperature range of the transition (Norton *et al*, 1984). This appeared to preclude the formation of a dimer. Furthermore the change in ion binding upon ordering, as determined from a plot of the reciprocal of the melting temperature versus the log of the ionic strength, was in good agreement with that calculated from the Manning electrolyte theory for a single stranded disorder-order transition, but appreciably lower than that for a double helix (Norton *et al*, 1984).

Milas and Rinaudo (1979) supported a similar single stranded mechanism. They observed that the melting temperature, as determined from the OR and CD spectra, were the same and concluded that since the chromophores involved in circular dichroism are located on the trisaccharide side chains, the "melting" process must correspond to the spreading of the lateral side arms. However, they also noted an increase in intrinsic viscosity of only 10% over the temperature course of the transition and surmised that no dramatic change in conformation occurs. A drop in hydrodynamic volume at temperatures well above the transition midpoint, they attributed to a continuous decrease in the rigidity of the molecule. Hence the transition, they stated, occurred via a one-step mechanism involving the breakdown of the helical conformation of the main chain and the release of the lateral side arms. More recently (1986) the same authors have provided evidence to suggest the existence of two different single-stranded ordered conformations at room temperature. Data from viscosity, intrinsic viscosity and conductance measurements, together with information from OR and light scattering, indicated that the pattern of side chain-backbone interactions that exists in the native polymer is broken down upon heating, but not re-established during renaturation. Instead a different pattern of interactions is set up which stabilizes a more extended backbone conformation. Interestingly since both Morris and coworkers, and Milas and Rinaudo, put forward their hypothesis Pérez and Vergalati (1987) have shown by molecular modelling, using potential energy calculations, that the side chains of xanthan in the ordered conformation show no preferred tendency to fold back along the backbone.

The second model for the conformational transition was put forward by a group of Japanese workers (Liu *et al*, 1987; Liu and Norisuye, 1988). They studied a series of different molecular weight xanthan fractions produced by sonication and showed that the molecular weight of each sample remained unchanged after heating but was double that of the same material in cadoxen, a solvent system in which the xanthan molecule has been shown to exist as a single-stranded flexible chain (Sato *et al*, 1984b). They therefore concluded that even in the disordered state, xanthan must exist as a dimer. The z-average radius of gyration for xanthan, determined by light scattering, and the intrinsic viscosity, were found to change with temperature in a manner dependent on the molecular weight. In 0.01M sodium chloride the high molecular weight samples showed a sigmoidal decrease in radius with rising temperature, but at a lower molecular weight of 2×10^5 the radius remained unchanged. Still smaller molecules showed an increase in hydrodynamic volume. Liu and coworkers suggested the following explanation for this data. They proposed that at ambient temperature the molecule exists as a double helix, but that upon heating it melts from both ends to produce an expanded dimer. The dimer consists of two molecules predominantly in the random coiled state but which are linked by a very short region of double helix (figure 4.8). At the higher molecular weights, each disordered "monomer" chain has a statistical radius much smaller than that of the rod-like monomer in the ordered dimer. The dimensions of the molecule will therefore decrease as the polymer

transforms from the ordered to the disordered state. At lower molecular weights, however, the difference in the statistical radius between the two structures becomes smaller and additional contributions from the distances between the subchains become more important. Thus, when the molecular weight falls below a certain limit value (2×10^5) the radius of the disordered dimer becomes greater than that of the double helix.

Hacche *et al* (1987) have proposed a similar model to that of Liu and coworkers. They studied the temperature-driven conformational change of a series of low molecular weight xanthan fractions in 0.005M sodium chloride using light scattering, intrinsic viscosity measurements and polarimetry. They found that the weight-average molecular weight, the root-mean-square-z-average radius of gyration and the intrinsic viscosity all increased slightly over the course of the transition, and particularly above the transition midpoint, whilst the osmotic second virial coefficient displayed a pronounced sigmoidal increase with temperature, consistent with the optical rotation behaviour, but with a midpoint 10°C higher than that of the melting temperature. They interpreted their data in terms of a native double-stranded xanthan which upon heating would partially dissociate to give a double-stranded dimer and, if heated to a higher temperature still, would dissociate completely to give disordered single strands.

The dissociation of a double-stranded structure was also suggested by Holzwarth and Prestridge (1977) who noted,in their electron micrographs, a halving of the diameter of the xanthan molecule upon denaturation. These authors also proposed the breakdown of a multistranded xanthan assembly composed of roughly 40 subunits. Their evidence for this was derived from electron microscopy and molecular filtration chromatography. The electron microscopy data, however, is nowadays generally considered to have been an artifact of the preparation procedure used, whilst the filtration chromatography data can be explained by molecular aggregation.

The melting temperature was initially envisaged as a two-state-all-or-none process (Morris *et al*, 1977a). However, Norton and colleagues (1980,1984), in their studies on the dynamics of the disorder-order transition, noted that the first order rate constant for the reaction increased as the temperature of the starting solution was reduced. Their explanation for this was that at high temperatures, where the polymer solution was initially completely disordered, nucleation was the rate limiting step but, at lower temperatures, regions of pre-existing order could act as nuclei for further helical growth and a more rapid propagation process therefore became rate limiting. This theory implied that regions of order and disorder could coexist within the same molecule and to test this deduction, Norton and coworkers (1984) analysed data from OR and differential scanning calorimetry (DSC) studies in terms of helix-coil transition theory. They were able to calculate the relative stability and sequence length distribution of the helix and coil sections of the

chain as a function of temperature and showed that the amount of helix increased as the temperature fell. Except at relatively high salt concentrations the average length of the helical sequence was much smaller than the total chain length as determined by light scattering. Thus, at any given temperature, the xanthan molecule contains both ordered and disordered regions in a state of equilibrium. Liu and coworkers (1988), whilst supporting a very different model for the transition, also ascribe to this view since they state that for any temperature the xanthan molecule quickly reaches a state of equilibrium, as monitored by OR.

The tendency of xanthan molecules to aggregate in solution is a well recognized phenomenon (Southwick *et al*, 1980; Norton *et al*, 1984). Indeed any concentrated solution of fairly rigid molecules would be expected to undergo some degree of alignment and aggregation. However, the role of aggregation in relation to the conformational transition is not clear cut. Southwick *et al* (1979, 1981) studied the transition using quasi-elastic light scattering and observed an increase in macromolecular polydispersity near to the transition temperature. This they attributed to a breakdown of multimolecular aggregates just prior to the conformational change. Rather, though, than being an integral part of the transition behaviour, as Southwick has suggested, it seems more likely that the time-dependent aggregation process is essentially separate and is promoted by a high degree of conformational order. This view is supported by the fact that urea, which is known to disrupt the non-covalent interactions between xanthan chains, also stabilizes the ordered conformation (Frangou *et al*, 1982). The importance of intramolecular order to the alignment of neighbouring molecules is indicated by the birefringence studies of Milas and Rinaudo (1979). They noted that solutions of xanthan at low temperatures showed birefringence with or without salt present, but that the birefringence disappeared at a temperature corresponding exactly to the transition midpoint.

4.5 Characterization of Materials by OR

OR was used to characterize the helix-coil transition behaviour of a range of native and chemically modified xanthans. The materials selected for study varied widely in acetyl and pyruvic acid content and an attempt was made to examine the effects of acyl substitution upon various aspects of the transition behaviour. These included not only the transition midpoint but also the transition breadth and transition height, the specific OR in the helix and coil plateau regions of the curve and the degree of thermal hysteresis. The effect of molecular weight (as indicated by the intrinsic viscosity) upon the transition was also considered. Computer analysis of the data was used to look for statistically significant correlations between the acetyl, pyruvate and intrinsic viscosity variables and aspects of the transition behaviour listed above. The effect of salt was studied on just four of the native materials, ps.646, ps.556, ps.1128 and ps.PXO_{61}. These xanthans each had very different levels of acetyl and pyruvic acid substituents. The transition

behaviour of ps.BD9A, a mutant polymer with the terminal mannose residue apparently absent from the side chains, was also examined. The helix-coil transition, interesting though it is, was studied not just for its own sake, but also so that at a later date it could be considered in relation to the gelling behaviour of the polymers (see section 7.14).

All of the OR measurements were made on 0.3% $^{w}/_{w}$ solutions of xanthan. This concentration was selected because it gave a readily measurable shift in OR upon heating but was not too viscous to give problems with manipulation ie. filtering, degassing etc. The samples were prepared by dissolution in deionized water and were filtered to ensure optical clarity. Where measurements were made in the presence of salt, both the polysaccharide and the sodium chloride solutions were prepared and filtered separately at double the required concentration. They were then mixed in equal quantities and stirred hot to ensure homogeneity. Measurements were made at 365 nm using 10 cm quartz cells. The temperature of the cell was controlled using a circulating water bath and readings were taken at 3°C intervals. Precise details of the handling procedure are given in Chapter 2.

Results

4.6 Influence of Acetyl and Pyruvic Acid Content Upon the Order-Disorder Transition

The thermally induced conformational change was studied for a range of xanthans with different levels of acetyl and pyruvic acid substitution, in the absence of added salt. Both the heating and cooling curves were monitored for each polymer and measurements were performed, at least in duplicate, on freshly prepared samples. Plots of the order-disorder transition for the native polymers and their respective chemically modified derivatives are shown in figures 4.9a-4.9e.

An attempt was made to quantify the data so that it could be tabulated and analysed statistically, and the following features of the transition curve were therefore measured:

1. Transition midpoint (melting temperature).
2. Range of temperature over which the transition occurred (transition breadth).
3. Shift in OR observed over the course of the transition (transition height).
4. Specific OR at 15°C ie. in the low temperature plateau region of the curve.
5. Specific OR in the high temperature plateau region of the curve.

The complete set of data is given in table 4.2, whilst the average measurements for each polymer, together with the acetyl and pyruvic acid contents, are shown in table 4.3. In the latter table the polymers are

grouped according to their acyl content so that for example, all of the high acetyl, low pyruvate polymers are listed together, and likewise the low acetyl, high pyruvate and low acetyl, low pyruvate polymers.

The parameters, 1 to 5 above, were assessed by eye and this therefore introduced a degree of subjectivity into the results. For example, it was sometimes difficult to discern at precisely what temperature the onset of the transition occurred and this in turn affected the estimation of the transition midpoint, the transition breadth and the transition height. In general, however, the results were fairly reproducible. The melting temperature varied by 1-2°C at most, except in the case of ps.PXO_{61} which showed a 6°C difference between the 3 solutions tested. The transition breadth, transition height and specific OR data usually varied more.

In the course of these experiments problems were encountered with specific polymers. Sample ps.646 at temperatures below about 25°C showed a large positive shift in OR and gave very erratic readings. This coincided with a fall in the amount of energy transmitted through the sample and is believed to have been due to aggregation. The pronounced tendency of ps.646 to aggregate in solution was demonstrated by Dr Ross-Murphy in his light scattering experiments (unpublished results; see section 5.6) and the formation of aggregates at low temperature may have caused, by excessive scattering of the light passing through the cell, the fall in energy and the optical artifacts observed. Because of this phenomenon, it was not possible to be certain that the apparent levelling off of the transition curve at low temperature was genuine and not due to the onset of aggregation and thus, the accuracy of the data must be called into question. Similar behaviour was observed intermittently for ps.1128, but here the onset of the transition occurred at higher temperatures and the position of the baseline in the low temperature plateau region of the curve could be established unequivocally. The specific OR at 15°C had, however, to be determined by extrapolation. The helix-coil transition for Flocon 4800C occurred at very low temperatures and for this sample the position of the low temperature plateau region was estimated from 2-3 data points only. This was really insufficient information from which to irrefutably establish the temperature for the onset of the transition, and once again the accuracy of the data is questionable. The sample from strain 556 showed unusual transition behaviour in the presence of salt (see figure 4.11d). What appeared in deionized water to be a single conformational change, on addition of salt became quite clearly resolved into two separate transition processes. The data recorded for ps.556, therefore, almost certainly describes a composite of two separate thermally induced transitions and, as such, it is probably not directly comparable with that of the other polymers.

The effect of deacetylation and depyruvylation upon the transition midpoint mirrors that described by other researchers (Holzwarth and Ogletree, 1979; Rinaudo *et al*, 1983; Dentini *et al*, 1984; Callet *et al*,

1987); deacetylation caused a decrease in melting temperature whilst depyruvylation produced an increase. For ps.1128 a drop of 13°C was observed and for ps.646, a fall of 12.5°C. Deacetylation of ps.PXO_{61} resulted in a fall of only 7.5°C, despite the fact that this polymer carries almost twice as much acetyl as ps.1128 and nearly three times as much as ps.646. However, the distribution as well as the quantity of acetyl in this polymer is known to be unusual and its behaviour might therefore differ from that of a normal xanthan. Depyruvylation of Flocon 4800C produced an increase of 17°C in the transition midpoint, but the rise for ps.646 was much smaller - only 7.5°C. Here the stabilizing influence of the acetyl groups may have opposed the destabilizing affect of the pyruvic acid. A fall of just 3°C was observed for ps.556 but, as already noted, the value for the native polymer at least, is probably not a genuine transition midpoint. The pattern of behaviour of ps.646 and its chemically modified derivatives was exactly the same as that recorded by Rinaudo *et al* (1983) and Dentini *et al* (1984). The depyruvylated polymer had the highest melting temperature and this was followed in turn by native xanthan, the deacetylated and depyruvylated derivative and finally the acetyl-free polymer. Callet and coworkers (1987), however, found that deacetylated and depyruvylated xanthan had a higher melting temperature than the native material. In table 4.3, where the polymers are grouped together according to their acyl content, the behaviour is essentially the same. The high acetyl, low pyruvate polymers have by far the highest melting temperatures, whilst the low acetyl, high pyruvate materials have the lowest. Those polymers with high levels of each substituent or alternatively very little of either, fall somewhere in the middle. Indeed, the transition midpoint for both categories is fairly similar, suggesting that both the acetyl and pyruvic acid groups make a significant contribution towards determining the overall stability of the ordered conformation. Figure 4.10 shows a plot of melting temperature versus acetyl to pyruvic acid ratio. The reliable data is shown in filled triangles, the less dependable data in open. Although the points are fairly scattered, there is a general increase in melting temperature as the ratio of acetyl to pyruvate goes up and the only polymer to deviate significantly from this relationship is ps.PXO_{61}.

The effects of acetyl and pyruvate content upon the other features of the transition curve are much less clear cut. Consider the transition breadth. The data, even for repeats of the same sample, varied considerably and trends are therefore difficult to pick out. Deacetylation appears to have caused a slight increase in the transition breadth for ps.1128 and ps.646, but not for ps.PXO_{61}. Samples ps.646 and Flocon 4800C were unaffected by depyruvylation but the transition breadth of ps.556 increased markedly when the pyruvic acid substituents were removed. Any trends observed upon chemical modification however, are not reflected by the groupings in table 4.3. Even omitting ps.PXO_{61} and ps.556 from the consideration, there is no discernible correlation between the transition breadth and the absolute levels of acetyl and pyruvic acid.

Removal of both the acetyl and pyruvate substituents caused a fall in the specific OR at 15°C and an increase in the transition height. This is reflected to some extent by the groupings in table 4.3. The specific OR in the high temperature plateau region of the curve was largely unaffected by deacetylation (except in the case of ps.PXO_{61} where a slight positive shift was observed) but depyruvylation caused a large positive shift in every case. Such a change is also seen in the data of Holzwarth and Ogletree (1979). Again, though, table 4.3 shows no consistent relationship between the OR of the polymer in the random coil state and the level of acyl substitution.

All of the polymers showed significant thermal hysteresis.

4.7 Computer Analysis

Detecting consistent patterns of behaviour within a set of data is often difficult when more than one variable is involved, and this particular set of data proved problematic. Apparent changes in the transition behaviour upon deacetylation and depyruvylation often failed to hold good when a series of polymers with similar levels of acetyl and pyruvic acid substituents were considered together, and variations in the data obtained for repeat experiments introduced additional difficulties. Because of this, an attempt was made to assess the data statistically using a commercially available computer package. The effects of acetyl and pyruvic acid upon the transition were considered, together with the molecular weight. Intrinsic viscosity measurements in 20mM sodium chloride were used in this study as an estimate of the relative molecular weights of the samples. The two are related as outlined in section 5.3, and the data included in the computer analysis is given in table 5.6. The suitability (or otherwise) of intrinsic viscosity as an indicator of molecular weight will be discussed in the next chapter.

A multiple regression analysis was carried out on the data using PROCEDURE RSQUARE from the SAS library (SAS Users Guide: Statistics, 1985) and the full correlation matrix of dependent and independent variables was outputted. Model dependent parameters, namely melting temperature, transition breadth, transition height and the specific OR readings in the helix and coil plateau regions of the curve, were then regressed against the independent variables acetyl, pyruvate and intrinsic viscosity. The independent parameters were tested singly, in pairs and all together to see whether any of the three acted in conjunction with one another. Initially the data for all of the polymers was used in the analysis. However, since evidence is available to suggest that ps.PXO_{61} and ps.556 behave atypically, the analysis was repeated, omitting first one and then both of the polymers, together with their chemically modified derivatives, from the data set. It should be noted that for the specific OR at 15°C the data had to be considered separately as no information was available for ps.646. The correlation matrix together with a table of model dependent versus independent variables is shown for the complete set of data and for

the data set minus ps.PXO_{61}, deacetylated ps.PXO_{61}, ps.556 and depyruvylated ps.556 in tables 4.5 and 4.6 respectively. (The values for the specific OR at 15°C are shown in brackets.) Values of 1 or -1 represent a complete correlation, whilst zero shows no correlation at all. Amounts greater than 0.7 are probably significant for the correlation matrix, whilst for the regression models the equivalent R-square value of 0.49 or above is a good overall indication of reliability, for the number of samples tested.

The correlations obtained in this analysis do, to a large extent, reflect the observations outlined in section 4.6, giving them a more objective basis. The melting temperature behaviour is particularly interesting. When all of the data was included in the analysis, the correlations between the melting temperature and acetyl or pyruvate were too low to be deemed significant, but acetyl and pyruvate together gave a just meaningful R-square value of 0.529. Removal of ps.556 and depyruvylated ps.556 from the data set made very little difference to the results, but removing ps.PXO_{61} and deacetylated ps.PXO_{61} resulted in a marked improvement. The effect of excluding all four polymers from the data set, however, was quite dramatic. An R-square value of 0.580 for acetyl alone increased to 0.904 when the two acyl substituents were considered together. Inclusion of intrinsic viscosity in the regression model barely improved the result. This demonstrates quite clearly that the melting temperature of xanthan is determined by both the acetyl and pyruvic acid substituents, but suggests that acetyl has the predominant effect. It also confirms the atypical behaviour of ps.556 and ps.PXO_{61}.

No correlations were observed between the transition breadth and any of the independent variables. When ps.556 and ps.PXO_{61} and their chemically modified derivatives were excluded from the analysis, a strong correlation was noted between pyruvic acid and the specific OR in the high temperature plateau region of the curve. This is consistent with the observed positive shift in OR upon depyruvylation. There was also a strong correlation between pyruvate and the transition height when ps.PXO_{61} and deacetylated ps.PXO_{61}, or all four polymers, were omitted from the data set. The correlation improved still further when acetyl and pyruvate were considered together, although there was no apparent correlation between the transition height and acetyl alone. The specific OR at 15°C was unaffected by acetyl and/or pyruvate. This appears to conflict with the observed decrease in OR upon deacetylation and depyruvylation but it should be borne in mind that in the absence of any data for ps.646, no high acetyl and high pyruvate polymer was considered in the analysis. This would have affected the computational results.

There was no detectable correlation between intrinsic viscosity and any of the dependent variables, suggesting that the transition behaviour of the polymers, as monitored by OR, is unaffected by molecular weight. The lowest molecular weight of any of the materials studied, as estimated from the intrinsic viscosity using the data of Sato *et al* (1984c; see

table 5.6) was 9.60 x 10^5. As noted above, according to Liu and Norisuye (1988), the OR scan for xanthan is independent of molecular weight at values of greater than 3 x 10^5 and this data seems to concur with their observation. Interestingly, a weak correlation did exist between the intrinsic viscosity and the percentage acetyl substitution when all four polymers were omitted from the analysis. This can be explained by the fall in the intrinsic viscosity of the materials, apparent upon deacetylation (see section 5.7).

4.8 Transition Behaviour of ps.BD9A

The heating curve for ps.BD9A is shown in figure 4.9f. The polymer appeared to undergo a conformational change upon heating, but the transition occurred at a low temperature and was not as sharp as for the other xanthans tested. The evidence for a low temperature plateau region, within the temperature range studied, was also extremely weak. One, or at most, two points appeared to indicate the levelling off of the transition curve. This data suggests that whilst ps.BD9A was capable of adopting an ordered conformation, the structure was rather weak and readily disrupted by heat. As such, it points to a stabilizing role for the terminal mannose residue, believed to have been absent from this polymer, but indicates that the complete trisaccharide side chain is unnecessary for the polymer to adopt an ordered conformation.

4.9 Influence of Salt Upon the Order-Disorder Transition

The influence of salt upon the order-disorder transition was studied for just four of the native polymers - ps.646, ps.1128, ps.PXO_{61} and ps.556. These polymers had vastly different levels of acetyl and pyruvic acid substituents. Sample ps.646 was a typical wild-type xanthan with a substantial amount of acetyl and pyruvic acid. Both ps.1128 and ps.PXO_{61} had high levels of acetyl (7.7% and 14.3% respectively) but very little pyruvate, and ps.556 was a high pyruvate, low acetyl xanthan. The transition behaviour of these polymers was studied at a range of sodium chloride concentrations up to 30mM. The effect of salt upon the transitions is illustrated in figures 4.11a - 4.11d.

Visually the behaviour of ps.646, ps.1128 and ps.PXO_{61} was the same as that reported in the literature; the transition moved to higher temperatures as the concentration of salt increased. Sample ps.556, however, behaved quite differently (figure 4.11d). As noted already, the OR curve for this polymer, upon addition of salt, resolved into two quite separate transition steps, each of which moved to higher temperatures as the concentration of sodium chloride rose. The basis for this dual transition behaviour will be considered in section 4.10 and in the discussion.

The transition midpoint for ps.646, ps.1128 and ps.PXO_{61} (table 4.7) was found to increase linearly with the log of the salt concentration, as illustrated in figure 4.12. The melting temperatures for

the highly acetylated polymers were greater than that of ps.646 at any given salt concentration, but the gradient of the ps.646 plot was steeper, indicating that the melting temperature increased more rapidly as a function of ionic strength. The data for ps.1128, which consisted of just three transition midpoints, was extremely close to that for ps.PXO_{61}. At between 2-4mM sodium chloride the linear relationship ceased and the melting temperature began to tail off. This would be expected ultimately for any log plot, since the log of zero salt on the abscissa is at infinity. However Holzwarth (1976), in his data for Keltrol (a polymer very similar to ps.646),observed a linear relationship at sodium chloride concentrations as low as 0.4mM. The explanation for the discrepancy is probably that the sodium chloride concentration considered here is the amount added and not the absolute concentration, taking into account the small quantity of salt carried by the freeze dried polymer. At high concentrations, the effect of the additional salt would be negligible, but at 2-4mM and below, it may have raised the effective concentration and therefore the melting temperature by a significant amount.

The position of the high temperature plateau region was unaffected by salt but in the low temperature plateau region, the baseline fell as the concentration of sodium chloride increased. A similar pattern was observed by Milas and Rinaudo (1979). The extent of the fall appeared to be related to the amount of charge carried by the polymers. For the highly acetylated materials, ps.1128 and ps.PXO_{61}, the fall at 15°C was only 16 and 24 mdeg respectively and the minimum OR level, which corresponded presumably to the maximum degree of attainable order, had been reached in both cases by a concentration of 1mM added salt. In contrast, for ps.556 with its high level of pyruvic acid, the fall in the low temperature plateau at 15°C was 102 mdeg and the baseline was still falling at concentrations of greater than 20mM sodium chloride. Sample ps.646 showed intermediate behaviour. A fall of 51 mdeg was recorded between 1mM salt and the minimum attainable OR, and the maximum level of order was achieved at between 5-10mM. Dentini *et al* (1984) noted similarly, that the OR of an acetyl-free xanthan (ie. high pyruvate polymer) in the ordered state was heavily dependent upon the level of calcium perchlorate, but that for native xanthan, depyruvylated xanthan and the deacetylated and depyruvylated derivative, the effect was negligible. Interestingly, the minimum specific OR was much the same for all of the polymers. At 15°C the lowest specific OR was -159 mdeg for ps.1128, -144 mdeg for both ps.PXO_{61} and ps.646, and -130 mdeg for ps.556. This suggests that in the presence of sufficient salt, each polymer was capable of adopting a comparable degree of conformational order.

The transition breadth for ps.646 remained unchanged as the concentration of sodium chloride increased. The same behaviour was observed by Holzwarth (1976) for Keltrol, a commercial polymer produced ostensibly by the same bacterial strain. For ps.PXO_{61} though, the transition breadth narrowed considerably as the concentration of salt

rose. The pattern of behaviour for ps.1128 was difficult to judge because of the small number of complete transition curves and the difficulty in discerning the precise temperature for the onset of the conformational change.

4.10 Transition Behaviour of ps.556

The molecular basis for the two-step transition behaviour observed for ps.556 in the presence of salt was obscure. A two-stage conformational change seemed unlikely, since it was difficult to imagine quite what the two separate conformational steps could be, especially since no such pattern had been observed in the past for other high pyruvate polymers. A more likely explanation was the existence of two well-defined chemical fractions within the sample, each of which underwent the usual helix-coil transition but did so over a quite different temperature range. The level of pyruvate substitution is known to vary within a population of xanthan molecules (see section 3.2) and the presence of both a high and a low pyruvic acid fraction in ps.556 seemed to provide a satisfactory explanation for the experimental data. The high pyruvate fraction would undergo the low temperature transition, and the low pyruvate fraction that at the higher temperatures. The pyruvic acid content of ps.556 determined colorimetrically was 6.0% and the theoretical maximum, assuming one pyruvate group per side chain, is 8.1%. Thus, if the high pyruvate fraction were fully substituted, the non-substituted polymer could only account for about 25% of the total. This is consistent with the relative height of the transitions in the OR scan. At high salt concentrations, the transition height for the low temperature conformational change was about three times that of the high temperature transition. Furthermore, the fall in the low temperature plateau region was observed in what would correspond to the high pyruvate fraction. Upon depyruvylation, the OR behaviour of ps.556 in deionized water changed from the rather unusual hyperbolic shaped curve, which represented a composite of the two transition steps, to a more convention sigmoidal curve. This suggested the switch from a dual to a single step transition event.

To investigate this hypothesis an attempt was made to separate ps.556 into both a high and a low pyruvic acid fraction using ion exchange chromatography. Unfortunately this experiment was carried out during the later stages of the research project and the original sample of ps.556 had by this time been exhausted. A second sample, prepared under identical cultural conditions was however available and this was used instead. (There is no reason to suppose that the second polymer would have behaved any differently to the first but, in the absence of a polarimeter at the Edinburgh laboratory, it was not possible to establish this unequivocally.)

Approximately 10 mg of the polysaccharide was separated on a column packed with DEAE-microgranular cellulose, using a gradient of 0-2M sodium chloride in phosphate buffer (pH, 7.0). The mobile phase was passed

through the column at a flow rate of 10 ml/hr and the eluant was collected in roughly 3 ml fractions. These were subsequently analysed for the presence of carbohydrate. Aliquots (200 µl) of each fraction were treated serially with 0.2 ml of 5% aqueous phenol and 1.0 ml of concentrated sulphuric acid, mixing well after each addition. The samples were then allowed to stand for 15 minutes at ambient temperature, before reading the absorbance at 490 nm against a reagent blank. The elution profile is given in figure 4.13. It shows, quite clearly, the presence of two separate xanthan fractions, a smaller fraction, thought to be the unsubstituted polymer, which was eluted first and a much larger fraction which came off at higher sodium chloride concentrations and was thought to be the pyruvylated xanthan.

Fractions 26-33 and 103-121 were pooled and dialysed exhaustively against distilled water to remove the salts. They were then reduced in volume, using a rotary evaporator, and freeze dried. 2.4 mg of polysaccharide was recovered from the first fraction and 6.0 mg from the second. Both samples were redissolved in 1M hydrochloric acid to give a concentration of approximately 0.3% $^{w}/_{v}$ xanthan and the solutions were heated for 3 hours at 100°C in sealed glass ampoules. After cooling, the hydrolysates were centrifuged and analysed by the 2,4-dinitrophenyl-hydrazine and phenol-sulphuric acid assays to determine the percentage pyruvic acid present in each fraction. The result was not consistent with the hypothesis above. The first fraction contained 6.6% pyruvate and the second, 6.1%. In other words, within the limits of experimental error, there was no difference in pyruvic acid content between the two fractions isolated and the original polysaccharide used in the polarimetry studies. This finding created the additional problem of understanding why the material, on ion exchange chromatography, had separated into two fractions carrying apparently the same level of charge.

One final definitive experiment which remains undone, was to examine the transition behaviour of the depyruvylated sample in the presence of salt. If depyruvylated ps.556 on heating had shown the same two-step OR behaviour as the parent polymer, it would have demonstrated beyond all doubt that the pyruvic acid content could not be responsible for the atypical transition behaviour.

4.11 Thermal Hysteresis and Storage Effects

All of the polymers (with the possible exception of ps.BD9A which was not tested) showed significant thermal hysteresis in the absence of salt (see figure 4.14a). In addition, storage of the polymers without salt at 10°C, overnight or for longer periods, resulted in a time-dependent fall in the specific OR. Both phenomena could be eradicated if sufficient sodium chloride was added to the sample. Similar behaviour was observed by Cutler in his studies on Keltrol (unpublished work), and by Hacche *et al* (1987) who reported that the OR monitored for a polymer in the ordered state was lower before heating than after repeatedly heating and cooling the sample.

Both the thermal hysteresis and storage effects can be explained in kinetic terms. When the rate of ordering is sufficiently fast in comparison with the rate of cooling, all of the conformational changes will have occurred during the course of the cooling routine and hysteresis is not therefore observed. If, however, the rate of ordering is much slower, then there is a time lag between the disordering and reordering of the molecules at any given temperature. This is observed as hysteresis between the heating and cooling curves. Addition of salt, by promoting the ordering process, reduces the amount of hysteresis.

To verify this hypothesis four of the xanthan samples, namely ps.646, ps.556, ps.PXO_{61} and Flocon 4800C were tested as follows: The samples were heated, in the absence of salt, to 88°C and then cooled according to the usual regime, to 37°C (in each case this temperature was close to the transition midpoint for the cooling curve). The OR was then monitored at half hourly intervals over the next three hour period. The results for ps.PXO_{61} are shown in figure 4.14b. The specific OR at 37°C on the heating curve was -86 mdeg but, subject to the normal cooling routine, it returned to a mere -68 mdeg. Storage at 37°C, however, resulted in a further drop in the OR and after a three hour period it had fallen to -83 mdeg. By the following morning (16 hours on) it had returned to its original value. The same pattern was observed for all four samples.

This type of kinetic behaviour would explain the discrepancies in the literature with respect to thermal hysteresis. Whether or not hysteresis is observed depends on two factors, firstly, how much salt is present in the sample and secondly, the time and temperature regime over which the measurements are made. Thus, whilst Liu *et al* (1987) noted a significant amount of hysteresis even in the presence of salt, Milas and Rinaudo (1979) may have failed to do so simply because the time course of their experiments was long enough to have allowed all of the conformational changes to occur.

4.12 Effect of Dialysis on the Transition Behaviour

Comparison of the thermally induced conformational transition for a series of different polymers should be at uniform ionic strength and the samples used in this study should therefore, strictly speaking, have been dialysed against deionized water instead of simply resuspended in it. Otherwise, small quantities of salt present in the freeze dried polymers, could affect the transition behaviour. The reasons for resuspending and not dialysing were two-fold. Firstly, dialysis can slightly alter the concentration of a polysaccharide solution and thereby influence the transition behaviour in a non-uniform manner. This became apparent when an attempt was made to compare the behaviour of polymers at different salt concentrations, using samples that had been dialysed against sodium chloride solutions of the requisite concentration. Although the melting temperature increased with the sodium chloride concentration as one would expect, the specific OR in the helix and coil plateau regions of the curve

varied erratically. Secondly it was intended to look for a correlation between the transition behaviour of the polymers and the strength of the gels that they formed with locust bean gum and konjac mannan. As the materials used in the gelling experiments were not dialysed, it was considered preferable to study the order-disorder transition, in so far as possible, under similar conditions.

In the course of their preparation, the polymers were passed through sodium and chloride ion exchange resins and then dialysed against distilled water, prior to lyophilization. (The dialysis step was necessary to remove sodium azide used as a preservative.) Initially it was felt that the small quantity of ions picked up by the polymers would have only a marginal effect upon the transition behaviour. However, to test this, the OR was monitored for samples ps.646, ps.PXO_{61} and Flocon 4800C in both the dialysed and undialysed state. A single stock solution of each material was divided into two; one half was dialysed against deionized water whilst the other was not. The order-disorder transition was then monitored for both samples simultaneously. The results for Flocon 4800C are shown in figure 4.15. The specific OR in the high temperature plateau region of the curve was affected only slightly by dialysis, presumably because of a change in concentration, but the melting temperature increased by 3°C and the specific OR in the low temperature plateau region fell significantly ie. by 40 mdeg at 15°C. A similar pattern was observed for both of the other polymers. This behaviour was surprising. A rise in the melting temperature and a fall in the baseline would be expected for an increase in ionic strength, but the effect of dialysing the polymer against deionized water could only be to reduce the amount of salt present. No satisfactory explanation can be offered for this behaviour, but the data does suggest that unbound salt, contributed by the distilled water, was not the determining factor. Clearly, had the samples been dialysed against deionized water first, the results would have been, quantitatively at least, slightly different.

Retrospectively the polymers should have been dialysed against deionized water instead of distilled water before freeze drying. This would have overcome the salt and concentration problems simultaneously. However, at the time, no ready source of deionized water was available.

Despite the preparation procedure, the results are by no means invalidated. All of the polymers were prepared under uniform conditions and, as a group, it is quite reasonable to make comparisons between them. This view is supported by the striking correlation observed between the melting temperature and the acetyl and pyruvic acid content, and by the pattern expected, and seen, in the presence of salt. Due care should be taken, though, when comparing this data with that of other authors.

4.13 Discussion

In line with the reports in the literature, an extremely good correlation was found between the melting temperature of the polymers and the levels of acetyl and pyruvic acid that they carried. Acetyl had a stabilizing effect upon the ordered conformation and raised the transition midpoint, whilst pyruvate destabilized the structure and lowered the melting temperature. The destabilizing influence of pyruvic acid was the result of charge-charge repulsion between the trisaccharide side chains but the reason for the stabilizing influence of the acetyl groups is less certain. As discussed in section 4.3, it could have been the result of intramolecular apolar interactions between the methyl groups of the acetyl substituents (Smith *et al*, 1981) or alternatively, it may have been due to hydrogen bonding between the polar oxygen atom of the acetyl residue and a hydrogen bond donor in some other part of the molecule (Dentini *et al*, 1984).

Sodium chloride, by charge shielding, repressed any intramolecular repulsion and stabilized the ordered conformation. The amount of salt necessary to achieve the maximum attainable level of order increased, as one might expect, with the amount of charge carried by the polymer. Thus, the fall in the specific OR at 15°C was much greater for ps.646 and ps.556 than for ps.1128 and ps.PXO_{61} and required a much higher concentration of added salt. The fractional increase in melting temperature with sodium chloride was also greater for the more highly charged materials, as indicated by the gradient of the melting temperature versus log of the ionic strength plot.

The polymers ps.PXO_{61} and ps.556 behaved atypically. The acetyl substituents in ps.PXO_{61} did have a stabilizing effect upon the ordered structure but the stability conferred was not proportional to the amount of acetyl carried. Sample ps.PXO_{61} had nearly three times the stoichiometric amount of acetyl, but the fall in melting temperature upon deacetylation was significantly less than that for ps.1128, which carried only half the number of acetyl groups. Thus the effect of the additional substituents was, if anything, to oppose the stabilizing influence of the normal O6-linked acetate ester. Evidence from fast atom bombardment spectroscopy (Dell and Sutherland - unpublished work) indicated that the extra acetyl groups in ps.PXO_{61} were situated on the internal mannose residue. However, with so little information available about the precise location and distribution, and in the absence of a satifactory explanation for the role of the O6-linked acyl group in normal xanthan, it is impossible to speculate with any certainty about the modifying influence of the additional acetyl residues.

The polysaccharide from strain 556 produced an unusual two-step transition response which was most pronounced in the presence of salt. An attempt was made to explain this behaviour in terms of a high and a low pyruvic acid fraction within the polymer, but whilst ion exchange

chromatography resolved the material into two fractions of appropriate size, analysis by colorimetric assay indicated that they both contained roughly the same amount of pyruvic acid. A satisfactory alternative explanation is not readily available. Different charge distributions within the molecules seems unlikely since with 6% total substitution there is very little scope for different arrangements of the side chain pyruvic acid residues. The presence of a high and a low molecular weight xanthan fraction also seems improbable. According to Liu and Norisuye (1988), for the molecular weight to have such a profound effect upon the transition behaviour, it would have to be well below 2×10^5 for one fraction at least. The molecular weight of ps.556, determined by light scattering, was 1.48×10^6 (table 5.5). The existence of two well defined fractions with such vastly different molecular weights seems unlikely, and furthermore, even if they did exist, it is doubtful whether the difference in molecular weight would account for their separation by ion exchange chromatography.

The effects of the acetyl and pyruvate substituents upon the transition breadth were not clear cut. Chemical deacetylation appeared to cause a slight increase in the temperature range over which the transition occurred whilst depyruvylation produced no change, but no correlation could be found between the transition breadth and the absolute levels of acetyl and pyruvic acid.

In theory there are two ways in which the acyl substituents could affect the breadth of the helix-coil transition. Firstly, they could alter the co-operativity of the transition process and secondly, as suggested by Holzwarth and Ogletree (1979; see section 4.3), they could affect it by virtue of their distribution within the population of molecules. The observed transition behaviour is difficult to explain in terms of either theory. One possibility would be that because acetyl stabilizes the ordered conformation to high temperatures, when sufficient energy is supplied to disrupt the helix, subsequent conversion to the disordered state is very rapid (ie. more cooperative). This would be consistent with the increase in transition breadth observed upon deacetylation but is difficult to equate with an equilibrium model for the transition. The acetyl content of ps.646 was almost stoichiometric, whilst ps.1128 carried slightly more than one acetyl group per side chain. Nothing is known about the distribution of the acetyl groups within the molecule or the population but, from the quantities alone, one would expect deacetylation to have produced either an increase in homogeneity or very little change. Neither is consistent with a broadening of the OR curve.

Pyruvate, by destabilizing the ordered structure, might be expected to increase the co-operativity of the helix-coil transition. If this were the case, then depyruvylation would bring about an increase in the transition breadth, but no change was observed to occur. In both ps.646 and Flocon 4800C, roughly one in every two side chains was substituted with pyruvic acid. If these substituents were evenly distributed within the molecule and throughout the population, then depyruvylation would have produced no change in heterogeneity and therefore no change in the

transition breadth. However, in the case of ps.646, Sutherland (1981b) has demonstrated the existence of both a high and a low pyruvate fraction within the population. For this polymer at least, therefore, an increase in homogeneity and a narrowing of the transition breadth would be expected upon depyruvylation if Holzwarth and Ogletrees' argument applied.

It seems that neither the acetyl nor the pyruvic acid substituents played an important role in determining the transition breadth via either of the mechanisms outlined above, and this view is supported by the lack of correlation found between the acyl content of the polymers and the transition breadth upon computer analysis. Other factors that may, theoretically, have affected the breadth of the transition are the molecular weight distribution and the concentrations of salt and polysaccharide. The molecular weight is unlikely to have been important. (As already pointed out, there is evidence to suggest that the transition behaviour, as monitored by OR, is unaffected by the molecular weight at above 3×10^5, and the average molecular weights of the materials used in this study were probably all well above this.) Variations in the ionic strength, resulting from slight differences in the amount of salt carried by the freeze dried polymers, could have affected the behaviour, but in the case of ps.646, at least, the transition breadth appeared to be unaffected by quite high levels of sodium chloride. The same was not true of ps.PXO_{61}. Dialysing the polymers against distilled water resulted in an increase in the transition breadth and one cannot ignore the possibility that the absence of any logical pattern in the experimental data was an artifact of the procedure used to prepare the polymers (see section 4.12). Differences in the concentration of pentasaccharide repeat unit may also have been significant but, again, this seems unlikely since the transition behaviour of xanthan at uniform ionic strength is concentration independent and since there was no detectable relationship between the transition breadth and the total level of acyl substitution.

In conclusion, it seems that there is no single, elementary explanation available for the transition breadth behaviour of xanthan and it is likely that a whole series of different factors interact to influence this. Workers may, in the past, have been too ready to produce simplistic explanations for the behaviour of what is a very complex system, on the basis of very limited experimental evidence.

There appeared to be a correlation between the transition height and the degree of acetyl and pyruvic acid substitution. The lower the level of each substituent, the greater the shift in OR over the course of the transition. The most obvious factor affecting the transition height would be the concentration of pentasaccharide repeat unit. Since all of the measurements were made on 0.3% $^{w}/_{w}$ polysaccharide solutions, those polymers with less acetyl and pyruvate will have contained more pentasaccharide as a proportion of the total weight. According to Rees (1970), the OR is related directly to the bond angles of the glycosidic linkages and the OR span would therefore be expected to increase upon

removal of the acetyl and pyruvic acid substituents, as indeed it did. In table 4.4 an attempt has been made to quantify the change in the sugar content and in the transition height in percentage terms. In every case the increase in the transition height was far greater than would be expected as a result of the increase in pentasaccharide repeat unit alone. At its most extreme a 224% increase was seen in the transition height of Flocon 4800C upon depyruvylation, but the increase in the sugar content was only 3.2%. Other factors affecting the concentration of polysaccharide, for example differences in the amount of water and other contaminants in the freeze dried polymer (section 3.9), or differences in the amount of polysaccharide filtered out in the form of microgels, would also have made only a minor contribution towards the change in transition height.

Another important factor will have been the degree of order attainable by the polymer at low temperature, under the prevailing ionic conditions. An examination of the effect of salt on the transition behaviour showed that if sufficient sodium chloride were present all of the polymers tested were capable of adopting a comparable degree of order, as judged from the specific OR in the low temperature plateau region of the curve. Under conditions of low ionic strength, however, the more highly charged polymers were prevented from adopting a very ordered structure by intramolecular repulsion between the charged trisaccharide side chains. Thus the acetyl and pyruvic acid content of the polymers was important in dictating the amount of order. Taking this argument to its logical conclusion, the specific OR at 15°C should have decreased as the pyruvic acid content of the polymers fell and the transition height should have increased simultaneously. This was observed to occur but, contrary to expectation, deacetylation produced the same effect. No correlation was detected between the specific OR in the low temperature plateau region of the curve and the levels of acetyl and pyruvic acid substitution.

The amount of order achieved by the polymers could have been restricted by ultrastructural features, such as the absence of side chains from regions of the cellulosic backbone. It may also have been influenced by the time of storage prior to the experiment (approximately 16 hours). A time dependent fall in the low temperature plateau region of the curve was observed upon cold storage and differences in the rate of ordering could have affected the specific OR and the transition height. The reason for the fall in the baseline is uncertain. It could have been the result of kinetic factors, as discussed in section 4.11. Alternatively it may have been related to the aggregation of molecules in the ordered state, as illustrated in the following equation. (A.N. Cutler - personal communication).

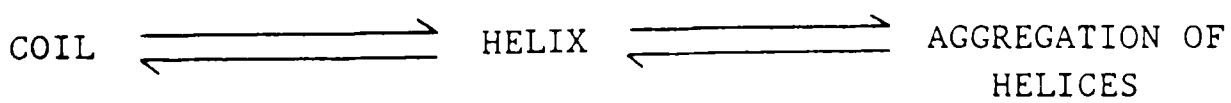

Assuming that regions of order and disorder can coexist within the same molecule, as they appear to do, then aggregation of the partially ordered strands could draw more of the molecule into the ordered form, thereby reducing the OR. The problem with such an equilibrium argument is the presupposition that order is essential, and not merely beneficial, for aggregation. This being the case the most highly ordered polymers should be the most aggregated and vice versa. This was clearly not the case for ps.646 which showed a pronounced tendency to aggregate but had a relatively high specific OR in the low temperature plateau region of the curve. Finally, the position of the baseline may have been influenced slightly by differences in the ionic strength as a result of ions carried by the freeze dried polymers.

The position of the high temperature plateau region could also have affected the transition height The pattern of behaviour for the specific OR in the high temperature plateau region of the curve was surprising. If, as Rees says, the OR is dictated by the bond angles of the glycosidic linkages, then the specific OR in the random coil state should have been much the same for all of the polymers, except for slight variations resulting from differences in the concentration of pentasaccharide repeat unit. Deacetylation and depyruvylation should also have had very little effect. In fact there were enormous differences between the polymers. For those materials carrying very little acetyl or pyruvate, the mean specific OR varied from -24 to +55 mdeg, a span greater than the total transition height for some polymers. Deacetylation produced no change in the specific OR, except in the case of ps.PXO_{61} where there was a slight positive shift, but depyruvylation produced a large positive shift in every case. Indeed, a significant correlation was found between the amount of pyruvate and the maximum specific OR when ps.PXO_{61} and ps.556, together with their chemically modified derivatives, were omitted from the computer analysis. This correlation was strengthened when pyruvate and acetyl were considered together. Although the disordered state of xanthan is normally referred to as a "random coil" and is believed by some authors to be literally that (Morris *et al*, 1977a), the available evidence, albeit limited, suggests that xanthan in the disordered state is still quite a stiff molecule. Such evidence includes the relatively small change in intrinsic viscosity reported by Milas and Rinaudo (1979; see section 4.4) and other authors, over the temperature range of the transition. If xanthan in the high temperature plateau region of the curve is not genuinely a random coil, then the local geometry might well be heavily influenced by structural features such as the level of acetyl and pyruvic acid substituents. Pyruvate could by some, as yet unknown mechanism, restrict the mobility of the sugar residues around the glycosidic linkages, thereby reducing the OR. This would account for the positive shift in OR upon depyruvylation, but still does not explain satisfactorily, the apparent random variation in the maximum specific OR among the polymers tested. The presence of an optically active contaminant is a simple and attractive possibility here, but all of the available evidence suggests that the xanthans were actually extremely pure (section 3.9).

Having considered the likely influences, one is led, once again, to the conclusion that the transition height, the low temperature specific OR and possibly also the high temperature specific OR, are dictated by a series of different structural and environmental factors.

As with other authors, attempts at explaining the OR behaviour of xanthan have so far centred on the behaviour of the individual molecule in solution and any possible concentration effects have been ignored. Nevertheless, for all of the polymers studied, a 0.3% $^{w}/_{w}$ solution of the polysaccharide was well above the overlap concentration (c^{*}) and it would be quite extraordinary if the interactions that must inevitably have occurred between molecules, had no effect at all on the OR measurements. Broadly speaking there are two ways in which the high polysaccharide concentration could affect the OR behaviour. Firstly, intermolecular interactions could alter the OR indirectly by promoting or inhibiting the adoption of the ordered conformation. The time-dependent fall in the low temperature specific OR due, it was suggested, to a shift in equilibrium towards the ordered form as a result of molecular aggregation would be an example of this type of behaviour. Alternatively, the intermolecular interactions might affect the OR directly via some other mechanism. The relationship demonstrated by Rees (1970) between the OR and the glycosidic bond angles was semi-empirical and it appears that no attempt has been made to derive this relationship from first principles. It is conceivable therefore, that other factors besides the bond angles could influence the chiroptical behaviour, and this view is supported by the wide variation in the specific OR at high temperatures observed for the polymers in this study. More direct evidence was supplied by Hjelm *et al* (1986) who showed that the CD spectrum in the soret region for sickle-cell deoxyhaemoglobin fibre gels was affected by the linear dichroism and linear birefringence of the individual molecules, even when no net linear dichroism or birefringence could be demonstrated. Since CD and OR are so closely related it is possible that the OR of a system like xanthan, which shows molecular anisotropy, could be affected by similar factors. Such concentration effects may account for certain of the anomalies observed in the xanthan systems studied.

Perhaps one of the most important conclusions one can draw from this discussion is that whilst it may be possible to explain some aspects of the transition behaviour of xanthan in relatively simple molecular terms, the system is extremely complicated. One should, therefore, be aware of the limitations of the experimental technique used to monitor the transition and not be to dogmatic in interpreting the evidence, especially where the amount of data is limited.

Table 4.1: Experimental techniques used to study the helix-coil transition of xanthan.

Method	Reference
Polarimetry	Callet *et al*, 1987 Dentini *et al*, 1984 Frangou *et al*, 1982 Gravanis *et al*, 1987 Hacche *et al*, 1987 Holzwarth *et al*, 1976 Holzwarth and Ogletree, 1979 Liu *et al*, 1987 Liu and Norisuye, 1988 Milas and Rinaudo, 1979; 1981; 1986 Morris, 1977 Morris *et al*, 1977a; 1983 Norton *et al*, 1984 Parry, 1985 Rinaudo *et al*, 1983 Smith *et al*, 1981
Stopped-flow polarimetry	Norton *et al*, 1980; 1984
Circular dichroism	Dentini *et al*, 1984 Milas and Rinaudo, 1979 Morris, 1977 Morris *et al*, 1977a Southwick *et al*, 1979
Nuclear magnetic resonance	Morris, 1977 Morris *et al*, 1977a
Viscometry	Gravanis *et al*, 1987 Jeanes *et al*, 1961 Holzwarth, 1976 Milas and Rinaudo, 1986 Morris, 1977 Morris *et al*, 1977a Southwick *et al*, 1979
Intrinsic viscosity measurements	Hacche *et al*, 1987 Liu *et al*, 1987 Liu and Norisuye, 1988 Milas and Rinaudo, 1979; 1986

Table 4.1: continued.

Method	Reference
Dynamic oscillatory shear testing	Rochefort and Middleman, 1987
Light scattering	Hacche *et al*, 1987 Liu *et al*, 1987 Norton *et al*, 1984 Rees, 1981 Southwick *et al*, 1979
Differential scanning calorimetry	Dentini *et al*, 1984 Norton *et al*, 1984 Paoletti *et al*, 1983
Photon correlation spectroscopy	Morris *et al*, 1983
Birefringence	Milas and Rinaudo, 1979; 1981
Potentiometry	Milas and Rinaudo, 1981
Conductance measurements	Milas and Rinaudo, 1986

Table 4.2: Optical rotation data for the helix-coil transition of a range of xanthans differing in acetyl and pyruvate content.

Polymer	% Ac	% Pyr	T_m (°C)	Transition Breadth (°C)	Transition Height (mdeg)	$[\alpha]_{365}$ at 15°C (mdeg)	Maximum $[\alpha]_{365}$ (mdeg)	Thermal Hysteresis
ps.646[a]	4.5	4.4	44	27	46	-	-23	+
			45	23	37	-	-23	
			44	21	38	-	-34	
DA ps.646	1.3	3.6	32	29	76	-101	-23	+
			31	36	96	-124	-27	
DP ps.646	4.4	0.6	52	24	99	-110	+14	+
			51	29	103	-107	+8	
DAP ps.646	1.0	0.6	40	23	135	-131	+31	+
			40	24	119	-125	+11	
ps.1128	7.7	1.7	54	20	78	-126[b]	-20	+
			55	20	80	-125[b]	-21	
DA ps.1128 (Batch 1)	1.6	1.3	42	29	151	-183	-22	+
			42	30	164	-195	-25	
$ps.PXO_{61}$	14.3	0.3	53	35	75	-115	-29	+
			49	29	63	-107	-34	
			47	38	75	-102	-23	
DA $ps.PXO_{61}$	2.3	0.8	42	34	113	-139	-17	+
			42	35	118	-130	-2	
ps.556[a]	1.6	6.0	38	22	56	-44	+13	+
			38	20	50	-30	+28	
DP ps.556	1.1	1.0	41	34	133	-79	+64	+
			41	28	101	-67	+46	
Flocon 4800C	2.0	4.9	28	20	43	-102	-58	+
			27	24	30	-91	-61	
DP Flocon 4800C	2.7	1.0	44	23	123	-151	-12	+
			46	26	116	-139	-7	

a Data unreliable; see text for details.
b Determined by extrapolation of the baseline.

Table 4.3: The influence of acetyl and pyruvate content upon the melting temperature, transition breadth, transition height and the specific optical rotation in the helix and coil plateau regions of the transition curve.

Polymer	% Ac	% Pyr	Ac/Pyr	T_m (°C)	Mean Optical Rotation Data			
					Transition Breadth (°C)	Transition Height (mdeg)	$[\alpha]_{365}$ at 15°C (mdeg)	Maximum $[\alpha]_{365}$ (mdeg)
High Ac, High Pyr								
ps.646[a]	4.5	4.4	1.02	44.0	23.5	40	-	-27
High Ac, Low Pyr								
DP ps.646	4.4	0.6	7.33	51.5	26.5	101	-109	+11
ps.1128	7.7	1.7	4.53	54.5	20.0	79	-126[b]	-21
ps.PXO_{61}	14.3	0.3	47.67	49.5	34.0	71	-108	-29
Low Ac, High Pyr								
DA ps.646	1.3	3.6	0.36	31.5	32.5	86	-113	-25
ps.556[a]	1.6	6.0	0.27	38.0	21.0	53	-37	+21
Flocon 4800C[a]	2.0	4.9	0.41	27.5	22.0	37	-97	-60
Low Ac, Low Pyr								
DAP ps.646	1.0	0.6	1.67	40.0	23.5	127	-128	+21
DA ps.1128 (Batch 1)	1.6	1.3	1.23	42.0	29.5	158	-189	-24
DA ps.PXO_{61}	2.3	0.8	2.88	42.0	34.5	116	-135	-10
DP ps.556	1.1	1.0	1.10	41.0	31.0	117	-73	+55
DP Flocon 4800C	2.7	1.0	2.70	45.0	24.5	120	-145	-10

a Data unreliable; see text for details.
b Determined by extrapolation of the baseline.

Table 4.4: Comparison between the percentage change in transition height and the percentage increase in sugar content of the polymer upon chemical modification.

Polymer	Modification	% Increase in Sugar Content[a]	% Increase in Transition Height
ps.646	Deacetylation	4.0	115
ps.1128	Deacetylation	6.5	100
ps.PXO_{61}	Deacetylation	11.5	63
ps.646	Depyruvylation	3.9	152
ps.556	Depyruvylation	5.5	121
Flocon 4800C	Depyruvylation	3.2	224
ps.646	Deacetylation and depyruvylation	7.3	218

a Equal to the percentage decrease in acyl substitution as a proportion of the total weight.

Table 4.5a: Correlation matrix relating acetyl, pyruvate and intrinsic viscosity to the helix-coil transition behaviour as monitored by optical rotation (all samples are included in the analysis).

	% Ac	% Pyr	Intrinsic Viscosity (dl/g)	T_m (°C)	Transition Breadth (°C)	Transition Height (mdeg)	$[\alpha]_{365}$ at 15°C (mdeg)	Maximum $[\alpha]_{365}$ (mdeg)
% Ac	1.000	-0.336	0.456	0.617	0.247	-0.303	(0.004)	-0.336
% Pyr	-0.336	1.000	0.305	-0.570	-0.470	-0.698	(0.546)	-0.259
Intrinsic Viscosity (dl/g)	0.456	0.305	1.000	0.310	-0.276	-0.474	(0.245)	-0.261
T_m (°C)	0.617	-0.570	0.310	1.000	0.011	0.152	(-0.217)	0.152
Transition Breadth (°C)	0.247	-0.470	-0.276	0.011	1.000	0.370	(-0.203)	0.046
Transition Height (mdeg)	-0.303	-0.698	-0.474	0.152	0.370	1.000	(-0.690)	0.432
$[\alpha]_{365}$ at 15°C (mdeg)	(0.004)	(0.546)	(0.245)	(-0.217)	(-0.203)	(-0.690)	(1.000)	(0.377)
Maximum $[\alpha]_{365}$ (mdeg)	-0.336	-0.259	-0.261	0.152	0.046	0.432	(0.377)	1.000

N.B. The data for the specific OR at 15°C is shown in brackets because in the absence of any information for ps.646, this particular variable had to be considered separately.

Table 4.5b: Regression models for the dependent variables

Number in Model	Variables in Model	R-Square for Dependent Variable				
		T_m (°C)	Transition Breadth (°C)	Transition Height (mdeg)	$[\alpha]_{365}$ at 15°C (mdeg)	Maximum $[\alpha]_{365}$ (mdeg)
1	% Ac	0.381	0.061	0.092	(0.000)	0.113
1	% Pyr	0.325	0.221	0.488	(0.298)	0.067
1	Intrinsic Viscosity	0.096	0.076	0.224	(0.060)	0.068
2	% Ac % Pyr	0.529	0.230	0.813	(0.351)	0.269
2	% Ac Intrinsic Viscosity	0.382	0.252	0.234	(0.075)	0.127
2	% Pyr Intrinsic Viscosity	0.583	0.240	0.562	(0.304)	0.103
3	% Ac % Pyr Intrinsic Viscosity	0.613	0.294	0.824	(0.361)	0.282

Table 4.6a: Correlation matrix relating acetyl, pyruvate and intrinsic viscosity to the helix-coil transition behaviour as monitored by optical rotation (ps.PXO_{61}, Deacetylated ps.PXO_{61}, ps.556 and depyruvylated ps.556 are not included in the analysis).

	% Ac	% Pyr	Intrinsic Viscosity (dl/g)	T_m (^oC)	Transition Breadth (^oC)	Transition Height (mdeg)	$[\alpha]_{365}$ at 15^oC (mdeg)	Maximum $[\alpha]_{365}$ (mdeg)
% Ac	1.000	-0.009	0.765	-0.761	-0.502	-0.371	(0.160)	-0.029
% Pyr	-0.009	1.000	0.216	-0.576	-0.054	-0.837	(0.475)	-0.807
Intrinsic Viscosity (dl/g)	0.765	0.216	1.000	0.351	-0.372	-0.359	(0.101)	-0.328
T_m (^oC)	0.761	-0.576	0.351	1.000	-0.299	0.216	(-0.243)	0.516
Transition Breadth (^oC)	-0.502	-0.054	-0.372	-0.299	1.000	0.391	(-0.267)	0.062
Transition Height (mdeg)	-0.371	-0.837	-0.359	0.216	0.391	1.000	(-0.853)	0.583
$[\alpha]_{365}$ at 15^oC (mdeg)	(0.160)	(0.475)	(0.101)	(-0.243)	(-0.267)	(-0.853)	(1.000)	(-0.126)
Maximum $[\alpha]_{365}$ (mdeg)	-0.029	-0.807	-0.328	0.516	0.062	0.583	(-0.126)	1.000

Table 4.6b: Regression models for the dependent variables.

Number in Model	Variables in Model	R-Square for Dependent Variable				
		T_m (°C)	Transition Breadth (°C)	Transition Height (mdeg)	$[\theta C]_{365}$ at 15°C (mdeg)	Maximum $[\theta C]_{365}$ (mdeg)
1	% Ac	0.580	0.252	0.137	(0.026)	0.001
1	% Pyr	0.332	0.003	0.700	(0.225)	0.651
1	Intrinsic Viscosity	0.124	0.139	0.129	(0.010)	0.107
2	% Ac % Pyr	0.904	0.256	0.844	(0.295)	0.652
2	% Ac Intrinsic Viscosity	0.708	0.252	0.151	(0.027)	0.226
2	% Pyr Intrinsic Viscosity	0.569	0.139	0.734	(0.225)	0.676
3	% Ac % Pyr Intrinsic Viscosity	0.933	0.257	0.878	(0.458)	0.696

Table 4.7: The influence of sodium chloride concentration upon the melting temperature of xanthan.

[NaCl] M x 10^{-3}	log [Na^+]	T_m (°C) ps.646	ps.1128	ps.PXO_{61}
0	-	-	56.0	57.0
0.5	-3.30	-	-	59.5
1.0	-3.00	43.0	61.0	61.5
2.0	-2.70	47.0	-	65.0
4.0	-2.40	-	-	-
5.0	-2.30	52.5	73.0	71.5
10.0	-2.00	62.0	81.0	78.5
20.0	-1.70	75.0	-	85.5
30.0	-1.52	81.0	-	90.0

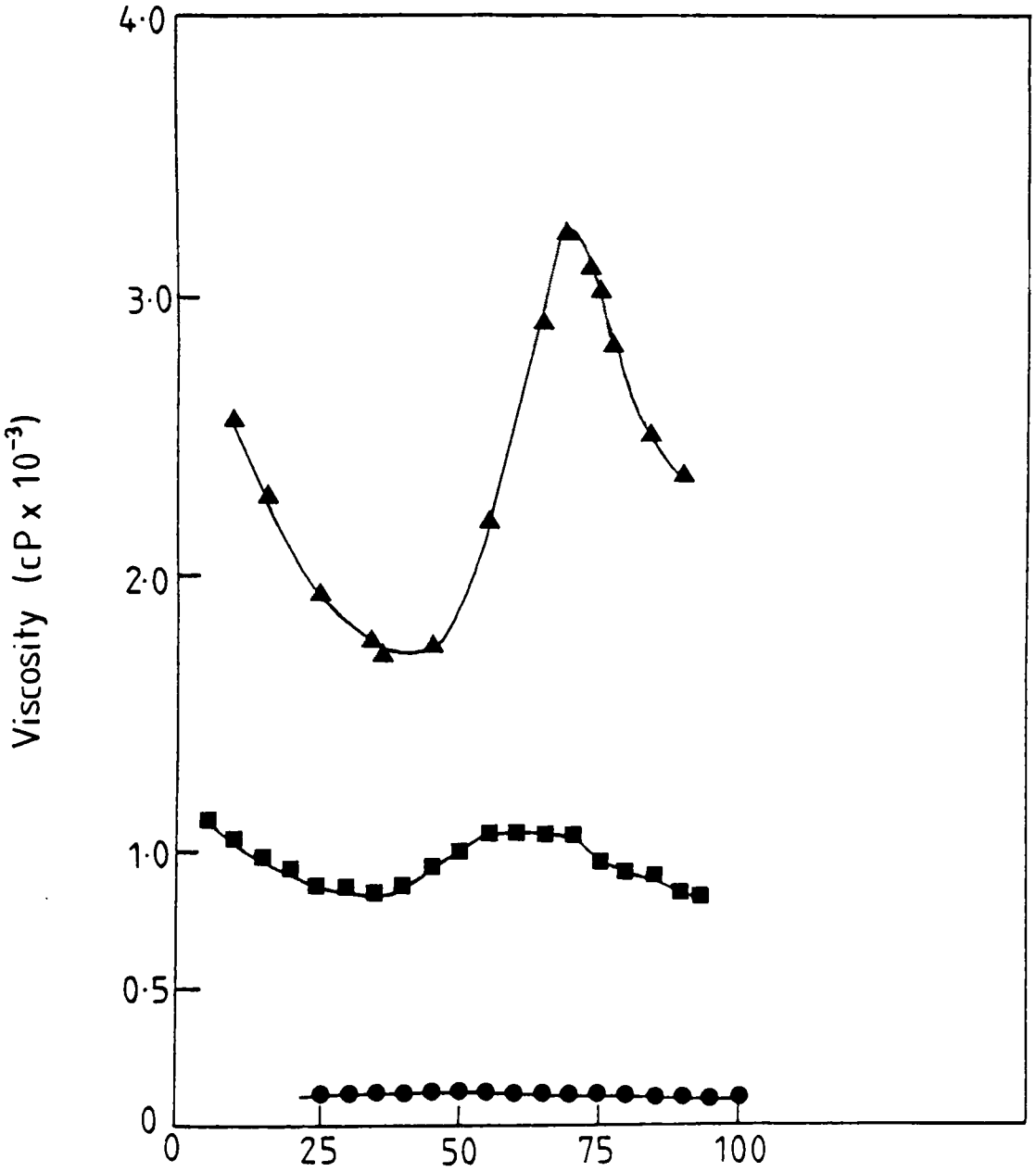

Fig. 4·1 Effect of temperature upon the viscosity of xanthan solutions at 0·1% (●), 0·5% (■) and 1·0% (▲) total polysaccharide concentration in the absence of salt (Jeanes et al, 1961)

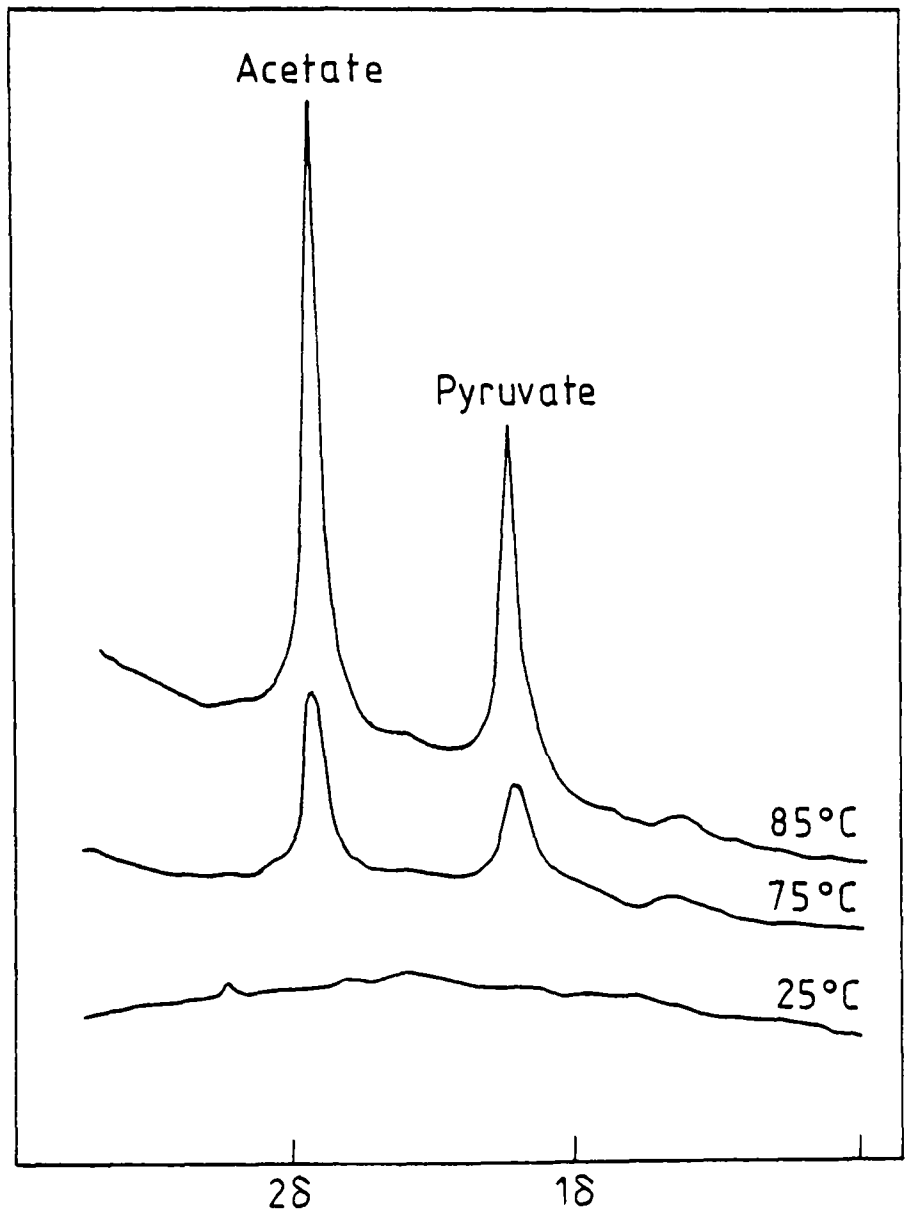

Fig. 4·2 Part of the high resolution proton magnetic resonance spectrum of xanthan, showing the effect of temperature on observable signal (Morris et al, 1977a).

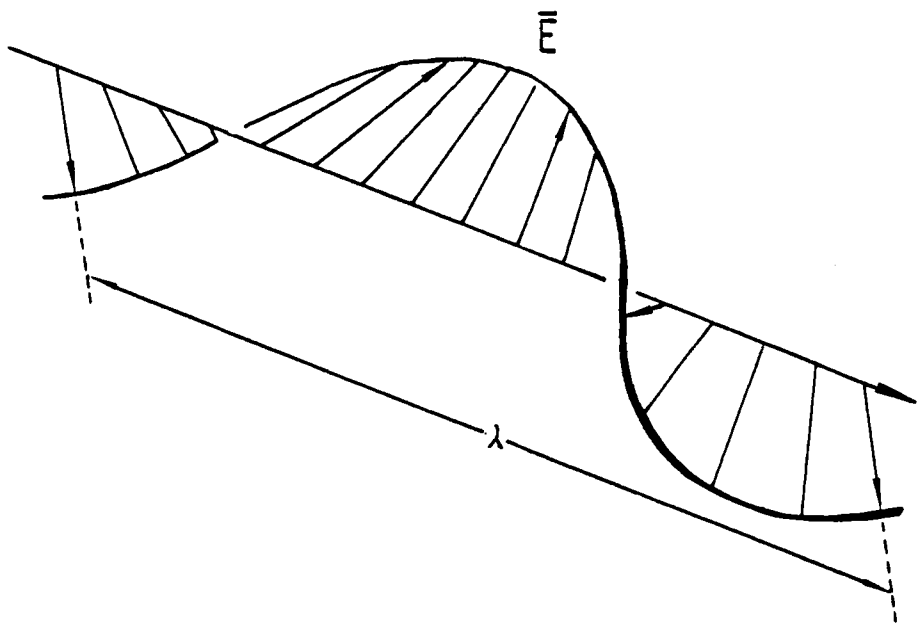

Fig. 4·3 Right circularly polarized radiation (only the electric field is shown).

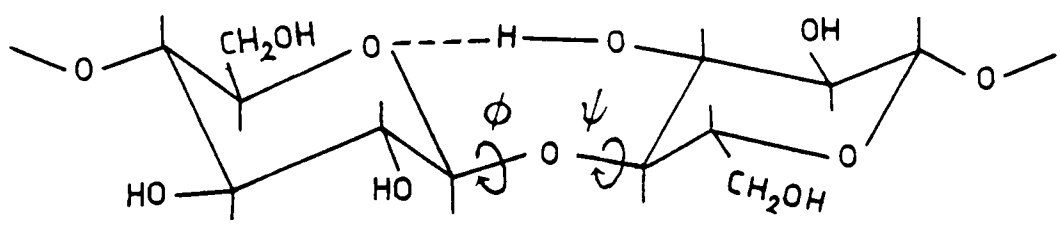

Fig. 4·4 Interresidue linkages in cellulose showing the dihedral angles ϕ and ψ.

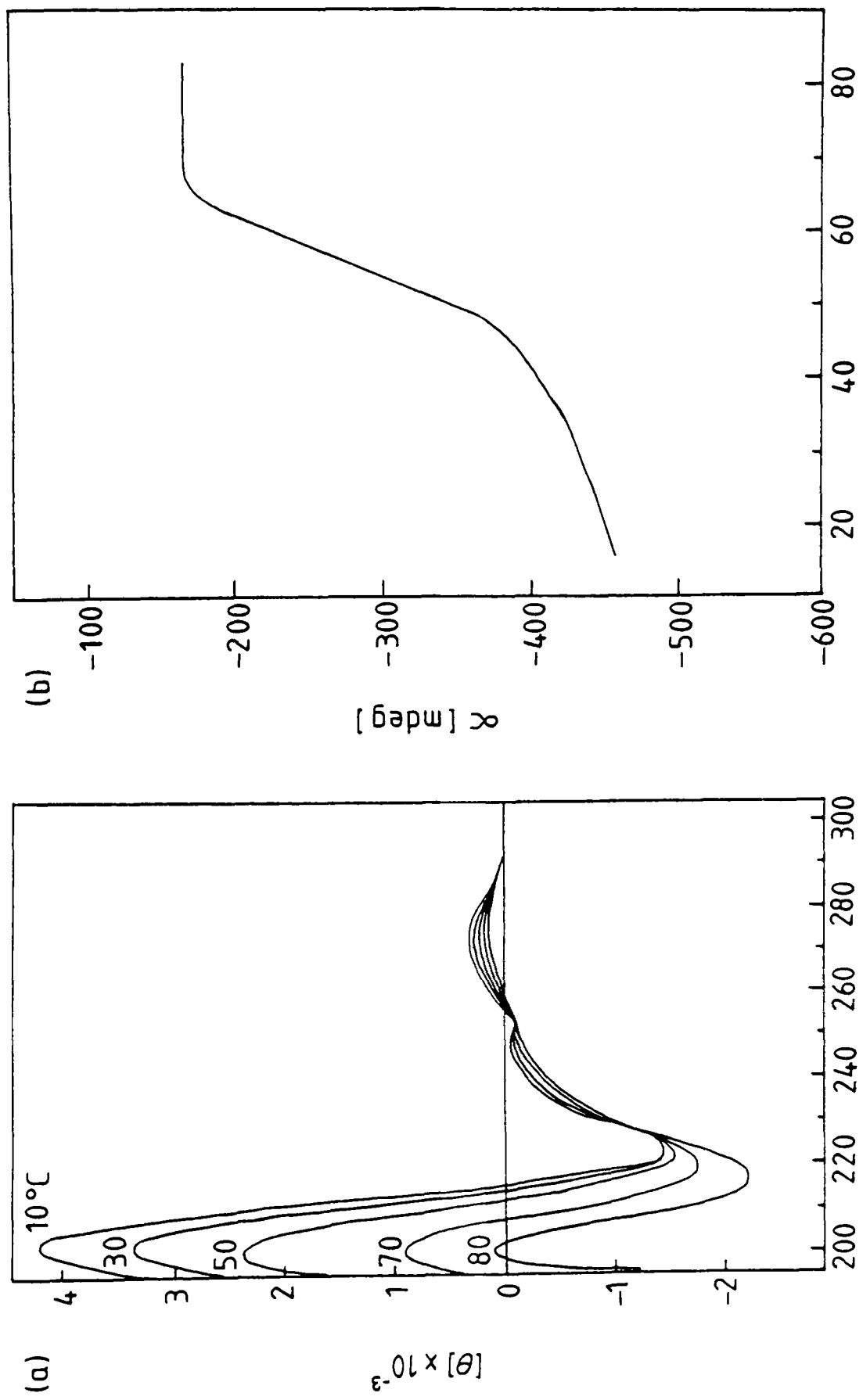

Fig. 4·5 Temperature dependence of the chiroptical behaviour of xanthan. (a) Circular dichroism. (b) Optical rotation at 365 nm (Morris et al, 1977a).

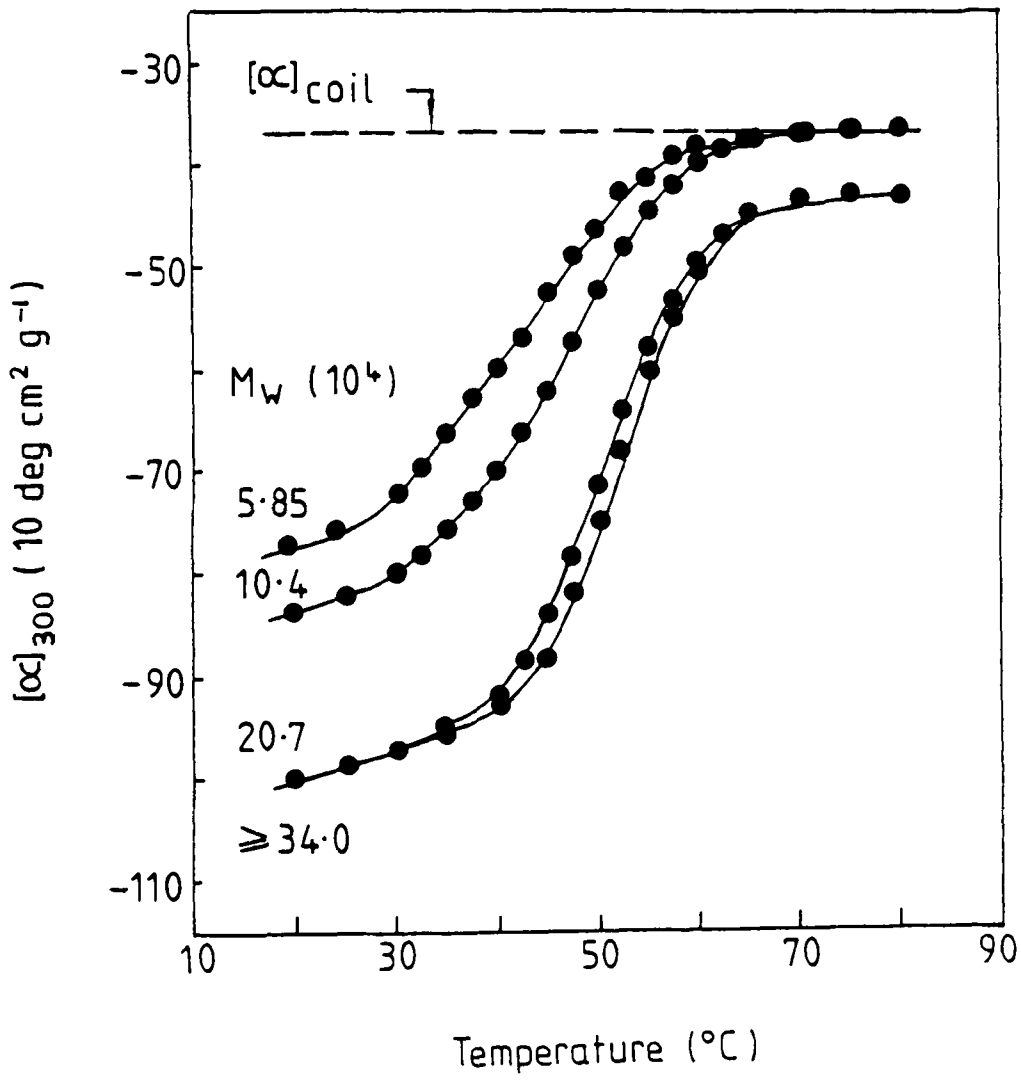

Fig. 4·6 Curves of $[\alpha]_{300}$ versus temperature as a function of molecular weight for xanthan in 0·01M aqueous NaCl (Liu and Norisuye, 1988).

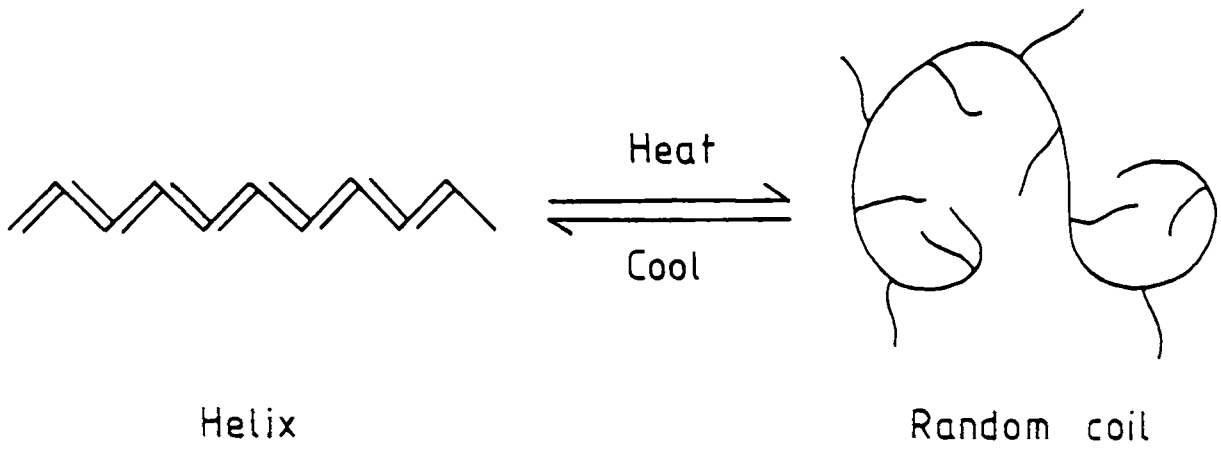

Fig. 4·7 Diagrammatic representation of the single-stranded helix to random coil model for the thermally induced conformational transition (Morris et al, 1977a).

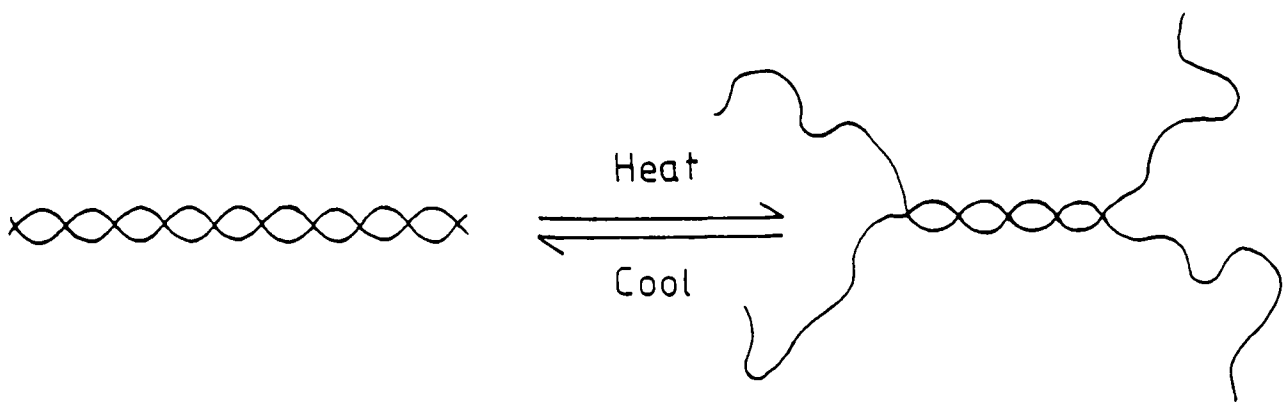

Fig. 4·8 Diagrammatic representation of the double helix to expanded dimer model for the thermally induced conformational transition (Liu and Norisuye, 1988).

Fig. 4·9 Order-disorder transition as monitored by optical rotation for a series of native and chemically modified xanthans (0·3 % $w/_w$) in the absence of salt.

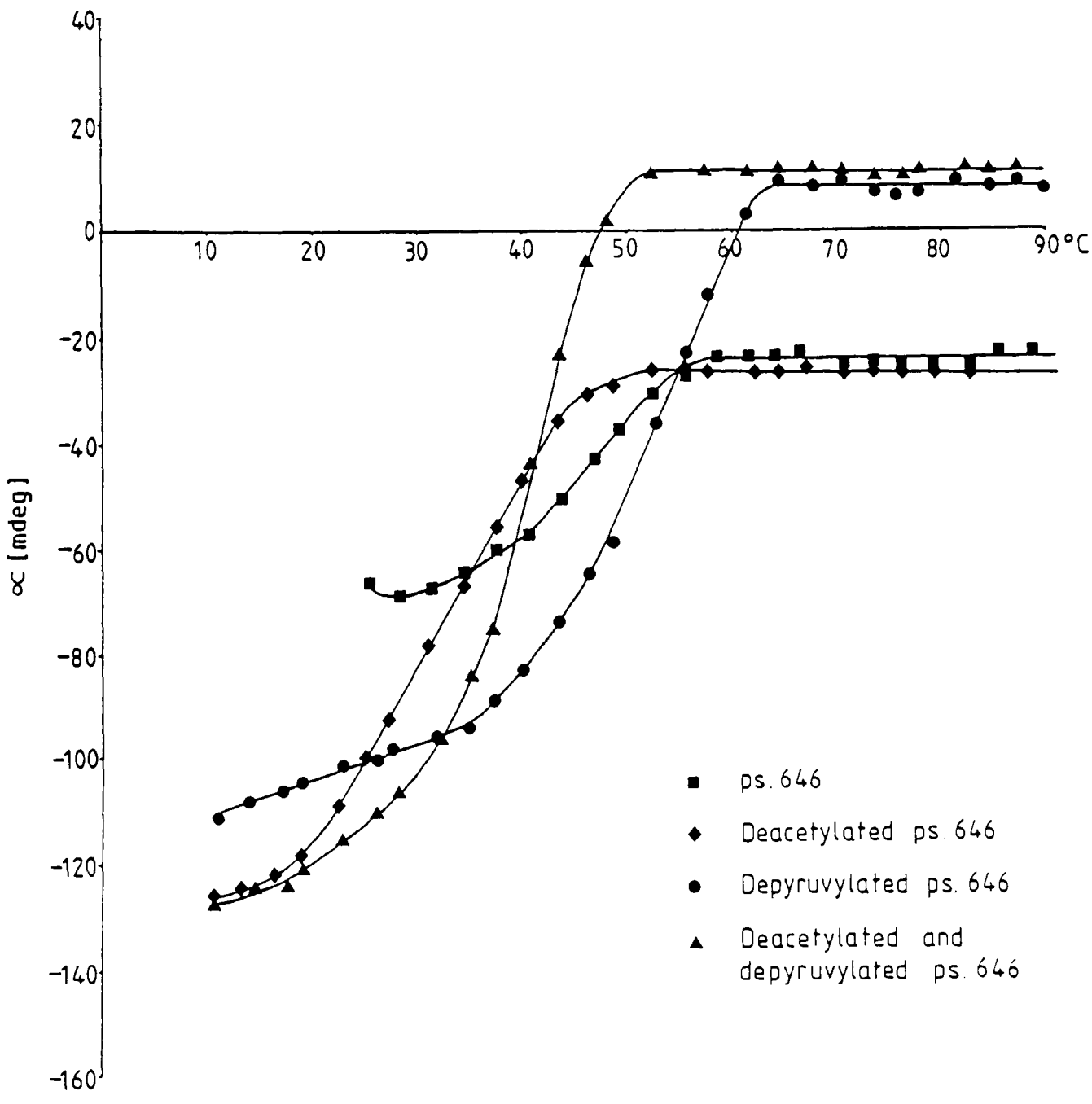

a) ps. 646 and its chemically modified derivatives

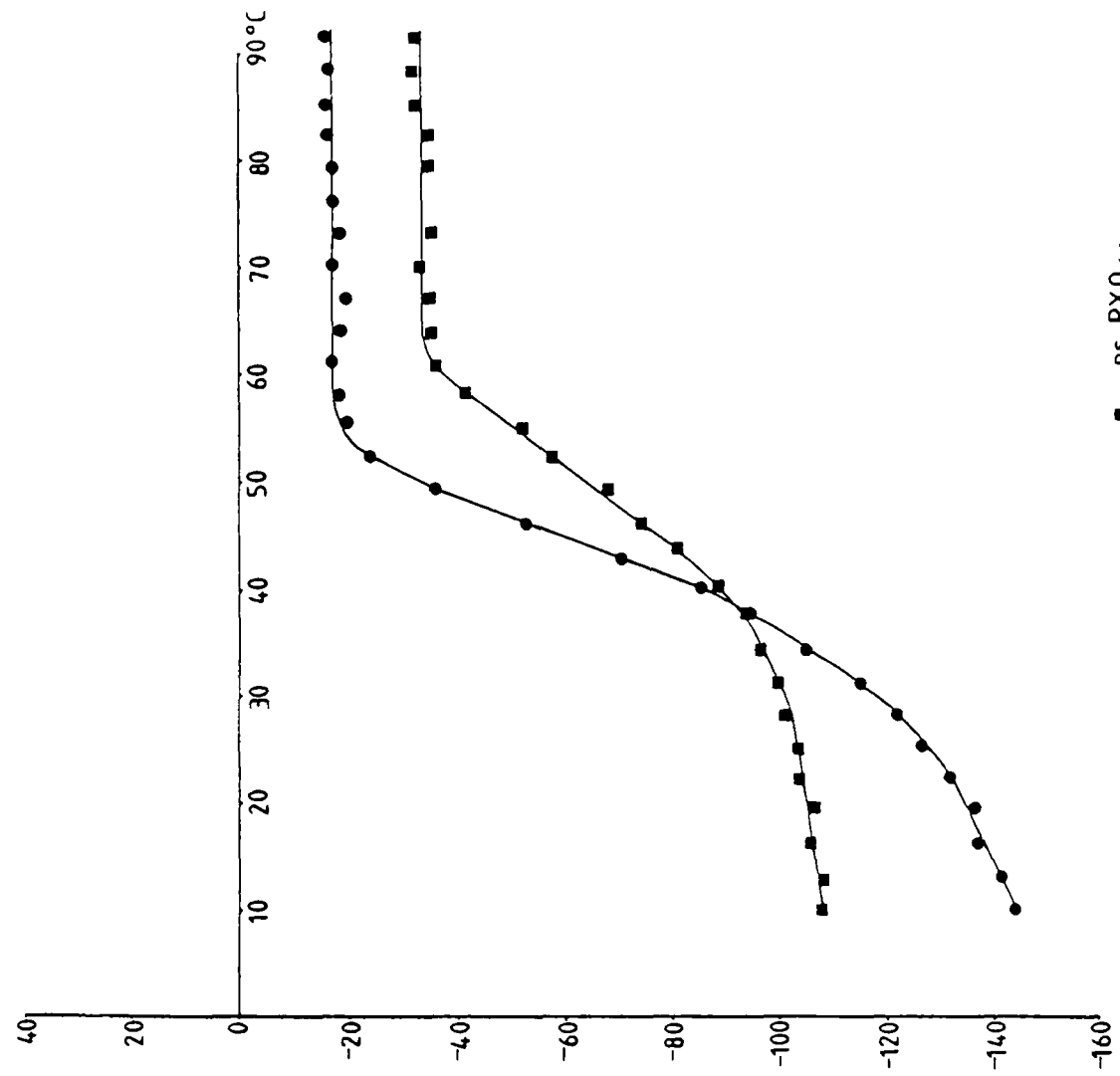

c) ps. PXO_{61} and deacetylated ps. PXO_{61}

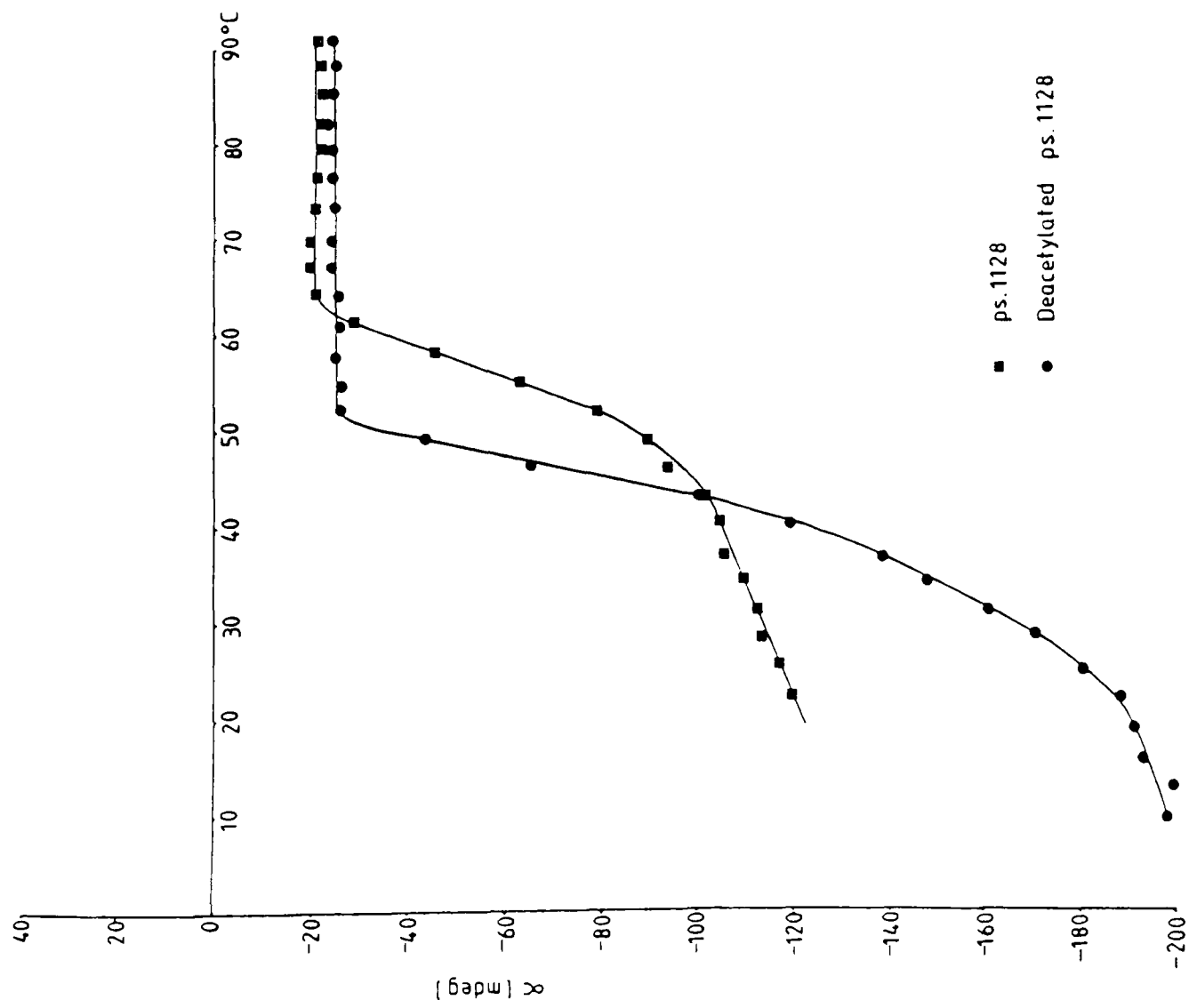

b) ps.1128 and deacetylated ps.1128

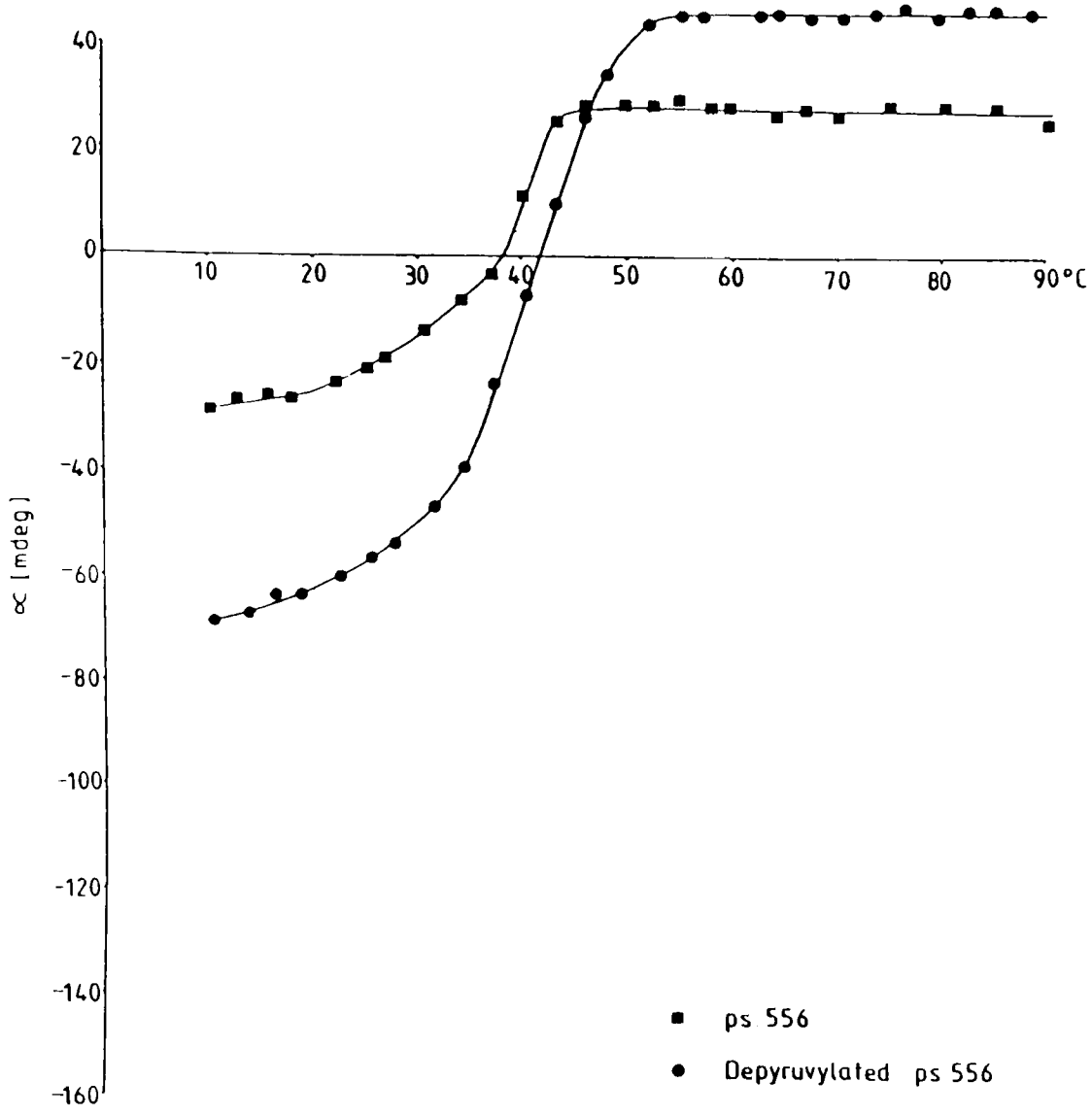

d) ps. 556 and depyruvylated ps. 556

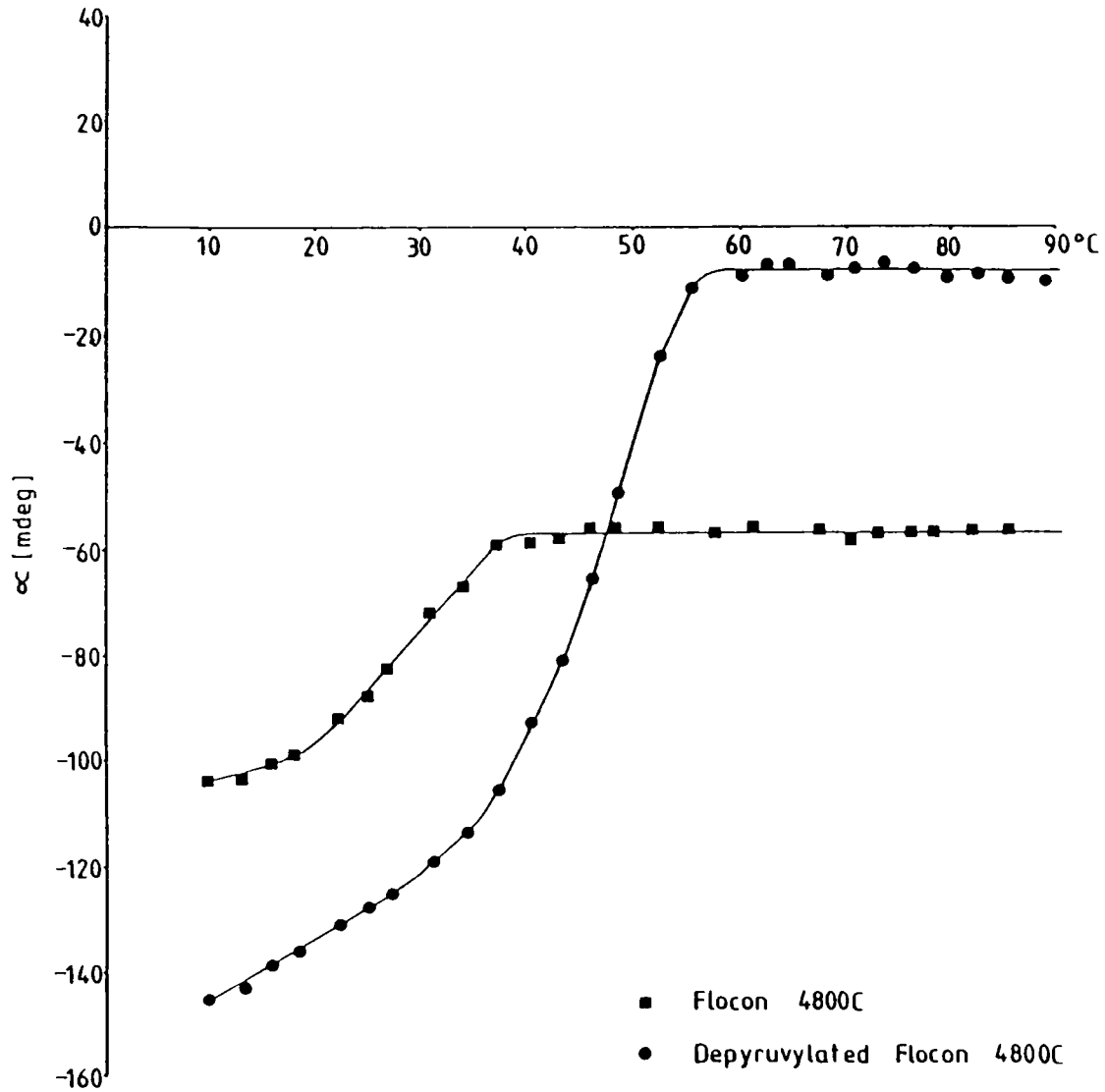

e) Flocon 4800C and depyruvylated Flocon 4800C

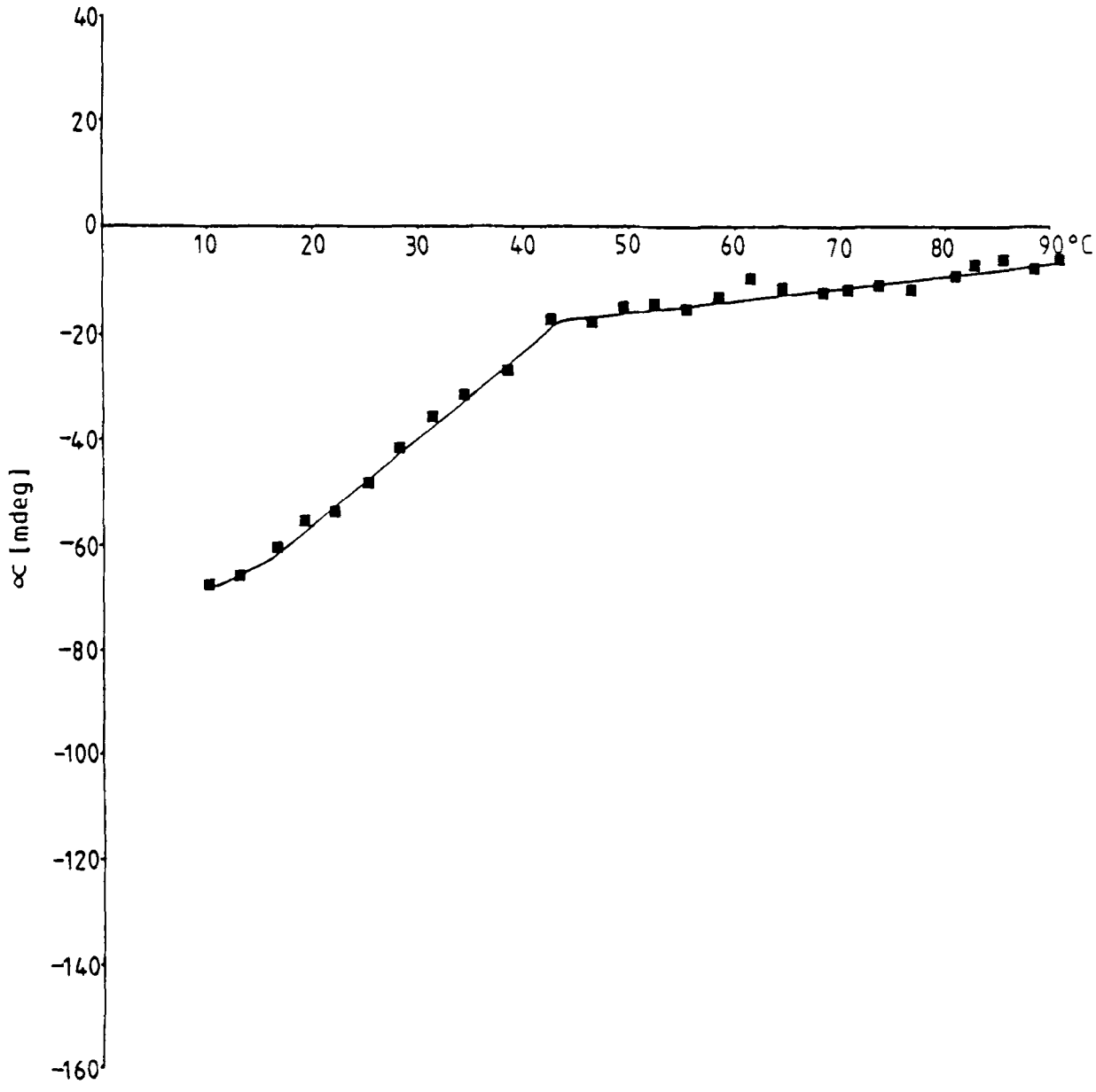

f) ps. B09A

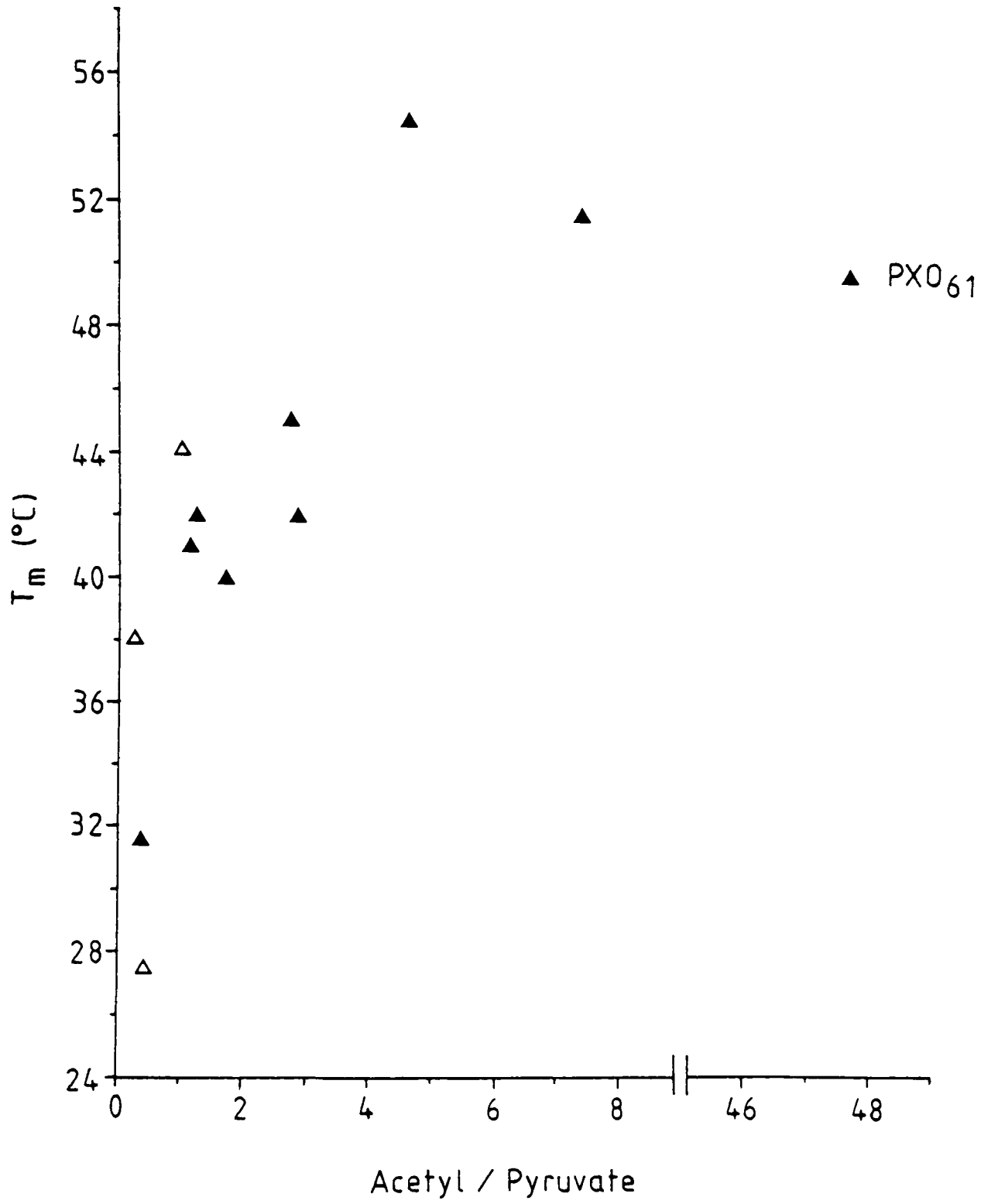

Fig. 4·10 Plot of melting temperature versus acetyl : pyruvic acid ratio.

Fig. 4·11 Order-disorder transition as monitored by optical rotation, for xanthan (0·3 %) at a series of different ionic strengths.

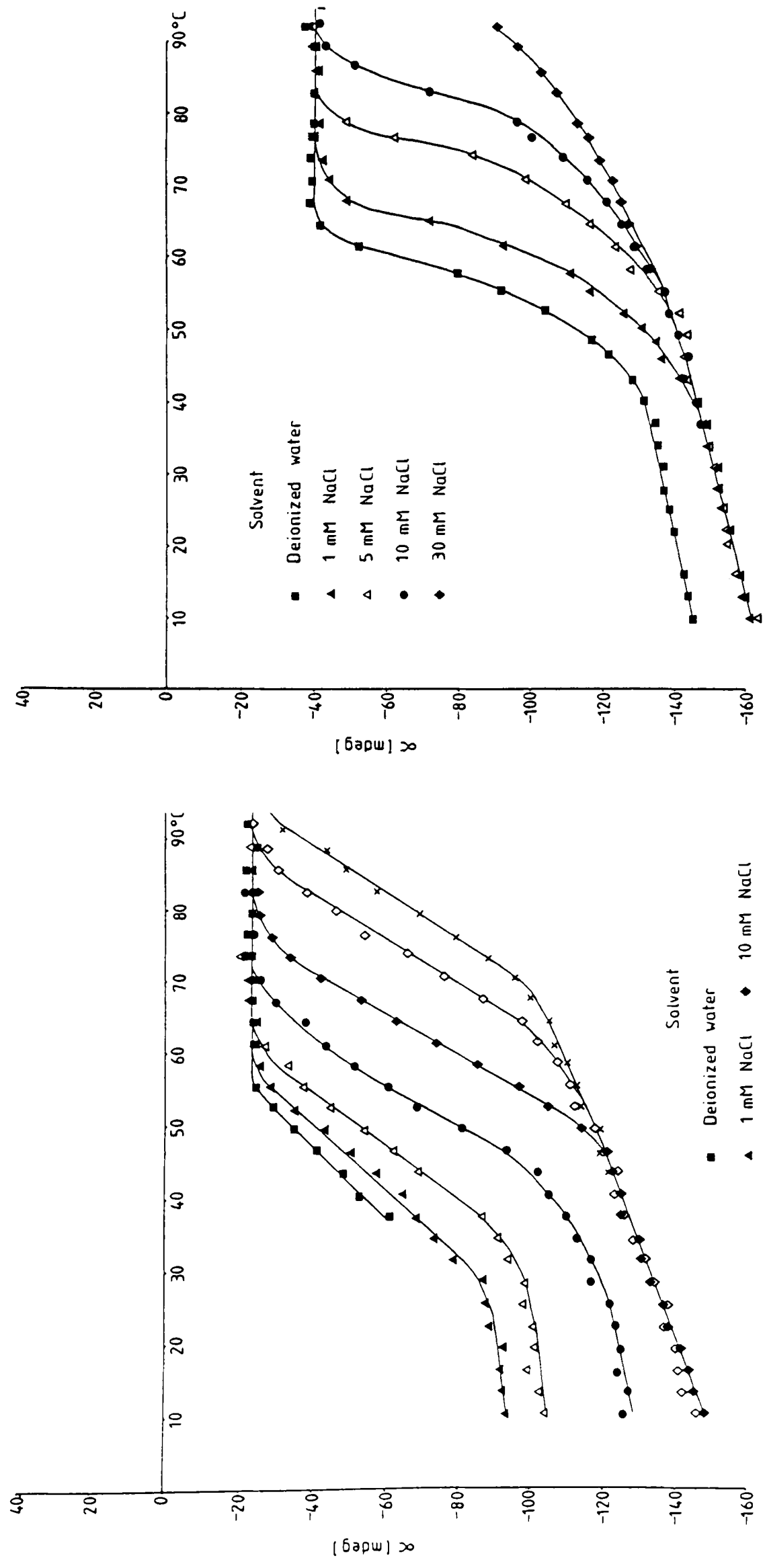

b) ps. 1128

a) ps. 646

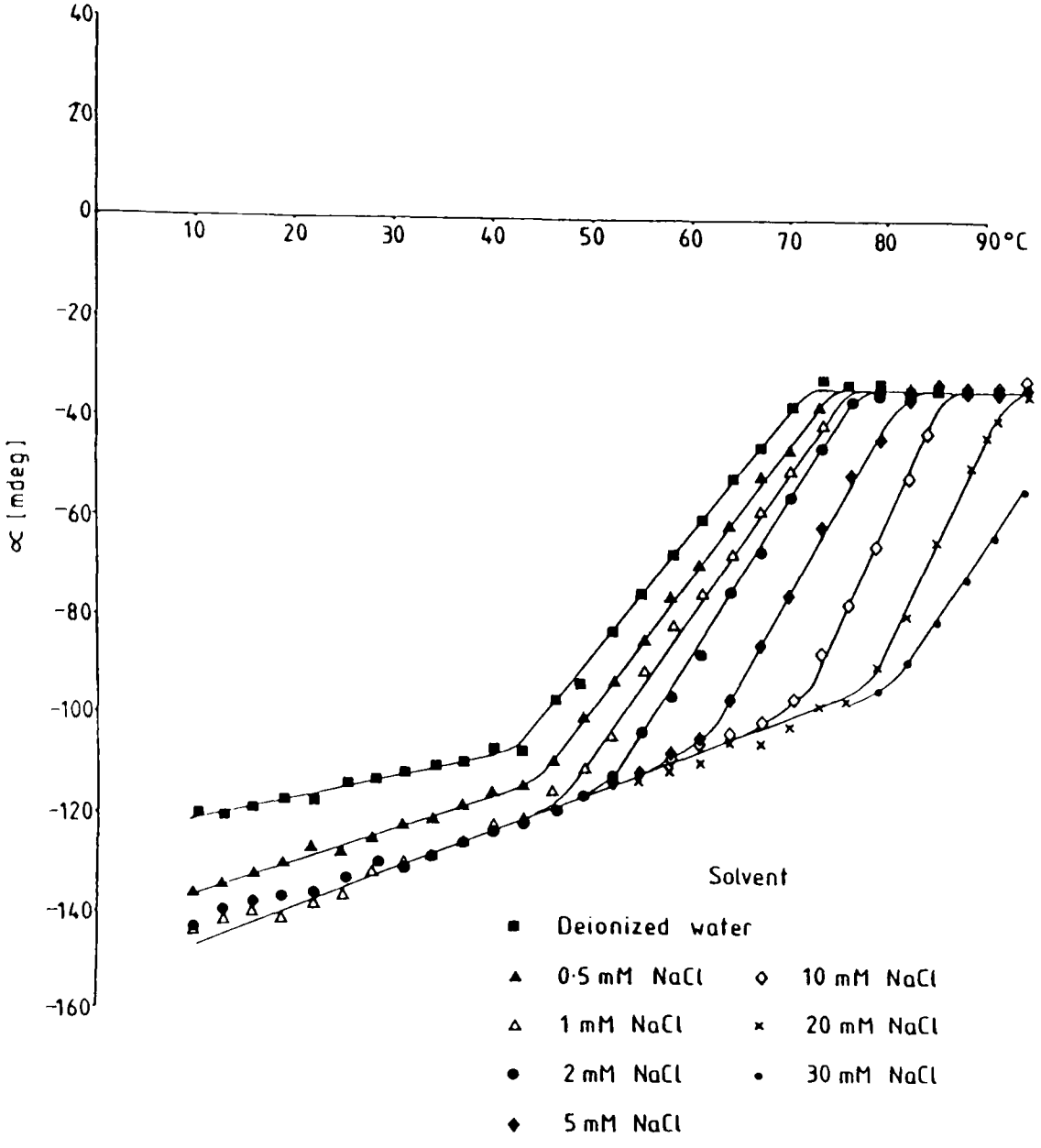

c) ps. PXO_{61}

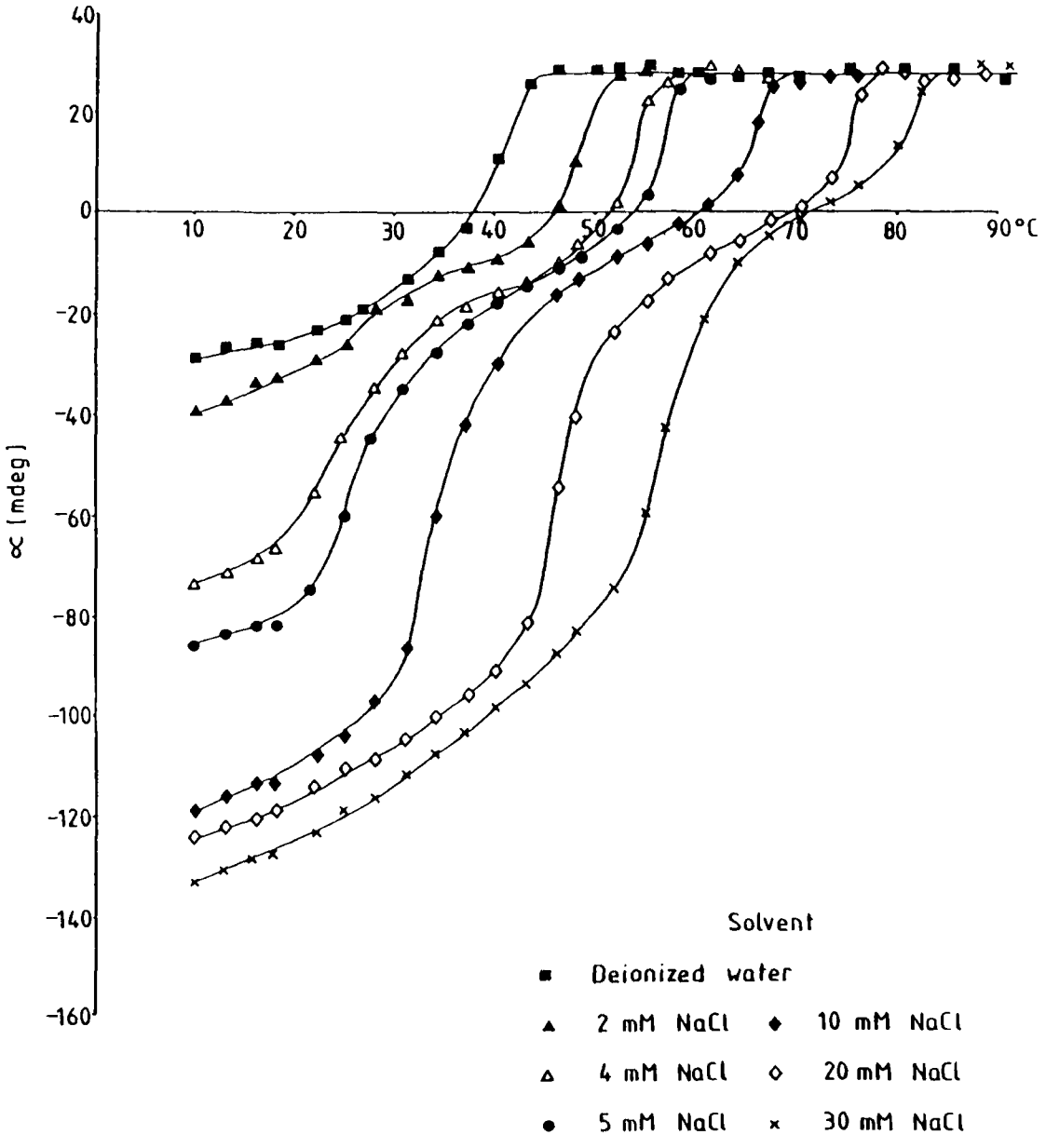

d) ps. 556

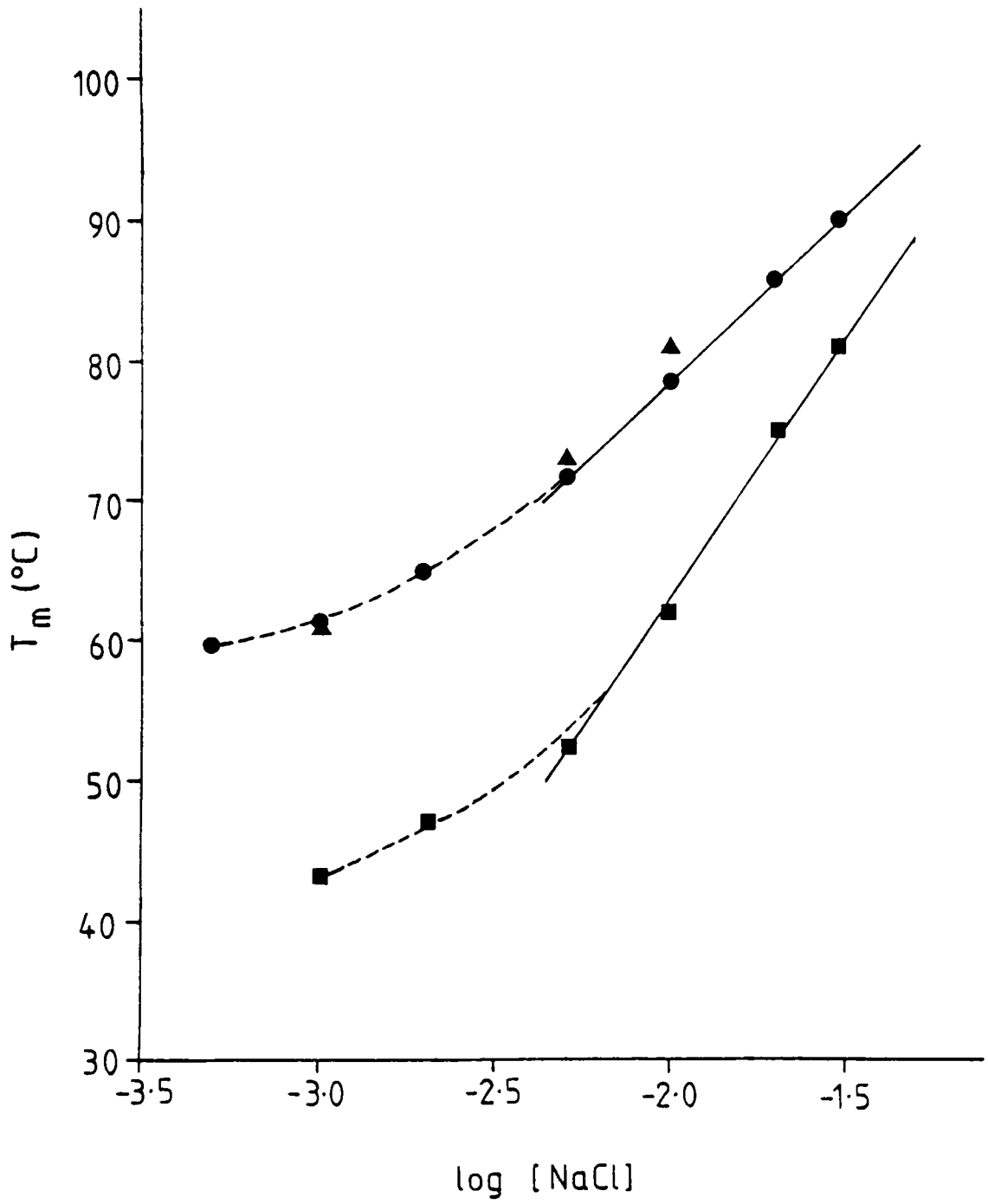

Fig. 4·12 Melting temperature of ps.646 (■), ps.1128 (▲) and ps. PXO_{61} (●) as a function of ionic strength.

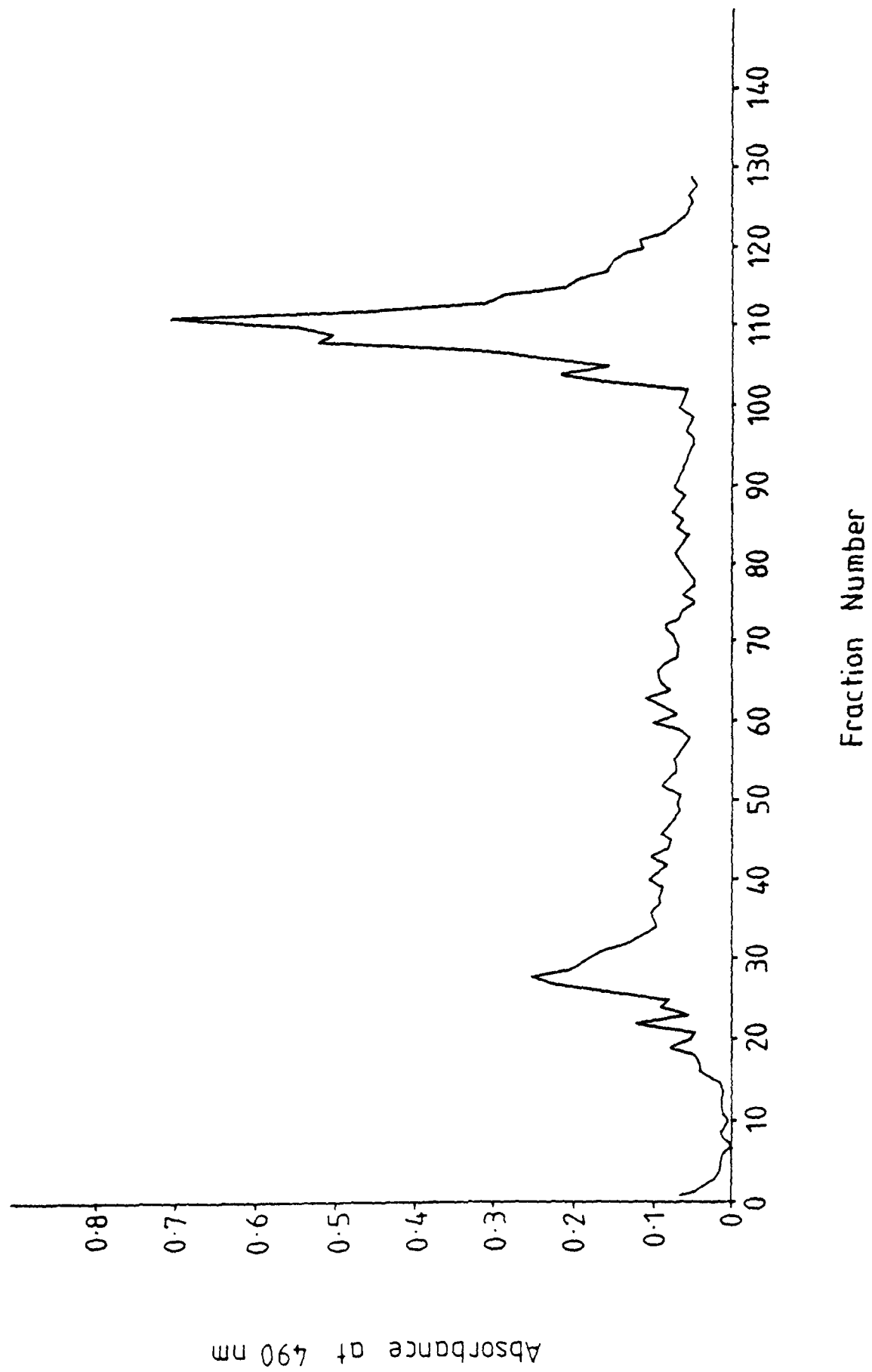

Fig. 4·13 Fractionation of ps.556 by ion exchange chromatography

Fig. 4.14 Thermal hysteresis of xanthan as monitored by optical rotation.

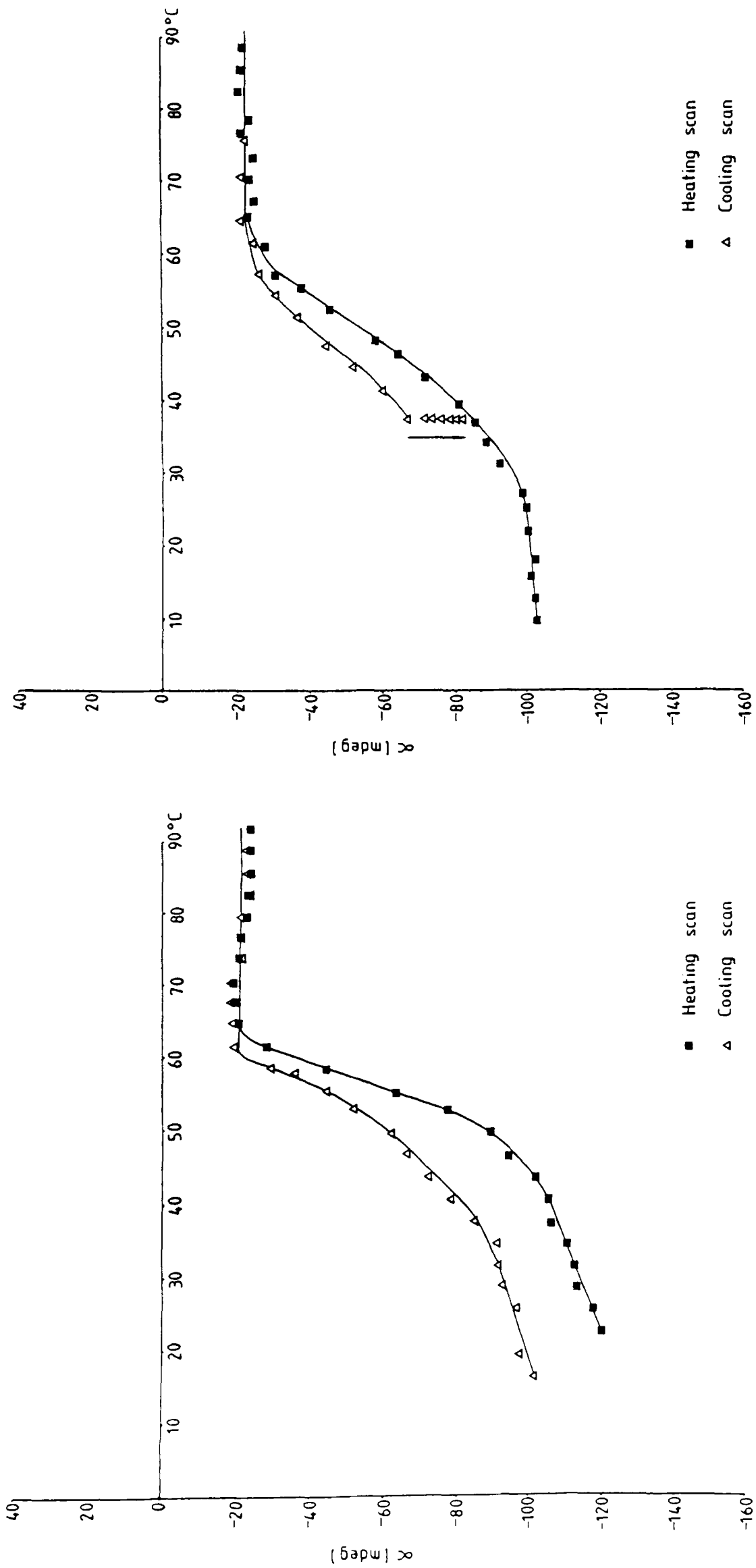

(a) Heating and cooling curves for ps.1128

(b) Heating and cooling curves for ps.PX061. The cooling curve has been halted at 37°C and the specific optical rotation monitored as a function of time.

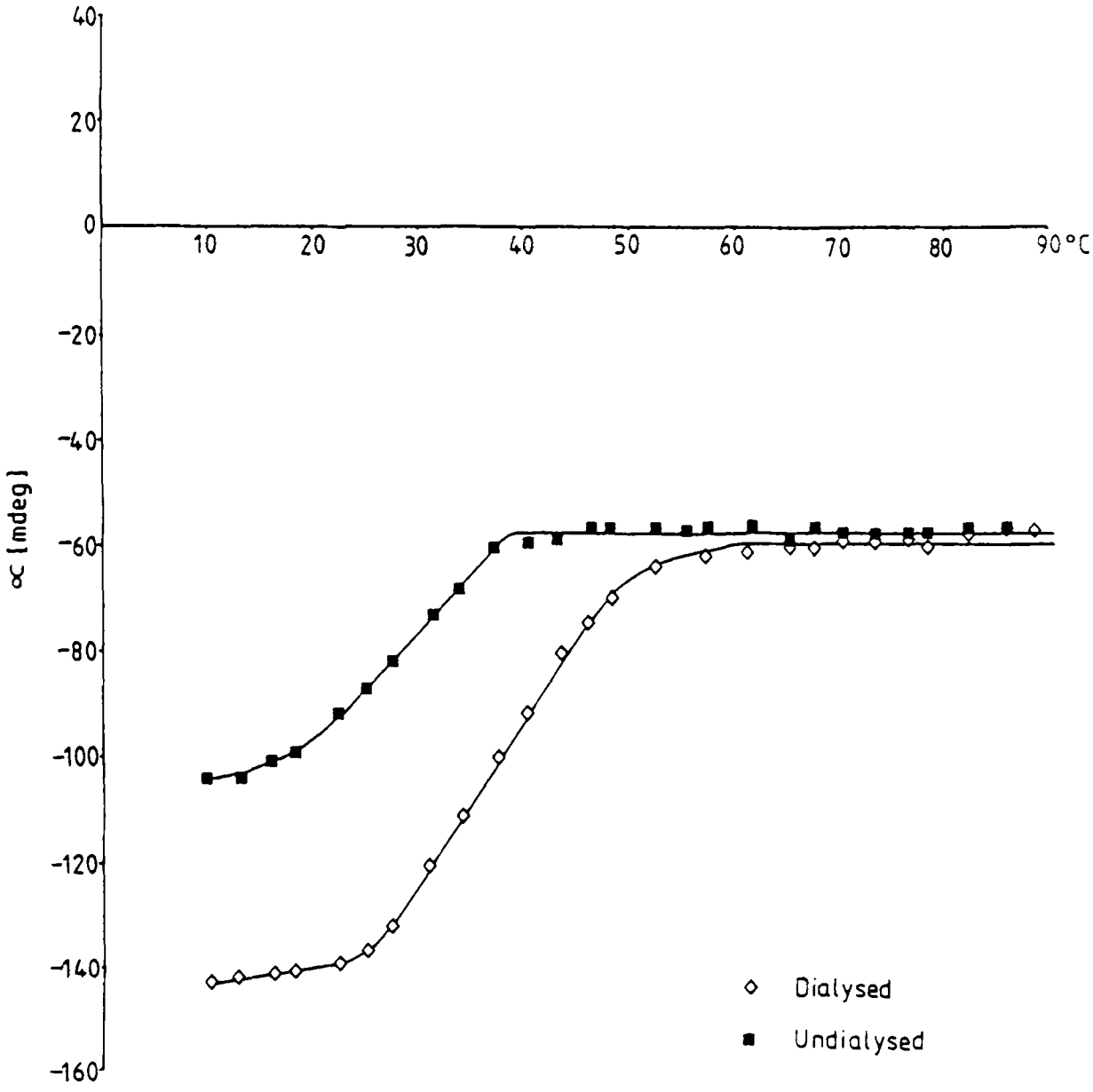

Fig. 4·15 Comparison of the helix-coil transition for 0·3% $w/_w$ solutions of Flocon 4800C, one of which has been dialysed against deionized water and another which has not.

CHAPTER 5

PHYSICAL CHARACTERIZATION II: INTRINSIC VISCOSITY AND LIGHT SCATTERING MEASUREMENTS

Introduction

5.1 Molecular Weight of Xanthan

Table 5.1 gives a list of published molecular weight (relative molecular mass) estimates for native xanthans, some of which were obtained from commercial sources, and others which were produced by bacterial fermentation in the laboratory. The values range from as little as 1.1×10^6 to as high as 62×10^6.

The variation in molecular weight could be attributed, at least in part, to differences in the cultural conditions used to synthesize the polymer. Alternatively the methods used to extract and purify the materials could affect the molecular weight of the final product. In the case of certain plant polysaccharides, the harsh conditions used to extract material from the plant tissue have been shown to result in some degradation. The traditional method for preparing konjac flour from the tubers of *Amorphophallus konjac*, for example, involves drying slices of the tuber in sunlight for several days and then pulverizing the dried material for 8 hours in a stamp mill, prior to recovery. Sugiyama *et al* (1972) showed that the molecular weight of konjac mannan, prepared by the traditional method, was a quarter of that of the same material extracted in the laboratory. Such a drastic reduction in the molecular weight of xanthan seems unlikely since the conditions used to isolate the polymer from the culture medium are relatively mild and since the cellulosic backbone of the molecule is fairly resistant to both chemical and mechanical degradation.

A more satisfactory explanation for the molecular weight heterogeneity is the tendency of xanthan molecules to form high molecular weight aggregates. Muller *et al* (1986) noted that when xanthan was freeze dried under certain conditions, molecular associates were formed which failed to break down when the polymer was redissolved. These so-called microgels raised the molecular weight, as determined by light scattering, irreproducibly. Southwick *et al* (1980), using quasi-elastic light scattering, demonstrated extensive time-dependent aggregation of xanthan molecules in deionized water and such aggregates could again raise the apparent molecular weight of the polymer.

Removal of microgels and aggregates may be achieved by filtration or high-speed centrifugation. Alternatively heating the solution to break up the aggregates may be successful, particularly in the presence of a compound like urea, which breaks down intermolecular hydrogen bonds and prevents the molecules from reassociating. Dintzis *et al* (1970) observed that the molecular weight of xanthan heated in the presence of 4M urea was approximately 2×10^6 whilst the molecular weights of two, admittedly different, xanthans which had been dissolved in 4M urea but not heated, were 13×10^6 and 50×10^6 - much higher. Morris *et al* (1983) obtained measurements of 1.1×10^6 and 47×10^6 for the same samples of xanthan

heated in 4M urea and deionized water respectively. Thus the procedure used to prepare the samples is absolutely critical when attempting to determine the molecular weight of xanthan experimentally.

The current consensus of opinion is that native xanthan has a molecular weight typically in the region of 2×10^6, and that the much higher values reported in the literature were the result of molecular aggregation or the presence of microgels.

5.2 Chain Flexibility

The solution viscosity of xanthan shows very little sensitivity towards salt and pH, in contrast to the behaviour of typical random coil polyelectrolytes. This suggests that the polymer is comparatively rigid and Morris *et al* (1977a), went so far as to propose that the solution properties of xanthan are consistent with those of a rigid rod. Whitcomb and Macosko (1978) subsequently modelled their non-Newtonian intrinsic viscosity data as a suspension of rods and Rinaudo and Milas (1978) adopted the rigid rod model to fit their intrinsic viscosity and sedimentation data. The bulk of the evidence currently available, however, favours a stiffened wormlike chain in preference to a rod, except for very low molecular weight fractions.

Holzwarth and Prestridge (1977) found that the hydrodynamic diameter of xanthan measured by membrane partition chromatography was a factor of 10 less than the particle length measured from electron micrographs. The molecules in the electron micrographs were extended and rod-like but Holzwarth and Prestridge attributed this to the method used to prepare the samples for electron microscopy, and expressed the view that the xanthan molecule does in fact have a small, but finite, amount of flexibility which allows substantial coiling at higher molecular weights. Stokke and coworkers (1986), using a quite different method of sample preparation, have recently produced electron micrographs for a range of molecular weight fractions of xanthan. They seem to show that whilst at low molecular weights the molecules are essentially rod-like, as the contour length increases the molecules become progressively more convoluted.

More satisfactory evidence for a degree of flexibility comes from static and dynamic light scattering studies (Paradossi and Brant, 1982; Muller *et al*, 1984; Sato *et al*, 1984b,c; Coviello *et al*, 1986). For example, from static light scattering, the decrease in curvature with increasing scattering angle in the Zimm plot (figure 5.2), and the clear maximum and asymptotic plateau observed in the so-called Holtzer plot (Coviello *et al*, 1986), are both characteristic of a stiffened wormlike chain. The curvature in the plot of z-average root mean square radius of gyration versus molecular weight, at higher molecular weight values (figure 5.3; Paradossi and Brant, 1982; Sato *et al*, 1984b, 1984c) is also indicative of this.

For a wormlike molecule, chain stiffness can be characterized by the persistence length (a). If the angle between the direction of the initial and final chain segments is λ, then the persistence length is defined by the equation

$$\langle \cos \lambda \rangle = \exp(-nl/a)$$

where the angled brackets denote a statistical average over all chain conformations and where nl is the chain length.

At one extreme the persistence length may be very large relative to the maximum fully extended chain length, in which case the wormlike chain approaches a rigid rod. For example, α-helical poly-benzyl-L-glutamate which behaves like a rigid rod, has a persistence length comparable to, or exceeding, the longest molecular length (300 nm). At the other extreme the persistence length can be very small, in which case the wormlike chain becomes a random coil. Polystyrene dissolved in benzene, for example, has a persistence length of around 1 nm.

Published estimates of the persistence length of xanthan range from 29 nm to 150 nm (Rinaudo and Milas, 1978; Muller *et al*, 1984; Sato *et al*, 1984b; Lecourtier *et al*, 1986; Stokke *et al*, 1986), with the majority of reliable estimates tending towards the larger value. The persistence length is high, indicating a fairly stiff chain. Indeed xanthan is one of the stiffest biopolymers known, the a value being comparable only with that of the triple helical polysaccharide from *Schizophyllum commune* (150-200 nm) and DNA (50-150 nm). The persistence length is, however, still well below the contour length, revealing a degree of flexibility.

The persistence length of a polyelectrolyte can be split into two parts, the geometrical persistence length which comes from steric hindrances and from intramolecular interactions such as hydrogen bonding, and the electrostatic persistence length which arises from charge-charge repulsion between neighbouring groups along the chain. With xanthan, as for other polyelectrolytes, the overall persistence length increases with decreasing salt as the electrostatic contribution towards the persistence length becomes more important. However, because of the innate stiffness of the molecule, the electrostatic persistence length is very small, and its contribution is negligible except at very low ionic strengths (Muller *et al*, 1986; Sho *et al*, 1986).

Considerable evidence exists to show that the acetyl group stabilizes the ordered conformation of xanthan, whilst pyruvic acid destabilizes it (section 4.3). Coviello *et al* (1986) looked for a correlation between the stability of the ordered structure and the Kuhn segment length, which characterizes the chain stiffness of the polymer (the Kuhn segment length is essentially equal to twice the persistence length) in 0.1M sodium chloride. They measured the Kuhn segment length for native xanthan and its chemically deacetylated and depyruvylated

derivatives using static light scattering and observed the following. The Kuhn segment length of the acetyl-free xanthan (198 nm) was lower than that of the native polymer (255 nm), consistent with the reported destabilization upon removal of the acetyl groups. The Kuhn segment length of the depyruvylated polymer (310 nm), in contrast, rose consistent with the observed increase in stability. This data would apparently suggest that the degree of acyl substitution has a significant effect upon the rigidity of the xanthan molecule.

5.3 Theory and Application of Intrinsic Viscosity Measurements

The theory and application of intrinsic viscosity measurements have been discussed in a number of reviews including those of Morris and Ross-Murphy (1981), Morris (1984) and Ross-Murphy (1984).

The viscosity of a solution may be expressed as the ratio of the solution viscosity (η) to that of the pure solvent (η_s) at a given temperature and shear rate. This ratio, which is dimensionless, is known as the relative viscosity (η_{rel}).

$$\eta_{rel} = \eta / \eta_s$$

The specific viscosity (η_{sp}) is defined as the fractional increase in viscosity due to the presence of solute.

$$\eta_{sp} = (\eta - \eta_s) / \eta_s$$

$$= \eta_{rel} - 1$$

The degree to which the viscosity is enhanced is dependent upon the concentration of solute (c) and the molecular size. Hence one can define a reduced viscosity (η_{red}).

$$\eta_{red} = \eta_{sp} / c$$

In the limit of infinite dilution, the reduced viscosity describes the fractional increase in viscosity due to each individual solute molecule and this is known as the intrinsic viscosity, $[\eta]$.

$$[\eta] = \lim_{c \longrightarrow 0} (\eta_{sp} / c)$$

The intrinsic viscosity is, in effect, the amount of volume "swept out" by the molecule in solution, expressed in dl/g. It is dependent not only upon the molecular weight, but also on the chain geometry, and hence the intrinsic viscosity of a random coil polymer will be much greater than that of a globular protein of equivalent molecular weight, even though much of the volume is in fact occupied by solvent.

The intrinsic viscosity can be determined by measuring the viscosity of the polymer at a range of concentrations and then extrapolating to infinite dilution.

Below the overlap concentration, c^*, (see section 6.1) the reduced viscosity is indirectly influenced by mutual interference of the solvent flow patterns around the solute, and this is expressed in the equation:

$$\eta_{sp} / c = [\eta] + K'[\eta]^2 c$$

The intrinsic viscosity can therefore be obtained from the intercept of a graph of η_{sp} / c versus c. This is the Huggins plot.

The alternative Kraemer extrapolation is a plot of $\ln \eta_{rel} / c$ against c and is obtained from the equation:

$$(\ln \eta_{rel}) / c = [\eta] + K''[\eta]^2 c$$

K' and K" are the so-called Huggins and Kraemer constants and are related thus:

$$K' = K'' + 0.5$$

The extrapolations should be carried out for relative viscosities in the range of approximately 1.2-2.0. Above this, higher order effects cease to be negligible and, below it, the experimental error becomes unacceptably large. The viscosities must be measured within the Newtonian region of the flow curve (ie. where viscosity is independent of shear rate) and this should be verified by determining the viscosity over a range of shear rates.

Measurements for polyelectrolytes must be made at constant ionic strength since the hydrodynamic volume will vary with the amount of salt. Experimentally this is achieved by first dialysing the concentrated polymer solution against a suitable salt solution and then preparing all subsequent dilutions using the dialysate.

The intrinsic viscosity can be used as a probe of molecular weight and molecular flexibility. It is related to the molecular weight by the Mark-Houwink-Sakurada equation.

$$[\eta] = KM^{\alpha}$$

Here M is the molecular weight, whilst K and α are the Mark-Houwink parameters. K is related to the local stiffness of the polymer backbone and α to the overall behaviour of the chain and its interaction with the solvent. Large values for α (say >1.2) indicate stiffened chains, with 1.8 being the value for a rigid rod, whilst for random coils values of 0.5-0.8 are typical. To find the molecular weight from the intrinsic viscosity,

the Mark-Houwink parameters must first be determined against a "primary" molecular weight technique such as light scattering but, thereafter, intrinsic viscosity measurements provide a relatively quick and simple index of molecular weight.

Published values of α, determined for xanthan, range between 0.93 and 1.35 (Holzwarth, 1978; Holzwarth, 1981; Muller *et al*, 1984, Gravanis *et al*, 1987) indicating, once again, a stiffened chain but not a rigid rod. The intrinsic viscosity versus molecular weight plot (figure 5.4) shows similar curvature to the plot of root-mean square radius of gyration against molecular weight (Sato *et al*, 1984c) and, this too, indicates an increase in overall chain flexibility at higher molecular weights.

For flexible polyelectrolytes the variation in intrinsic viscosity with ionic strength can be used as a measure of chain flexibility. At low ionic strength the polymer exists in an expanded state as a result of electrostatic repulsion between the chain segments but, with increasing salt, the random coil dimensions of the polymer lessen due to charge shielding. The more flexible the polymer, the greater the fractional decrease in intrinsic viscosity with increasing salt.

Smidsrød and Haug (1971) have developed a simple semi-empirical method for characterizing the chain flexibility of a polymer from measurements of the intrinsic viscosity, over a range of ionic strengths. A plot of intrinsic viscosity against $I^{-1/2}$ (where I is the ionic strength) for a particular polyelectrolyte gives a straight line, the slope of which (S), is an indicator of chain flexibility (figure 5.6a). Smidsrød and Haug found that a double logarithmic plot of S against the intrinsic viscosity at 0.1M salt ($[\eta]_{0.1}$), for different chain lengths, was also linear and had essentially the same slope ie. 1.3 +/- 0.1, for all of the polyelectrolytes tested (figure 5.6b). This relationship can be expressed by the general equation:

$$\log S = \log B + 1.3 \log[\eta]_{0.1}$$

The intercept B is inversely proportional to the persistence length as illustrated in figure 5.6c, and the persistence length can therefore be determined approximately from the following equation:

$$Ba \simeq 0.26$$

The Smidsrød and Haug B-value method has been applied successfully to a range of polysaccharides including, for example carboxymethyl-cellulose, alginate and even DNA, but never to a polymer as stiff as xanthan.

5.4 Molecular Weight and Chain Flexibility Studies

As well as characterizing them chemically, it was important to have an indication of the relative molecular weights of the materials used in this study. Ideally such measurements should have been made using a direct, quantitative technique such as static light scattering. However since the necessary instrumentation was not accessible, a more approximate method had to be substituted. Gel permeation chromatography was one possibility - it has been used successfully in the past to determine the molecular weight profile of xanthans (eg. Bradshaw *et al*; 1983) but as the equipment was readily available at Colworth, in this instance intrinsic viscosity measurements were the method of choice.

The intrinsic viscosities of the xanthans and also the gluco- and galactomannans were determined in 20mM sodium chloride, and an attempt was made to estimate the approximate molecular weights from intrinsic viscosity and molecular weight data reported in the literature.

In the case of ps.646, ps.1128, ps.PXO_{61} and ps.556, the intrinsic viscosities were determined at a range of sodium chloride concentrations in an attempt to compare the relative flexibility of the four polymers, and the Smidsrød and Haug B-value method was applied to the data to try to estimate the persistence lengths. The information derived from the intrinsic viscosity measurements was compared with the more accurate light scattering data obtained by Dr Ross-Murphy at the University of Freiburg.

Results and Discussion

5.5 Intrinsic Viscosity Measurements

A 0.1% solution of xanthan, or a 0.2% solution of the gluco- or galactomannan, was prepared and dialysed against aqueous sodium chloride to the required concentration. It was then filtered through a 1.2 μm millipore filter and a series of five dilutions, with relative viscosities in the range of 1.2-2.0, were prepared from the stock, using the dialysate as diluent. The relative viscosities of the solutions were measured in triplicate, at 25°C, using a Contraves Low Shear (LS30) viscometer under computer control, and the intrinsic viscosity was computed directly using both the Huggins and Kraemer extrapolations.

The intrinsic viscosity was calculated by the computer using the nominal concentration ie. the apparent concentration prepared on a weight/weight basis, not taking into account any changes that may have occurred upon dialysis or filtration. This value had therefore to be corrected for the true polysaccharide concentration. This required two additional measurements - firstly the percentage carbon determined by elemental analysis and secondly, the dry weight obtained by weighing freeze dried aliquots of the stock solution and adjusting the value to

take into account the amount of salt present as a result of dialysis. The intrinsic viscosity was corrected according to the method outlined in Appendix 2.

The majority of the experimental data from which the intrinsic viscosities were determined will not be included in this thesis. However, as an illustration of the procedure used, the viscosity measurements and the Huggins and Kraemer plot data for ps.556 and guar galactomannan are given in table 5.2. Figure 5.1 shows the Huggins and Kraemer extrapolations for both polymers. For ps.556 the Huggins and Kraemer extrapolations intercept the ordinate at 49.4 dl/g and 48.3 dl/g respectively. These apparent intrinsic viscosities were corrected as shown in Appendix 2 and the true values are therefore slightly higher, 51.3 dl/g and 50.2 dl/g.

Table 5.3 gives a summary of the intrinsic viscosity measurements for the xanthans, whilst table 5.4 shows the data for the gluco- and galactomannans. In theory the Huggins and Kraemer extrapolations should intercept the ordinate at the same point but because of the limited amount of experimental data, they rarely coincided exactly. The maximum discrepancy observed between the two values was around 13-14% but, in general, the agreement was very much better than this.

Where the measurements were repeated under uniform conditions, the reproducibility of the data was not very good. There were probably two reasons for this. Firstly, this method for determining the intrinsic viscosity has a margin of error of +/- 3-5%. Secondly, aggregates formed upon freeze drying may have failed to break up when the polymer was redissolved and these could have raised the intrinsic viscosity irreproducibly. Such factors should be borne in mind when comparing the intrinsic viscosities of the different materials.

5.6 Static Light Scattering Measurements

Static light scattering measurements were carried out on samples of ps.646, ps.1128, ps.PXO_{61} and ps.556 by Dr Ross-Murphy at the Institut für Makromolekulare Chemie, University of Freiburg.

Measurements were made at 20°C and in 0.1M potassium chloride, according to the procedure outlined in Chapter 2. The results were processed using the so-called Zimm/Holtzer analysis of the angular dependence of the zero concentration scattered light, described by Coviello *et al* (1986). An example of the familiar Zimm plot is shown for ps.1128 in figure 5.2. The molecular weight of the polymer can be determined from the intercept at zero concentration and zero scattering angle, and the curvature is, as mentioned in the introduction, typical of a stiffened wormlike chain.

The information derived from the Zimm/Holtzer analysis included the weight average molecular weight (M_w), the z-average root mean square radius of gyration (R_g), which is a measure of the average size of the molecule, the linear mass density (M_L), the Kuhn segment length (l_K), the contour length (L) and the number of Kuhn segment lengths per chain (N_K). A summary of this data is given in table 5.5. The second virial coefficients are not shown since they were close to zero in each case.

The data for ps.1128, ps.PXO_{61} and ps.556 is believed to be of good quality and this view is supported by figure 5.3 which shows a plot of z-average root mean square radius of gyration versus molecular weight. The data obtained in this study are plotted, together with that of Paradossi and Brant (1982) and Coviello *et al* (1986), and are found to be in good agreement. (The dashed lines show the curves calculated by Coviello *et al* for polydisperse double-stranded chains with Kuhn segment lengths of 200 and 300 nm.) The data for ps.646 could not be calculated to the same degree of precision, as this polymer showed pronounced time dependent aggregation which interfered with the measurements.

As these experiments were not performed by the author, the analysis of the data and the results will not be discussed any further, except in the context of her own work.

5.7 Xanthan Molecular Weight Estimation

The approximate molecular weights of the various xanthans have been estimated from the intrinsic viscosity values using the data of Sato *et al* (1984c). Sato and coworkers studied a series of xanthan fractions generated from Keltrol by sonication, and a combination of fractional precipitation and gel filtration. They determined the intrinsic viscosity of the samples in 0.1M sodium chloride at 25°C, and measured the molecular weight under the same conditions using static light scattering. A double logarithmic plot of their intrinsic viscosity versus molecular weight data is shown in figure 5.4. The curvature at the higher molecular weight values indicates increasing flexibility, whilst the dashed line shows the values calculated for a rigid rod with a mass per unit length of 1940/nm and a diameter of 2.2 nm, using the Yoshizaki-Yamakawa theory.

The data obtained by Holzwarth (1978) at a somewhat higher salt concentration are also plotted in figure 5.4. Like Sato *et al*, Holzwarth used fractions of Keltrol produced by sonication but the molecular weights, in this case, were calculated from the sedimentation coefficient (determined by band sedimentation of molecules tagged with a fluorescent group) and the intrinsic viscosity, using the Mandelkern-Flory-Scheraga equation. The plot shows similar curvature to that of Sato *et al*, but the intrinsic viscosity at any given molecular weight is lower.

The intrinsic viscosities used to estimate the molecular weights from the data of Sato *et al* were determined by the Kraemer extrapolation. In theory, because of the lower slope, this plot should give a more

accurate intrinsic viscosity value than the alternative Huggins extrapolation but, in practice, the two values were generally so close that the choice was largely academic. For the majority of polymers the intrinsic viscosity measured in 20mM sodium chloride was used to obtain the molecular weight, but for ps.646, ps.1128, ps.PXO_{61} and ps.556, the intrinsic viscosities in both 20mM and 100mM salt were used. These were determined from the plot of intrinsic viscosity versus $I^{-1/2}$ (figure 5.7).

Table 5.6 gives a summary of the molecular weight data. For typical xanthans, the molecular weight ranged from 0.96 x 10^6 for depyruvylated Flocon 4800C to 8.80 x 10^6 for ps.646 produced in continuous culture under potassium limiting conditions. Sample ps.BD9A, a mutant polymer with less than the usual complement of mannose, may have had a still lower molecular weight (around 0.85 x 10^6), but the loss of the terminal mannose residue could have altered the flexibility of the polymer, thereby preventing the molecular weight from being accurately determined.

As the intrinsic viscosity measurements in this study were made predominantly in 20mM sodium chloride, whilst those of Sato *et al* were made in 0.1M salt, one is bound to ask whether it is really valid to use data produced at a higher ionic strength to estimate the molecular weights. In the case of typical random coil polyelectrolytes, for example, one would expect the concentration of salt to have a pronounced effect upon the intrinsic viscosity values, and the molecular weight estimates would therefore be significantly affected.

The choice of 20mM sodium chloride was made initially on the basis of the available OR data. The OR scans at a range of salt concentrations (figures 4.11a-4.11d) indicated that in 20mM salt the polymers had achieved their maximum attainable degree of order at 25°C, except probably in the case of ps.556 (this data was not available at the time). If the amount of order remained unchanged at higher salt concentrations, then it seemed likely that the degree of flexibility and the intrinsic viscosity would be similarly unaffected. Data published subsequently by Muller *et al* (1986) and Sho *et al* (1986) largely support this view. These authors demonstrated that the electrostatic contribution to the persistence length of xanthan was significant only at very low ionic strengths, and that above 20mM sodium chloride, any additional increase in persistence length or decrease in intrinsic viscosity, upon the addition of more salt, was minimal. It is possible to quantify the extent of the decrease by comparing the intrinsic viscosities in 20mM and 100mM sodium chloride for ps.646, ps.1128, ps.PXO_{61} and ps.556. Among these four polymers, which represent the extremes in terms of the amount of acetyl and pyruvic acid carried, the maximum difference between the two values was 11.4% for ps.646. This is only 2-3 times the level of experimental error and represents a molecular weight of 2.65 x 10^6 instead of 2.40 x 10^6. Thus the effect of ionic strength upon the molecular weight estimates will have been only marginal.

The data of Sato and coworkers was for a double-stranded molecule. They established this quite conclusively by showing that the molecular weight of the polymer in sodium chloride solution was invariably twice that of the same fraction in cadoxen, a solvent system in which xanthan appears to exist as single-stranded flexible chains.

Although the majority of evidence favours a double-stranded model for xanthan (section 1.4), it is possible that the polymer adopts different conformations depending on the thermal history, the level of acyl substitution and the prevailing environmental conditions. Stokke *et al* (1986), for example, demonstrated using electron microscopy that in 2mM ammonium acetate the polysaccharide from strain PXO_{61} existed predominantly in the single-stranded form. However, when the concentration of salt was increased to 0.1M, molecular association occurred to give double strands. Kelzan appeared to behave in a similar fashion but in 2mM ammonium acetate this polymer consisted of a mixture of both single and double strands. Coviello *et al* (1986) showed using static light scattering that whilst native and deacetylated xanthan existed in the double-stranded form in 0.1M sodium chloride, the depyruvylated derivative contained apparently fewer double strands. It is possible, therefore, that a proportion of the polymers prepared for use in this study favoured a single-stranded form in 20mM salt. Since little is known about the relative effects of single and double-strandedness upon the intrinsic viscosity behaviour of xanthan, it is impossible to say what influence this would have had upon the molecular weight estimate.

An indication of the strandedness of four of the polymers in 0.1M potassium chloride may be obtained by comparing the theoretical mass per unit length for the materials with those measured experimentally by light scattering. Coviello and coworkers calculated the theoretical mass per unit length for Keltrol and its chemically modified derivatives using a repeat unit length of 1.08 nm. (This is slightly greater than the 0.94 nm estimated for the polymer in the crystalline state using X-ray fibre diffraction data and corresponds, instead, to the stretched cellulosic backbone which is believed to exist in solution.) They obtained values of 899 for the native polymer, 860 for deacetylated xanthan and 835 for the depyruvylated derivative. These values have been used to calculate the approximate ratio of the experimental to theoretical mass per unit length for ps.646, ps.1128, $psPXO_{61}$ and ps.556. The first three polymers all had ratios of 1.9 which suggests a predominantly double-stranded structure but for ps.556 the ratio was only 1.5, indicating the presence of a significant number of single strands. Whether the same was true in 20mM sodium chloride is uncertain, but there is no evidence to suggest a significant change in the strandedness of these polymers between 20mM and 100mM salt.

The problem of aggregation has already been alluded to (sections 5.1 and 5.5). The formation of high molecular weight aggregates by the time-dependent aggregation mechanism, demonstrated by Southwick *et al*

(1980), is unlikely to have had a marked effect upon the intrinsic viscosity since, generally speaking, such assemblies are very compact and contribute little towards the intrinsic viscosity measurement. However, lower molecular weight aggregates formed upon freeze drying are usually less compact, and were these to have remained intact when the polymer was redissolved, they could have distorted the intrinsic viscosity value upwards by a significant amount. The presence of aggregates in a proportion of the samples is suggested by the following observations. Firstly, as mentioned earlier, intrinsic viscosity measurements made for particular polymers, under identical conditions, often showed greater variation than would be expected from the level of experimental error alone. Secondly the molecular weight estimates were in some cases well above the value of 2×10^6 considered typical for a native xanthan. The polymers produced by strain 646 in continuous culture, for example, had an apparent molecular weight in the range of $7.8\text{-}8.8 \times 10^6$, whilst that of the same material produced in batch culture was only 2.65×10^6. A greater propensity to aggregate would explain the very high molecular weight values, although this is by no means the only possible explanation. Sato and coworkers (1984c) obtained molecular weights of up to 7.4×10^6 for double-stranded Keltrol in 0.1M sodium chloride and values of up to 3.56×10^6 for the same materials in cadoxen. The fact that the ratio of the molecular weights in the two solvent systems was close to 2.0 for a wide range of molecular weight fractions, indicates that aggregation was unlikely in their system and shows, quite clearly, that molecular weights of greater than 2×10^6 are possible for at least some xanthans. The higher molecular weight estimates might, therefore, conceivably be genuine, and in the case of ps.646 could reflect the very different cultural conditions used to grow the organism.

The third observation which suggests aggregation upon freeze drying is the apparent increase in the intrinsic viscosity of ps.646 upon lyophilization. Values of between 33.1 and 45.9 dl/g were obtained for solutions of ps.646 prepared from the freeze dried polymer, but the same material prior to lyophilization had an intrinsic viscosity of only 23.3 dl/g. Fourthly and finally, there is the fact that the molecular weights estimated from the intrinsic viscosity values were invariably higher than those obtained for the same polymers using static light scattering (table 5.8). In the case of ps.1128 the difference was particularly marked. Because light scattering is an absolute measurement of molecular weight, and because the samples prepared for light scattering were pressure cooked at 116°C for a total of 40 minutes, precisely in order to break up any high molecular weight aggregates present, one is inclined to believe this data in preference to that obtained using the intrinsic viscosity values. However, it is possible that the high temperature and pressure used to break up the aggregates could have resulted in some depolymerization and that this could also account for the relatively low molecular weights. On balance though, this seems unlikely to have occurred, since the data obtained in this study agrees well with that of both Coviello *et al*, who did pressure cook their samples, and

Paradossi and Brant who did not. In addition Kierulf and Sutherland (1988) have demonstrated that most xanthans, in the presence of salt, will remain stable at 80-90°C for periods of up to 800 days and just 40 minutes at the higher temperature, therefore, seems unlikely to have had a pronounced effect.

Deacetylation and depyruvylation in each case resulted in a reduction in the intrinsic viscosity and, therefore, the apparent molecular weight of the polymers. A number of possible explanations are available for this. Perhaps the most likely is the breakdown of the polymer molecule during chemical modification. The conditions used to depyruvylate the materials were particularly harsh and accordingly, some degree of depolymerization was to be expected. Chemical characterization of the materials produced no satisfactory evidence for degradation, but when the dialysates from aliquots of deacetylated and depyruvylated ps.646 and Flocon 4800C were examined by paper chromatography (section 3.6), a number of low molecular weight products were detected. The amounts were substantial only in the case of the depyruvylated materials, suggesting a considerable degree of degradation. By contrast deacetylation appeared to have very little effect.

It is interesting to note that the molecular weight estimates for the chemically modified derivatives of ps.646, ps.1128, ps.PXO_{61} and ps.556 were actually very much closer to the values obtained for the native materials by light scattering, than were the estimates for the native materials themselves. An alternative, or possibly complementary, explanation for the data, therefore, would be that by removing the acyl groups one reduced the propensity of the polymers to aggregate upon freeze drying and thus enabled the true intrinsic viscosity to be determined.

The foregoing discussion indicates that whilst intrinsic viscosity can be used as an indicator of molecular weight, problems with the xanthan system, and in particular the tendency to form aggregates, can adversely influence the results. Thus where intrinsic viscosity is used directly, in this thesis, as a measure of molecular weight - notably in the computer analyses of the optical rotation data (section 4.7) and the data from oscillatory shear measurements on the mixed gel systems (section 7.14) - the results should be regarded with a suitable amount of caution.

5.8 Molecular Weight Estimation for the Galactomannans and Konjac Mannan

The molecular weights of the guar gum and locust bean gum samples used in this study were estimated from the intrinsic viscosity values using the data of Robinson *et al* (1982).

Robinson and coworkers measured the intrinsic viscosity, and the molecular weight using static light scattering, for a series of five guar gum fractions in 0.1M urea, and demonstrated that the relationship between the two was:

$$[\eta] = 3.8 \times 10^4 M^{0.723}$$

The low α value corresponds to the known random coil behavior of guar gum in solution. Their data is shown in figure 5.5.

The mean intrinsic viscosity of guar was found to be 15.6 dl/g and this corresponds to a molecular weight of 22.5×10^5 (table 5.7). The intrinsic viscosities in this study were measured in 20mM sodium chloride but, since guar gum is not a polyelectrolyte, the difference in solvent should not have significantly affected the result. The intrinsic viscosity and the estimated molecular weight agree well with most of the reports in the literature. McCleary *et al* (1985) measured the intrinsic viscosity of a range of guar gum samples from different sources and obtained values of 15 +/- 2 dl/g. Dea *et al* (1986) reported a value of 14.3 dl/g and Gaisford and colleagues (1986) a value of approximately 12 dl/g. This corresponded to a molecular weight of 6.3×10^5, determined by sedimentation equilibrium..

McCleary and coworkers (1981) studied the effect of galactose content upon the solution properties of the galactomannans and demonstrated that in dilute solution, the viscosity is totally dependent upon the nature of the D-mannan backbone, providing of course that sufficient galactose is present to maintain the polymer in solution. This being the case, it is not unreasonable to use the guar gum data of Robinson *et al* to estimate the molecular weight of locust bean gum, and Tako and Nakamura (1984) have in set a precedent for this, by using the Mark-Houwink parameters of Robinson and coworkers to determine the molecular weight of their locust bean gum sample from the intrinsic viscosity. The approximate 20% difference in galactose content will affect the molecular weight estimate, but by probably no more than the amount of error in the molecular weight of an arbitrary sample of guar gum interpolated from the Mark-Houwink plot.

The average intrinsic viscosity of the locust bean gum used in this study was 7.1 dl/g and this corresponds, therefore, to a molecular weight of 8.2×10^5. The intrinsic viscosity is slightly lower than most of the reports in the literature but the molecular weight, surprisingly, is a little higher. McCleary *et al* (1985), who again studied a wide range of samples from different sources, obtained values of 9.9-14.3 dl/g for total locust bean gum but slightly lower values, down to 7.4 dl/g, for the cold water soluble fraction alone. Gaisford *et al* (1986) achieved values of 6.0-9.2 dl/g for the hot and cold water soluble fractions of one polymer and 10.3-14.7 dl/g for the hot and cold water soluble fractions of another. These were equivalent, they said, to molecular weights (determined by sedimentation equilibrium) of $3.0\text{-}3.2 \times 10^5$ for the cold water soluble fractions, and $2.66\text{-}2.70 \times 10^5$ for the hot water soluble. Tako and Nakamura (1984) calculated a value of 2.63×10^5 for their sample.

An attempt was made to estimate the molecular weight of the konjac mannan using the data of Kishida *et al* (1978). Kishida and coworkers studied the methyl-derivative of konjac mannan instead of the native polymer, since the former shows greater solution stability. They stated, however, that the intrinsic viscosity versus molecular weight relationship could be "useful for the purpose of estimating the molecular weight of konjac glucomannan by viscometric methods". Using the methylated derivatives of four native konjac mannans and seven partial hydrolysates, these authors determined the intrinsic viscosities of the samples in water at 30°C, and the molecular weights, also in water, but at ambient temperature, using static light scattering. Their data is shown in figure 5.5. The Mark-Houwink-Sakurada equation determined from this data was as follows:

$$[\eta] = 6.37 \times 10^4 M^{0.74}$$

The low α value, as for the galactomannans, is indicative of random coil behaviour.

The average intrinsic viscosity of the glucomannan sample prepared for this study was 5.2 dl/g and this, using the data of Kishida *et al*, corresponds to a molecular weight of 18×10^4 (table 5.7). Both the intrinsic viscosity and the estimated molecular weight are very much lower than the values found by the Japanese group for their own unhydrolysed polymers. They obtained measurements of 18.6-19.9 dl/g for the intrinsic viscosities and $98.5\text{-}116 \times 10^4$ for the molecular weights. Sugiyama *et al* (1972) who determined the molecular weights of a selection of native konjac mannan samples using static light scattering also obtained much higher values, ranging from $25.5\text{-}112 \times 10^4$, and Shimahara *et al* (1975b) found a value of 120×10^4.

The reason for the very low intrinsic viscosity and molecular weight is not immediately obvious. As already noted in section 5.1, Sugiyama and colleagues (1972) have shown that the molecular weight of the glucomannan can vary significantly depending on the source and the method used to recover the material from the plant tuber. It is possible, therefore, that during the course of preparation, the polymer was subjected to very harsh treatment and, as a result, underwent considerable degradation. The crude flour used in this study was supplied by Dr I.C.M. Dea of Unilever Research but its original source and the method of preparation are unknown. The mild procedures used to extract the material from the crude flour, however, are unlikely to have resulted in degradation.

A more satisfactory explanation for the discrepancy may be found by comparing the data for methyl-konjac mannan with that of guar gum. Native konjac mannan is a slightly acetylated β-(1→4)-linked copolymer of D-glucose and D-mannose which may or may not have some branching. The galactomannan comprises a β-(1→4)-linked D-mannan backbone, partially

substituted with single residue D-galactose side chains. The side chains serve to solubilize the polymer but do not, according to McCleary *et al* (1981), affect the dilute solution behaviour. Both polysaccharides appear to behave as random coils. Since glucose and mannose are epimers, differing only in the orientation of one hydroxyl group and, further, as both polymers are /3-(1→4)-linked, one would expect them to show a similar degree of rotational freedom about the backbone glycosidic linkages. This being the case, they should also give very similar intrinsic viscosity versus molecular weight plots. The data in figure 5.5, however, shows an enormous difference between the plots for methyl-konjac mannan and guar gum. This suggests that partial methylation of konjac mannan causes a marked increase in the stiffness of the polymer relative to guar gum and that, as a result, the intrinsic viscosity for any given molecular weight is higher. This view is supported by the high K value for the glucomannan relative to that of guar gum. Thus, despite the authors' claims, it may not be valid to estimate the molecular weight of the native polymer from the intrinsic viscosity and molecular weight data for the methylated derivative.

Assuming that native konjac mannan does in fact behave in a similar fashion to guar gum, one can estimate the approximate molecular weight using the data of Robinson *et al*. The resulting value of 55 x 10^4 is more in line with the previously reported values. Of course, the additional contribution to the molecular weight made by the galactose side-chains of the galactomannan will affect the molecular weight estimate, but by nowhere near as much as the more than 300% difference in the molecular weights estimated from the data of Kishida *et al* and Robinson *et al*.

5.9 Chain Flexibility of Xanthan: Application of the Smidsrød and Haug B-value Method.

The ionic strength dependence of the intrinsic viscosity was studied for ps.646, ps.1128, ps.PXO_{61} and ps.556, in an attempt to compare the relative flexibility of these four polymers.

The intrinsic viscosities were measured over a range of ionic strengths between 2mM and 1M sodium chloride and the data is plotted against $I^{-1/2}$ in figure 5.7. The data shows a considerable amount of scatter and the likely reasons for this, namely experimental error (5% error bars are shown for ps.556), and aggregation upon freeze drying, have already been discussed. It was noted during the course of these experiments that where the samples at different ionic strengths were prepared from a single stock solution (as for example in the case of ps.PXO_{61}) the data fell much closer to a straight line. Because of this, the linear interpolation of figure 5.7 is weighted towards these points.

The slope of the intrinsic viscosity versus $I^{-1/2}$ plot is the so-called S value (table 5.8), which is a measure of chain flexibility. None of the four polymers studied showed pronounced ionic strength dependence and even ps.556, which appeared to be the most flexible,

displayed only a 32% change in intrinsic viscosity over the range of concentrations studied. This is consistent with the known rigidity of the xanthan molecule and with the findings of Muller *et al* (1986) and Sho *et al* (1986), who demonstrated that the electrostatic contribution towards the total persistence length of xanthan is very small. The amount of flexibility, however, did appear to vary between the polymers. Sample ps.556 was the most flexible, followed in turn by ps.646, ps.PXO_{61} and ps.1128.

Application of the Smidsrød and Haug B-value method to the intrinsic viscosity data failed to give satisfactory results. The persistence lengths calculated for the polymers in 0.1M salt (table 5.8) were in the case of ps.646, ps.PXO_{61} and ps.556 very much lower than the values determined by static light scattering, but the persistence length calculated for ps.1128 was greater.

Clearly the semi-empirical Smidsrød and Haug method cannot be applied to a molecule as stiff as xanthan. To illustrate this, the hypothetical position of xanthan, assuming a persistence length of 100 nm, has been marked on the plot of B versus 1/a (figure 5.6b). It falls, to all intents and purposes, at the origin. Although the data in the plot has been linked with a straight line, the behaviour of the polymers in this region of the curve must in fact deviate from linearity. DNA, which is itself a fairly rigid molecule, would appear to comply with the B-value rule. However, it is interesting to note, that the persistence length given by Smidsrød and Haug (ie. 25 nm) is very much lower than the majority of values reported in the literature. Presumably for the B-value method to apply, as it does for materials such as carboxymethylcellulose and alginate, the polymer requires a minimum amount of flexibility which enables it to expand and contract freely with the prevailing ionic conditions. Xanthan and possibly DNA lack the necessary flexibility. Far more exacting theories do exist to describe the electrostatic contribution to the persistence length for rigid chains, for example the Skolnick-Fixman-Odijk theories which were originally conceived to explain data for DNA (Odijk, 1977; Skolnick and Fixman, 1977).

The relative flexibility of the four polymers, as judged from their S values, appears to agree with the known conformational stability. In other words, the more acetyl and the less pyruvic acid present, the greater the stability of the ordered form and the lower the apparent flexibility. It would also appear to agree with the data of Coviello and coworkers (1986) who demonstrated that the depyruvylated derivative of Keltrol had a greater Kuhn segment length than the native polymer, and that this in turn, was higher than that of the deacetylated derivative. The light scattering data presented in this study, however, does not support the observations of Coviello *et al*. The Kuhn segment lengths of the pyruvylated polymers, ps.556 and ps.646, were a little lower than those of the highly acetylated materials, but the difference was really too small to be considered significant. Thus, in 0.1M potassium chloride

at least, the four polymers showed a similar degree of flexibility. This finding is substantiated by data from Callet *et al* (1987). These authors prepared an acetyl-free xanthan, a pyruvate-free xanthan, and an acetyl and pyruvate-free xanthan, by chemical hydrolysis of a single native polymer. They then obtained from each of the four materials, by sonication, a series of low molecular weight samples. The intrinsic viscosity and molecular weight of these were determined in 0.1M sodium chloride. A double logarithmic plot of intrinsic viscosity versus molecular weight gave a single curve. In other words, in 0.1M salt, the flexibility and therefore the intrinsic viscosity were essentially unaffected by the level of acetyl and pyruvate substitution. It is also interesting to note that in 0.1M salt the degree of local order for each of the four polymers, as indicated by the specific OR at 365 nm, appeared to be very similar (section 4.9).

The real anomaly in these results was the behaviour of ps.1128. The molecular weight of this polymer was, as judged from the intrinsic viscosity values, very much higher than that of the other materials and yet the contour length and molecular weight, as estimated from the light scattering data, were much the same. The intrinsic viscosity of ps.1128 showed virtually no ionic strength dependence and the polymer should therefore, on the basis of this behaviour, have been essentially a rigid rod. The persistence length in 0.1M potassium chloride, however, was not significantly different to that of the other xanthans. It seems likely, from these observations, that ps.1128 showed a particular predisposition toward aggregation upon freeze drying, and that the aggregates failed to break down under the regime used to prepare the polymer for the intrinsic viscosity measurements. That is, prolonged stirring, and heating at 90°C for one hour. Pressure cooking at 116°C, on the other hand, did break up the aggregates. The intrinsic viscosity behaviour of ps.1128 is probably not, therefore, directly comparable with that of ps.646, ps.PXO_{61} and ps.556.

Table 5.1: Molecular weight estimates for xanthan reported in the literature.

Reference	Method of Measurement	Molecular weight
Callet *et al*, 1987	Low-angle light scattering	5.2×10^6
Coviello *et al*, 1986	Light scattering	2.9×10^6
Dentini *et al*, 1984	Low-angle light scattering	1.5×10^6
Dintzis *et al*, 1970	(i) Determined from sedimentation and diffusion measurements using the Svedberg equation	1.4×10^6
	(ii) Light scattering	3.6×10^6 13×10^6 50×10^6
Holzwarth and Prestridge, 1977	Estimated from the contour length in electron micrographs	$4\text{-}20 \times 10^6$
Holzwarth, 1978	Estimated from the sedimentation coefficient (determined by band sedimentation) and intrinsic viscosity, using the Mandelkern-Flory-Scheraga equation.	14.8×10^6 62×10^6
Holzwarth and Ogletree, 1979	As for Holzwarth, 1978	7.0×10^6
Lambert *et al*, 1982	Light scattering	3.0×10^6
Lecourtier *et al*, 1986	Light scattering	4.8×10^6
Milas and Rinaudo, 1979	Light scattering	3.6×10^6
Milas and Rinaudo, 1984	Light scattering	6.1×10^6
Milas and Rinaudo, 1986	Light scattering	7.0×10^6
Morris *et al*, 1983	Light scattering	47×10^6 1.1×10^6

Table 5.1: continued.

Reference	Method of Measurement	Molecular Weight
Muller *et al*, 1986	Low-angle light scattering	1.8×10^6
Norton *et al*, 1984	Low-angle light scattering	3.0×10^6
Paradossi and Brant, 1982	Light scattering	1.95×10^6
Rinaudo and Milas, 1978	Light scattering	2.0×10^6
Sato *et al*, 1984b	Light scattering	7.4×10^6
Southwick *et al*, 1980	Estimated from the translational diffusion coefficient (determined by quasi-elastic light scattering) and the intrinsic viscosity, using the Flory-Mandelkern equation.	2.16×10^6
Whitcomb and Macosko, 1978	As for Holzwarth, 1978	7.6×10^6

Table 5.2: Huggins and Kraemer plot data for ps.556 and guar gum in 20mM sodium chloride.

Polymer	Nominal Concentration % $^{w}/_{w}$ x 10^{-2}	Huggins Plot ηsp	Huggins Plot $\eta sp/c$	Kraemer Plot ηrel	Kraemer Plot $\ln \eta rel/c$
ps.556	0.3985	0.227	56.88	1.227	51.27
		0.218	54.72	1.218	49.50
		0.208	52.22	1.208	47.44
	0.6000	0.332	55.39	1.332	47.82
		0.336	55.98	1.336	48.26
		0.341	56.87	1.341	48.93
	0.8005	0.478	59.68	1.478	48.78
		0.474	59.27	1.474	48.50
		0.485	60.63	1.485	49.42
	0.9980	0.640	64.12	1.640	49.57
		0.638	63.90	1.638	49.43
		0.628	62.97	1.628	48.86
	1.196	0.759	63.40	1.759	47.18
		0.794	66.40	1.794	48.87
		0.791	66.14	1.791	48.73
Guar Gum	2.001	0.392	19.57	1.392	16.51
		0.394	19.69	1.394	16.60
		0.445	22.26	1.445	18.41
	2.444	0.563	23.03	1.563	18.27
		0.542	22.18	1.542	17.72
		0.509	20.82	1.509	16.83
	2.935	0.661	22.51	1.661	17.28
		0.671	22.87	1.671	17.50
		0.667	22.73	1.667	17.41
	3.493	0.823	23.57	1.823	17.19
		0.833	23.84	1.833	17.34
		0.809	23.17	1.809	16.98
	4.000	1.049	26.23	2.04	17.94
		1.042	26.05	2.042	17.85
		1.008	25.21	2.008	17.43
		1.027	25.67	2.027	17.66

NB. These data were calculated by the computer to a higher number of decimal places than are actually shown. The figures in each column do not therefore correspond exactly.

Table 5.3: Intrinsic viscosity measurements for xanthans, determined using both the Huggins and Kraemer extrapolations.

Polymer	Sodium Chloride Concentration (mM)	Intrinsic Viscosity (dl/g) Huggins Plot Data	Huggins Plot Mean	Kraemer Plot Data	Kraemer Plot Mean
ps.646	2	46.9		50.1	
	3	45.4		45.0	
	5	42.0		41.6	
	10	32.0	32.0	34.7	33.5
		32.1		32.2	
	20	41.9	40.0	41.7	40.2
		31.0		33.1	
		47.1		45.9	
	50	30.4		30.5	
	200	38.6		38.3	
ps.646[a]	20	22.3		23.3	
DA ps.646	20	30.1		29.8	
DP ps.646	20	15.6		15.5	
DAP ps.646	20	14.2		14.4	
ps.646[b1]	20	81.8		84.2	
ps.646[b2]	20	103.9		103.6	
Kelzan	20	68.8		67.7	
ps.1128	2	76.4		76.4	
	5	79.6		78.8	
	10	80.7		82.1	
	20	70.1	79.6	73.2	82.5
		85.0		89.0	
		83.8		85.2	
	200	80.1		78.5	
	1000	78.1		77.5	
DA ps.1128 (Batch 1)	20	24.9		24.5	
DA ps.1128 (Batch 2)	20	21.8		22.1	

Table 5.3: continued.

Polymer	Sodium Chloride Concentration (mM)	Intrinsic Viscosity (dl/g) Huggins Plot Data	Huggins Plot Mean	Kraemer Plot Data	Kraemer Plot Mean
ps.PXO_{61}	2	53.4		53.7	
	3	45.8		47.3	
	5	47.9		46.7	
	10	45.5		46.1	
	20	45.4	42.7	45.9	43.7
		40.0		41.4	
	200	38.2		38.3	
DA ps.PXO_{61}	20	27.5		26.8	
ps.556	2	77.8		79.2	
	3	67.6		67.4	
	5	58.8		58.8	
	10	55.4		54.9	
	20	50.2	52.3	51.3	52.9
		54.4		54.4	
	200	46.5		47.2	
	1000	52.3		52.9	
DP ps.556	20	16.4		16.4	
Flocon 4800C	20	28.0		28.4	
DP Flocon 4800C	20	10.1		10.5	
ps.BD9A	20	8.8		8.9	

a Polymer had not been lyophilized at any stage.

b1 Polymer produced by strain 646 in continuous culture under conditions of potassium limitation and at a dilution rate of 0.024/hr.

b2 Polymer produced by strain 646 in continuous culture under conditions of potassium limitation and at a dilution rate of 0.12/hr.

Table 5.4: Intrinsic viscosity measurements for the gluco- and galactomannans, determined using both the Huggins and Kraemer extrapolations.

Polymer	Sodium Chloride Concentration (mM)	Intrinsic Viscosity (dl/g) Huggins Plot Data	Huggins Plot Mean	Kraemer Plot Data	Kraemer Plot Mean
Konjac Mannan	20	4.6 5.8	5.2	4.6 5.8	5.2
Locust Bean Gum	20	7.1 6.4	6.8	7.4 6.7	7.1
Guar Gum	20	18.0 11.7 14.2	14.6	18.1 13.4 15.4	15.6

Table 5.5: Static light scattering measurements.

Polymer	$M_w \times 10^6$	R_g (nm)	N_K	M_L	L (nm)	l_K (nm)
ps.646	0.9 - 1.2	152	~3	1700	575	~200
ps.1128	1.27	197	3.3	1550	833	254
ps.PXO_{61}	1.60	220	4.0	1625	994	247
ps.556	1.48	231	4.9	1320	1130	230

Table 5.6: Xanthan molecular weights determined from the data of Sato *et al* (1984c).

Polymer	Sodium Chloride Concentration (mM)	Intrinsic Viscosity (dl/g)	Molecular Weight $x10^6$
ps.646	20	34.1*	2.65
	100	30.2*	2.40
ps.646[a]	20	23.3	1.92
DA ps.646	20	29.8	2.35
DP ps.646	20	15.5	1.32
DAP ps.646	20	14.4	1.25
ps.646[b1]	20	84.2	7.80
ps.646[b2]	20	103.6	8.80
Kelzan	20	67.7	5.30
ps.1128	20	79.5*	6.40
	100	79.0*	6.30
DA ps.1128 (Batch 1)	20	24.5	2.00
DA ps.1128 (Batch 2)	20	22.1	1.84
$ps.PXO_{61}$	20	42.1*	3.20
	100	39.4*	3.05
DA $ps.PXO_{61}$	20	26.8	2.18
ps.556	20	53.8*	4.10
	100	49.6*	3.80
DP ps.556	20	16.4	1.40
Flocon 4800C	20	28.4	2.25
DP Flocon 4800C	20	10.5	0.96
ps.BD9A	20	8.9	(0.85)

a, b1, b2 As for table 5.3.
* Determined from the plot of $[\eta]$ vs. $I^{-1/2}$

Table 5.7: Molecular weights of the gluco- and galactomannans estimated from the data of Kishida *et al* (1978) and Robinson *et al* (1982) respectively.

Polymer	Intrinsic Viscosity (dl/g)	Estimated Molecular Weight
Konjac Mannan	5.2	18.0×10^4
Locust Bean Gum	7.1	8.2×10^5
Guar Gum	15.6	22.5×10^5

Table 5.8: Molecular weight and flexibility of xanthans as determined by static light scattering and from the intrinsic viscosity data.

Polymer	%Ac	%Pyr	Salt Concentration (mM)	Intrinsic Viscosity Data				Static Light Scattering Data	
				[η] dl/g	Mw x 10^6 *	S	a (nm)**	Mw x 10^6	a (nm)
ps.646	4.5	4.4	20	34.1	2.65	1.01	-	-	-
			100	30.2	2.40		21.6	0.9-1.2	~100
ps.1128	7.7	1.7	20	79.5	6.40	0.13	-	-	-
			100	79.0	6.30		586.1	1.27	127
ps.PXO_{61}	14.3	0.3	20	42.1	3.20	0.73	-	-	-
			100	39.4	3.05		42.2	1.60	124
ps.556	1.6	6.0	20	53.8	4.10	1.06	-	-	-
			100	49.6	3.80		39.2	1.48	115

* Estimated from the data of Sato et al (1984c).
** Estimated from the intrinsic viscosity data using the Smidsrød and Haug B-value method.

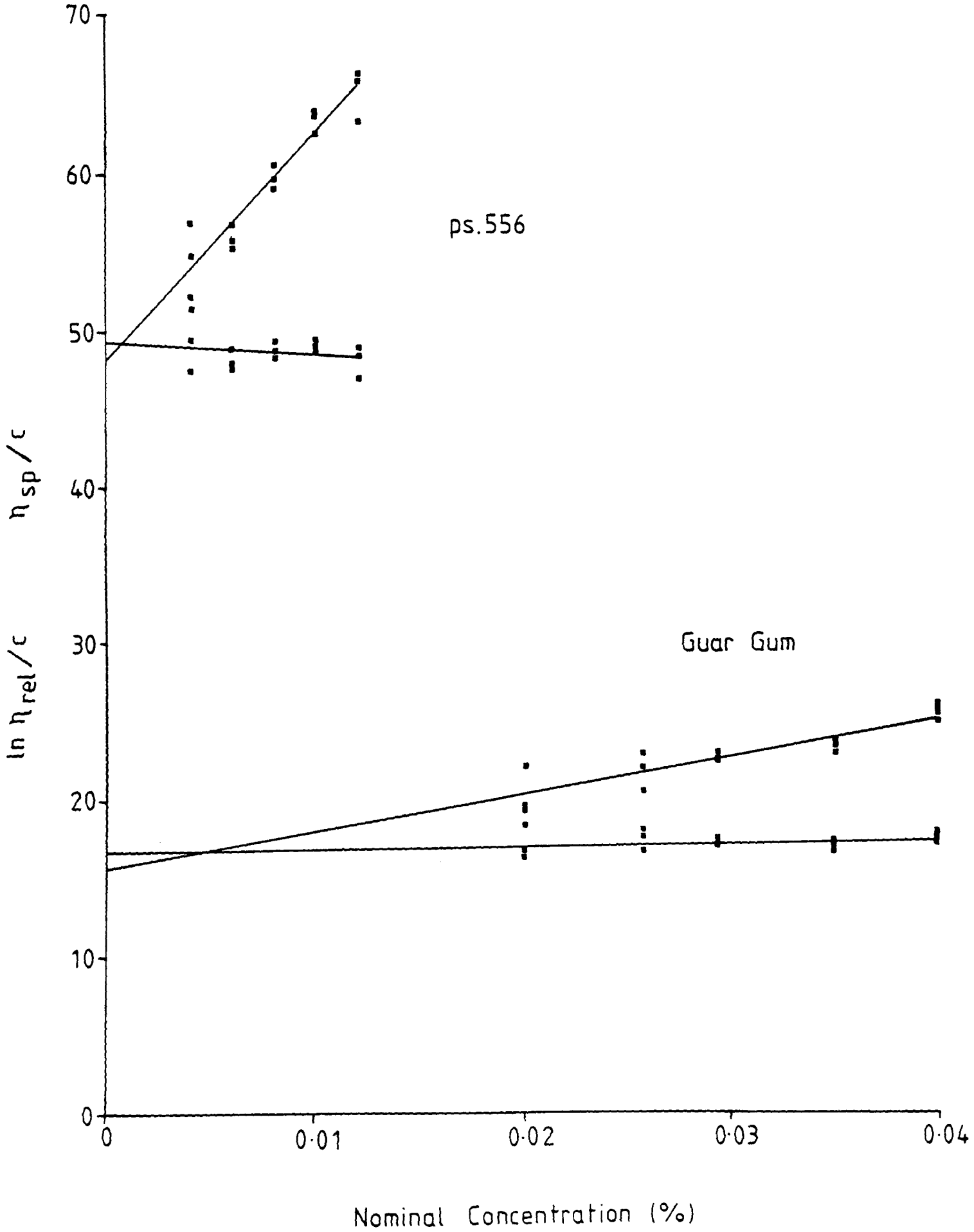

Fig. 5·1 The Huggins and Kraemer extrapolations for ps.556 and guar gum in 20 mM sodium chloride.

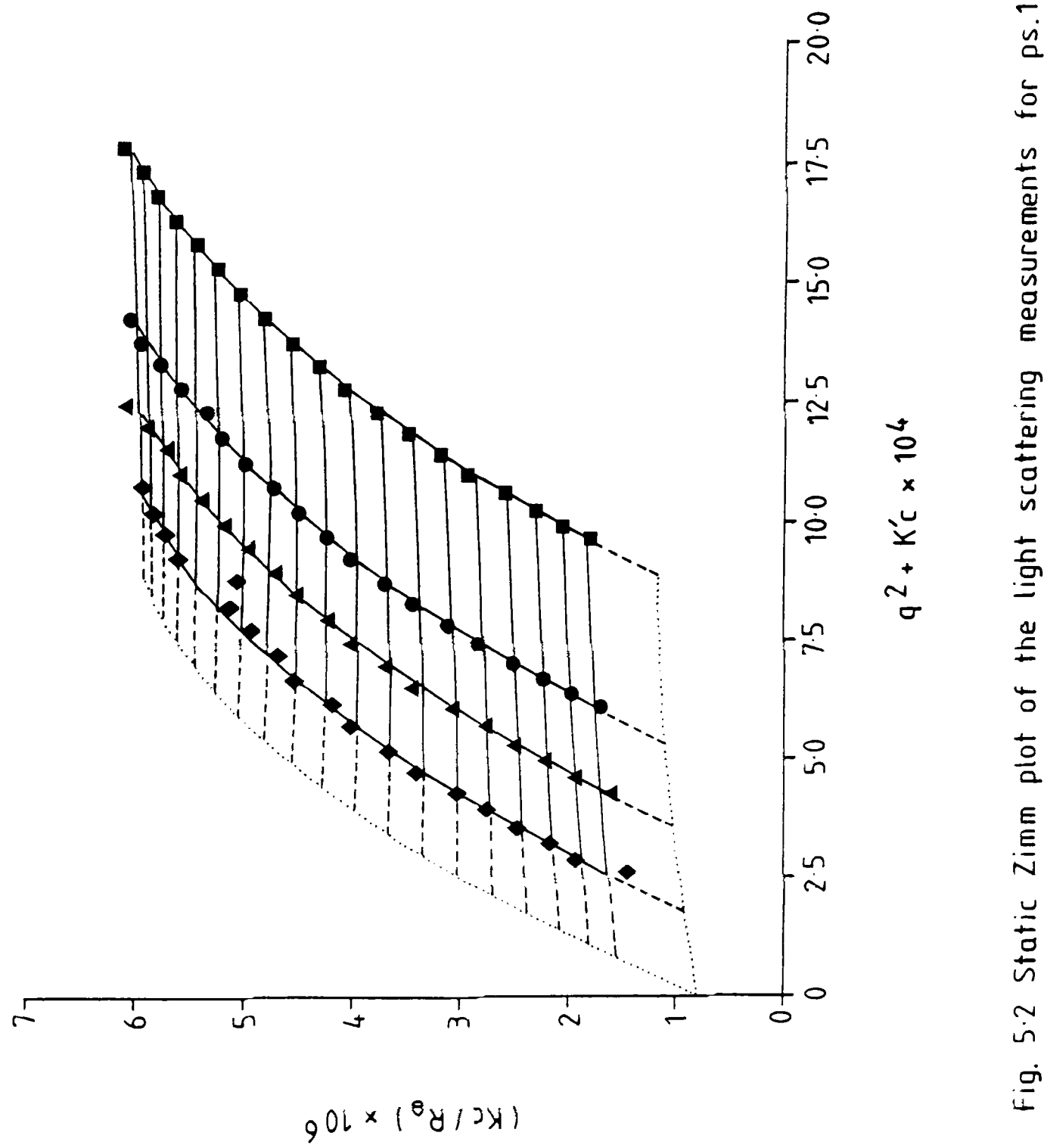

Fig. 5·2 Static Zimm plot of the light scattering measurements for ps.1128 in 0·1M potassium chloride.

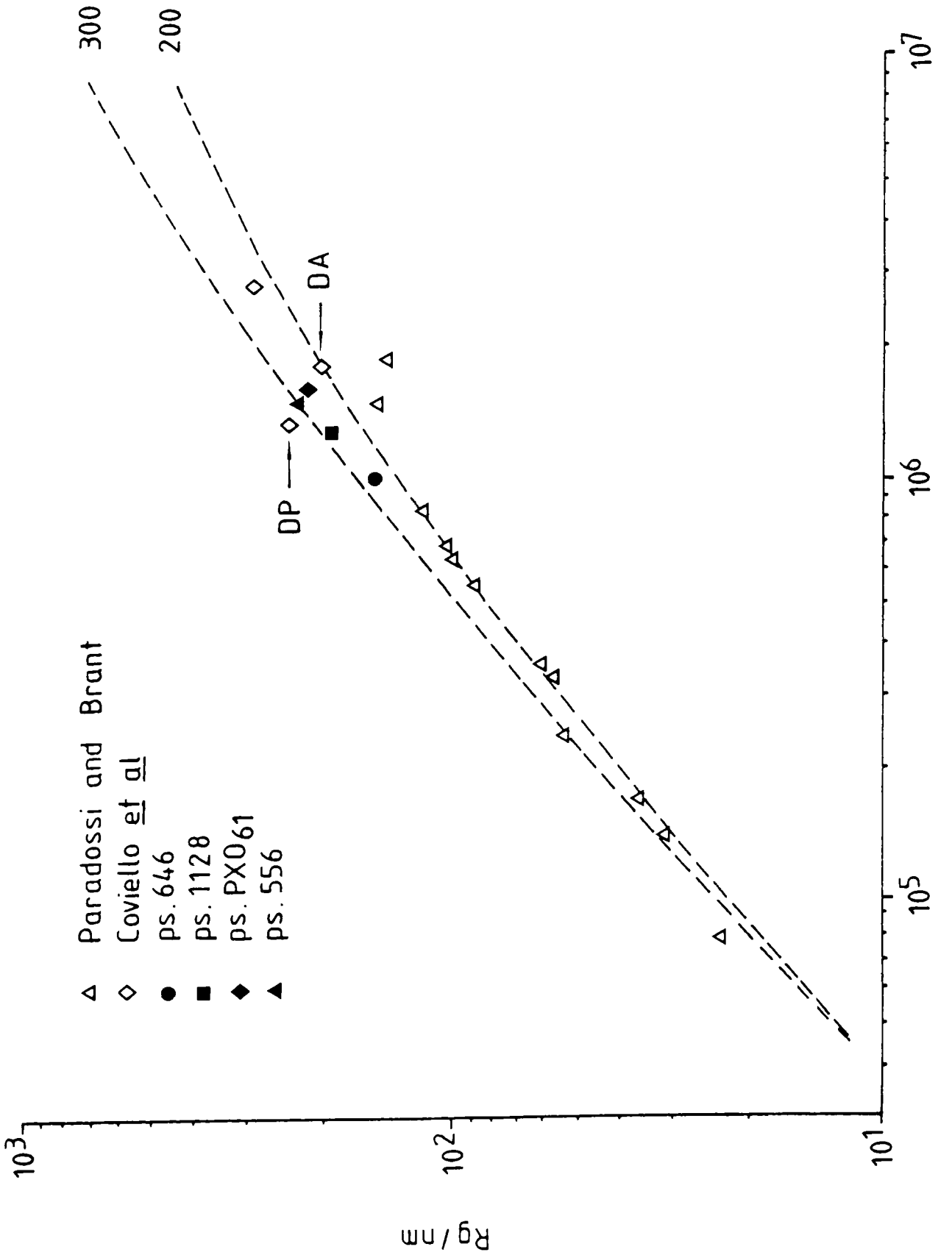

Fig. 5·3 Molecular weight dependence of the z-average root mean square radius of gyration for various xanthan fractions.

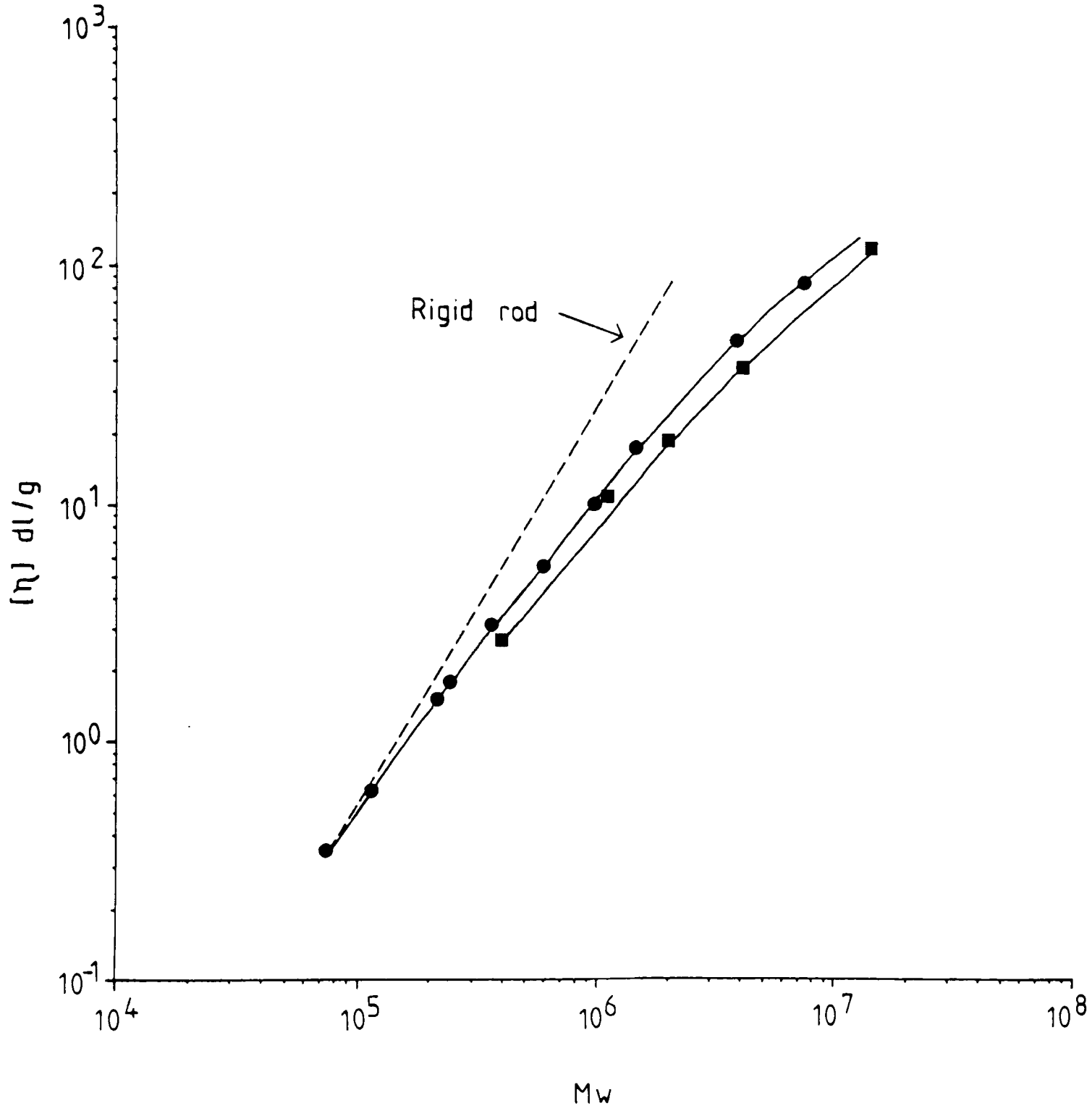

Fig. 5·4 Intrinsic viscosity versus molecular weight plot for xanthan. Data from Sato et al, 1984c (●) and Holzwarth, 1978 (■).

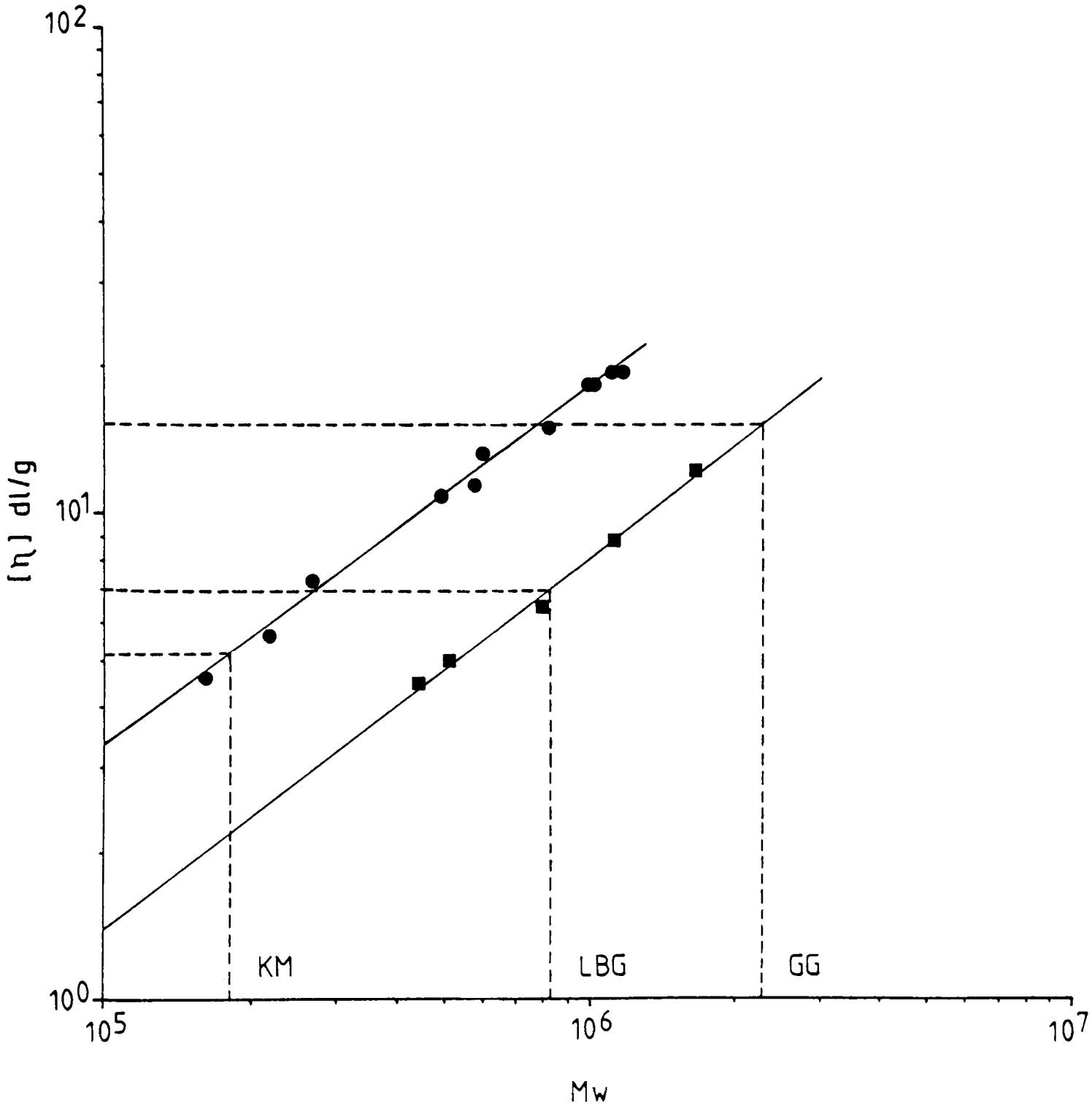

Fig. 5·5 Intrinsic viscosity versus molecular weight plots for methyl-konjac mannan, Kishida et al, 1978 (●), and guar gum, Robinson et al, 1982 (■).

Fig. 5·6 The Smidsrød and Haug "B-value" method (Morris and Ross-Murphy, 1981).

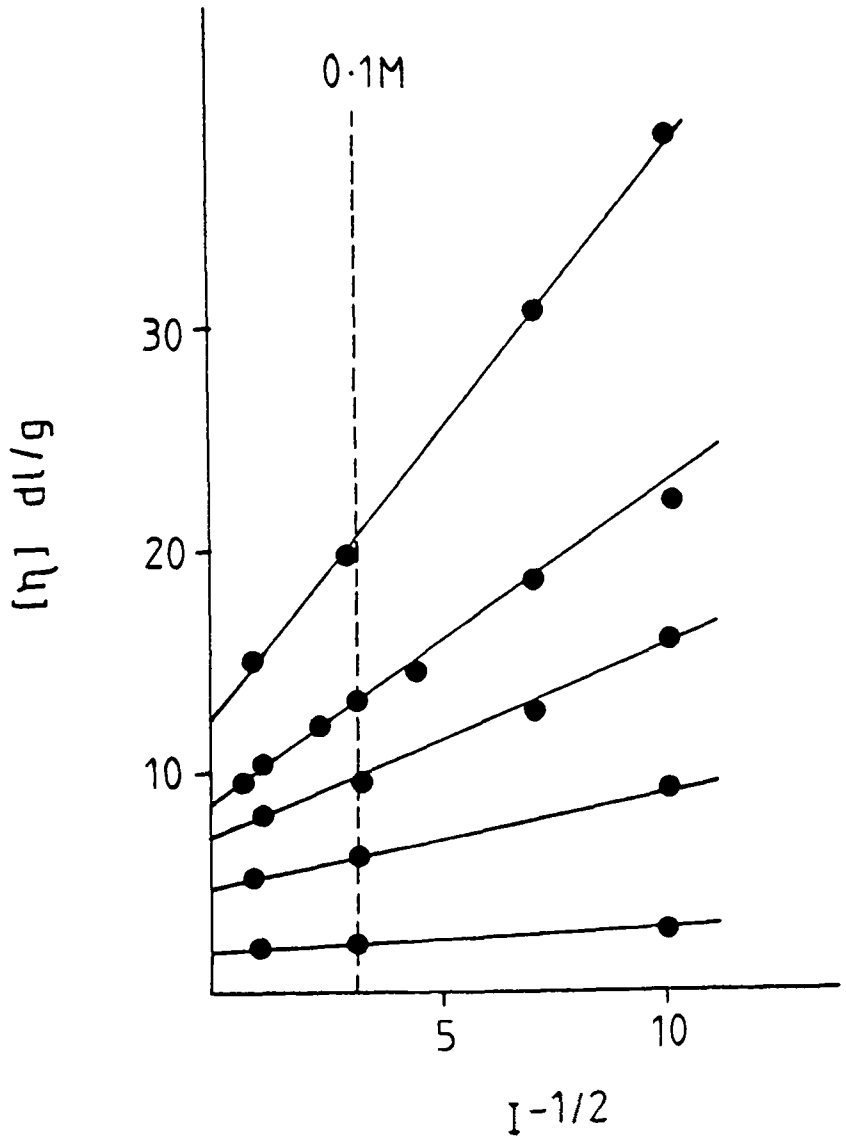

a) Ionic strength dependence of intrinsic viscosity for a range of alginate samples of different chain length.

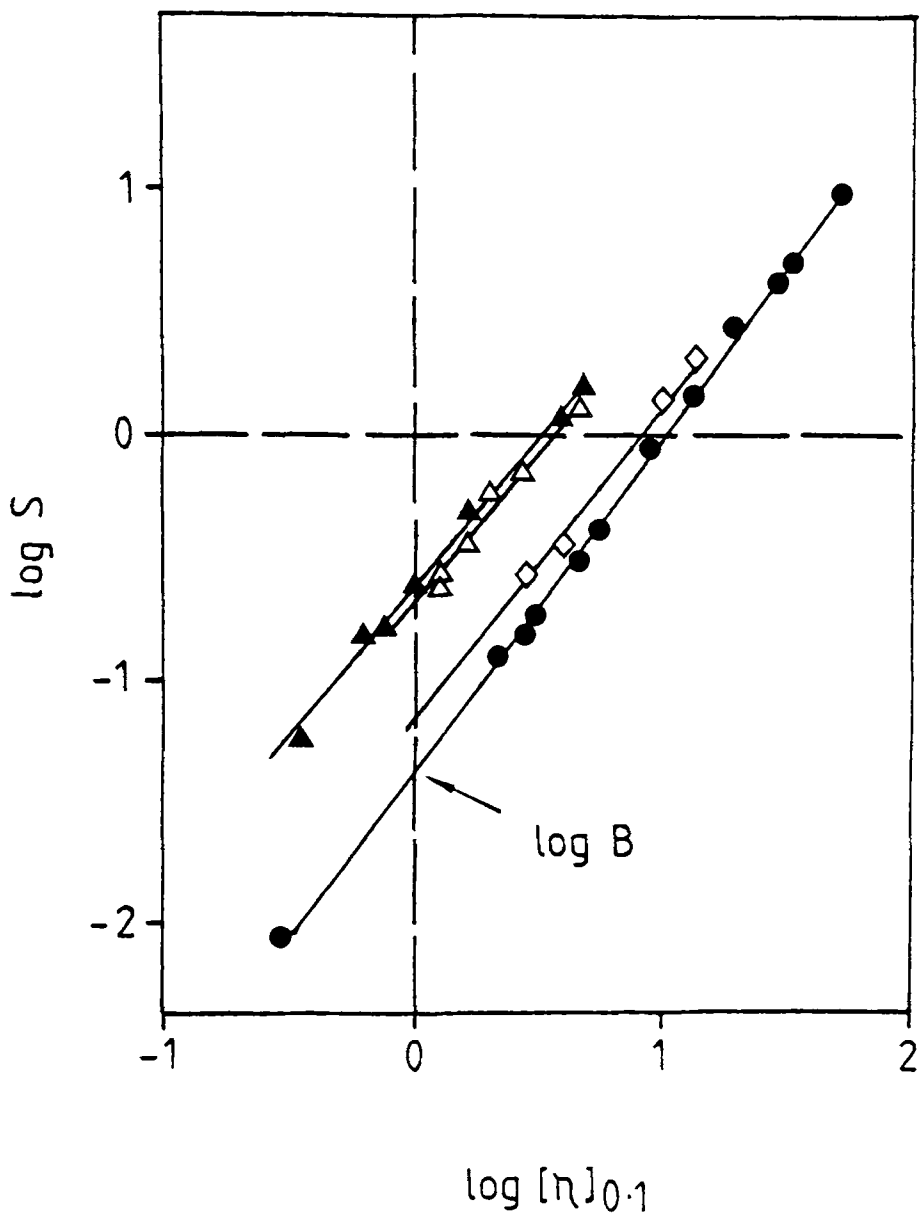

b) The variation with chain length (characterised by $[\eta]_{0\cdot1}$) of the ability of polyelectrolyte coils to expand or contract in response to changes in ionic strength (characterised by the slope S). This is shown for alginate (●), carboxmethyl-cellulose (◇), carboxymethylamylose (△) and polyacrylate (■).

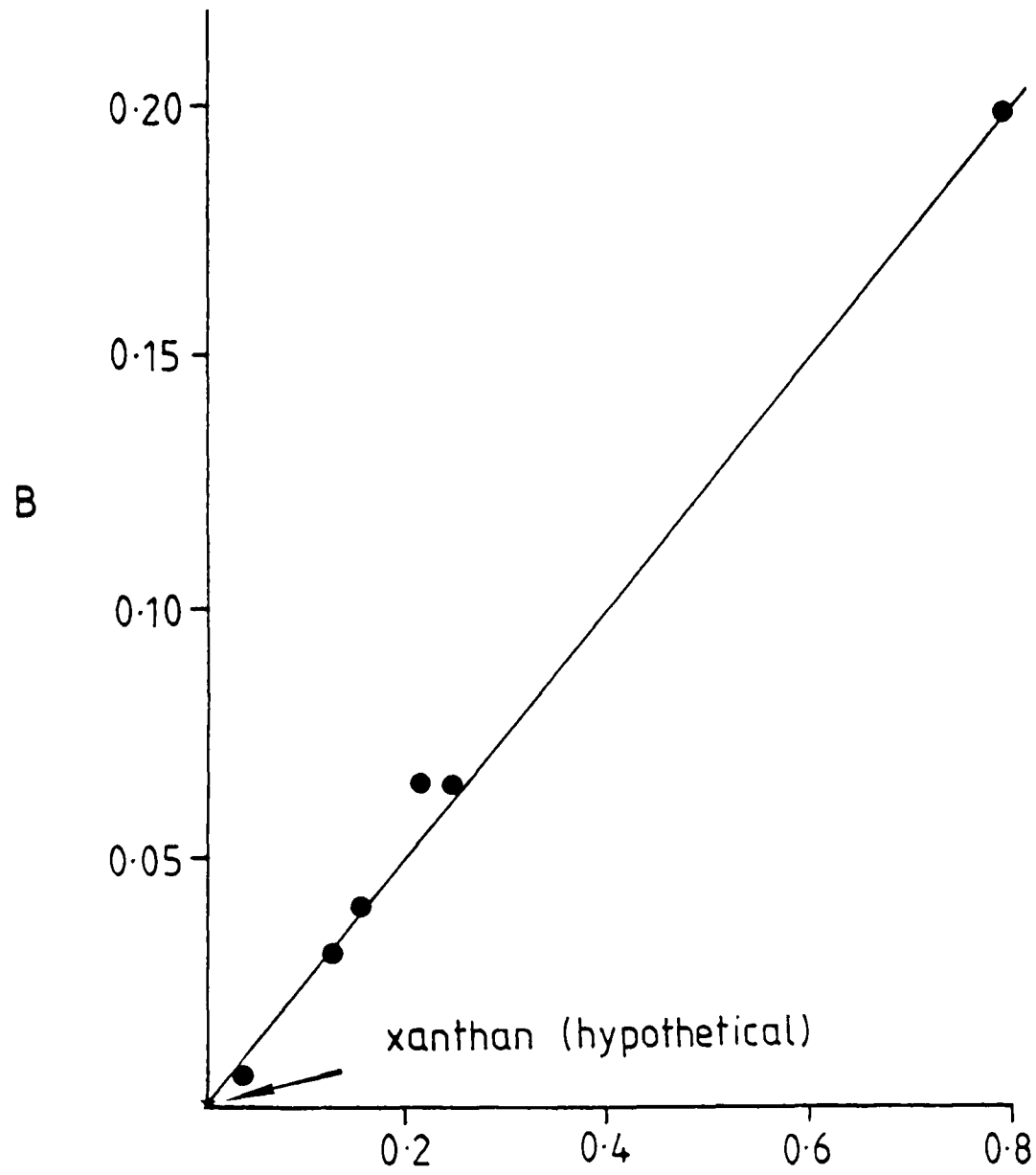

c) Correlation of the empirical flexibility parameter B with persistence length (a) for a series of polyelectrolytes. These are, in order of increasing B value, DNA, alginate relatively rich in polyguluronate, polymannuronate and alternating sequences respectively, carboxymethylcellulose and carboxymethylamylose.

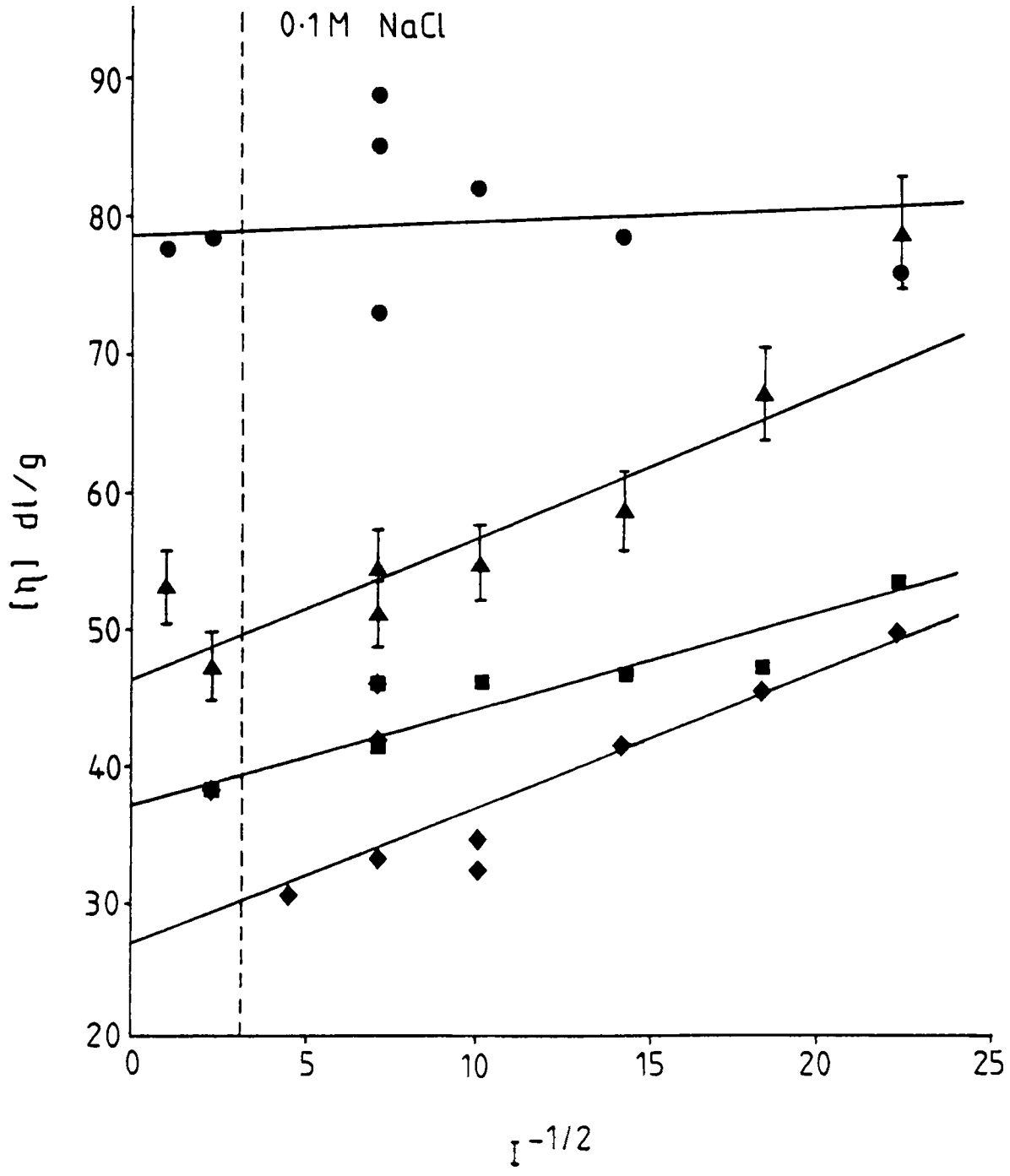

Fig. 5·7 Plot of intrinsic viscosity versus $I^{-\frac{1}{2}}$ for ps.646 (◆), ps.1128 (●), ps.PXO_{61} (■) and ps.556 (▲).

CHAPTER 6

PHYSICAL CHARACTERIZATION III: VISCOMETRY

Introduction

6.1 Viscosity of Xanthan Solutions

Xanthan gum, even at relatively low concentrations, produces very viscous solutions with excellent particle suspending and emulsion stabilizing properties. The solutions are highly pseudoplastic, with a low shear Newtonian plateau region detectable only at comparatively low polysaccharide concentrations - typically less than 0.2% (Cuvelier and Launay, 1986). Some thixotropy is evident (Morris, 1984; Zatz and Knapp, 1984; Richardson and Ross-Murphy, 1987b; Rochefort and Middleman, 1987) but most of the solution viscosity recovers quickly after deformation, except under conditions of low ionic strength (Rochefort and Middleman, 1987). It is these aspects of the xanthan solution rheology which make it an invaluable asset in a wide range of industrial products and processes (see section 1.3).

The concentration dependence of viscosity for xanthan solutions appears to be somewhat different to that of typical random coil polysaccharides (Morris *et al*, 1981; Morris, 1984). A double logarithmic plot of "zero shear" specific viscosity (η_{sp0}) against concentration, for most random coil hydrocolloids, shows a pronounced increase in slope at a specific critical concentration, referred to here as c^* (the precise definition of c^* varies from one publication to another). Under the dilute solution conditions below c^* the individual molecules are present as isolated coils, but above c^* coil overlap is believed to occur and the molecules interpenetrate to form an "entangled" network. It is the change in flow properties resulting from entanglement that gives rise to the abrupt change in the concentration dependence of η_{sp0}.

The value of c^* for a particular polymer is dependent upon the volume occupied by each molecule in isolation ie. the intrinsic viscosity, $[\eta]$ (see section 5.3). The total volume occupied by all of the molecules in solution, therefore, may be characterized by the dimensionless "coil overlap parameter", $c[\eta]$, irrespective of the type of polymer or its molecular weight. Experimental data for a wide range of random coil polysaccharides has revealed a striking generality in the behaviour of such polymers (Morris *et al*, 1981). A double logarithmic plot of η_{sp0} versus $c[\eta]$ produces a single master curve (figure 6.1) in which the c^* transition occurs at a value of $c[\eta]$ close to 4. This corresponds to a specific viscosity of roughly 10. The slope of the curve below c^* is approximately 1.4 and above it, approximately 3.3.

Launay and coworkers (1984; see also Cuvelier and Launay, 1986) studied the variation in η_{sp0} with $c[\eta]$ for xanthan under a range of solvent conditions (ie. in water and in solutions of sucrose and sodium chloride at different concentrations) and found that instead of the usual master curve, solutions of xanthan gave a series of plots which did not superpose and which showed two apparent critical concentrations. These

they denoted c^* and c^{**}. In the dilute solution region (ie. below c^*) the slopes of the curves were typically 1.2-1.3, comparable with that of the random coil polysaccharides, but the onset of coil overlap occurred at relatively low concentrations and the slope above c^* increased to approximately 2 for solutions of xanthan in water and 0.1M sodium chloride. Above c^{**} the gradient of the curve increased still further, reaching values of 4-5. At high concentrations, therefore, the concentration dependence of η_{sp0} was greater for xanthan than for polysaccharide systems showing purely physical entanglements. This suggests that some other sort of interaction mechanism must be involved. The existence of two critical concentrations has also been suggested by Southwick *et al* (1981), on the basis of their quasi-elastic light scattering measurements and these authors suggested that the c^{**} transition could result from the development of more permanent associations between the xanthan molecules in concentrated solution. Analogous results have, in addition, (as noted by Cuvelier and Launay, 1986) been reported for synthetic polymer solutions and for hydroxyethylcellulose in 0.1M aqueous sodium chloride.

The viscosity of typical random coil polyelectrolyte solutions is dramatically affected by changes in the pH or ionic strength. Addition of salt, for example, brings about a huge fall in the solution viscosity as a result of charge shielding and the subsequent reduction in the random coil dimensions of the polymer. Solutions of xanthan, however, are not affected to anything like the same extent and this may be attributed to the innate stiffness of the xanthan molecule (see section 5.2). Changes in the viscosity in response to pH are relatively small, even in water, and they diminish still further in the presence of salt (Jeanes *et al*, 1961; Rocks, 1971; Kovacs and Kang, 1977; Sandford *et al*, 1977). The effect of salt upon the viscosity is dependent upon the polysaccharide concentration. Below concentrations of about 0.2-0.3% (different publications give different values) increasing the ionic strength results in a fall in viscosity but at higher polysaccharide concentrations the viscosity actually increases (Jeanes *et al*, 1961; Sandford *et al*, 1977; Symes, 1980; Zatz and Knapp, 1984; Rochefort and Middleman, 1987). At the lower concentrations, as with other polyelectrolytes, the fall in viscosity is due to the decrease in hydrodynamic volume resulting from charge shielding but at higher polysaccharide concentrations, the decrease in hydrodynamic volume is believed to be offset by molecular association.

The possibility of molecular associations other than physical entanglement is a recurring theme and a number of authors have suggested that the solution rheology of xanthan could be explained by the non-covalent association of molecules to form a three dimensional "weak gel" network (Morris *et al*, 1977a; Ross-Murphy *et al*, 1983; Morris, 1984; Cuvelier and Launay, 1986). The formation of such a network would explain the high viscosity, and the particle suspending and emulsion stabilizing properties of xanthan, whilst the breakdown of the system under shear would account for the pseudoplasticity. The mechanical spectrum for

xanthan provides tangible evidence for such a network (Frangou *et al*, 1982; Ross-Murphy *et al*, 1983; Morris, 1984; Richardson and Ross-Murphy, 1987). The frequency sweep for a concentrated solution of xanthan (2% $^{w}/_{w}$) in the presence of salt is given in figure 7.10b . It shows quite definite elastic behaviour. G' is greater than G" throughout the accessible frequency range, with little frequency dependence of either modulus, and the dynamic viscosity (η^*) decreases sharply with increasing frequency.

The nature of the intermolecular interaction is uncertain. Morris (1984) has suggested that long stretches of the polymer chains could associate to form conformationally ordered "junction zones", stabilized by co-operative arrays of non-covalent interactions. These would be analogous to those in a true gel (section 7.1) but of lower binding energy. Alternatively, as suggested by Cuvelier and Launay (1986), parallel packing of the xanthan chains might occur at high concentrations, with the domains of associated chains being stabilized by hydrogen bonding. There is, however, no evidence to favour any one particular mechanism.

Frangou and coworkers (1982) reported that in the presence of 4M urea, the normal elastic frequency sweep observed for xanthan in the presence of salt disappeared and the material showed typical polymer solution behaviour (ie. an entanglement system). They also noted that the viscosity of a 0.5% xanthan solution at low shear rates, fell progressively as the concentration of urea increased. The apparent decrease in the amount of association in the presence of high concentrations of urea indicates that hydrogen bonding plays an important role in the mechanism of association. The increase in viscosity with salt, at high polysaccharide concentrations, also suggests the involvement of some sort of ionic interaction. For example, specific chelation of counterions between the participating chains might occur, as it does in certain gelling polysaccharides, notably alginate and the carrageenans (Clark and Ross-Murphy, 1987). The possible involvement of a third type of non-covalent interaction, namely hydrophobic bonding between the apolar methyl groups of the pyruvic acid substituents located at the periphery of the helix, will be discussed in the next section.

At higher concentrations (>3%) there is evidence to suggest that xanthan adopts an even more highly ordered liquid crystalline arrangement in solution. Such evidence includes the existence of significant optical birefringence in very concentrated, quiescent solutions of xanthan (Maret *et al*, 1981; Salamone *et al*, 1982; Lim *et al*, 1984).

The effect of temperature on the solution viscosity is complex. Reports in the literature vary and it is likely that the viscosity is influenced by a range of other factors including the ionic strength, the shear rate and possibly also the polysaccharide concentration. To summarize, however: in the presence of salt the viscosity is fairly stable to high temperatures. A slight decrease may be observed, particularly at

low polysaccharide concentrations (Jeanes *et al*, 1961; Sandford *et al*, 1977; Launay *et al*, 1984), but the overall stability reflects the maintenance of the ordered conformation and therefore the majority of the solution structure (Rochefort and Middleman, 1987), under conditions of high ionic strength. In the absence of salt, the viscosity appears to be heavily dependent upon the shear rate. At low shear rates there is a marked decrease in viscosity as the temperature increases and this appears to correlate with the fall in the intrinsic viscosity as the polymer undergoes the transition from the ordered to the disordered state (Morris *et al*, 1977a). At high shear rates, however, the onset of helix melting is accompanied by an anomalous increase in viscosity (Jeanes *et al*, 1961; Holzwarth, 1976; Morris *et al*, 1977a; Sandford *et al*, 1977). This is generally considered to be the result of molecular extension and the formation of non-specific entanglements under the high shear conditions.

6.2 The Influence of Acetyl and Pyruvate Upon Viscosity

The effect of different degrees of acetyl and pyruvate substitution on the viscosity of xanthan solutions has been the subject of a considerable amount of research in recent years.

Callet and coworkers (1987) produced a series of different molecular weight samples, prepared from native xanthan and its chemically deacetylated and depyruvylated derivatives, by sonication. They then determined the molecular weight of each sample, together with the intrinsic viscosity and the specific viscosity below c^*, in 0.1M sodium chloride. Double logarithmic plots of intrinsic viscosity versus molecular weight, and specific viscosity versus $c[\eta]$, gave single curves, indicating that in dilute solution, at least, the acetyl and pyruvic acid contents of the polymer have no effect upon the viscosity.

At higher concentrations, however, there is evidence to suggest that the acyl groups can influence the degree of macromolecular association. Sandford *et al* (1977) studied xanthans from both commercial sources and laboratory fermentations. They observed that at concentrations of 0.1% and 0.5% polysaccharide, the high pyruvate polymers were more viscous than the low pyruvate materials, although in this study no account was taken of the molecular weight.

Smith and coworkers (1981), using seven different polymers, mostly from commercial sources, calculated the fractional change in viscosity resulting from the addition of 0.1M potassium chloride to a previously salt-free 1% solution of the polysaccharide. They found that where the fraction of side chains substituted with pyruvic acid was less than 0.31, there was a fall in the viscosity upon addition of salt, but that above this critical value, the viscosity increased rapidly as the pyruvate content rose. The fall in viscosity below 0.31 was attributed to a reduction in the electroviscous effects at higher ionic strength, but

above the critical value this effect was believed to be at first offset, and then completely surpassed, by the positive contribution to the viscosity from macromolecular association.

Smith *et al* (1981) also studied the effect of polysaccharide concentration on the viscosity of two polymers, with similar intrinsic viscosities but different degrees of pyruvic acid substitution (0.34 and 0.39). Measurements were made in water and in 0.1M potassium chloride. At low concentrations there was a net decrease in viscosity with salt for both polymers, but at higher concentrations the effect of the reduction in hydrodynamic volume appeared to be surpassed by the viscosity enhancing effects of the intermolecular interactions. A net increase in viscosity was therefore observed in the presence of salt. Each polymer displayed a cross-over concentration where the solution rheology in water was identical to that in 0.1M potassium chloride. The polymer with the higher degree of pyruvate substitution had a lower c^* value in both water and salt solution, and a greater slope above c^*. This, then, also appeared to indicate that macromolecular association becomes increasingly favourable as the amount of pyruvate increases, and that there is a more rapid build up of association with concentration, the higher the level of pyruvic acid.

Bradshaw *et al* (1983) prepared chemically deacetylated and depyruvylated derivatives of Keltrol under optimized conditions, in order to avoid depolymerization. They then compared the viscosity of 0.3% solutions of each in water and in 1% potassium chloride. The viscosity and pseudoplasticity in both solvents, appeared to be essentially unaltered by removal of the acetyl and pyruvic acid groups. A series of polymers with varying amounts of pyruvate were also prepared by hydrolysis of the native material for different time periods. The viscosity of these polymers at 0.3%, was found to be independent of the amount of pyruvic acid and insensitive to the addition of salt.

At first sight this data would appear to contradict the earlier evidence, but as Smith *et al* pointed out in a subsequent publication (1984), the 0.3% concentration used by Bradshaw was very close to the cross-over that they themselves had observed. Hence no appreciable change in viscosity was to be expected at this concentration.

The reason for the apparent enhancement of molecular association by pyruvic acid is uncertain. However Smith and coworkers (1981) have suggested that apolar interactions between the pyruvate methyl groups could be responsible. Enough pyruvic acid substituents, located in sufficiently close proximity, could act co-operatively to form apolar regions stretching not only around the helix, but also parallel to the axis. Hydrophobic interactions between adjacent chains could, therefore, increase the polymer-polymer affinity relative to the polymer-solvent affinity and thereby raise the viscosity, particularly in the presence of salt.

The effect of acetyl substitution on viscosity has not been studied to anything like the same extent as pyruvic acid, but there is some evidence to suggest that the acetyl groups inhibit macromolecular association at higher concentrations. Jeanes *et al* (1961) noted that the deacetylated derivative of xanthan was more viscous than the native polymer in both water and salt solution, whilst Tako and Nakamura (1984) reported a higher dynamic viscosity (η') and elasticity (G') for the deacetylated derivative at concentrations of greater than 0.5% (at below 0.3% η' and G' were lower). The explanation for the inhibitory effect, if it genuinely exists, is obscure. However, Tako and Nakamura (1984) have proposed a model in which the xanthan molecules in solution are "associated in quaternary" between the charged trisaccharide side chains which are aligned parallel or antiparallel. They have suggested that an increase in the flexibility of the side chains upon deacetylation, would facilitate an increase in the degree of intermolecular association.

In this particular study, an attempt has been made to compare the effect of polysaccharide concentration and ionic strength upon the viscosity of two very different native polymers - ps.1128 and ps.556. These materials appeared to be of similar molecular weight (table 5.5), but whilst ps.1128 was a fully acetylated, low pyruvate xanthan, ps.556 had roughly three out of every four side chains substituted with pyruvic acid and very little acetyl. Viscosity measurements were made on these two polymers over a wide range of polysaccharide and sodium chloride concentrations.

6.3 Results

Samples of xanthan at different salt and polysaccharide concentrations were prepared by the addition of deionized water and aqueous sodium chloride to a stock solution of the polymer (see Chapter 2). The samples were prepared on a weight/weight basis and were homogenized using a vortex mixer. Viscosity measurements were made at 25°C, over a range of shear rates between 0.02 and 128.5 per second, using a Contraves Low Shear (LS30) couette viscometer.

The "zero-shear" specific viscosity of ps.1128 and ps.556 was measured over a range of polysaccharide concentrations between 0.001% and 0.5%. Measurements were made in the absence of salt, and in 2mM and 20mM sodium chloride. In the case of ps.556 additional measurements were made in 5mM salt. A summary of the data is given in table 6.1. Double logarithmic plots of η_{sp0} against concentration are shown in figures 6.3 and 6.4.

The "zero-shear" specific viscosity was also measured for 0.002% and 0.2% solutions of ps.1128 and ps.556, over a range of sodium chloride concentrations up to 1M. Solutions of ps.646 and ps.PXO_{61} at 0.2% were tested for comparison. This data is given in table 6.2, whilst figure 6.5 shows a double logarithmic plot of η_{sp0} versus sodium chloride concentration.

The shear rate dependence of viscosity was essentially the same for all of the polymers tested, and is illustrated by the data in figure 6.2. A low shear Newtonian plateau was detectable up to concentrations of 0.3% for ps.556 (higher concentrations were not tested), and for ps.1128 in the presence of salt. In the absence of added salt, however, it was evident for ps.1128, only up to concentrations of 0.2%. (Values of η_{sp0}, at higher polysaccharide concentrations, were estimated to be where the curve appeared to be levelling off). As the concentration decreased, the beginning of the shear thinning zone was shifted towards higher shear rates and at the very lowest concentrations, no shear thinning was discernible. In the case of ps.1128, for example, shear thinning could not be detected at or below concentrations of 0.005% in the presence of salt, or 0.002% in its absence.

Both ps.1128 and ps.556 showed the expected sharp increase in η_{sp0} with concentration (figures 6.3 and 6.4). The viscosity fell between zero salt and 2mM sodium chloride, and the fall was most marked at low polysaccharide concentrations. It was, however, detectable across the entire range of concentrations tested. The material from strain 556 (figure 6.4) exhibited a further slight decrease in viscosity in the presence of 5mM salt but in 20mM sodium chloride, the fall in the dilute solution region was followed by an increase in η_{sp0} (relative to that in 2mM and 5mM salt) at higher polysaccharide concentrations. The polymer from strain 1128, in contrast, showed only the slightest additional fall in viscosity between 2mM and 20mM salt (figure 6.3).

Addition of small amounts of salt to a 0.002% solution of ps.1128 and ps.556 resulted in an initial sharp fall in viscosity. This then levelled off as the concentration of sodium chloride increased still further (figure 6.5). At the higher concentration of 0.2% polymer, the early fall in viscosity was followed by a gradual increase in η_{sp0} with salt. This general pattern was observed, not only for ps.1128 and ps.556, but also for ps.646 and ps.PXO_{61}. Polymer ps.556 at 0.2% showed an anomalous jump in viscosity between 5mM and 10mM salt. Such an increase was not observed for any of the other materials tested and has not, to the author's knowledge, been previously reported in the literature. To confirm its authenticity, therefore, a fresh set of solutions at a range of sodium chloride concentrations between 2mM and 20mM were prepared, and the η_{sp0} value of each determined. This data is given, together with the original, in figure 6.5 and shows quite clearly the presence of a "salt jump". In addition, the corresponding increase in viscosity can be seen at between 5mM and 20mM salt, and at the higher polysaccharide concentrations, in figure 6.4.

The comparative viscosities of ps.1128, ps.556, ps.646 and ps.PXO_{61} will depend, of course, upon both the polysaccharide concentration and the amount of salt present in solution. The data in figure 6.5, nevertheless, suggests that at a concentration of 0.2%, the "zero shear" specific viscosity of ps.1128 was greater than that of ps.556 and that this in turn

was greater than that of ps.646 and ps.PXO_{61}. (The viscosities of the latter two were very similar.) There is, however, an apparent discrepancy between the data for ps.1128 in this experiment and in table 6.1. In table 6.1 the η_{sp0} values for the 0.2% solutions of ps.556 appear to be slightly greater than those for ps.1128, in both water and salt solution. It would appear then, that the viscosities of the two polymers (ie. ps.1128 and ps.556) were actually quite similar, and on the basis of the present measurements, one cannot conclude that either material produced the more viscous solutions.

6.4 Discussion

The marked fall in viscosity observed (typically in the region of 70%) when small amounts of sodium chloride were added to aqueous solutions of xanthan, at both high and low polysaccharide concentrations, is believed to have been due to the decrease in hydrodynamic volume resulting from charge shielding. The subsequent increase in viscosity at higher salt and polymer concentrations, however, resulted probably from the viscosity enhancing effects of macromolecular association discussed in section 6.1. Support for this view is presented in figure 6.6. The diagram shows a reduced variable plot of the effect of salt on both the η_{sp0} and intrinsic viscosity values for ps.1128, ps.556, ps.646 and ps.PXO_{61} at 0.2%. In each case the η_{sp0} and intrinsic viscosity numbers have been divided by their respective values in 10mM salt (ie. at or close to the minimum attainable viscosity, except in the case of ps.556). Two polymers deviate from the general trend. The sample from strain 556 shows the pronounced jump in viscosity described in the last section (this data is linked by a dash-dot line) whilst the intrinsic viscosity of ps.1128 is essentially independent of the sodium chloride concentration (this data is connected by a dashed line). Leaving aside these two exceptions, it is clear that up to about 20mM salt the fall in viscosity is roughly proportional to the drop in the intrinsic viscosity, but at higher ionic strengths, the viscosity begins to rise again even though the intrinsic viscosity continues to decrease. The increase in viscosity with salt is particularly pronounced in the case of ps.646 and this is consistent with the known high tendency of this polymer to aggregate in solution (section 5.6). It is interesting to note that the increase in viscosity at high salt levels occurred not only with ps.556 and ps.646, the pyruvylated polymers, but also with ps.1128 and ps.PXO_{61}. These materials carried negligible quantities of pyruvic acid. This appears to conflict with the conclusions of Smith and coworkers (1981), namely that a minimum critical degree of pyruvic acid substitution is necessary for macromolecular association.

There was no obvious relationship between the viscosity of the four polymers and either the degree of acyl substitution or the molecular weight, although it is likely that both factors played a role in determining the viscosity.

The reason for the unusual jump in viscosity reported for ps.556 at concentrations of between 5mM and 10mM sodium chloride is obscure. Chemical analysis (section 3.5) and light scattering studies (Chapter 5) revealed no major differences between the structure and behaviour of this polymer and any other, and certainly none that would account for the unusual solution behaviour. However, the OR scan for the polymer was different (sections 4.9 and 4.10) and the material, on ion exchange chromatography, became inexplicably resolved into two fractions (section 4.10). It is likely that these phenomena are in some way connected.

The plots of η_{sp0} versus polymer concentration, for both ps.1128 and ps.556 (figures 6.3 and 6.4), have been drawn following Launay *et al* (1984), that is, with two critical concentrations. The positioning of c^* and c^{**} though, given the available number of data points, was somewhat subjective and the values have not, for this reason, been tabulated. Indeed, the data could just as readily have been linked by a smooth curve and, in many respects, such an interpretation would be more acceptable. For example, no satisfactory explanation has ever been given for the sudden sharp increase in viscosity at the critical concentrations. If c^* is due to the onset of coil overlap then one might expect it to occur, in a plot of η_{sp0} against $c[\eta]$, at a value of $c[\eta] = 1$. Instead, according to Morris *et al* (1981), c^* occurs at an overlap concentration of approximately 4, for a wide range of polymers. A gradual increase in viscosity may therefore be a more realistic interpretation, with c^* and c^{**} representing the intercepts of the more extreme slopes. Close examination of the guar gum data of Robinson *et al* (1982) supports this view.

Figure 6.7 shows the master plot of η_{sp0} against $c[\eta]$ for the ps.1128 and ps.556 data, in the presence of salt (the measurements made in deionized water are not included because the intrinsic viscosity of xanthan under these conditions could not be accurately determined). The concentrations in this instance have been corrected using the carbon contents ascertained by elemental analysis (table 3.9).

The majority of the data for ps.556 falls on a single master curve. Only those measurements made in 20mM salt and at relatively high polysaccharide concentrations (in other words those made after the "salt jump") deviate significantly. The η_{sp0} data for 0.2% ps.PXO_{61} in 2, 5 and 20mM sodium chloride, and ps.646 in 2 and 5mM salt can also be included in the master curve. This is perhaps surprising in the light of earlier suggestions that the presence of aggregates in solution may have distorted the intrinsic viscosity values upwards (section 5.7). However, assuming that such aggregates were not, in fact, present in large numbers, one might suggest that at low salt concentrations superposition occurs because the viscosity essentially reflects the degree of space occupancy by the molecules but that at higher salt concentrations, where significant macromolecular association begins, the data deviates more and more from

the master plot. The data for ps.1128 gives a completely separate master curve but this was to be expected since the presence of higher molecular weight aggregates in this system is in little doubt (section 5.9).

The data of Morris *et al* (1981) for random coil polysaccharides is shown in figure 6.7 as a dotted line. Interestingly there is quite good superposition between this data and the ps.556 master curve. The slight deviation at very low concentrations is readily explained since ultimately the viscosity must become proportional c^1 rather than $c^{1.4}$. In the upper region of the curve there is also a slight disparity but this can be attributed to the relative inaccuracy of the Contraves LS30 with the more viscous solutions.

The slopes of the master curves for ps.556 and ps.1128 are as follows: c<c*, 1.12 and 1.10: c*<c<c**, 1.50 and 1.53: c>c**, 3.00 and 3.25. These are somewhat lower than those reported by Launay and coworkers (1984), particularly at the higher polysaccharide concentrations (typically in the range 4-5, above c**). There are two points to be noted here. Firstly, at the relatively low sodium chloride concentrations used (up to 20mM) the degree of macromolecular association, as judged from figure 6.6, was relatively small. One might therefore expect the curves to become steeper at higher salt concentrations. Secondly, it is possible that if the data were actually curved, as discussed above, then the plots may not have achieved their maximum attainable slopes over the range of concentrations tested.

Table 6.1: Viscosity of ps.556 and ps.1128 at a range of polysaccharide and sodium chloride concentrations.

Concentration (%)	η_{sp0} (mPa s)							
	Deionized water		2mM NaCl		5mM NaCl		20mM NaCl	
	ps.1128	ps.556	ps.1128	ps.556	ps.1128	ps.556	ps.1128	ps.556
0.001	0.166	-	-	0.090	-	0.051	-	0.040
0.002	0.417	0.829	0.080	0.151	-	0.106	0.075	0.088
0.003	0.588	1.35	0.140	0.223	-	0.151	0.128	0.134
0.005	0.982	2.87	0.228	0.340	-	0.315	0.206	0.252
0.007	1.34	3.40	0.358	0.578	-	0.419	0.340	0.360
0.01	2.12	5.54	0.574	0.871	-	0.639	0.503	0.567
0.02	7.30	24.6	1.38	2.18	-	1.47	1.19	1.33
0.03	15.0	38.7	2.41	3.90	-	2.60	2.05	2.47
0.05	32.2	75.2	5.46	8.55	-	5.77	4.72	5.99
0.07	36.7	104	10.7	15.8	-	10.9	8.98	11.9
0.1	80.3	172	22.6	34.1	-	23.5	19.1	27.1
0.15	189	315	65.6	88.9	-	62.7	57.0	81.7
0.2	373	533	151	196	-	155	116	202
0.3	1208	1204	630	670	-	581	532	829
0.4	3261	-	2159	-	-	-	1858	-
0.5	4092	-	-	-	-	-	-	-

Table 6.2: Influence of sodium chloride concentration upon the viscosity of ps.646, ps.1128, ps.PXO_{61} and ps.556.

NaCl Concentration (mM)	η sp0 (mPa s) ps.646 0.2%	ps.1128 0.002%	ps.1128 0.2%	ps.PXO_{61} 0.2%	ps.556 0.002%	ps.556 0.2%	ps.556 Repeat 0.2%
0	115	0.398	1076	164	0.489	457	-
1	89.6	0.168	581	99.2	0.202	218	-
2	69.7	0.153	455	76.8	0.148	157	135
4	-	-	-	-	-	-	96.8
5	54.2	0.128	359	58.6	0.108	108	96.4
6	-	-	-	-	-	114	95.0
7	-	-	-	-	-	-	101
8	-	-	-	-	-	139	111
9	-	-	-	-	-	-	125
10	50.5	0.119	345	54.9	0.103	153	124
15	-	-	-	-	-	-	121
20	49.1	0.121	337	57.4	0.090	146	123
50	60.1	0.106	375	63.9	0.081	150	-
100	68.5	0.111	403	67.8	0.074	160	-
200	84.2	0.128	441	73.3	0.079	179	-
500	104	0.108	502	82.7	0.060	200	-
1000	134	0.108	611	96.1	0.071	224	-

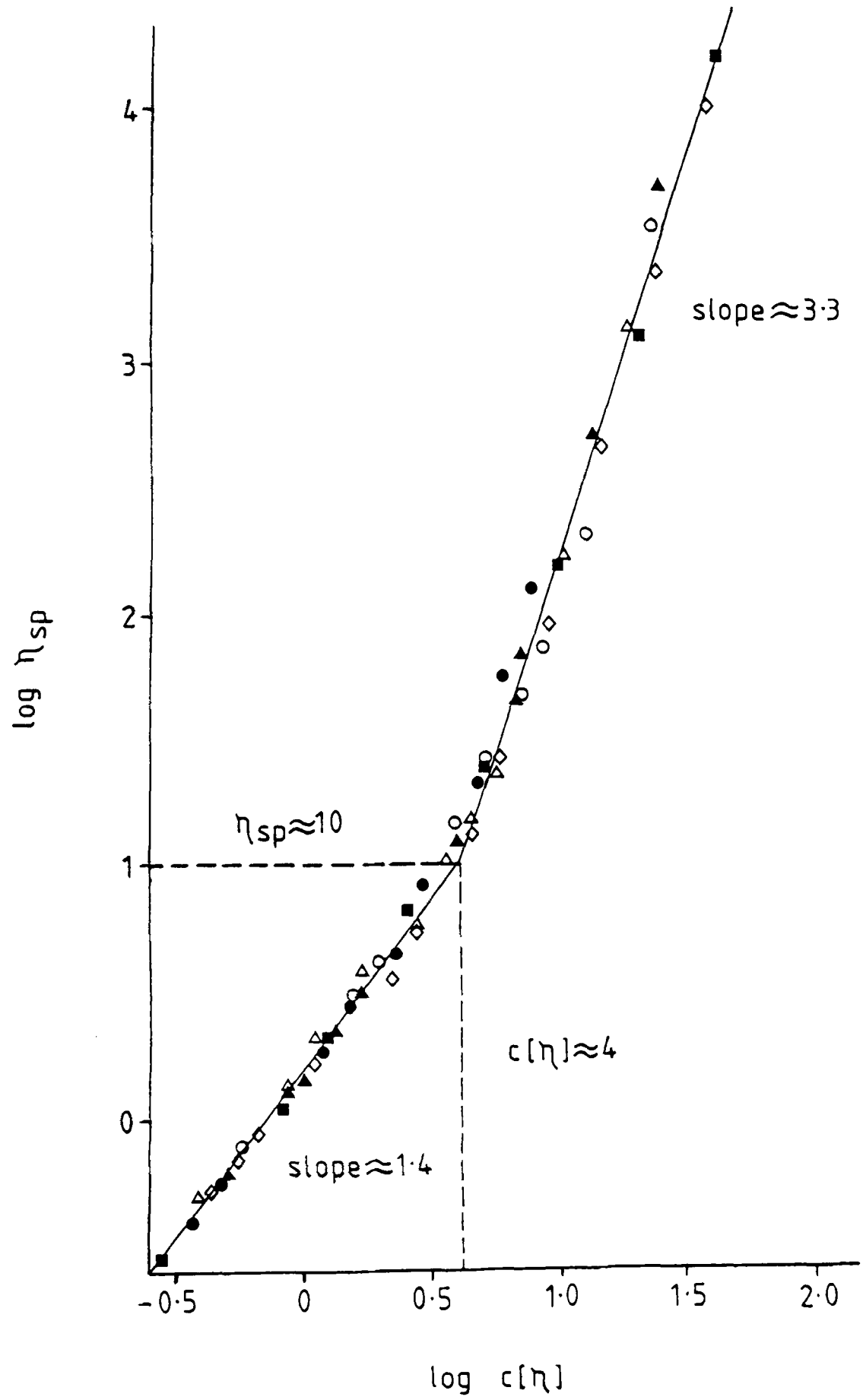

Fig. 6·1 "Zero shear" specific viscosity as a function of c[η] for a range of polysaccharides. These are dextran (○); carboxymethylcellulose (●); high mannuronate alginate (△); high guluronate alginate (▲); lambda carrageenan (◇) and hyaluronate (■), (Morris et al, 1981).

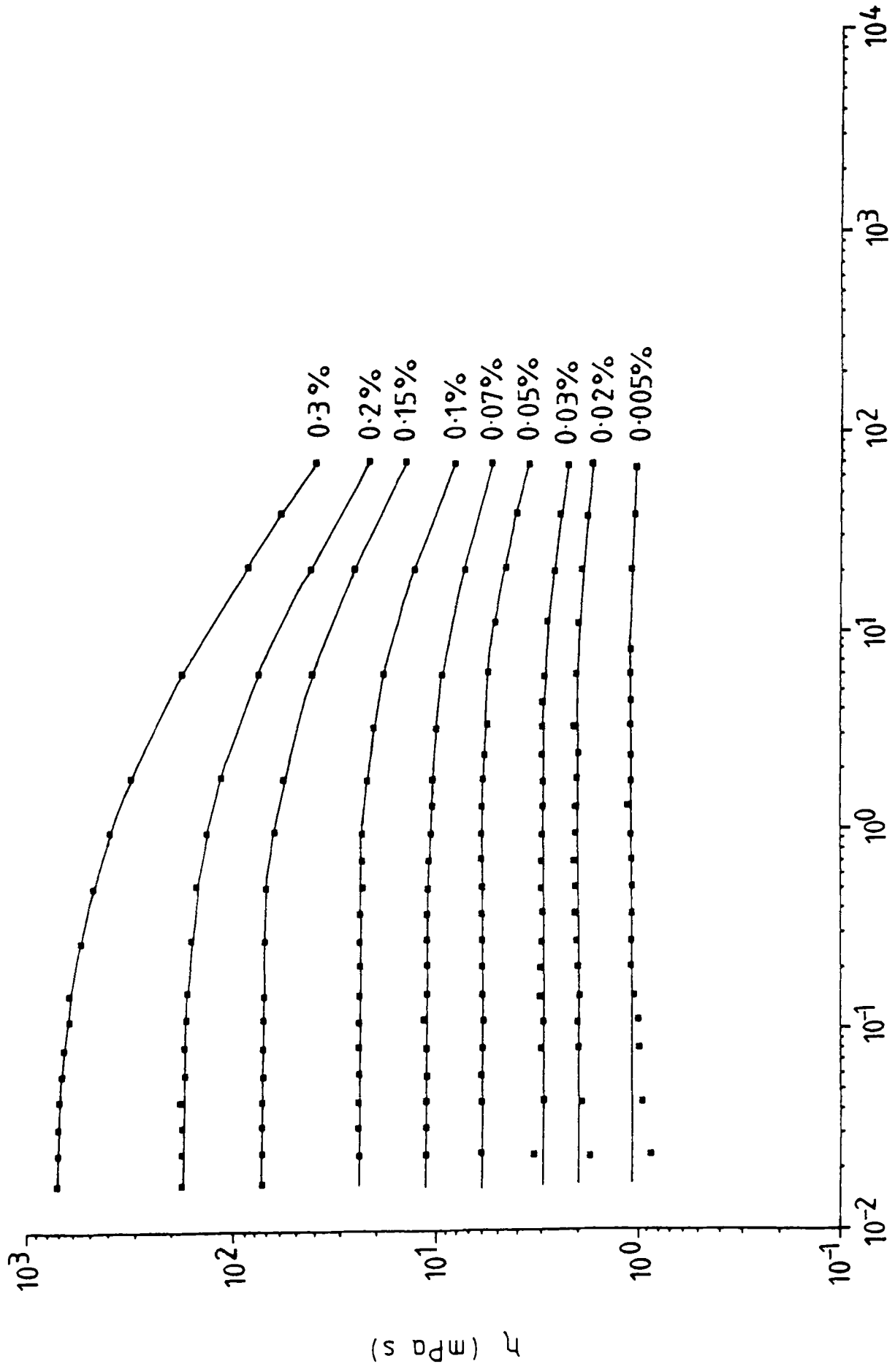

Fig. 6·2 Shear rate dependence of viscosity for ps.556 in 20 mM sodium chloride.

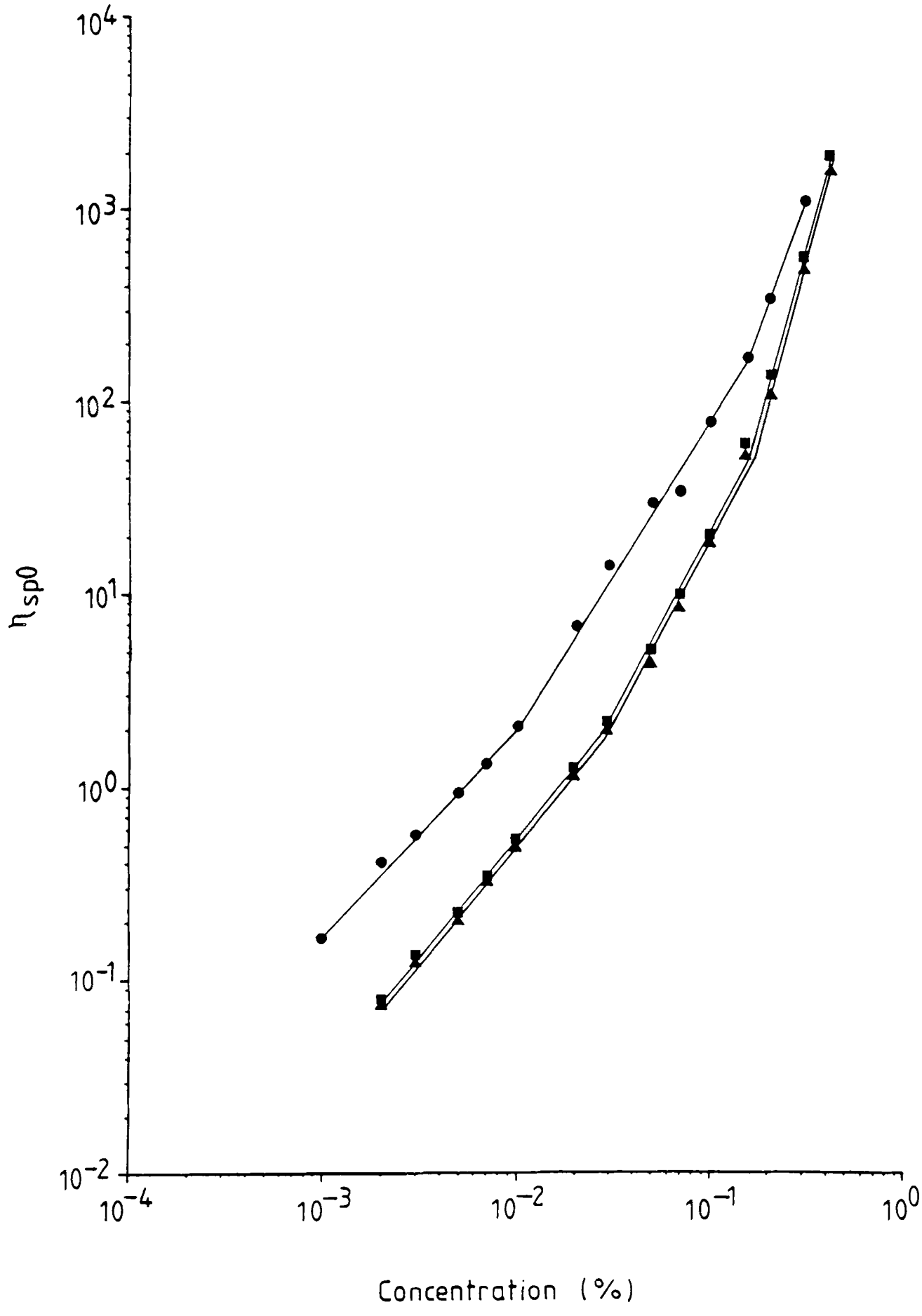

Fig. 6·3 Concentration dependence of "zero shear" specific viscosity for ps.1128 in the absence of salt (●) and in 2 mM (■) and 20 mM (▲) sodium chloride.

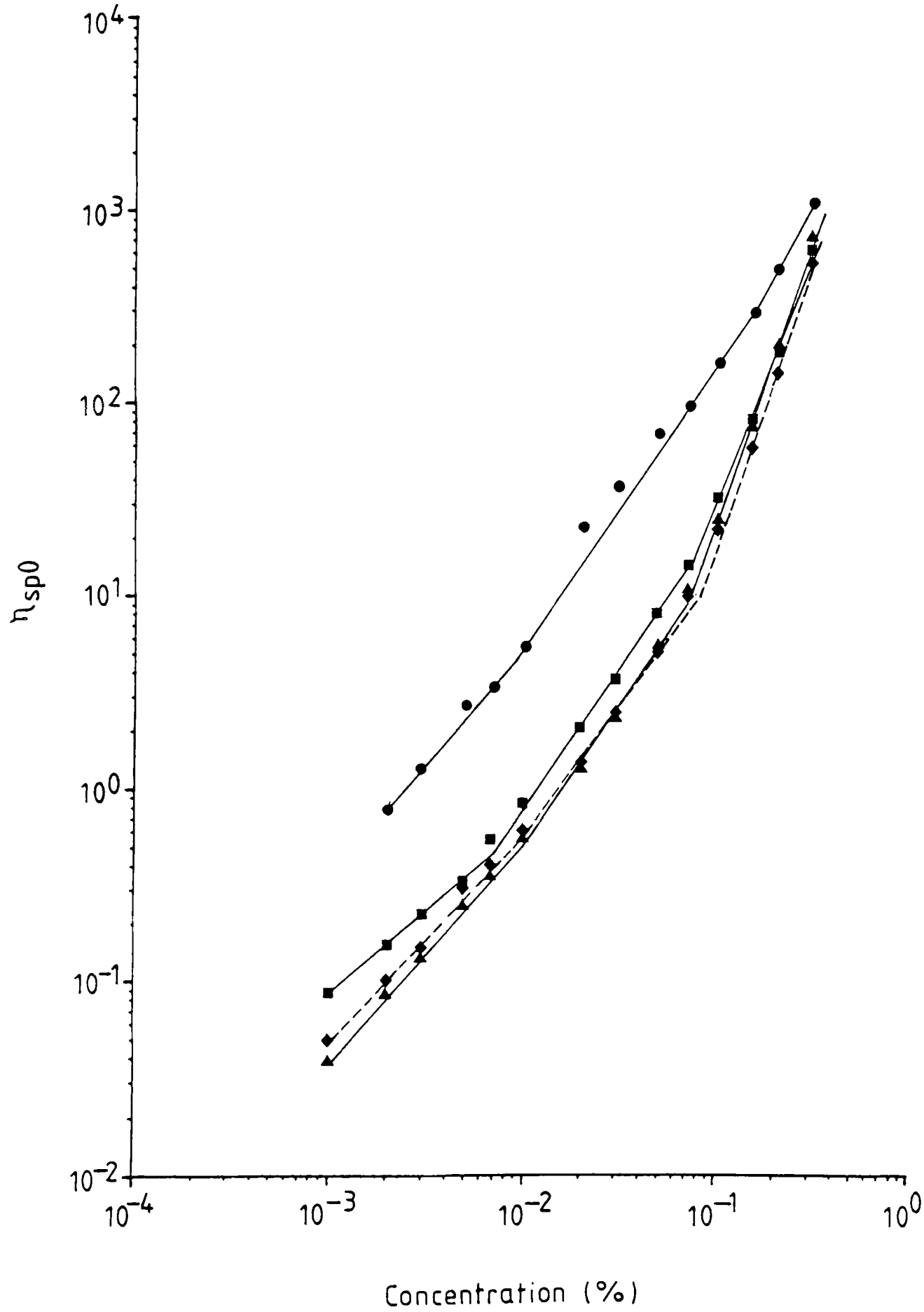

Fig. 6·4 Concentration dependence of "zero shear" specific viscosity for ps.556 in the absence of salt (●) and in 2 mM (■), 5 mM (◆) and 20 mM (▲) sodium chloride.

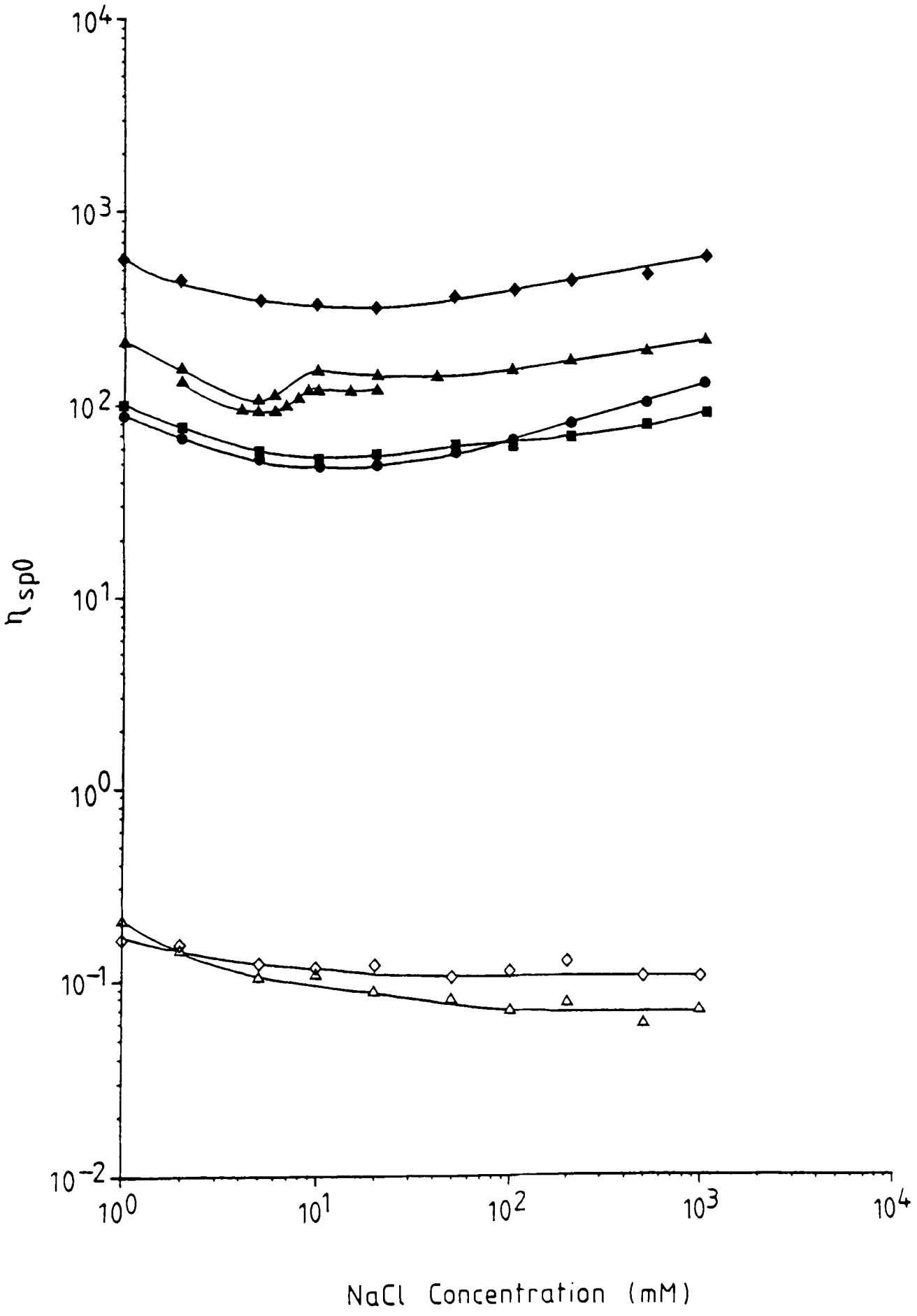

Fig. 6·5 "Zero shear" specific viscosity for 0·2% ps.646 (●), ps.1128 (◆), ps.556 (▲) and ps.PXO_{61} (■), and 0·002% ps.1128 (◇) and ps.556 (△), at a range of sodium chloride concentrations.

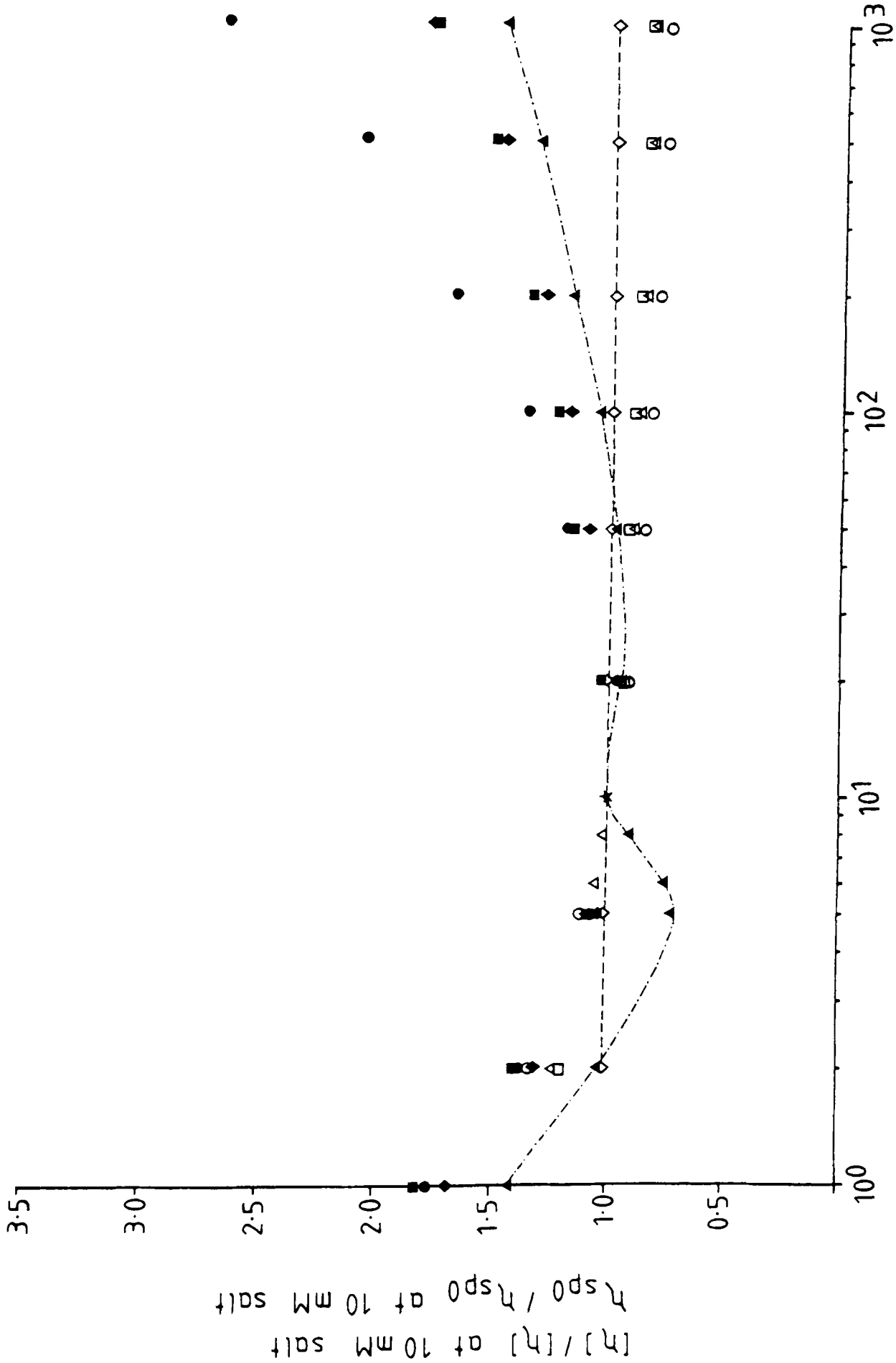

Fig. 6·6 Reduced variable plot of effect of salt on the "zero shear" specific viscosity and intrinsic viscosity of 0·2% ps.646 (●○), ps.1128 (◆◇), ps.PXO$_{61}$ (■□) and ps.556 (▲△).

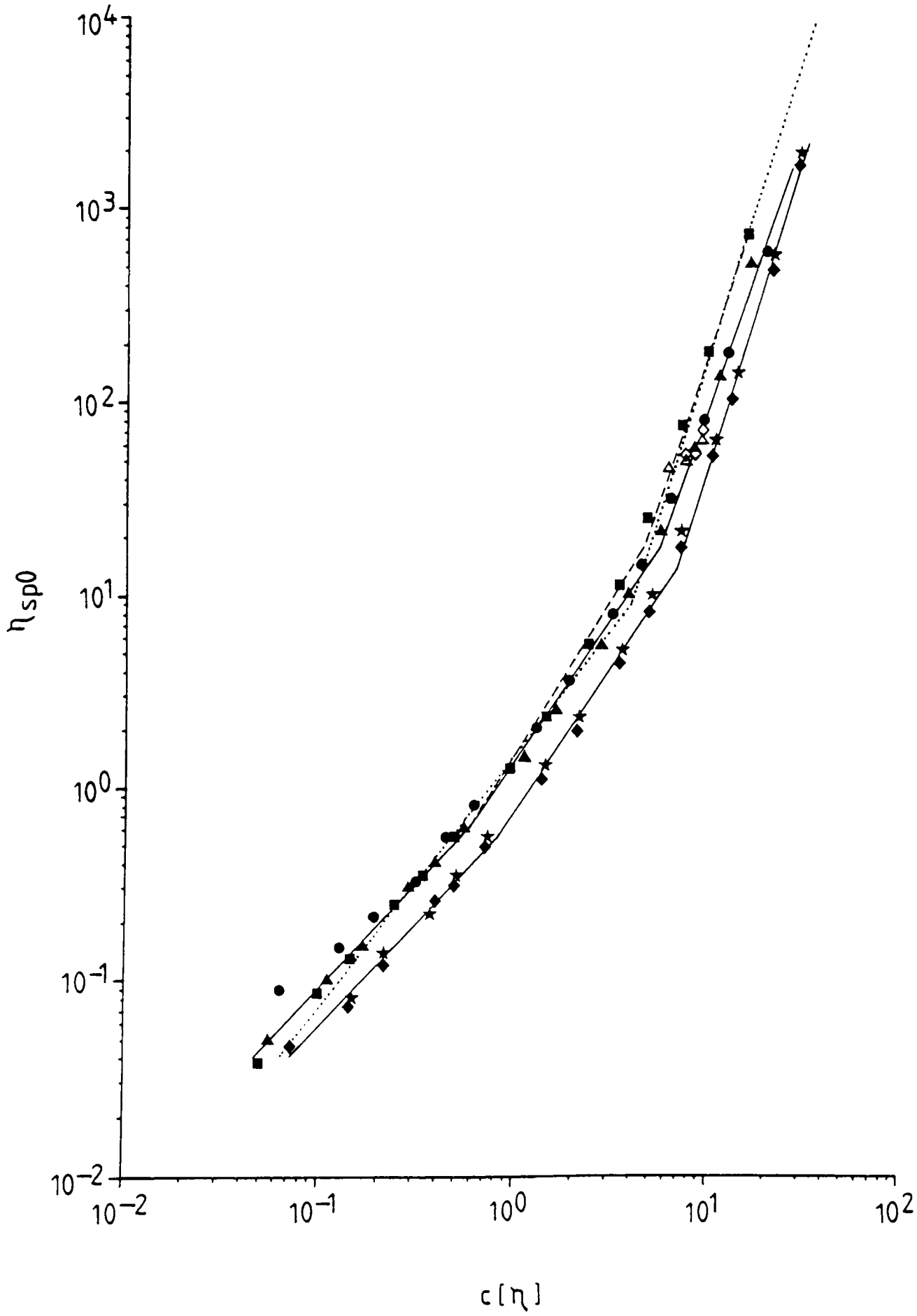

Fig. 6·7 "Zero shear" specific viscosity as a function of c[η] for ps.1128 in 2 mM (★) and 20 mM (◆) sodium chloride, and ps.556 in 2 mM (●), 5 mM (▲) and 20 mM (■) sodium chloride. (Data for 0·2% ps.646 (△) and ps.PXO_{61} (◇) at 2, 5 and 20 mM salt are also plotted.)

CHAPTER 7

GELLING INTERACTIONS

Introduction

7.1 The Gel State

A working definition for a hydrocolloid gel is a sample capable of supporting its own weight against gravity (ie. maintaining its shape) over a practical timescale of days or weeks (Morris, 1984). At the molecular level this type of behaviour is believed to result from the association of long stretches of the polymer chain into conformationally ordered "junction zones". The junction zones are essentially crystalline in nature and are held together by regular arrays of non-covalent bonds. These may include van der Waals' forces, hydrogen bonds, electrostatic forces (both attractive and repulsive), hydrophobic bonds and ion bridging interactions. The junction zones are linked by regions of the molecule which are structurally incapable of forming stable associations or are prevented from doing so by network constraints. These regions are extensively hydrated and serve to solubilize the gel network.

The nature of the junction zones in a number of single component systems has been extensively studied. Figure 7.1 shows the currently favoured junction zone models for three algal polysaccharides, iota-carrageenan and agarose, both of which form brittle, thermoreversible gels after heating and cooling, and alginate which forms a stiff, brittle gel in the presence of certain divalent cations, in particular Ca^{++}. Both carrageenan and agarose have a disaccharide repeat unit structure. Carrageenan consists of alternating (1→3)-linked β-D-galactose and (1→4)-linked 3,6-anhydro-α-D-galactose residues, one (kappa) or both (iota) of which may be sulphated. Agarose consists of (1→3)-linked β-D-galactose alternating with (1→4)-linked 3,6-anhydro-α-L-galactose. Both polymers carry so-called "kinking" residues. In carrageenan the 3,6-anhydro-α-D-galactose is replaced at intervals by a (1→4)-linked galactose-6-sulphate or 2,6-disulphate residue, whilst in agarose the anhydro ring may be replaced by galactose itself or galactose-6-sulphate. These sequence breaking residues are thought to be extremely important in the gelation mechanism since, by preventing perfect ordering, they limit association and thereby prevent precipitation of the polysaccharide during the sol-gel transition. Junction zone development in iota-carrageenan is believed to involve both right-handed double helix formation and the subsequent limited association of double helices, possibly promoted by specific counterion effects (figure 7.1a; Morris *et al*, 1980). The junction zones in agarose appear to consist of many left-handed double helices associated into large bundles (figure 7.1b; Clark and Ross-Murphy, 1987).

Alginate is a block copolymer of (1→4)-linked β-D-mannuronic acid (M) and (1→4)-linked α-L-guluronic acid (G). The residues are arranged in MM..... and GG..... homopolymer blocks and in mixed blocks containing irregular sequences of both M and G. Gelling results from the specific, and highly co-operative, binding of Ca^{++} ions to the guluronate sequences

and the subsequent conformational change. The chains, which normally exist in solution in the random coil state, associate to form a regular two-fold, ribbon-like conformation, with the Ca^{++} ions bound during the process sitting inside electronegative cavities like eggs in an egg-box (figure 7.1c). Grant *et al* (1973) envisaged the formation of relatively large aggregates via this mechanism, but Morris and coworkers (1978) have more recently restricted the process to side-by-side dimerization under non-forcing conditions of calcium concentration. Ion induced gelation of pectin - a plant cell wall polysaccharide - is believed to involve the formation of essentially the same type of junction zone, the galacturonic acid blocks of pectin being almost mirror images of the guluronic acid blocks in alginate (Thom *et al*, 1982).

Binary polymer gels are an order of magnitude more complex than the single component systems. According to Brownsey and Morris (1988) they can be divided into four broad categories. In their type I gels only one of the two polymers is actively involved in network formation, the second soluble polymer being entrapped within the network. Mixtures of kappa-carrageenan or furcellaran (a carrageenan with a relatively low sulphate content) with locust bean gum (Carroll *et al*, 1984; Miles *et al*, 1984; Cairns *et al*, 1986c, 1987), tara gum (Cairns *et al*, 1986b,c,d, 1987) or konjac mannan (Cairns *et al*, 1988) may all form systems of this type. X-ray fibre diffraction evidence indicates, in each case, a kappa-carrageenan or furcellaran network within a galactomannan or glucomannan solution.

In type II gels both polymers are incorporated into the molecular network. In coupled networks cross-linking occurs between the two components to form mixed junction zones. Evidence has been obtained to suggest a synergistic interaction between alginate and pectin and the near mirror image similarity between the guluronic acid and galacturonic acid sequences suggests a stereochemically possible mechanism for inter-molecular binding (Thom *et al*, 1982; Morris and Chilvers, 1984). The interactions between xanthan and the galactomannans, and xanthan and konjac mannan are also believed to be of this type (see sections 7.4 and 7.5). In general, however, mixed junction zones are far less well characterized than those of the single component systems. Certain biopolymers are mutually incompatible. In this case phase separation occurs with both polymers cross-linking only with self. Protein-polysaccharide mixed gels are often of this type (Clark *et al*, 1982). Finally there are the interpenetrating networks. These consist of two polymer networks, at least one of which is formed in the immediate presence of the other. Such systems are very rare.

Although most people would claim to be able to recognize a gel, in reality, sensory evidence alone is rarely sufficient to distinguish a gel network from a concentrated polymer solution. Rheological techniques such as compression testing, stress relaxation experiments or mechanical spectroscopy are required to make the distinction.

When a hydrocolloid gel is compressed, the stress generated in resistance to the applied deformation at first increases linearly with strain. At higher strains, the slope of the stress-strain curve usually increases slightly, and then more pronouncedly, until eventually the sample breaks. The maximum stress needed to rupture the gel network is sometimes referred to as the "yield stress". However, the actual behaviour is complex since in compression there is often no clear point of failure before the gel is severely macerated. Measurements made within the initial linear region are known as "small deformation" measurements and those at higher strains, "large deformation" measurements.

If a gel is deformed by a fixed amount over a long time period then the stress required to maintain this constant strain will gradually decrease. This is known as "stress relaxation". On release of the strain the sample will only partially recover its original dimensions. Conversely, if a constant stress is applied then the amount of strain gradually increases with time. This is referred to as "creep". Both phenomena can be explained in terms of network rearrangement. In other words many of the original junction zones dissociate and new ones are formed which accommodate the applied deformation.

Mechanical spectrometry is a particularly powerful technique for characterizing polymer systems. If a sinusoidal strain wave is applied to a perfectly elastic material (solid) then the resultant sinusoidal stress will be exactly in phase with the imposed strain (figure 7.2a). For a purely viscous (Newtonian) solution, however, the stress and strain waves will be exactly 90^{o} out of phase (figure 7.2b). The ratio of the in-phase stress to applied strain is known as the elastic or storage modulus (G'), whilst the 90^{o} out-of-phase stress to strain is known as the viscous or loss modulus (G").

Any real material will possess a combination of both solid and liquid-like properties (ie. is viscoelastic) and by applying an oscillatory strain wave and comparing the strain with the resultant stress, one is able to extract the two viscoelastic parameters from the overall response of the sample, the complex modulus (G^*)and the tangent of the phase angle ($\tan \delta$).

$$G^* = (G'^2 + G''^2)^{1/2}$$

$$\tan \delta = \frac{G''}{G'}$$

Measuring G' and G" together with the so-called dynamic viscosity (η^*) - the ratio of total stress to frequency of oscillation (ω) - over a range of frequencies is particularly informative. Figure 7.3 shows the mechanical spectra for an elastic gel network (agarose) and a Newtonian solution (dextran). For the elastic network G' is much greater than G" and the two are essentially frequency independent. The dynamic viscosity on

the other hand decreases sharply with increasing frequency. This is in stark contrast to the behaviour of the Newtonian solution. Here G" has the larger value and both G' and G" are heavily frequency dependent. The dynamic viscosity, though, is not. Thus the mechanical spectrum alone can essentially define the type of system one is dealing with, provided the measurements are carried out at small enough strains ie where G^* is independent of strain.

7.2 The Galactomannans - Guar Gum and Locust Bean Gum

This chapter will be concerned principally with the interactions between xanthan, the galactomannans guar gum and locust bean gum (carob gum), and the glucomannan konjac mannan. Before proceeding further though, it is worth considering in a little more detail the nature of these three plant polysaccharides.

The vast majority of the plant galactomannans are obtained from seeds of the *Leguminosae*. Guar gums comes from the seeds of *Cyamopsis tetragonoloba* and locust bean gum from *Ceratonia siliqua*. The polymers are located in the endosperm where they function principally as reserve carbohydrate (Dea and Morrison, 1975; Dey, 1978; Meier and Reid, 1982; Reid, 1985). After germination they are broken down into their constituent monosaccharides and these are then taken up and utilized by the growing embryo. Three principal enzymes are involved in galactomannan mobilization, α-galactosidase, endo-β-mannanase and β-mannosidase (Meier and Reid, 1982; Reid, 1985). The galactomannans are hydrophilic and readily absorb water. A second possible function, therefore, may be to imbibe water from the environment, which is then distributed around the embryo and protects it against desiccation during transient periods of water stress (Dea and Morrison, 1975; Reid, 1985).

The galactomannans consist of a β-(1→4)-linked D-mannan backbone with single α-(1→6)-linked D-galactose side chains. The amount of galactose varies widely from one species to another. Guar gum contains typically about 36-40% galactose and locust bean gum, 21-23% (McCleary *et al*, 1985; section 3.9). The distribution of the galactose side-chains has been a matter of some controversy. A wide range of chemical and enzymic techniques have been used to try to elucidate the fine structure, but the results have been inconclusive. In the case of locust bean gum, for example, everything from a block structure (Baker and Whistler, 1975; Painter *et al*, 1979) to a completely random distribution (Grasdalen and Painter, 1980) has been suggested. A recent rather elegant study by McCleary and coworkers (1985) is probably among the most reliable. These authors studied the distribution of D-galactose in locust bean gum and guar gum, using a computer analysis of the amounts and structures of the oligosaccharides produced upon degradation with two highly purified β-D-mannanases. Computer programs were developed to account for the specific substrate binding requirements of the enzymes and to simulate the synthesis of the galactomannan by a process in which the D-galactosyl

groups were transferred to the growing D-mannan chain, in either a statistically random manner, or as influenced by nearest-neighbour/second-nearest-neighbour substitution. The results indicated a non-regular distribution in locust bean gum with a high proportion of substituted couplets, lesser amounts of triplets and an absence of block substitution. The probability of sequences in which alternate D-mannose residues are substituted was found to be very low but there were more unsubstituted blocks of intermediate length than would be expected for a statistically random galactose distribution. The distribution in guar gum was also found to be non-regular with the side-chains arranged mainly in pairs and triplets. This is consistent with the data of Hoffman and Svensson (1978).

Limited X-ray fibre diffraction data for guar gum suggests that the galactomannans in the solid state exist in an extended ribbon-like conformation (Dea and Morrison, 1975). In solution they appear to behave as slightly stiffened random coils (Robinson *et al*, 1982). The solutions are extremely viscous and the viscosity is largely unaffected by pH or ionic strength as one would expect for a polymer with no charged groups.

The galactomannans will not normally gel alone, but they can be induced to do so in the presence of certain ions, notably borate (Pezron *et al*, 1988a, b) and the transition metal cations (Chrisp, 1967). Gelation can also be promoted by lowering the water activity, for example by addition of sucrose (60% $^{w}/_{v}$), glycerol (50% $^{v}/_{v}$) or ethylene glycol (50% $^{v}/_{v}$), or by cycles of freeze thawing (Dea *et al*, 1977, 1986). On freezing the polymer solution, ice formation progressively raises the effective concentration in the residual unfrozen solution and this promotes association. The less galactose the polymer carries, the greater the amount of gelation (McCleary *et al*, 1981; Dea *et al*, 1986). Hence locust bean gum will gel whereas guar gum will not. Dea and coworkers (1977) have suggested that chain-chain association occurs by aggregation of the "smooth" (unsubstituted) regions of the mannan backbone into a regular two-fold, ribbon-like conformation, with the substituted regions of the galactomannan serving to solubilize the gel network.

The galactomannans can also be used to enhance the gelation of other polysaccharides. For example, addition of even small amounts of locust bean gum to carrageenan or agarose will lower the minimum gelling concentration considerably and produce gels that are firmer and more elastic (Dea and Morrison, 1975). The gelation of xanthan in the presence of certain galactomannans is a major topic in this thesis.

The galactomannans were used by man as long ago as 3000 B.C. The ancient Egyptians used them for mummification. Hence the name "Pharaoh's" polysaccharides. Current commercial exploitation is restricted almost exclusively to guar gum and locust bean gum (Dea and Morrison, 1975; Reid, 1985). These polymers are used extensively in the food industry where their ability to produce very viscous solutions makes them invaluable as a thickener in products such as soups, desserts, pie fillings, sauces and

mayonnaise. They are also widely used in combination with other polysaccharides for gelled food products. In contact with water the galactomannans hydrate and become mucilaginous, eventually forming a thick paste which is impervious to further water. This property is made use of commercially for water-proofing explosives, plugging leaking wells and improving the wet strength of paper. The relatively slow hydration of guar gum has also been exploited by the pharmaceutical companies in the manufacture of delayed release drug preparations.

7.3 Konjac Mannan

Konjac mannan is derived from the tubers of *Amorphophallus konjac*, where it is located in specialized cells known as idioblasts. These are distributed throughout the tuber tissue. Its primary function appears to be that of a storage polysaccharide, the material being broken down during germination to provide sugars for the newly growing leaves, stems and tubers. Two enzymes involved in mobilization have so far been identified, mannanase I and mannanase II. These cleave the konjac mannan into manno-oligosaccharides and glucomanno-oligosaccharides. Like the galactomannans, konjac mannan is hydrophilic and a second possible role in water storage has therefore been suggested (Bewley and Reid, 1985).

Konjac mannan is a β-(1$\rightarrow$4)-linked copolymer of mannose and glucose. The mannose to glucose ratio is approximately 1.4:1.0 (Bewley and Reid, 1985) but the distribution of the residues is uncertain. Partial repeat unit structures have been proposed by Kato *et al* (1970) and Shimahara *et al* (1975b) but the presence of only a few weak meridional reflections in the X-ray fibre diffraction pattern for konjac mannan, indicates that there is in fact no regular repeating structure and no cellulosic or mannan blocks (Brownsey *et al*, 1988). Some branching may occur through the C3 of the glucose and mannose residues (Smith and Srivastava, 1959; Kato and Matsuda, 1973; Shimahara *et al*, 1975a). The polymer carries about 4% acetyl (Dea *et al*, 1977; Cheetham and Punruckvong, 1985), but the precise location of these groups is unknown.

In solution the polymer behaves as a random coil. At concentrations in excess of 5% it forms a viscoelastic dough or "putty" which can be moulded, heals after mechanical damage and flows over long periods, but which on a shorter time scale bounces like rubber (Dea *et al*, 1977).

Native konjac mannan does not gel alone but it will do so when warmed in the presence of alkali. Gelation is believed to be due to the elimination of the acetyl group under alkaline conditions (Maekaji, 1974). It has been suggested that the acetyl ester sterically inhibits molecular association (Dea, 1981) but the highly crystalline X-ray fibre diffraction pattern obtained for the native polymer (Brownsey *et al*, 1988) is not consistent with this view. Instead as Maekaji has suggested the acetyl group may suppress intermolecular hydrogen bonding, in which case its removal would decrease the solubility of the polymer by enhancing intermolecular association, leading eventually to gelation.

Konjac mannan will interact synergistically with xanthan to form a gel (Dea *et al*, 1977) and can be used to modify the properties of both the agarose (Dea, 1981) and carrageenan systems (Dea, 1981; Cairns *et al*, 1988).

The major commercial use of the polymer is as a food product. Edible konnjaku, a gel of konjac mannan, is one of the most popular foods in Japan.

7.4 Xanthan-Galactomannan Interactions

Xanthan, like the galactomannans, will not normally gel alone, although it may do so in the presence of certain di- and trivalent metal ions at an appropriate pH (Pettitt, 1979). A mixture of the two polymers, however, will often form a gel. With locust bean gum, for example, xanthan gives a firm, rubbery thermoreversible gel network at total polysaccharide concentrations of greater than 0.5% (Dea and Morrison, 1975). The gels show sharp melting and setting behaviour, the melting temperature increasing with the total polysaccharide concentration, but showing little dependence upon the relative concentrations of the two polymers (Dea *et al*, 1977). Maximum gel strength occurs over a pH range of 6-8 and there is a dramatic decrease in gel strength at both the acid and alkaline ends of the pH spectrum (Kovacs, 1973). The optimum ratio of xanthan to locust bean gum is uncertain. Kovacs (1973) has reported an optimum ratio of 1:1, Tako and coworkers (1984) a ratio of 1:2 and Dea and Morrison (1975) a ratio of 1:3. The ratio will vary though with the molecular weight of the polymers.

The gelling behaviour is heavily dependent upon the galactose content of the galactomannan. The less galactose, the stronger the gel, generally speaking (Dea *et al*, 1977, 1986). Hence the polymer from *Caesalpinia vesicaria* with 29% galactose, forms a significantly weaker gel with xanthan, than locust bean gum (~23% galactose). Guar gum which carries about 38% galactose will not gel at all, although the viscosity of the mixture is greatly enhanced. If galactose is removed from guar gum, using a highly purified α-galactosidase enzyme, not only can gelation be induced, but the strength of the gel is observed to increase as the galactose content diminishes (McCleary *et al*, 1981, 1984). It was the importance of the galactose content in gelation that lead Dea and coworkers (1977) to propose the first model for a xanthan-galactomannan junction zone. They noted that the characteristic sigmoidal OR curve which accompanies the order-disorder transition for xanthan, persists in the presence of the galactomannan and is essentially complete before the onset of gelation (Dea and Morris, 1977), and also that the X-ray fibre diffraction pattern for the xanthan-galactomannan mixtures is similar to that of xanthan alone. They suggested, therefore, a synergistic interaction between the xanthan helix and the unsubstituted or poorly substituted regions of the galactomannan (figure 7.4a). A similar interaction between the agarose and carrageenan double helices and the

unsubstituted regions of the galactomannan had been proposed earlier by the same group (Dea *et al*, 1972). Moorhouse *et al* (1977b) took the model one stage further. They observed that the 5/1 helical conformation favoured for xanthan presents two distinct faces, one with the side-chains and charged groups and the other comprising essentially the cellulosic backbone. They suggested therefore that the interaction with the galactomannan might take place at the cellulosic "groove" - in other words between the similar β-(1→4)-linked cellulosic and mannan backbones.

More recent research has indicated that the distribution of the galactose groups is as important as the quantity in determining the interaction properties of the galactomannans. Locust bean gum and the polymer from *Caesalpinia pulcherima* for example, have very similar levels of galactose substitution and yet the locust bean gum interacts very much more strongly with both xanthan and agarose. Dea and coworkers (1986) using the technique of McCleary *et al* (1985) outlined in section 7.2 have shown that the *C. pulcherima* galactomannan has a galactose distribution approaching statistically random, whereas locust bean gum has a non-regular, non-statistically random distribution with a higher proportion of unsubstituted blocks of intermediate length. The greater interactivity of the locust bean gum can therefore be attributed to the larger number of unsubstituted blocks. The same situation applies with the *Caesalpinia vesicaria* and *Gleditsia triacanthos* polymers. In this case the *G. triacanthos* galactomannan carries the higher proportion of unsubstituted blocks and interacts more strongly with xanthan and agarose (Dea *et al*, 1986).

The polymer from *Leucaena leucocephala* is particularly unusual. It carries approximately the same amount of galactose as guar gum and yet interacts with xanthan to roughly the same extent as locust bean gum. Quantitation and characterization of the oligosaccharides produced from this polymer upon hydrolysis with β-D-mannanase, showed an extremely high proportion (more than 25% of the total carbohydrate in the hydrolysate) of $Gal\text{-}Man_2$. On the basis of this evidence (McCleary, 1979; Dea *et al*, 1986) it was concluded that large sections of the *L. leucocephala* galactomannan consist of mannose residues alternately substituted with galactose. Because of steric hindrance there is unlikely to be any rotation about the mannose-mannose glycosidic bond in these regions, and the galactose groups will therefore be located on one side of the mannan chain. The model of Dea and coworkers has therefore been modified to include an interaction between the xanthan helix and regions of the galactomannan backbone where the galactose groups are positioned on one side only (figure 7.4a).

A second model proposing an interaction between the xanthan helix and locust bean gum has been put forward by Tako *et al* (1984). Rheological evidence obtained by these workers apparently indicates the involvement of the xanthan side-chains in xanthan-galactomannan binding and this group have suggested, therefore, that the side-chains of the xanthan, which is in the helical conformation, are inserted into adjacent unsubstituted

regions of the galactomannan backbone. The galactomannan is extended in a two-fold, ribbon-like conformation. This produces the lock and key-type effect illustrated in figure 7.4b. Measurements made by this group in the presence of urea showed a marked fall in the dynamic viscoelasticity (G' and η') of the mixed systems, suggesting that hydrogen bonding plays a major role in the interaction.

X-ray fibre diffraction is the only method presently available for studying gels at the level of atomic resolution, and even then the gel sample has to be stretched and at least partially dried to form a fibre, so that it may no longer be in its "native" state. This technique has been used by Cairns and coworkers to study the interaction between xanthan and locust bean gum (Cairns *et al*, 1986a, 1987), and xanthan and tara gum (Cairns *et al*, 1987) - the galactomannan from *Caesalpinia spinosa*. It was found that the diffraction patterns for the xanthan-galactomannan systems showed reflections characteristic of both aligned xanthan helices and mixed junction zones. To test whether helix formation was essential for xanthan-galactomannan binding, solutions of xanthan and locust bean gum were mixed at room temperature. The xanthan under these conditions was in the ordered conformation. No mixed junction zones were subsequently detected in the X-ray fibre diffraction pattern, indicating that gelation had not occurred. If, however, the mixture was heated to 95°C (ie. above the helix-coil transition temperature) and then recooled to room temperature prior to X-ray diffraction, xanthan-galactomannan binding was evident. Addition of sufficient calcium chloride to raise the melting temperature above 100°C, inhibited gelation even after heating and cooling. This indicated that denaturation, rather than the helical conformation, was necessary in order for intermolecular association to occur. The authors noted that glucose and mannose differ only in the orientation of the -OH group at the C2 position and proposed therefore that binding occurs between the sterically compatible cellulosic backbone of xanthan in the disordered state, and the mannan backbone of locust bean gum. The remaining xanthan, they suggested, readopts the ordered helical conformation. This would account for the substantial recovery of the OR for the mixed systems upon cooling and gelation, and for the presence of reflections characteristic of the xanthan helix in the X-ray fibre diffraction pattern.

The precise structure of the xanthan-galactomannan junction zones cannot be discerned from the X-ray fibre diffraction data, but possible models have been suggested based upon the available information. According to Cairns *et al*, the reflections for the mixed junction zones indicate a possible sandwich structure in which the xanthan side-chains are staggered as illustrated in figure 7.4c. Staggering is suggested by the repeat unit distance of 0.52 nm. Other simpler binding schemes would be expected to give an axial advance per repeat unit of 1.04 nm. The exact stoichiometry of binding is unknown. Several galactomannan molecules may be sandwiched between the xanthan backbones and the interior of the sandwich might need

to accommodate galactose substituted regions of the galactomannan backbone as well as the bare mannan regions. There is also evidence to suggest that growth of the sandwich structure can occur in two dimensions only.

Cheetham and Mashimba (1988) have recently produced more evidence to support the Cairns model for xanthan-galactomannan binding. Using OR, they monitored the helix-coil transition for a sample of Keltrol that had been dialysed exhaustively against distilled water (ie. to constant conductivity) and for another sample that had been only partially dialysed. The former had a much less negative OR at lower temperatures than the latter, indicating a lesser degree of conformational order. This polymer formed a gel with locust bean gum, whereas the partially dialysed sample did not. A series of experiments were carried out in which solutions of xanthan and locust bean gum were combined at equal concentrations, under a variety of conditions to give mixed systems. These systems were examined for gel formation at room temperature and the apparent melting points were determined using a falling ball method similar to that described in section 7.8. A selection of the results, together with the interpretations given, are shown in table 7.1.

It appears, from this data, that for the formation of a cohesive gel network the xanthan molecules must exist predominantly in the disordered state. When the xanthan was not disordered, as was the case in the presence of external salt, gel islands were formed. These were considered to be very tightly cross-linked gel structures. The authors suggested that, in the presence of potassium chloride, xanthan molecules exist not as single, largely disordered chains (as they were assumed to do in distilled water) but partly as coaxial or side-by-side helices, joined by some single chain regions. The single chain regions, according to Cheetham and Mashimba, would exist in the flat ribbon conformation, and could therefore interact with the galactomannan backbone to form the gel islands.

It was noted that the gels formed in the presence of 0.05M potassium chloride had a somewhat higher melting temperature than those formed in distilled water and it was suggested that once the xanthan-galactomannan interactions have become established, the presence of salt restores the ordered conformation in the non-junction zone regions of the xanthan chain, "locking" the junction zones in place. The melting point for the gels formed in the presence of 4M urea was found to be markedly lower than that of the gels formed in distilled water or salt solution, indicating once again that hydrogen bonding may play an important role in the gelling interaction.

The explanations given account quite satisfactorily for the behaviour of native Keltrol. Unfortunately though, the results for a similar set of experiments carried out on the chemically deacetylated and depyruvylated derivatives of Keltrol showed some inconsistencies. For example, the pyruvate-free xanthan, in distilled water, failed to form a

gel with locust bean gum even after heating and cooling, although the helix-coil transition midpoint for this polymer should have been well below 95°C. In the presence of 0.05M potassium chloride, however, gel islands were formed upon mixing, and a cohesive gel network with a melting temperature of 46°C, was established after heating and cooling. The acetyl-free xanthan did not gel with locust bean gum in distilled water until after it had been heated and yet this polymer should have been the least stable and the most disordered of the three materials under the prevailing conditions (see Chapter 4).

Cheetham and Mashimba have suggested two possible, rather more detailed, models for the xanthan-galactomannan junction zones based upon their own observations, and those of Cairns *et al*, but which accommodate to some extent the proven effects of galactomannan fine structure on the interaction. These models are shown in figure 7.4d. A single mannan backbone is sandwiched between the two xanthan chains in the disordered ribbon conformation and the side-chains (shown as triangles) are arranged to give the repeat distance of 0.52 nm observed by Cairns and coworkers. The galactomannan chains are substituted on one face only. Additional galactose side-chains shown in dotted lines indicate that with a fully substituted region of the galactomannan chain there would be a considerable amount of steric hindrance. Other locust bean gum molecules could stack above and below the xanthan, extending the junction zones in two dimensions, but probably not in the third.

7.5 Xanthan-Konjac Mannan Interaction

To date relatively little work has been carried out on mixed xanthan-konjac mannan systems and the nature of this interaction is even more obscure than that of xanthan with the galactomannans.

Evidence from Dea and coworkers (1977) has indicated that xanthan-konjac mannan gels are stronger than those of the equivalent galactomannan systems. The melting point for a 0.25% xanthan plus 0.25% konjac mannan mixed gel for example was found to be 63°C, 20°C higher than the highest melting point obtained for a xanthan-locust bean gum gel (total polysaccharide concentration, 2%). Recognizable gels were also apparently formed at much lower concentrations - down to a total polysaccharide concentration of only 0.02%.

Brownsey *et al* (1988) studied the interaction using X-ray fibre diffraction and obtained evidence for intermolecular binding. They were, however, unable to suggest a model for the junction zones, since analysis of the diffraction patterns was complicated by the complex and possibly irregular structure of the glucomannan. Analogous experiments to those performed on the xanthan-locust bean gum system (Cairns *et al*, 1986a, 1987) indicated that denaturation of the xanthan helix was necessary for intermolecular binding, although in this instance gelation was detected using simple creep compliance tests instead of X-ray fibre diffraction.

The stereochemical similarity between the xanthan and glucomannan backbones is obvious and an interaction mechanism similar to that proposed by Cairns *et al* (1986a, 1987) for the xanthan-galactomannan interaction is therefore a possibility.

7.6 Influence of Substituents on Gelation

Acetyl substitution affects the gelling properties of a range of polysaccharides including alginate, XM-6, gellan gum, pectin and konjac mannan (sections 7.3 and 7.17). It also appears to have some influence on the interaction properties of xanthan. Both Dea *et al* (1977) and Tako *et al* (1984) have reported a stronger interaction between deacetylated xanthan and locust bean gum, than with the native polymer. Tako and coworkers suggested that an increase in the flexibility of the xanthan molecule upon deacetylation could facilitate easier association between the xanthan side-chains and galactomannan backbone giving rise to a stronger gelling interaction. The same group (Tako and Nakamura, 1985) have also reported a stronger interaction between deacetylated xanthan and guar gum. Figure 7.5 shows the G' and η' values measured for a series of xanthan-guar gum mixtures at a range of different polysaccharide ratios (total concentration, 0.2%). For the mixtures of native xanthan and guar gum the dynamic viscoelasticity changes very little, but with deacetylated xanthan it increases approaching a xanthan to guar gum ratio of 2:1. It has been suggested (Tako and Nakamura, 1985) that native xanthan and guar gum interact only weakly because the presence of the galactose side-chains on every 2-4 backbone residues of the galactomannan prevents insertion of the xanthan side-chains into the galactomannan backbone. An increase in the flexibility of xanthan upon deacetylation might therefore facilitate greater association, as has been suggested with locust bean gum. Cheetham and Mashimba (1988) found that in terms of gel melting temperature, the gel formed by deacetylated xanthan and locust bean gum after heating and cooling, was of a similar strength to that formed by the parent polymer, but that the interaction was significantly stronger than that of depyruvylated xanthan with locust bean gum.

The interaction between xanthan and konjac mannan, according to Dea *et al* (1977), is weakened by deacetylation. These authors reported an approximate 20°C reduction in the gel melting and setting temperatures for mixtures of deacetylated xanthan and konjac mannan.

To date there is very little evidence to suggest that pyruvic acid affects the strength of the gelling interaction with either the galacto-mannans or konjac mannan. However, Cheetham and Mashimba (1988) did find that a depyruvylated derivative of Keltrol failed to gel with locust bean gum in distilled water, although it interacted quite strongly in the presence of 0.05M potassium chloride. This suggests that pyruvate may in fact promote gelation, at least under conditions of low ionic strength.

7.7 Studies on the Interaction Between Xanthan and the Gluco- and Galactomannans.

The two major aims of this study were to characterize, in rheological terms, the nature of the interaction between xanthan and the polymers locust bean gum, guar gum and konjac mannan, and to examine in more detail the effects of both acetyl and pyruvic acid substitution on the strength of the interaction. A range of techniques was employed to this end. Techniques such as polarimetry, falling ball experiments and compression testing were used but were found, for various reasons, to be unsuitable. They were therefore abandoned, having yielded little useful information. Mechanical spectrometry, on the other hand, was found to be invaluable and this, together with estimation of the minimum gelling concentrations, provided most of the data in this study. A large number of xanthans were used in the gelling experiments but most of the data was obtained from ps.646, ps.1128, deacetylated ps.1128, ps.PXO_{61}, ps.556 and depyruvylated ps.556. These materials represented the complete range in terms of acetyl and pyruvic acid substitution and illustrated the effects of deacetylation and depyruvylation upon specific polymers.

The behaviour of the individual polysaccharides was characterized, both in the presence and absence of added salt, using steady and oscillatory shear measurements. That of the mixed systems was studied using a combination of oscillatory shear measurements and estimation of the minimum gelling concentrations. The majority of measurements were made in the absence of salt and at a xanthan to galactomannan (or glucomannan) ratio of 1:2. This was a compromise between the optimum ratios reported in the literature. The effects of temperature, strain and frequency upon the oscillatory shear response were examined.

G', tan δ and the slope of η^* were all found to be suitable measures of gel strength and an attempt was made to analyse the data for the xanthan/locust bean gum and xanthan/konjac mannan systems in statistical terms, to look for significant correlations between gel strength and the levels of acetyl and pyruvate substitution. The effect of molecular weight (as indicated by the intrinsic viscosity) was also considered. The same statistical package was used to look for a correlation between gel strength and the helix-coil transition midpoints obtained in the optical rotation studies of Chapter 4.

The interaction between ps.BD9A and locust bean gum was examined by mechanical spectrometry. Sample ps.BD9A was produced by a mutant strain of *X. campestris* 646 and was believed to lack the terminal mannose residue from the trisaccharide side-chain (section 3.8). The study of this interaction would, it was hoped, throw some light upon the role of the xanthan side-chain in gelation.

The effect of salt upon the interaction properties of xanthan was examined for a limited number of samples, but this particular aspect of the study was hampered by instrumental problems.

Finally, the observation by Cairns *et al* (1986a, 1987) and Brownsey *et al* (1988) that denaturation of the xanthan helix is necessary for the interaction between xanthan and both locust bean gum and konjac mannan was tested by mixing the samples cold, both in the presence and absence of added salt, and looking for gelation using mechanical spectrometry.

Results

7.8 Techniques Used to Study the Interaction Properties of the Mixed Systems

Polarimetry

Polarimetry has been used to study the interaction behaviour of a number of mixed polysaccharide systems including, for example, the interactions of both agarose and kappa-carrageenan with the galactomannans (Dea *et al*, 1972, 1986). Dea and coworkers (1977) used optical rotation to study the interaction of xanthan with tara gum, locust bean gum and guar galactomannan. These authors observed that, in the presence of tara gum, the order-disorder transition for xanthan remained but was shifted to a higher temperature by approximately 10°C. This they interpreted as evidence for stabilization of the xanthan helix by interaction with the galactomannan. They also noted a significant flattening of the temperature profile below the gel point. This, they suggested, was due to inhibition of xanthan aggregation by network constraints. Xanthan/locust bean gum gels appeared to show analogous behaviour, although measurements of optical activity below the gel point in this system were irreproducible, presumably as a result of stress birefringence. Guar gum, like the other galactomannans, was found to stabilize the xanthan helix to a temperature of approximately 10°C higher, but in this case the OR profile at low temperature was hardly affected, consistent with the absence of gel network formation.

In this study an attempt was made to assess the viability of OR as a technique for comparing the interaction behaviour of different xanthans with locust bean gum, guar gum and konjac mannan. The methodology used was similar to that employed for the studies on xanthan alone (Chapters 2 and 4). A concentration of 0.2% $^{w}/_{w}$ xanthan and 0.4% $^{w}/_{w}$ gluco- or galacto-mannan was used. Solutions of each polysaccharide were prepared at double the required concentration, by dispersing the polymer in deionized water (dissolution by stirring and heating at 90°C in a water bath). The solutions were passed through a series of Millipore filters down to a minimum pore size of 0.45 μm, and then combined by weight in equal quantities. They were reheated and stirred to ensure homogeneity.

Measurements were made, as before, at 365 nm using a Perkin-Elmer 241 polarimeter and 10 cm quartz thermostatted cells. The procedure adopted for sample handling was the same as that described in Chapter 2 for the xanthan solutions, except that in this case the temperature was lowered to only 15°C, instead of 10°C.

No satisfactory measurements were made on the mixed xanthan/locust bean gum or xanthan/konjac mannan systems. In the case of the former, practical problems were encountered in preparing the sample. The 0.8% locust bean gum solution, from which the mixed system should have been prepared, failed to pass through the Millipore filters, presumably because of the presence of the hot water soluble fraction which precipitated out at ambient temperature and clogged the filter. (A similar problem was encountered when samples of locust bean gum were prepared for the intrinsic viscosity measurements - section 5.5 - but here, because the concentration of the polymer was so much lower, the difficulty could be overcome by frequently renewing the filters.) Although certainly not insurmountable (for example the locust bean gum solution could have been forced through the filter under high pressure instead of under vacuum) no attempt was made to overcome this problem. With the xanthan/konjac mannan mixed systems, large irreproducible optical artifacts occurred at about the onset of gelation (between 50-60^{o}C) making any comparison between the systems meaningless. These optical phenomena are analogous to those reported by Dea *et al* (1977) and Morris *et al* (1977a) for mixtures of xanthan and locust bean gum and were presumably the result of stress birefringence.

The only interesting data acquired using OR was for the xanthan/ guar gum systems. Figure 7.6 shows the temperature profiles obtained for ps.1128, deacetylated ps.1128 (batch 1) and guar gum in isolation, and as mixtures of xanthan and galactomannan. The ps.1128 and deacetylated ps.1128 samples showed the typical helix-coil transition behaviour for xanthan, with transition midpoints close to those reported for the same samples in table 4.2. There was significant hysteresis between the heating and cooling curves. Guar gum, on the other hand, showed only a slight and gradual decrease in OR with increasing temperature, consistent with a slightly stiffened random coil, and there was no thermal hysteresis.

The heating and cooling curves for a mixture of ps.1128 and guar gum appeared to be a composite of those of the two individual components. The transition curve for xanthan was, in effect, shifted upwards but the shape was essentially unaltered except in the high temperature plateau region of the curve, where there was a slight drop in OR, consistent with that observed for the galactomannan. The thermal hysteresis was retained. With deacetylated ps.1128 the behaviour was somewhat different. The OR curve for xanthan was once again shifted upwards and the slight drop in OR in the high temperature plateau region of the curve remained, but this time there was a significant flattening of the transition curve at below 37^{o}C and, at still lower temperatures, optical artifacts analogous to those observed for the gelling systems were found to occur. Furthermore, the cooling curve, which showed initial hysteresis, fell to meet the heating curve at about 30^{o}C. This suggests the possibility of a weak interaction between the deacetylated derivative of ps.1128 and guar gum. This would be consistent with the observations of Tako and Nakamura (1985). An alternative explanation involving the precipitation at low

temperature of one or both of the polymers as a result of mutual incompatibility cannot, however, be completely ruled out, although no precipitate was visible in the cell. Interestingly, in contrast to the observations of Dea and coworkers (1977), there was no increase in the transition midpoint or in the temperature at which the upper plateau region was reached for either system. In other words there was no evidence for stabilization of the xanthan helix by interaction with guar gum.

Falling Ball Experiments

The falling ball experiments were used in an attempt to compare the gel strength in terms of "melting temperature", for a range of xanthan/locust bean gum and xanthan/konjac mannan mixtures. The apparatus used is shown in figure 2.1. A small lead sphere, roughly 2 mm in diameter, was set into a gel comprising 0.5% $^{w}/_{w}$ xanthan and 1.0% $^{w}/_{w}$ gluco- or galactomannan in deionized water, and the temperature was increased at a rate of 0.5°C/minute from ambient. The lead sphere was observed continuously through a travelling microscope and the temperature at which it began to drop constantly through the gel was taken to be the "melting point". Strictly speaking, this was not a true melting point, but the temperature at which the gel had softened sufficiently to enable the lead sphere to "rip" through the molecular network. The apparent "melting points" for a number of mixed systems are given in table 7.2.

The major problem with this type of experiment was in discerning the precise temperature at which the ball began to move through the gel. The melted systems were, generally speaking, quite viscous and the lead sphere therefore fell extremely slowly. In addition any slight lack of homogeneity within the system could markedly affect the result. Because of this it is unreasonable to place too much reliance on single measurements. Had the experiments been repeated a number of times and the results averaged, then the data would have been more meaningful. However, to do this would have been extremely time consuming, and was not considered to be worthwhile when more exacting techniques were available for comparing gel strength. In conclusion, therefore, the data in table 7.2 may be regarded as accurate to within about only +/-3°C. Bearing this in mind, only two conclusions may realistically be drawn from the data. Firstly, the "melting points" for the xanthan/konjac mannan systems were consistently and significantly higher than those of the xanthan/locust bean gum gels. Secondly, deacetylation of ps.1128 appeared to cause a marked increase in gel strength with both locust bean gum and konjac mannan. With locust bean gum deacetylation of ps.1128 caused an apparent increase in the "melting temperature" of 12°C. With konjac mannan, ps.1128 actually failed to form a gel at ambient temperature, whereas the deacetylated derivative gave quite a strong gel with a "melting point" of approximately 56°C.

Compression Testing

Measuring an apparent "yield stress" is a technique widely used in the food industry for estimating gel strength. Indeed McCleary and coworkers (1984) have used it to compare the gel strengths of mixtures of xanthan and galactose-depleted guar gum. Whilst accepting the very obvious theoretical limitations of this approach (Ross-Murphy, 1984) an attempt was made to use compression testing as a purely empirical, comparative technique for estimating the gel strength of the xanthan/locust bean gum and xanthan/konjac mannan mixed gels.

Small cylindrical gel plugs comprising 0.5% $^{w}/_{w}$ xanthan and 1.0% $^{w}/_{w}$ gluco- or galactomannan in deionized water were prepared using perspex moulds (sample preparation as for the minimum gelling concentration experiments; Chapter 2) and the samples were allowed to age for 24 hours prior to testing. They were then compressed between two parallel plates using an Instron Materials Tester and a cross-head speed of 10 mm/minute. The apparent "yield stress" was obtained from the height of the first peak on the chart recorder trace.

A series of measurements were made on different samples, but the technique was found to be an unsuitable measure of gel strength for two reasons. Firstly, the measurements were confined to those samples capable of maintaining their shape against gravity. Secondly, and more importantly, repeat measurements for the same samples differed significantly, and the variation was deemed to be too great when one was looking for possibly quite small differences in gel strength between the systems.

Mechanical Spectrometry

Oscillatory shear measurements (see section 7.1) and, in some instances, steady shear measurements were made using the Rheometrics Mechanical Spectrometer (RMS-605). This instrument is not widely available and it is worth therefore describing briefly how the equipment operates.

A photograph of the RMS-605 is given in figure 7.7 and a block diagram in figure 7.8. A range of test geometries can be used with the instrument. In this study both the 50 mm parallel plate and 72 mm cone and plate (cone angle 0.04 radians) assemblies were used. The sample is loaded between the parallel plates (or the cone and plate), the upper of which is connected to a motor and the lower to a torque transducer. The user selects the deformation history to be applied to the material (strain, shear rate, oscillatory frequency etc.) and the computer translates this into motion of the servo-controlled motor, based upon the geometry in use. The torque generated in response to the imposed motion is measured by the transducer, and the computer calculates the stress from this value. From the stresses, and the strains determined from the measured sample motion, the instrument is able to calculate values for the rheological properties of the sample (G^*, G', G'', η, η^*, tan δ etc.). These values are then outputted to the data terminal and plotter.

The sample temperature history can be controlled during the test using convected gas in the environmental chamber (oven). This facility was only available for use with the 50 mm parallel plate assembly, as the 72 mm cone and plate assembly was not designed to fit inside the oven. The lower of the two parallel plates was specially fitted with an outer cup. This enabled the periphery of the sample to be sealed with a light silicone oil which prevented the sample from drying out at high temperatures.

The Mechanical Spectrometer was used to study the behaviour of both the individual polymers and the mixed systems. A considerable amount of data was obtained using this approach and the methodology and results will be discussed later in this Chapter (sections 7.9-7.12).

Estimation of Minimum Gelling Concentrations.

Experiments to estimate the minimum gelling concentration were carried out on a wide range of xanthan/locust bean gum and xanthan/konjac mannan mixed systems. Starting at a concentration of 0.5% $^{w}/_{w}$ xanthan and 1.0% $^{w}/_{w}$ gluco- or galactomannan, serial 1/2 dilutions were made upon the gel in the melted state (ie. at 80°C). Dilutions down to 1/64 (ie. approximately 0.008% xanthan and 0.016% gluco- or galactomannan) were prepared and the samples were allowed to age for 24 hours at ambient temperature. They were then examined for gel formation, using the criteria outlined in table 2.3. The majority of the measurements were made in distilled water and this data is shown in table 7.5. Samples ps.646, ps.1128 and ps.556, however, were also tested in the presence of sodium chloride and this additional information is given in table 7.6. The results will be discussed in more detail in sections 7.13 and 7.15.

This is, of course, a somewhat subjective technique and as has already been pointed out, it is not always possible to distinguish a gel from a concentrated polymer solution. This type of problem was encountered with certain of the xanthan/guar gum mixtures which at a concentration of 0.5% xanthan and 1.0% galactomannan, to the eye at least, resembled a weak gel network. Nevertheless a high proportion of the xanthan/locust bean gum and xanthan/konjac mannan systems tested in this way had been shown by other techniques to form true gel networks and, despite its subjectivity, this type of experiment yielded a number of interesting results.

7.9 Oscillatory and Steady Shear Measurements on the Individual Polymers

The original aim of these experiments was to examine the individual polymers under conditions identical to those used for the mixed systems (ie. at the same concentration and with the same test geometry and deformation history). This, however, proved to be impossible, as the torque generated was too low. The 72 mm cone and plate assembly was therefore substituted for the 50 mm parallel plates in order to increase the resultant torque, and where necessary (ie. for xanthan) the concentration of the polymer solution was also increased.

Because the 72 mm cone and plate assembly would not fit inside the oven, the instrument could not be used in cure mode and all of the measurements had to be made at ambient temperature (24 +/-1°C). The experiments were therefore restricted to rate sweeps in both the dynamic oscillatory and steady shear modes. Measurements were made in deionized water and in 20mM and 50mM sodium chloride, the samples being prepared exactly as for the mixed systems (section 7.10). The applied strain was 10%.

The Galactomannans

Figure 7.9a shows the steady and oscillatory shear sweeps for a solution of 1.0% guar gum in deionized water. The behaviour is typical of an entanglement system (Robinson *et al*, 1982; Richardson and Ross-Murphy, 1987a). At low frequencies the response is predominantly liquid-like. G" is greater than G' and the two are heavily frequency dependent. As the oscillatory frequency increases, however, G' rises faster than G" and the two eventually cross at a frequency of about 1.5 rad/sec. Above this the behaviour resembles that of a solid. G' is greater than G" and the two are far less frequency dependent. η^* shows the converse behaviour. At low frequencies it is essentially frequency independent but the slope of η^* increases with the oscillatory frequency. The viscosity of the guar gum solution decreases with increasing shear rate and η and η^* are closely superimposable, except at the highest frequencies. Such behaviour is typical of a random coil polymer.

A simple explanation for this type of behaviour is that, at high frequencies the interchain entanglements do not have sufficient time to come apart within the period of one oscillation, and so the solution behaves essentially like a gel. At lower frequencies the principle response is rearrangement of the network to accommodate strain (flow) and so here G" becomes predominant, as is the case for dilute solutions.

Guar gum appears to obey the Cox-Merz rule (Richardson and Ross-Murphy, 1987a). This states that for many polymer solutions the frequency dependence of η^* and the shear rate dependence of η are closely superimposable when the same numerical values of ω and $\dot{\gamma}$ are compared (except for slight deviations which occur for dilute solutions and at high frequencies). This empirical correlation is followed by most solutions of disordered polysaccharides (Morris and Ross-Murphy, 1981)

As one might expect for an uncharged polymer, the behaviour of the guar gum solution was essentially unaltered in 20mM and 50mM sodium chloride.

Figure 7.9b shows the equivalent plot for a 1.0% solution of locust bean gum in deionized water. The behaviour of this polymer was similar to that of guar gum except that the viscosity of the solution was very much lower. Because of this the torque generated was less and sensible data was

only attainable at the higher frequencies. (Note that steady shear data obtained for the same solution at low frequencies, using the Contraves LS30, is shown on the plot as filled circles.) The frequency sweep shows only that region of the plot below the cross-over point for G' and G". Had higher frequencies been accessible or alternatively, a higher concentration of the polymer been used, the frequency sweep might be expected to resemble more closely that in figure 7.9a (Robinson *et al*, 1982). As for guar gum, the locust bean gum solution obeyed the Cox-Merz rule and the behaviour was essentially unaffected by the addition of salt.

Konjac Mannan

The steady and oscillatory shear sweeps for a 1.0% konjac mannan solution in deionized water are shown in figure 7.9c. The plot is almost identical to that of locust bean gum, except that the viscosity is lower and the mechanical spectrum therefore restricted to even higher frequencies. The similarity between the plots, the agreement between η and η^* and the apparent insensitivity of the behaviour towards sodium chloride, indicates that the glucomannan, like guar gum and locust bean gum, behaves in solution as an uncharged, random coil polysaccharide and at higher concentrations forms an entanglement system.

Xanthan

The steady and oscillatory shear response of xanthan was studied for a limited number of samples at a concentration of 2.0% $^{w}/_{w}$. Figure 7.10b shows the so-called Cox-Merz plot for a 2.0% $^{w}/_{w}$ solution of ps.646 in 20mM aqueous sodium chloride (that in 50mM salt was essentially the same). The frequency sweep is typical of a weak gel network (section 6.1). G' is greater than G" and the two are essentially frequency independent. η^*, on the other hand, decreases sharply with increasing frequency. A similar weak gel response has been reported for xanthan by Frangou *et al* (1982), Richardson and Ross-Murphy (1987b) and Clark (1988). The xanthan solution in the presence of salt does not obey the Cox-Merz rule. η^* is significantly greater than η, particularly at high frequencies. The failure of the Cox-Merz rule has, as noted by Richardson and Ross-Murphy (1987b), been reported for other weak gel systems.

In the absence of added salt the behaviour of xanthan was quite different. Figure 7.10a shows the steady and oscillatory shear response for a 2.0% $^{w}/_{w}$ solution of ps.646 in deionized water. The viscosity of this solution was significantly lower than that of the same sample in the presence of salt and reliable data was therefore obtainable only at the higher frequencies. The frequency sweep actually looks more like the high frequency region of an entanglement system than that of a weak gel. G' is only slightly greater than G" and the two approach one another at low frequencies. η and η^* are almost superimposable.

The very different behaviour of xanthan in deionized water may be explained by considering the nature of the polymer under the conditions used in the experiment. The sample was prepared as for the mixed gel experiments and the solution was then allowed to cool to ambient temperature before loading onto the RMS. Optical rotation studies on xanthan (section 4.11) revealed that in the absence of added salt the polymer took longer to readopt the ordered conformation on cooling, than it did to undergo the initial helix-coil transition. This suggests that under the conditions of the experiment, xanthan existed predominantly in the disordered state. It seems likely, therefore, that in the disordered state the intermolecular interactions between xanthan molecules were reduced and the viscoelastic behaviour of the polymer was governed by purely topological entanglements, as it is for other polymers, particularly random coil polysaccharides. Had the polymer solution been allowed longer to cool (eg. overnight storage in a refrigerator) the system may have become more gel-like.

Only the behaviour of ps.646 is illustrated in the figures. However, a 2.0% $^{w}/_{w}$ solution of ps.1128 showed exactly analogous behaviour, both in deionized water and in 20mM sodium chloride. The frequency sweep for a 2.0% $^{w}/_{w}$ solution of deacetylated ps.1128 (batch 2) in deionized water, approached that of an entanglement system but was slightly more gel-like than that of ps.646 and ps.1128.

7.10 Oscillatory Shear Measurements on the Mixed Systems

Oscillatory shear measurements were made upon mixed systems comprising 0.5% $^{w}/_{w}$ xanthan and 1.0% $^{w}/_{w}$ gluco- or galactomannan in deionized water. The samples were prepared by hydrating the polymers overnight in deionized water and then shearing for 5 minutes at 85°C using a top-drive Atomix. They were pressure cooked for 5 minutes at about 110°C and resheared for a further 5 minutes at maximum speed. After centrifugation the samples were remelted and loaded onto the RMS. There is evidence to suggest that pressure cooking solutions of xanthan can result in depyruvylation. Cheetham and Punruckvong (1985) found that when Keltrol was autoclaved for 20 minutes at 120°C in 0.1M sodium chloride, there was a 25% loss of pyruvic acid and this increased to almost total removal of the pyruvate in deionized water. Rinaudo *et al* (1983) reported the complete removal of pyruvate from a partially enzymically degraded xanthan after heating for 48 hours at 90°C in the disordered form, and a significant drop also occurred in the presence of external salt. It is possible, therefore, that pressure cooking the samples in deionized water, even for a relatively short period, will have resulted in some depyruvylation. Some depolymerization could also have occurred although there is no experimental evidence to suggest that this was likely.

Because of the possibility of degradation, before including the pressure cooking step as a routine part of the sample preparation procedure, an attempt was made to ascertain whether autoclaving actually

affected the experimental results. A sample of 0.5% $^{w}/_{w}$ ps.646 and 1.0% $^{w}/_{w}$ locust bean gum was prepared in double the usual amount (I) and the sample was divided into two after the first shearing step. One half was autoclaved and resheared according to the standard procedure. The other was tested directly. A second sample comprising 0.5% $^{w}/_{w}$ ps.646 and 1.0% $^{w}/_{w}$ locust bean gum was prepared from scratch according to the usual procedure (II). After centrifuging, the samples were loaded onto the RMS at 85°C and cooled at a rate of 1°C/minute down to 25°C. A frequency sweep was then performed. (The deformation history used in these tests was the same as for the routine experiments described below.) The values for G', G" and tan δ at the end of the cooling sweeps are given in table 7.3, together with the temperature for G' = G", and the slope of η^* in the frequency sweep. The variation in the data for the autoclaved and unautoclaved halves of sample I was no greater than that for the duplicate autoclaved samples (I and II). This does not mean that no loss of pyruvic acid or depolymerization occurred, merely that any degradation was insufficient to produce a change in the gelling behaviour over and above that of normal sample to sample variation.

Oscillatory shear measurements were performed upon 7 samples of xanthan in combination with locust bean gum, guar gum and konjac mannan. As already noted, the xanthans were selected to give the widest possible range of acetyl and pyruvic acid contents, as well as to examine the effects of chemical deacetylation and depyruvylation. Two samples of deacetylated ps.1128 were included in the study to give an indication of the reproducibility of the data. These samples were prepared by deacetylating two separate batches of ps.1128 produced under identical conditions and the polymers were found to have a very similar chemical composition (table 3.1) and intrinsic viscosity (table 5.3). Sample ps.BD9A was tested with just locust bean gum as only a small amount of this material was available.

The following standard set of experiments was performed on each system:

1. The samples were loaded at 85°C and the temperature was then adjusted to 75°C and held there for 5 minutes. It was subsequently reduced at a rate of 1°C/minute down to 25°C and held there for a further 30 minutes. The G', G" and tan δ values were monitored throughout the cooling process, using 10% strain and a frequency of 10 rad/sec.

2. After 30 minutes ageing a strain sweep was performed at 25°C. The values for G', G" and tan δ were measured over a range of strains between 0-25%, using a frequency of 10 rad/sec. This was necessary to ensure that, at the strain used in the other experiments (ie. 10%), the behaviour of the system was not heavily strain dependent.

3. A frequency sweep was performed next. G', G" and η^* were measured over a range of frequencies between 0.01-100 rad/sec, using a value of 10% strain.

4. Finally the sample was reheated to 75°C at a rate of 1°C/minute and the G', G" and tan δ values were monitored using the same deformation conditions as for the cooling sweep.

The pattern of behaviour for each type of system is discussed below. Examples of the RMS spectra are given in figures 7.11-7.13 and the main features of the spectra are summarized in tables 7.4a and 7.4b.

7.11 Characterization of Mixed Systems in Deionized Water

Xanthan/Locust Bean Gum Mixed Systems

Figure 7.11a shows a typical cooling sweep for a mixture of xanthan and locust bean gum. The behaviour is characteristic of a thermoreversible gel system. At 75°C (ie. at the far left of the trace) the gel is in the melted state and the system behaves as a liquid, the G" value being significantly greater than G'. As the temperature drops and the gel begins to set up, the G' value increases sharply and tan δ falls as the system becomes more elastic. G" also increases, although by nowhere near as much as its elastic counterpart. This phenomenon is usually observed upon gelation but the reason for it is unknown. A number of theories have been proffered (Clark and Ross-Murphy, 1987) but to date none has proved entirely satisfactory. The G' value continues to increase and the tan δ value to decrease long after the gel network has become established and the two are, in fact, still changing at the end of the 30 minutes ageing time. This apparent gradual increase in gel strength over a long period of time has been reported by other authors. Kovacs (1973) noted that for a 1% xanthan/locust bean gum mixture it was 4 hours before the increase in gel strength began to level off and, even then, it continued to increase very slowly for a further 6-7 days. Figure 7.11b shows the tan δ plot for the same system upon cooling and reheating. There is significant hysteresis between the cooling and heating curves and this may be attributed to the increase in gel strength with time.

A strain sweep for the gel is shown in figure 7.11d. Here G' (and G^* which is not shown but which was almost superimposable) can be seen to be virtually independent of strain up to a value of 25%. G" and tan δ are slightly more strain dependent, particularly at the lowest values.

The frequency sweep for the same system is given in figure 7.11e. This is quite clearly that of a strong gel network. G' is much greater than G" and both show very little frequency dependence. η^* decreases markedly with increasing frequency. The G' plot is essentially linear but that of G" increases slightly at both the highest and the lowest

frequencies. This may be an indication of some sort of relaxation phenomenon although the precise nature of such a phenomenon at the molecular level, is not understood.

All of the spectra discussed so far have been for a mixture of ps.646 and locust bean gum. The behaviour of the other xanthans, however, was broadly similar, with the exception of ps.1128 and ps.BD9A. The cooling sweep for ps.1128 and locust bean gum is given in figure 7.11c. The transition is nowhere near as sharp as that for ps.646. G' increases only slowly as the temperature falls and tan δ, in particular, fails to show a definite transition. It decreases steadily over the course of the experiment. (The cooling sweep for ps.PXO_{61} and locust bean gum also showed a somewhat slower than usual transition but the difference was nowhere near as marked as for ps.1128.) The cooling sweep for ps.BD9A is shown in figure 7.11f and the frequency sweep in figure 7.11g. This polymer does appear to undergo some sort of a transition, as indicated by the cooling sweep, but the resultant "gel" is significantly weaker than that of the other systems (see section 7.12).

Xanthan/Guar Gum Mixed System

Figure 7.12a shows a typical cooling sweep for a xanthan/guar gum mixed system. G' increases very slightly upon cooling whilst tan δ decreases, but G" remains essentially unchanged throughout the cooling process. The lack of any significant transition is consistent with the known inability of xanthan to gel with guar gum. The tan δ plots for the same system upon cooling and reheating are shown in figure 7.12b. They illustrate, once again, the very slight decrease in tan δ with falling temperature and there is no thermal hysteresis.

The strain sweep for the xanthan/guar gum system is not shown. G', G", G^* and tan δ, however, showed no strain dependence (except at the very lowest strains) up to a value of 25%.

The frequency sweep for ps.646 and guar gum is shown in figure 7.12c. The spectrum somewhat resembles that of an entanglement system. At high frequencies G' is significantly greater than G" and the two are fairly frequency independent. At lower frequencies they approach one another and the frequency dependence increases. (In the case of ps.646, ps.1128, ps.PXO_{61} and depyruvylated ps.556, G' and G" were actually observed to cross; see table 7.4a.) η^* decreases with increasing frequency and becomes more frequency dependent. Similar behaviour was reported by Clark (1988) for a 0.5% xanthan/guar gum blend (ratio 1:1) in 0.01M sodium chloride.

The behaviour of ps.646, ps.1128, ps.PXO_{61} and depyruvylated ps.556 appears to be a composite of that for the individual polymers in deionized water (figures 7.9a and 7.10a). This is not surprising considering that the two polymers do not normally interact. The behaviour of ps.556 and

deacetylated ps.1128, however, was a little different. The frequency sweeps for ps.556 and deacetylated ps.1128 (batch 2) are given in figures 7.12d and 7.12e respectively. In these spectra G' and G" show markedly less frequency dependence at the lower frequencies, and instead of crossing over, run almost parallel. This may be an indication of some weak intermolecular association within the system.

Xanthan/Konjac Mannan Mixed Systems

The cooling sweep for a typical xanthan/konjac mannan mixed system (figure 7.13a), broadly speaking, resembles that of the xanthan/locust bean gum gels. At high temperatures G" is greater than G'and as the temperature drops and the gel forms, G' increases rapidly and tan δ falls. There are though, a number of significant differences. The gel in the melted state was far less viscous than for the xanthan/locust bean gum mixtures and the torque generated was therefore lower. Consequently the data on the far left of the spectrum is more erratic. The gel begins to set up at a higher temperature and the transition itself is very much sharper. In addition, once the gel has formed, the G' and tan δ plots soon level off and there is little additional increase in gel strength with time. This is reflected in the tan δ plots (figure 7.13b) which show no thermal hysteresis between the cooling and heating curves.

A strain sweep for the xanthan/konjac mannan mixtures is not given but the behaviour was typical of a strong gel system. G' (and G^*) were largely independent of strain except at the lowest values, whilst G" and tan δ, as for the xanthan/locust bean gum systems, showed a slight increase with increasing strain. The frequency sweep for the same system is shown in figure 7.13c and is, once again, that of a strong gel network.

The majority of the xanthan/konjac mannan systems showed the pattern of behaviour described above. However, as with locust bean gum there were exceptions. The transition from liquid to gel in the cooling sweep was less sharp for ps.PXO_{61} than for most of the other systems, whilst ps.1128 actually failed to form a recognizable gel. The mixture, at ambient temperature, flowed freely and was of too low a viscosity to generate sensible data on the RMS. The frequency sweep for this system is, nevertheless, shown in figure 7.13d and although the data is very erratic, there may be evidence for weak cross-linking at the lowest frequencies. Here G' and G" do appear to be relatively frequency independent and η^* decreases with increasing frequency.

7.12 Comparative Gel Strengths

Tables 7.4a and 7.4b give a summary of the major features of the RMS spectra and, in particular, those features that could be of value in comparing the strength of interaction for the different systems. For the xanthan/locust bean gum and xanthan/konjac mannan mixed systems table 7.4a shows the temperature at which G' = G" both upon cooling and reheating,

together with the slope of η^* for the frequency sweeps. For the xanthan/guar gum mixed systems the slope of η^* is given both at high and low frequencies and, where relevant, the cross-over frequency for G' and G" is shown. Table 7.4b gives the tan δ, G' and G" values at the start of the cooling sweep (ie. at 75°C) and at the end (ie. at 25°C), for each system. The most useful measures of gel strength are the G' and tan δ values at 25°C and the slope of η^*.

Generally speaking, the stronger the gel, the higher the elastic modulus. However, G' is not an absolute measure of gel strength. It can depend a great deal upon the frequency at which it is measured. A viscous solution, for example, may at appropriate frequencies have a higher G' value than a true gel network. This is seen for certain of the xanthan/ guar gum mixtures which at 10 rad/sec have a G' value approaching or exceeding that of the equivalent xanthan/konjac mannan gel.

A true gel network has associated with it an equilibrium modulus, that is, an elastic modulus at zero frequency and zero strain. A Newtonian solution or an entanglement system does not. When comparing different systems one would ideally measure the equilibrium modulus since this eliminates any problems of frequency or strain dependence, but this is not, of course, possible. Some workers have attempted to determine a pseudoequilibrium modulus by extrapolation of the G' plot. In this study the G' value at a frequency of 10 rad/sec was taken as a comparative measure of gel strength. This was satisfactory for the majority of the mixed gel systems since, for a true gel network, G' shows very little frequency dependence. However, for the weaker systems, in particular ps.BD9A with locust bean gum, the frequency dependence of G' increased at the higher frequencies (see figure 7.11g) due to a greater contribution from dynamic entanglements. It should be borne in mind that for such systems the G' value at 10 rad/sec will actually tend to underemphasize the difference between the weaker and the stronger networks.

The tan δ value at 25°C is a measure of the elasticity of the system. The lower the tan δ value, the more elastic the gel network. Likewise, the greater the slope of η^*, the more elastic the gel. A perfectly elastic system has a slope of -1.

The temperatures at which G' = G" in the cooling and heating sweeps may be regarded as a "setting" and "melting temperature" since this is the point at which the behaviour of the system is exactly midway between a liquid and a gel. The G' = G" values are, therefore, a possible additional indicator of gel strength.

The extremely good agreement between the data for the samples of deacetylated ps.1128 suggests that the overall reproducibility of the data was good.

If one compares the data for the xanthan/locust bean gum and xanthan/konjac mannan gels, one finds that the G' values were generally somewhat lower for the xanthan/konjac mannan systems, and the tan δ values a little higher. The slopes of η^*, on the other hand, were very similar. The G' = G" values for the xanthan/konjac mannan gels were significantly greater than those for the xanthan/galactomannan systems. This is consistent with the results for the falling ball experiments. Indeed the data for the falling ball experiments and for the oscillatory shear measurements, broadly speaking, followed the same pattern, although the "melting temperatures" determined using the former method were a little lower. This suggests that the xanthan/konjac mannan junction zones were rather more resistant to disruption by heat than the xanthan/locust bean gum junctions, but that the overall gel strength at 25°C was, if anything, a little lower.

The majority of the xanthans tested formed a relatively strong gel network with locust bean gum, but there were exceptions. Sample ps.1128 gave a markedly weaker gel in combination with the galactomannan. The G' value and the slope of η^* were significantly lower than for most of the other systems and the tan δ value was somewhat higher. In addition, as already noted, the transition from the liquid to the gel state upon cooling was not as sharp as usual. The G' = G" values though, were exceptionally high for this system, which appears to conflict with the other evidence for a weaker interaction This suggests that G' = G" is not, after all, a particularly good criterion for estimating the gel melting temperature, especially for comparatively weak systems. Sample ps.PXO_{61} appeared to form a slightly weaker gel than normal but the difference was not as marked as for ps.1128.

Deacetylation of ps.1128 resulted in a significant increase in gel strength. The G' value and the slope of η^* increased dramatically and the tan δ value fell. In contrast, depyruvylation of ps.556 hardly affected the gel strength. The G' = G" values dropped by 7-8°C but G', tan δ and the slope of η^* barely changed. This suggests that the acetyl group had an inhibitory effect upon gelation but that the pyruvate group played no role in the gelling interaction.

The polymer from strain BD9A produced a much weaker gel than any of the other xanthans tested. The G' value for this system was exceptionally low and the tan δ value very high. The slope of η^* was low and likewise the G' = G" value upon cooling. In addition, as already noted, this polymer showed increasing frequency dependence at the higher frequencies. This indicates that the terminal mannose residue on the trisaccharide side-chain played an important role in the xanthan-locust bean gum interaction.

As for the xanthan/locust bean gum systems, the interaction between ps.1128 and konjac mannan was very weak. Indeed, ps.1128 and konjac mannan failed to form a recognizable gel at room temperature and yielded no useful data on the RMS. No data for this system is therefore given in

tables 7.4a and 7.4b, except for an estimate of the slope of η^* at low frequencies, determined from figure 7.13d. This value, -0.74, is significantly lower than that for any of the other systems and approaches the expected result for an entanglement network. The deacetylated derivative of ps.1128, in contrast, formed quite a strong gel with konjac mannan. Once again, therefore, the acetyl group appears to have had an inhibitory effect upon gelation. This, however, was probably not true in the case of ps.PXO_{61} or, at least, not to any great extent. The gel for this polymer was marginally weaker than that for ps.646 and ps.556 but about the same strength as that for deacetylated ps.1128.

Depyruvylation of ps.556, in this case, resulted in a slight drop in the strength of the interaction with konjac mannan. G' decreased significantly, as did the G' = G" values, and tan δ rose. The slope of η^*, however, changed very little.

The strength of the interaction between xanthan and both the gluco- and galactomannans will depend upon the concentration of the two polysaccharides involved. It is possible, therefore, that differences in the concentration of pentasaccharide repeat unit between xanthans with very different levels of acetyl and pyruvate substitution, could similarly influence the strength of the interaction. To what extent this might occur is uncertain. However, the lack of any obvious relationship between the gel strength and the total percentage of acyl substituents in either type of mixed system, suggests that in these experiments, the relative concentrations of pentasaccharide repeat unit was not an important determinant of gel strength. There was also no apparent correlation between the gel strength and the molecular weight of the xanthan samples as indicated by their intrinsic viscosity values.

Since xanthan and guar gum do not interact to form a gel, the G' and tan δ values listed in table 7.4b say very little about the strength of interaction between the polymers. Instead more informative data is found at the lower frequencies. Samples ps.646, ps.1128, ps.PXO_{61} and depyruvylated ps.556 all showed apparent entanglement behaviour with G' and G" crossing at low frequencies. However, for deacetylated ps.1128 and ps.556, G' and G" did not cross and the slope of η^* in the low frequency region was significantly greater than that for the other systems. This has already been interpreted as a possible indication of weak intermolecular association and it is interesting to note that, with the exception of depyruvylated ps.556, it was the polymers with little or no acetyl that appeared to interact in this way.

7.13 Minimum Gelling Concentration Experiments

The data for the minimum gelling concentration experiments carried out on the xanthan/locust bean gum and xanthan/konjac mannan systems in distilled water, is given in table 7.5. The data indicates that the xanthan/locust bean gum systems were capable of forming gels down to a much lower total polysaccharide concentration than the konjac mannan

systems. This is in marked contrast to the findings of Dea and coworkers (1977). Dea *et al* stated that recognizable gels were formed with konjac mannan down to a total polysaccharide concentration of 0.02%, yet in this study, the lowest total polysaccharide concentration at which a gel was formed with konjac mannan was 0.375%. This was true for ps.646, Kelzan and deacetylated ps.1128 (batch 1) and it compares with a total polysaccharide concentration of 0.094% for a mixture of deacetylated ps.1128 (batch 1) and locust bean gum. The minimum gelling concentration data also appears to conflict with the findings from mechanical spectrometry. As discussed in the last section, evidence from the oscillatory shear measurements suggests that the xanthan/konjac mannan gels may have been marginally weaker than the xanthan/locust bean gum gels at 25°C, but that they were significantly more resistant to disruption by heat. One might therefore have expected xanthan to gel with konjac mannan down to concentrations at least approaching those of the xanthan/locust bean gum systems.

The answer to the apparent discrepancy may lie in the relative molecular weights of the galacto- and glucomannan. The estimated molecular weight for the locust bean gum sample was 8.2×10^5, whereas that for konjac mannan was 18×10^4 using the data of Kishida *et al* (1978), or 55×10^4 using the guar gum data of Robinson *et al* (1982; section 5.8). The effect of molecular weight upon gel strength is not clear cut (section 7.17) but it is possible that although xanthan and konjac mannan interacted fairly strongly at high concentrations, because of its low molecular weight, the glucomannan was incapable of forming a well-defined, cross-linked gel network at concentrations as low as for the xanthan/locust bean gum mixed systems. The apparent molecular weight of the konjac mannan sample used in this study was unusually low compared with reports in the literature and the discrepancy between the present observations and those of Dea *et al* may be at least partially accounted for by a difference in the molecular weight of the samples.

Deacetylation of ps.1128 caused a marked decrease in the minimum gelling concentration of the polymer with both locust bean gum and konjac mannan. Sample ps.1128 gelled with locust bean gum down to a minimum total polysaccharide concentration of 0.3% and it failed to gel at all with konjac mannan over the range of concentrations tested. The deacetylated derivative, however, gelled with locust bean gum at a total concentration as low as 0.094% and with konjac mannan at a concentration of 0.375%. The decrease in the minimum gelling concentration is consistent with the apparent increase in gel strength reported for both the falling ball experiments and the oscillatory shear measurements. Deacetylation of ps.646 produced a slight decrease in the minimum gelling concentration with konjac mannan and deacetylation of ps.PXO_{61}, a slight decrease with locust bean gum. However, the gels formed by all of the deacetylated derivatives were found to be firmer to the touch than those of the equivalent native polymers, even though this is not always reflected by the gradings in table 7.5.

Sample ps.556 was a native low acetyl, high pyruvate polymer. This material formed a gel with locust bean gum down to a minimum total concentration of 0.094%, the same as for deacetylated ps.1128, but with konjac mannan a gel was formed only down to a concentration of 0.75%.

Depyruvylation of ps.556 produced a slight increase in the minimum gelling concentration with locust bean gum and the same was true for ps.646. For Flocon 4800C there was no change. With konjac mannan, depyruvylation of ps.646 produced a slight increase in the minimum gelling concentration but for ps.556 and Flocon 4800C, the minimum gelling concentration remained unaltered. In general though, the gels formed by the native polymers were slightly firmer to the touch than those of their depyruvylated derivatives. Hence, evidence from the minimum gelling concentration experiments and from the oscillatory shear measurements suggests that depyruvylation usually caused a slight decrease in gel strength with locust bean gum and konjac mannan.

Interestingly, there was fairly good agreement between the data for ps.646 produced in batch culture, ps.646 produced in continuous culture under potassium limiting conditions, and Kelzan which was produced by the same bacterial strain as ps.646. There was also quite good agreement between the data for the low acetyl, low pyruvate polymers. Deacetylated ps.PXO_{61}, depyruvylated ps.556, depyruvylated Flocon 4800C and deacetylated and depyruvylated ps.646 all formed gels with locust bean gum down to a total concentration of 0.188% and with konjac mannan down to a concentration of 0.35%. Deacetylated ps.1128 (batch 1), however, formed gels down to a slightly lower total polysaccharide concentration. There appeared to be no consistent correlation between the molecular weight of the xanthan samples, as indicated by the intrinsic viscosity, and the minimum gelling concentrations.

7.14 Computer Analysis

Virtually all of the data presented so far has indicated that the strength of the interaction between xanthan and both locust bean gum and konjac mannan is heavily dependent upon the level of acetyl substitution. The role of pyruvate and the molecular weight, however, is much less clear cut. An attempt was therefore made to look for statistically significant correlations between the gel strength, the levels of acetyl and pyruvate substitution and the molecular weight (as indicated by the intrinsic viscosity) using the same computer package as was used in Chapter 4 (section 4.7) to analyse the helix-coil transition behaviour of the polymers.

In this instance the dependent variables were the main measures of gel strength, tan δ, G' and the slope of η^*, together with the ratios of tan δ and G' at 75°C and 25°C. Using PROCEDURE RSQUARE from the SAS library (SAS Users Guide: Statistics, 1985) a multiple regression analysis was carried out on the data. The model dependent parameters were regressed

against the independent variables, acetyl, pyruvate and intrinsic viscosity, and the full correlation matrix of dependent and independent variables was outputted. The independent variables were then tested singly, in pairs and all together to see whether any of the three acted in conjunction with one another.

Initially the data for all of the polymers studied by mechanical spectrometry was included in the analysis, with the exception of that for ps.BD9A (sample ps.BD9A was not a conventional xanthan). Subsequently that for ps.PXO_{61} was also excluded since this polymer appeared to have an atypical acetyl distribution (section 3.2). As no data was available for ps.1128 with konjac mannan, except for an estimate for the slope of η^* at low frequencies, arbitrary values below the limit of resolution of the RMS-605, were included for this sample, in the analysis. A value of 500 was used for tan δ and a value of 50 for G'. For the ratios of tan δ and G' a value of 1.0 was used. This was necessary because the number of samples in the data set was already very small and to have omitted ps.1128 would, not only have reduced the number still further, but would have excluded one of the most important polymers in the study.

The complete correlation matrices for the xanthan/locust bean gum and xanthan/konjac mannan systems are given in tables 7.7a and 7.8a respectively. The same data determined in the absence of ps.PXO_{61} is given in tables 7.7b and 7.8b.

Because the number of samples included in this analysis was so small (6 or 7) a much higher value is required to indicate statistical significance than was the case for the OR studies. Here a value of 0.85 or above may be considered a reasonable indication of statistical significance. This is equivalent to an R-square value of 0.72.

For the xanthan/locust bean gum system a significant correlation was found between tan δ and the slope of η^*, and between the ratios of tan δ and G'. Quite a strong negative correlation was also found between tan δ and G'. This was true when the data for ps.PXO_{61} was included in the analysis and when it was not. Such correlations were to be expected since all of these variables are measures of gel strength.

A weak correlation ie. 0.896, was found between the percentage acetyl and the slope of η^* when all of the data was included in the analysis, and this increased to 0.939 when the data for ps.PXO_{61} was excluded from the data set. In the absence of the data for ps.PXO_{61} a strong correlation was also observed between the percentage acetyl and tan δ. This seems to confirm the previous finding that acetyl has a strong influence upon gel strength. There were no consistent correlations between gel strength and either the percentage pyruvate or the molecular weight. However, in the absence of the data for ps.PXO_{61}, there was a weak, and probably spurious, negative correlation between the intrinsic viscosity and the ratio of the tan δ values (such findings are an almost inevitable problem when such a small data set is used).

The findings for the xanthan/konjac mannan mixed systems were quite similar to those just described. Strong correlations were found between tan δ and the slope of η^*, between G' and the tan δ ratio, and between the ratios of G' and tan δ, both with and without the data for ps.PXO_{61}. When the complete data set was used there were no significant correlations between any of the dependent and independent variables, but when the data for ps.PXO_{61} was omitted from the analysis, a weak correlation was observed between the percentage acetyl and tan δ, and the percentage acetyl and the slope of η^*. Thus, the role of the acetyl group in the xanthan/konjac mannan interaction appears to be a little less clear cut than for the xanthan/locust bean gum systems. However, care should be taken in interpreting these correlations because of the very small number of samples in the data set. Indeed, the data obtained from the regression models for the dependent variables was found to be unusable for precisely this reason. Because of the small number of samples considered, when more than one of the independent variables was included in the model, the R-square values all tended to be very high and true significance could not, therefore, be established.

An attempt was made to investigate whether or not there was a statistically significant correlation between the gel strength and the helix-coil transition midpoint (T_m). Using PROCEDURE RSQUARE the tan δ, G' and slope of η^* values for all of the polymers were regressed against the mean helix-coil transition midpoints given in table 4.3 (the same values for tan δ and G' were included for ps.1128 and konjac mannan as in the previous analysis). The resultant correlation matrices for the xanthan/ locust bean gum and xanthan/konjac mannan mixed systems are given in tables 7.9a and 7.9b respectively.

For the xanthan/locust bean gum systems a strong positive correlation was found between T_m and both tan δ and the slope of η^*. A strong negative correlation was obtained between T_m and the G' value, ie. the higher the transition midpoint, the weaker the gel formed with locust bean gum. This could be taken as evidence to support the Cairns model for the xanthan-galactomannan interaction (section 7.4). In other words, the higher the transition midpoint temperature, the more rapidly the polymer readopts the ordered conformation upon cooling and the less time is therefore available for junction zones to become established between xanthan and the galactomannan. The relationship, however, need not necessarily be causal.

No significant correlations were found between the melting temperature and the gel strength for the xanthan/konjac mannan mixed systems.

7.15 Effect of Salt Upon Gelation

The effect of salt upon the interaction properties of xanthan was studied for three polymers, ps.646, ps.1128 and ps.556.

Oscillatory shear measurements were made upon these polymers in combination with locust bean gum, guar gum and konjac mannan, in the presence of 20mM and 50mM sodium chloride. The protocol used was identical to that described in section 7.10, except that the samples were prepared directly in sodium chloride solution instead of deionized water. Unfortunately the results obtained in these experiments proved to be unsatisfactory. When the samples were reheated to 75°C at the end of the normal sequence of measurements, they were found to retain a considerable amount of structure. That is, the G' values were markedly higher and the tan δ values somewhat lower than they had been at the start of the experiment. The apparent structure was thought to be due to some drying out of the sample at the rim of the lower plate and a hair-line fracture was subsequently discovered between the lower plate and the outer cup. Because of this, the data collected in the presence of sodium chloride had to be discarded.

Some data was, however, obtained for the xanthan/locust bean gum and xanthan/konjac mannan systems using the minimum gelling concentration method. This data is given in table 7.6. In the majority of cases the minimum gelling concentration increased in the presence of sodium chloride and the gels were found to be noticeably less firm to the touch. The most startling change was observed for the ps.1128 and locust bean gum system. In distilled water these materials appeared to form a gel down to a total polysaccharide concentration of 0.75% but in the presence of 50mM sodium chloride, gelation failed to occur at any of the concentrations tested and the mixture flowed freely. This indicates that salt inhibits the gelling interaction between xanthan and both locust bean gum and konjac mannan. Tako and coworkers (1984) reported a similar decrease in the strength of interaction between xanthan and locust bean gum in the presence of sodium chloride. Cheetham and Mashimba (1988), however,found that gels formed between xanthan and locust bean gum in the presence of 50mM potassium chloride were, at least in terms of their melting temperature, stronger than the equivalent gels formed in distilled water. This appears to conflict with the findings in this study. Furthermore, the depyruvylated derivative of Keltrol (ie. a polymer with a moderate amount of acetyl but no pyruvate) used by Cheetham and Mashimba failed to form a gel with locust bean gum in distilled water but gave quite a strong gel in 50mM potassium chloride. This is in direct contrast to the behaviour of ps.1128, a high acetyl, low pyruvate polymer used in this study, and also conflicts with the findings for depyruvylated ps.646, a polymer that should, theoretically at least, have been very similar to depyruvylated Keltrol.

7.16 Experiments to Determine whether or not Denaturation of the Xanthan Helix is Necessary for Gelation to Occur with Locust Bean Gum and Konjac Mannan

According to the models of Cairns *et al* (1986a, 1987) and Cheetham and Mashimba (1988), denaturation of the xanthan helix is necessary for the gelling interaction between xanthan and locust bean gum, and evidence from Brownsey *et al* (1988) suggests that the same is true for the xanthan/konjac mannan interaction. In this study an attempt was made to test this assertion using oscillatory shear measurements to determine unequivocally whether or not gelation had occurred.

A 1.0% $^{w}/_{w}$ solution of ps.646 and a 2.0% $^{w}/_{w}$ solution of both locust bean gum and konjac mannan were prepared in deionized water and in 50mM aqueous sodium chloride (sample preparation was essentially the same as for the mixed gel systems). The solutions were then combined in equal quantities to give the following four mixed systems:

i) 0.5% $^{w}/_{w}$ ps.646 plus 1.0% $^{w}/_{w}$ locust bean gum in deionized water.

ii) 0.5% $^{w}/_{w}$ ps.646 plus 1.0% $^{w}/_{w}$ locust bean gum in 50mM sodium chloride.

iii) 0.5% $^{w}/_{w}$ ps.646 plus 1.0% $^{w}/_{w}$ konjac mannan in deionized water.

iv) 0.5% $^{w}/_{w}$ ps.646 plus 1.0% $^{w}/_{w}$ konjac mannan in 50mM sodium chloride.

The samples were mixed cold (ie. at ambient temperature) using a top-drive Atomix. They were sheared for 1 minute at high speed and were then centrifuged for 2 minutes at 20,000 rpm in a bench centrifuge, before loading onto the mechanical spectrometer. As before, the 50mm parallel plates were used in conjunction with the normal (TC-2000) transducer. The samples were loaded onto the instrument at ambient temperature and the temperature was adjusted to 25°C. The G', G" and tan δ values were monitored for a period of 40 minutes at 25°C, using 10% strain and a frequency of 10 rad/sec. A frequency sweep was then performed. Thereafter, the sample was heated quickly to 75°C, held there for 5 minutes and then cooled at a rate of 2°C/minute back down to 25°C. The G', G" and tan δ values were monitored throughout the heating and cooling process.

All four mixed systems showed essentially the same pattern of behaviour. Gelation appeared to occur as soon as the polymers were mixed and so, when the samples were loaded onto the RMS, the gel was broken up by the lowering of the upper plate. The G', G" and tan δ values monitored over the initial 40 minute period hardly changed, but the frequency sweep for each system at 25°C was quite clearly that of a gel. Figure 7.14 shows the frequency sweep obtained for ps.646 and locust bean gum in the presence of 50mM sodium chloride and figure 7.15, the frequency sweep for

ps.646 and konjac mannan, also in the presence of salt. The gels do not appear to be particularly strong, as one might expect for a system that has been well and truly macerated, but there can be little doubt that a gelling interaction did occur. The frequency sweeps for the same polymers in deionized water are not shown but they were very similar. The gels appeared to be somewhat stronger, but absolute values of G' mean very little for a broken gel network. In addition, salt has been shown, in this study, to have an inhibitory effect upon gelation.

When the samples were heated to 75°C, the G' value decreased and tan δ increased as the gel melted out. The reverse happened upon cooling and it was noted that the G' value attained at 25°C, after cooling, was slightly higher than that at the start of the experiment. This was to be expected as the system was now a single, cohesive gel network and since there was probably also an increase in the overall homogeneity of the sample after heating.

That gelation occurred when the samples were mixed cold in deionized water came as no great surprise. The solution of ps.646 was prepared in essentially the same way as the sample in figure 7.10a and it is therefore likely that when the two polymers were mixed the xanthan still remained largely in the disordered state. In the presence of 50mM sodium chloride, however, there can be no doubt that the xanthan had readopted the ordered conformation prior to mixing and yet gelation occurred with both locust bean gum and konjac mannan. Furthermore the gel, in each case, appeared to have melted out at 75°C and yet, judging from the results for the helix-coil transition experiments performed upon ps.646 in the presence of salt (table 4.7), in 50mM sodium chloride the transition midpoint for the polymer should have been well above 75°C. The results for these experiments, therefore, appear to contradict the findings of Cairns *et al*, Cheetham and Mashimba, and Brownsey *et al*, and indicate that denaturation of the xanthan helix is unnecessary for the polymer to interact with locust bean gum and konjac mannan.

7.17 Discussion

The two main aims of this study were, as outlined in section 7.7, to characterize in rheological terms the nature of the interaction between xanthan and the polysaccharides locust bean gum, guar gum and konjac mannan, and to examine the effects of structure, in particular the level of acetyl and pyruvate substitution, on the strength of the interaction.

The first of these goals was achieved satisfactorily. The majority of xanthans were shown to interact with locust bean gum and konjac mannan, in the absence of added salt, to form a strong gel network. The gels formed between xanthan and locust bean gum took a relatively long time to set up and the gel strength continued to increase well beyond the time scale of the experiments. The melting point was quite low, typically in the region of 40-50°C. The xanthan-konjac mannan gels, in contrast, set up

and achieved maximum strength extremely quickly and the melting point was significantly higher, usually between 50-60°C. Xanthan, in general, failed to interact with guar gum and the two polymers formed an entanglement system, the behaviour of which appeared to be a composite of that of the two individual materials.

The second goal, namely to define the effects of acetyl and pyruvate substitution on the interactions, was only partially achieved. Almost all of the data collected in this study indicated that the acetyl substituent had an inhibitory effect on intermolecular association. The high acetyl xanthans generally formed weaker gels with locust bean gum and konjac mannan, than their acetyl-free counterparts and the gels were formed at higher concentrations. This was particularly true in the case of ps.1128. Furthermore, there was evidence to suggest that certain low acetyl xanthans were capable of interacting weakly with guar gum. whereas the more highly acetylated materials were not.

Inhibition of intermolecular association by acetyl groups is quite a common phenomenon in biopolymer systems (Morris and Miles, 1986). For example, when salt is added to an aqueous solution of XM-6, an exocellular polysaccharide produced by a species of *Enterobacter* (NCIB 11870), a thermoreversible gel is formed (Nisbet *et al*, 1984). The capsular polysaccharide from *Klebsiella aerogenes* serotype K54, however, which is a naturally acetylated polymer with the same basic tetrasaccharide repeat unit as XM-6, will not form a gel unless it is first chemically deacetylated (O'Neill *et al*, 1986). Gellan gum, an acetylated polysaccharide secreted by *Pseudomonas elodea* will gel both in the native state and after deacetylation but the texture of the gels is significantly different (Moorhouse *et al*, 1981). The native polymer forms a soft, elastic gel after heating and cooling, whereas that of the deacetylated derivative is firm, non-elastic and rather brittle. The difference in texture is believed to be due to a much stronger interaction between the deacetylated molecules. Bacterial alginate which is secreted by certain strains of *Pseudomonas aeruginosa* and *Azotobacter vinelandii*, unlike algal alginate, carries O-acetyl groups which are associated with the polymannuronic acid blocks. Polymers with a high level of acetyl substitution form relatively weak gels. Inhibition of gelation by the acetyl groups in konjac mannan has been discussed in section 7.3 and acetyl groups have also been shown to inhibit gelation in plant pectin (Pippen *et al*, 1950).

In the case of bacterial alginate the reason for inhibition is well established. Alginate is synthesized as polymannuronic acid and the block copolymer is produced by epimerization of mannuronic acid to guluronic acid by the enzyme mannuron C-5 epimerase. The O-acetyl groups inhibit epimerization and so those polymers with a high level of acetyl substitution remain rich in mannuronic acid (Skjak-Braek *et al*, 1985). Since it is predominantly the guluronic acid blocks that are involved in gelation, the more acetyl groups the polymer carries, the lower its ability to bind cations and form a gel.

The reason for inhibition in the other four polysaccharides is not so well understood. For konjac mannan (Cairns *et al*, 1988), the K54 capsular polysaccharide (Atkins *et al*, 1987) and gellan gum (Carroll *et al*, 1982) X-ray fibre diffraction studies have shown that the ordered conformation of the polymers is not significantly affected by deacetylation and that the only change is an increase in the propensity of the polymers to co-crystallize. Exactly how the acetyl group inhibits co-crystallization has still to be established. In the case of konjac mannan, Maekaji (1974) has suggested that the acetyl group suppresses intermolecular hydrogen bonding but this has not been proven conclusively.

Thus, despite the frequency with which acetyl is found to inhibit gelation, examination of other biopolymer systems throws very little light upon the role of the acetyl group in xanthan/galactomannan and xanthan/glucomannan mixed systems. The absence of a well-established mechanism for each interaction makes speculation that much more difficult. Broadly speaking there are three ways in which the acetyl group could inhibit intermolecular association. The first is direct steric hindrance. The second is suppression of the intermolecular attractive forces, particularly hydrogen bonding, as has been suggested for konjac mannan. (The weakening of the gelling interaction between xanthan and locust bean gum in the presence of urea (Tako *et al*, 1984; Cheetham and Mashimba, 1988), indicates that hydrogen bonding plays an important role in the interaction). The third possibility is that the acetyl group influences the gelling properties of xanthan through its effect upon the ordered conformation. Acetyl has been shown to stabilize the xanthan helix and to raise the helix-coil transition midpoint (Chapter 4). There is also limited evidence to suggest that high acetyl polymers are less flexible than low acetyl materials in solution (section 5.9). Tako and coworkers observed a stronger interaction between deacetylated xanthan and both locust bean gum (Tako *et al*, 1984) and guar gum (Tako and Nakamura, 1985) than with the native polymer and suggested that an increase in the flexibility of the xanthan molecule upon deacetylation could facilitate easier association between the xanthan side-chains and the galactomannan backbone. The models of Cairns *et al* and Cheetham and Mashimba, state that gelation can only occur when xanthan is in the disordered state, and this implies that by raising the helix-coil transition midpoint the acetyl group could limit the ability of the polymer to gel under certain conditions. The strong negative correlation observed between T_m and gel strength, for the xanthan/locust bean gum mixed systems, would be consistent with this view.

In agreement with the findings of Tako and Nakamura (1985), evidence from both the OR studies and oscillatory shear measurements indicated a possible weak interaction between low acetyl xanthan and guar gum. It should be noted, however, that whilst both ps.556 and deacetylated ps.1128 showed signs of weak association, depyruvylated ps.556, another low acetyl xanthan, did not. A possibility not so far considered is that the apparent weak interaction occurred not between xanthan and guar gum

but between the xanthan molecules alone. Both Jeanes *et al* (1961) and Tako and Nakamura (1984) have produced evidence to suggest a stronger association between deacetylated xanthan molecules than between molecules of the native polymer (section 6.2), although presumably in both cases, unlike here, the xanthan was in the ordered state. (Evidence presented in section 7.9 suggests that under the conditions employed in the mixed gelling experiments xanthan existed predominantly in the disordered state, at least prior to any interaction.) The frequency sweep for a 2.0% $^{w}/_{w}$ solution of deacetylated ps.1128 in deionized water (not shown) showed slightly more gel-like behaviour than that of 2.0% $^{w}/_{w}$ ps.646 and 2.0% $^{w}/_{w}$ ps.1128 (unfortunately a 2.0% solution of ps.556 could not be tested because of a shortage of the material), lending support to a possible xanthan-xanthan interaction. On balance though, in light of the findings of Tako and Nakamura, a weak interaction between xanthan and guar gum is still favoured by the author.

The role of pyruvic acid in gelation is even less well understood than that of the acetyl group. The findings in this study indicated a slight decrease in gel strength upon depyruvylation, particularly in the xanthan/konjac mannan mixed systems, and this suggests possible promotion of the gelling interaction by the pyruvic acid group. Cheetham and Mashimba (1988) reported that depyruvylated Keltrol failed to interact with locust bean gum in distilled water, whereas the native polymer gelled readily, and this too would be consistent with the enhancement of gelation by pyruvic acid. If the pyruvate substituent does indeed promote gelation then, assuming that xanthan can only interact in the disordered state, it might do so via its destabilising effect upon the ordered conformation (Chapter 4). The evidence presented in this study though, is by no means definitive. The changes observed upon depyruvylation were small and any apparent trends were not reflected by the data from the statistical analysis. Furthermore, it is by no means certain that the changes observed were actually due to loss of the pyruvic acid group. Evidence outlined in section 7.10 suggests that autoclaving the polymer in deionized water, even for a relatively short period of time, may have brought about a significant reduction in the level of pyruvate substitution and if this were the case, then many of the materials used for the oscillatory shear measurements may have contained less pyruvic acid than was thought. In addition it is possible that the reduction in gel strength was due, not to depyruvylation itself, but to the concomitant decrease in molecular weight that is believed to have occurred (sections 3.6 and 5.7).

The effect of molecular weight on gel strength has so far been largely ignored. No obvious correlation was found between the intrinsic viscosity of xanthan and the gel strength and this was confirmed by the statistical analysis. However, the suitability of intrinsic viscosity as a measure of molecular weight has been called into question (section 5.7).

In theory the rigidity of a polymer gel should increase with the molecular weight, since the chance of macromolecular association rises as the length of the molecules increases (Janus/Flory, 1974). In practice

though, this appears only to be true in the low molecular weight region. Data presented by Smidsrød (1974) for alginate gels, namely a plot of modulus of rigidity against degree of polymerization, showed that for this system, above a minimum critical degree of polymerization (approximately 500) the modulus of rigidity did not change. This is consistent with the view that above a minimum critical molecular weight the concentration of cross-linkages remains fixed as the primary molecular weight increases (Janus/Flory, 1974).

What the minimum critical molecular weight for xanthan would be in xanthan/locust bean gum and xanthan/konjac mixed mannan gels is unknown. There is therefore no way of telling whether the apparent reduction in the molecular weight of xanthan after depyruvylation could have been responsible for the decrease in gel strength in the mixed systems. The problem does not arise in the case of deacetylation since here the gel strength appeared to increase in spite of possible depolymerization. Interestingly, marked differences in gel strength were recorded for the systems prepared with ps.646, ps.1128, ps.PXO_{61} and ps.556 and yet the molecular weights of these polymers, determined in the light scattering experiments, were quite similar (table 5.5). This suggests that over the molecular weight range 0.9-1.6 x 10^6, at least, factors other than the molecular weight were of overriding importance. (The molecular weight obtained by light scattering is a weight average molecular weight. For this type of comparison a number average molecular weight would be more relevant. The number average molecular weight range should, in fact, be narrower.)

Although the acetyl groups appeared to have an inhibitory effect on gelation for all of the polymers tested, the effect upon ps.1128 was particularly marked. If one compares the strength of the gels formed with ps.1128 with that of the gels formed with PXO_{61} and ps.646, the ps.1128 systems were substantially weaker, even though the acetyl content of this polymer was only about half that of ps.PXO_{61}. Deacetylation of ps.PXO_{61} produced nothing like the same decrease in the minimum gelling concentrations as deacetylation of ps.1128, and the same was true for ps.646. This suggests that there was something special about the structure of ps.1128 that was particularly antagonistic towards intermolecular association. It may have been the acetyl distribution. The acetyl content of this polymer (7.7%) was slightly more than stoichiometric and the location of the additional acetyl groups is unknown. Alternatively it may have been some other aspect of the fine structure. A possibility that cannot be ignored, however, was the tendency of ps.1128 to form a stable aggregated structure which was not broken down at 90°C or by vigorous stirring (section 5.9). Had this aggregated structure persisted in the mixed gel systems then the amount of xanthan available for cross-linking would have been less and the gel may, as a consequence, have been significantly weaker. (The deacetylated derivative of ps.1128, judging from its intrinsic viscosity, showed no such tendency to aggregate.) The samples used for the oscillatory shear measurements were autoclaved.

albeit for short time. This should have broken down any aggregates, as indicated by the light scattering experiments, but one cannot be absolutely certain of this. Neither can one guarantee that the regime used in the minimum gelling concentration experiments was sufficient to break up any aggregates.

Of all the xanthan-locust bean gum interactions studied, that of ps.BD9A was by far the weakest. As ps.BD9A is believed to have lacked the terminal mannose residue from the trisaccharide side-chain, this suggests some fundamental role for the side-chain in the xanthan-galactomannan interaction. The side-chain could be directly involved in binding, as Tako *et al* (1984) have suggested, or alternatively, assuming that the ordered helical conformation is necessary for xanthan-galactomannan binding (Dea *et al*, 1977), loss of the terminal mannose residue could have inhibited the interaction by preventing adoption of the ordered state. The helix-coil transition curve for ps.BD9A indicated that, in deionized water, the polymer was capable of adopting at least a partially ordered conformation (section 4.8). However, close examination of the OR data in figure 4.9f reveals that at 25°C, the temperature at which the oscillatory shear measurements were made, the polymer had already lost a substantial amount of order. The weakness of the interaction between ps.BD9A and locust bean gum is difficult to equate with a backbone-backbone interaction of the type described by Cairns *et al* and Cheetham and Mashimba, since there is no obvious role for the side chain in such an interaction. The very low intrinsic viscosity for ps.BD9A ie. 8.9 dl/g in 20mM sodium chloride (Table 5.6), suggests that the molecular weight of this polymer was also quite low and this might provide a complete, or partial alternative explanation for the very weak interaction.

The few experiments carried out in this study in the presence of sodium chloride indicated that salt brings about a reduction in gel strength, both in xanthan/locust bean gum and xanthan/konjac mannan mixed systems. Salt might inhibit the interaction between polymers in a number of ways. One way would be to modify the intermolecular behaviour directly by altering the dielectric constant of the medium. Another would be to inhibit a backbone-backbone interaction of the type described by Cairns *et al*, by promoting the ordered helical conformation of xanthan. A third possibility, and the one favoured by the author, is that salt promotes the interaction between xanthan molecules in preference to the xanthan-galactomannan or xanthan-glucomannan interaction. In concentrated solutions, salt has been shown to promote intermolecular association between xanthan molecules, leading to weak gel network formation and enhanced viscosity (section 6.1). Thus, by favouring intermolecular association between xanthan molecules, salt could reduce the gel strength of the system as a whole.

On the basis of the evidence presented in this study it is impossible to decide which of the currently available models for the xanthan-galactomannan interaction is most likely. Different pieces of experimental evidence appear to support different models and much of the

data, for example the apparent inhibitory effect of the acetyl group, cannot be regarded as favouring any one particular type of interaction. No doubt the proponents of each model could find an explanation compatible with their own convictions. This particular worker prefers to remain impartial and to await either more definitive evidence, or until the weight of evidence points more firmly in one direction. It may be that none of the current models is correct. The seemingly contradictory nature of much of the experimental evidence suggests that this might be the case.

One alternative that has been largely ignored in favour of junction zone models is that of a mutual incompatibility between the polymer species. Although no evidence has ever been obtained for gross phase separation, this possibility should not be dismissed out of hand. The fact that certain galactomannans, including locust bean gum, can be induced to gel by freeze-thawing or by lowering the water activity indicates that this polymer at least will form a gel if the concentration of molecules is high enough. It is possible therefore, that by mixing xanthan and locust bean gum the effective concentration of one or both of the materials is raised to above the critical gelling concentration, resulting in gelation. The finding of mixed junction zones in the X-ray fibre diffraction data for mixtures of xanthan and locust bean gum (Cairns *et al*, 1986a, 1987) is not consistent with this explanation but, as has already been pointed out, the need to stretch and dry the fibres prior to X-ray diffraction may well give rise to abnormal behaviour. The X-ray fibre diffraction data for denatured globular proteins has proved misleading for precisely this reason (Clark and Ross-Murphy, 1987). It is, nevertheless, true that incompatibility must be limited to small domain sizes compared to the wavelength of light, otherwise the resultant gels would tend, in the absence of refractive index matching, to be turbid. Most of the gels in this study were, at least relatively, transparent.

All of the models outlined in section 7.4 seem to imply that to interact xanthan, be it in the ordered or disordered state, must be single stranded. Yet the bulk of available evidence (section 1.4) indicates that, at least in the ordered state, xanthan exists predominantly as a double-stranded molecule. This would tend to argue against the models of Dea *et al* (1977) and Tako *et al* (1984). There is, however, mounting evidence to suggest that the ordered conformation can vary depending on the particular polymer, its thermal history and the prevailing environmental conditions. Depending on these factors, xanthan may interact differently in different situations. This may account for some of the apparent contradictions in the experimental data.

As far as the xanthan/konjac mannan interaction is concerned, apart from contradicting the findings of Brownsey *et al* (1988), which indicate that xanthan must be in the disordered state to interact, this study throws little new light on the mechanism of interaction. Compared with the xanthan/galactomannan interaction, that of xanthan with konjac mannan has received very little attention so far. This combined with the apparent irregular structure of the glucomannan makes any detailed speculation difficult, and rather profitless.

Table 7.1: Melting points for xanthan (0.25% $^{W}/_{V}$)/locust bean gum (0.25% $^{W}/_{V}$) gels formed under a variety of conditions (Cheetham and Mashimba, 1988)

Experiment	Melting Point (^{o}C)	Interpretation
1. Xanthan + LBG in cold water. Mix cold.	40	Enough single, non-helical regions are present to allow gelation.
2. Heat[a] and cool gel from Experiment 1.	42	Heating causes rearrangement of xanthan and LBG to allow more favourable interactions.
3. Xanthan + LBG in 0.05M KCl. Mix cold.	Gel islands	Very tight mixed gel forms.
4. Heat and cool Experiment 3.	45	Non-helical xanthan interacts with LBG to form a firm gel on cooling. KCl enhances xanthan-xanthan interactions, and increases melting point.
5. Xanthan + LBG in 0.05M KCl. Heat and cool separately. Mix.	Gel islands	Though the helical form was largely destroyed on heating, it reformed on cooling and gel islands formed as in Experiment 3.
6. Heat and cool Experiment 5.	45	Reasoning as in Experiment 4.
7. Xanthan + LBG in 0.05M KCl. Heat, mix hot, then cool.	45	Non-helical xanthan (at 95^{o}C) cooled in the presence of LBG interacts strongly to yield a firm gel on cooling, as in Experiments 4 and 6.
8. Xanthan + LBG in 0.2M KCl (or 0.1M $CaCl_2$). Mix cold.	Gel islands	As for Experiment 3.
9. Heat and cool Experiment 8.	Gel islands	Xanthan at 95^{o}C retained the ordered helical conformation and therefore failed to form a cohesive gel network upon cooling
10. Take solution from Experiment 3. Dialyse KCl away in stirred cell (without heating).	Firm gel ~40	Removal of KCl gives conditions similar to Experiment 1, and the gel is of similar strength. No exact melting point, as the original volume was not exactly maintained during dialysis.
11. Add solid urea to gel from Experiment 2.	Clumps	Urea destroys the gel, indicating involvement of hydrogen bonds.
12. Heat and cool Experiment 11.	31	Urea stabilises the helical conformation but destabilises the interaction with LBG causing a lower melting point.

N.B. In 50mM KCl T_m is below 95^{o}C. In 0.2M KCl and 0.1M $CaCl_2$ T_m is above 95^{o}C.
a 95^{o}C for 30 minutes.

Table 7.2: Gel "melting temperatures" determined using the falling ball method (gels comprised 0.5% $^{w}/_{w}$ xanthan and 1.0% $^{w}/_{w}$ locust bean gum or konjac mannan).

Xanthan	Melting Point (°C) Xan/LBG	Xan/KM
ps.646	44	58
Kelzan	38	58
ps.1128	33	-
DA ps.1128 (Batch 1)	45	56
ps.PXO_{61}	43	50
ps.556	48	58
Flocon 4800C	43	56
DP Flocon 4800C	41	52

Table 7.3: Effect of autoclaving on the gelling behaviour of 0.5% $^{w}/_{w}$ ps.646 plus 1.0% $^{w}/_{w}$ locust bean gum samples.

Sample	G'	G"	tan δ	G' = G" °C (Setting)	Slope η*
I (autoclaved)	5700	540	0.094	55	-0.93
I (unautoclaved)	4500	480	0.107	51	-0.94
II (autoclaved)	5000	390	0.077	52	-0.93

NB. See text (section 7.10) for details of samples.

Table 7.4: Oscillatory shear measurements made on mixed systems (0.5% $^{w}/_{w}$ xanthan and 1.0% $^{w}/_{w}$ gluco- or galactomannan) in the absence of added salt.

a) The G' = G" values determined upon cooling and reheating the sample are given for the gelling systems, together with the slope of η^* determined from the frequency sweep. For the xanthan/guar gum mixtures the slope of η^* at both high and low frequencies is given, together with the cross-over frequency for G' and G" when present.

Xanthan	% Ac	% Pyr	$[\eta]^a$ (dl/g)	Xan/LBG			Xan/KM			Xan/GG		
				G' = G" (^{o}C/set)	G' = G" (^{o}C/melt)	Slope η^*	G' = G" (^{o}C/set)	G' = G" (^{o}C/melt)	Slope η^*	Slope η^* (LF)	Slope η^* (HF)	Cross-over Frequency (rad/sec)
ps.646	4.5	4.4	34.1	49	50	-0.92	60	60	-0.93	-0.53	-0.77	0.0143
ps.1128	7.7	1.7	79.5	62	63	-0.88	-	-	-0.74 (LF)	-0.54	-0.69	0.082
DA ps.1128 (Batch 1)	1.6	1.3	24.5	46	47	-0.95	56	57	-0.93	-0.73	-0.73	None
DA ps.1128 (Batch 2)	1.5	1.3	22.1	45	48	-0.94	56	56	-0.93	-0.71	-0.77	None
ps.PXO_{61}	14.3	0.3	42.1	43	45	-0.88	61	61	-0.91	-0.59	-0.73	0.27
ps.556	1.6	6.0	53.8	52	53	-0.94	60	62	-0.94	-0.75	-0.84	None
DP ps.556	1.1	1.0	16.4	44	46	-0.93	54	56	-0.92	-0.41	-0.70	0.3
ps.BD9A	2.3	2.0	8.9	37	-	-0.88 (LF) -0.69 (HF)	-	-	-	-	-	-

a Intrinsic viscosity in 20mM NaCl.
LF Determined at low frequencies.
HF Determined at high frequencies.

b) Tan δ, G' and G" values at the start (0 mins, 75°C) and end (85 mins, 25°C) of the cooling sweep (values determined at 10% strain and 10 rad/sec)

Xanthan	Xan/LBG						Xan/KM						Xan/GG					
	tan δ		G'		G"		tan δ		G'		G"		tan δ		G'		G"	
	0	85	0	85	0	85	0	85	0	85	0	85	0	85	0	85	0	85
ps.646	2.2	0.095	36	4300	80	410	2.7	0.106	10.3	3000	26	320	0.86	0.41	540	1350	460	550
ps.1128	1.5	0.25	33	930	49	240	-	-	-	-	-	-	0.97	0.57	370	770	360	440
DA ps.1128 (Batch 1)	2.1	0.049	19	3300	41	160	1.7	0.16	12.6	1100	21	170	0.84	0.47	570	1130	480	530
DA ps.1128 (Batch 2)	3.1	0.049	13	3800	42	180	1.5	0.15	14.6	1140	22	170	1.05	0.39	290	1100	310	420
ps.PXO_{61}	2.1	0.165	35	2200	75	370	2.2	0.11	13.0	1660	27	190	0.98	0.50	430	950	420	480
ps.556	1.3	0.048	57	5100	76	240	1.2	0.075	23.0	2300	28	170	0.76	0.24	610	2050	460	500
DP ps.556	3.5	0.049	11	5200	39	250	1.7	0.11	4.2	930	5.8	107	1.1	0.46	310	990	340	450
ps.BD9A	5.0	0.41	4.0	620	25	250	-	-	-	-	-	-	-	-	-	-	-	-

Table 7.5: Estimation of minimum gelling concentrations for xanthan/locust bean gum and xanthan/konjac mannan mixed systems, in the absence of added salt.

				Gelation						
				Dilution	0	1/2	1/4	1/8	1/16	1/32	1/64
				~% LBG/KM	1.0	0.5	0.25	0.125	0.063	0.031	0.016
				~% Xan	0.5	0.25	0.125	0.063	0.031	0.016	0.008
Xanthan	% Ac	% Pyr	[η]* (dl/g)	System							
ps.646	4.5	4.4	34.1	Xan/LBG	++	++	+	+	+/-	-	-
				Xan/KM	++	+	+/-	-	-	-	-
DA ps.646	1.3	3.6	29.8	Xan/LBG	++	++	+	+	+/-	-	-
				Xan/KM	++	++	+	+/-	-	-	-
DP ps.646	4.4	0.6	15.5	Xan/LBG	++	+	+	+/-	-	-	-
				Xan/KM	++	+/-	-	-	-	-	-
DAP ps.646	1.0	0.6	14.4	Xan/LBG	++	++	+	+	-	-	-
				Xan/KM	++	+	+/-	-	-	-	-
ps.646[a]	7.4	3.6	103.6	Xan/LBG	++	++	+	+	+/-	-	-
				Xan/KM	++	++	+	+/-	-	-	-
Kelzan	6.6	4.8	67.7	Xan/LBG	++	++	+	+	+/-	-	-
				Xan/KM	++	++	+	-	-	-	-
ps.1128	7.7	1.7	79.5	Xan/LBG	+	+	+/-	-	-	-	-
				Xan/KM	-	-	-	-	-	-	-
DA ps.1128 (Batch 1)	1.6	1.3	24.5	Xan/LBG	++	++	+	+	+	+/-	-
				Xan/KM	++	++	+	+/-	-	-	-

Table 7.5: continued.

Xanthan	% Ac	% Pyr	[η]* (dl/g)	Gelation Dilution	0	1/2	1/4	1/8	1/16	1/32	1/64
				~% LBG/KM	1.0	0.5	0.25	0.125	0.063	0.031	0.016
				~% Xan	0.5	0.25	0.125	0.063	0.031	0.016	0.008
				System							
ps.PXO$_{61}$	14.3	0.3	42.1	Xan/LBG	++	+	+	+/-	-	-	-
				Xan/KM	++	+	+/-	-	-	-	-
DA ps.PXO$_{61}$	2.3	0.8	26.8	Xan/LBG	++	++	+	+	+/-	-	-
				Xan/KM	++	+	+/-	-	-	-	-
ps.556	1.6	6.0	53.8	Xan/LBG	++	++	++	+	+	+/-	-
				Xan/KM	++	+	+/-	-	-	-	-
DP ps.556	1.1	1.0	16.4	Xan/LBG	++	++	+	+	+/-	-	-
				Xan/KM	++	+	+/-	-	-	-	-
Flocon 4800C	2.0	4.9	28.4	Xan/LBG	++	++	+	+	+/-	-	-
				Xan/KM	++	+	+/-	-	-	-	-
DP Flocon 4800C	2.7	1.0	10.5	Xan/LBG	++	++	+	+	+/-	-	-
				Xan/KM	++	+	+/-	-	-	-	-

NB. The criteria used for estimating gel strength are given in table 2.3.
a Polymer produced by strain 646 in continuous culture under conditions of potassium limitation and at a dilution rate of 0.120/hr.
* Intrinsic viscosity in 20mM sodium chloride.

Table 7.6: Estimation of minimum gelling concentration for xanthan/locust bean gum and xanthan/konjac mannan mixed systems in the presence and absence of sodium chloride.

						Gelation						
				Dilution		0	1/2	1/4	1/8	1/16	1/32	1/64
				~% LBG/KM		1.0	0.5	0.25	0.125	0.063	0.031	0.016
				~% Xan		0.5	0.25	0.125	0.063	0.031	0.016	0.008
Xanthan	% Ac	% Pyr	[η] (dl/g)	System	NaCl Conc (mM)							
ps.646	4.5	4.4	34.1	Xan/LBG	0	++	++	+	+	+/-	-	-
				Xan/LBG	50	++	++	+	+/-	-	-	-
				Xan/KM	0	++	+	+/-	-	-	-	-
				Xan/KM	20	+	+	-	-	-	-	-
				Xan/KM	50	+	+/-	-	-	-	-	-
ps.1128	7.7	1.7	79.5	Xan/LBG	0	+	+	+/-	-	-	-	-
				Xan/LBG	50	-	-	-	-	-	-	-
				Xan/KM	0	-	-	-	-	-	-	-
				Xan/KM	50	-	-	-	-	-	-	-
ps.556	1.6	6.0	53.8	Xan/LBG	0	++	++	++	+	+	+/-	-
				Xan/LBG	50	++	++	+	+	+/-	-	-
				Xan/KM	0	++	+	+/-	-	-	-	-
				Xan/KM	50	++	+	+/-	-	-	-	-

Table 7.7: Correlation matrix relating acetyl, pyruvate and intrinsic viscosity to gel strength in mixed xanthan (0.5% $^{w}/_{w}$)/locust bean gum (1.0% $^{w}/_{w}$) systems.

a) All samples are included in the analysis.

	% Ac	% Pyr	Intrinsic Viscosity (dl/g)	tan δ	tan δ Ratio	G'	G' ratio	Slope η^*
% Ac	1.000	-0.358	0.444	0.753	-0.710	-0.696	0.584	0.896
% Pyr	-0.358	1.000	0.271	-0.258	-0.242	-0.485	-0.318	-0.318
Intrinsic viscosity (dl/g)	0.444	0.271	1.000	0.797	-0.827	-0.629	-0.774	0.643
tan δ	0.753	-0.258	0.797	1.000	-0.766	-0.883	-0.618	0.931
tan δ Ratio	-0.710	-0.242	-0.827	-0.766	1.000	0.646	0.950	-0.708
G'	-0.696	0.485	-0.629	-0.883	0.646	1.000	0.605	-0.757
G' Ratio	-0.584	-0.318	-0.774	-0.618	0.950	0.605	1.000	-0.514
Slope η^*	0.896	-0.318	0.643	0.931	-0.708	-0.757	-0.514	1.000

b) Data for ps.PXO_{61} is omitted from the analysis.

	% Ac	% Pyr	Intrinsic Viscosity (dl/g)	tan δ	tan δ Ratio	G'	G' ratio	Slope η^*
% Ac	1.000	0.019	0.799	0.965	-0.812	-0.804	-0.657	-0.939
% Pyr	0.019	1.000	0.329	-0.126	-0.491	0.387	-0.527	-0.086
Intrinsic viscosity (dl/g)	0.799	0.329	1.000	0.832	-0.875	-0.655	-0.798	-0.764
tan δ	0.965	-0.126	0.832	1.000	-0.728	-0.865	-0.568	0.962
tan δ Ratio	-0.812	-0.491	-0.875	-0.728	1.000	0.582	0.947	-0.641
G'	-0.804	0.387	-0.655	-0.865	0.582	1.000	0.551	-0.716
G' Ratio	-0.657	-0.527	-0.798	-0.568	0.947	0.551	1.000	-0.424
Slope η^*	0.939	-0.086	0.764	0.962	-0.641	-0.716	-0.424	1.000

Table 7.8: Correlation matrix relating acetyl, pyruvate and intrinsic viscosity to gel strength in mixed xanthan (0.5% $^{W}/_{W}$)/konjac mannan (1.0% $^{W}/_{W}$) systems.

a) All samples are included in the analysis.

	% Ac	% Pyr	Intrinsic Viscosity (dl/g)	tan δ	tan δ Ratio	G'	G' ratio	Slope η^*
% Ac	1.000	-0.358	0.444	0.278	0.122	-0.041	-0.133	0.371
% Pyr	-0.358	1.000	0.271	-0.124	0.333	0.673	0.235	-0.225
Intrinsic viscosity (dl/g)	0.444	0.271	1.000	0.814	-0.435	-0.227	-0.550	0.788
tan δ	0.278	-0.124	0.814	1.000	-0.734	-0.640	-0.585	0.991
tan δ Ratio	0.122	0.333	-0.435	-0.734	1.000	0.891	0.862	-0.707
G'	-0.041	0.673	-0.227	-0.640	0.891	1.000	0.689	-0.669
G' Ratio	-0.133	0.235	-0.550	-0.585	0.862	0.689	1.000	-0.561
Slope η^*	0.371	-0.225	0.788	0.991	-0.707	-0.669	-0.561	1.000

b) Data for ps.PXO_{61} is omitted from the analysis.

	% Ac	% Pyr	Intrinsic Viscosity (dl/g)	tan δ	tan δ Ratio	G'	G' ratio	Slope η^*
% Ac	1.000	0.019	0.799	0.881	-0.366	-0.254	-0.258	0.874
% Pyr	0.019	1.000	0.329	-0.216	0.552	0.788	0.255	-0.278
Intrinsic viscosity (dl/g)	0.799	0.329	1.000	0.838	-0.485	-0.235	-0.551	0.795
tan δ	0.881	-0.216	0.838	1.000	-0.730	-0.636	-0.594	0.997
tan δ Ratio	-0.366	0.552	-0.485	-0.730	1.000	0.915	0.917	-0.730
G'	-0.254	0.788	-0.235	-0.636	0.915	1.000	0.693	-0.667
G' Ratio	-0.258	-0.255	-0.551	-0.594	0.917	0.693	1.000	-0.563
Slope η^*	0.874	-0.278	0.795	0.997	-0.730	-0.667	-0.563	1.000

Table 7.9: Correlation matrices relating gel strength to the helix-coil transition midpoint.

a) Xanthan/Locust bean gum mixed systems.

	tan δ	G'	Slope η^*	T_m (^oC)
tan δ	1.000	-0.904	0.924	0.975
G'	-0.904	1.000	-0.774	-0.937
Slope η^*	0.924	-0.774	1.000	0.909
T_m (^oC)	0.975	-0.937	0.909	1.000

b) Xanthan/Konjac mannan mixed systems.

	tan δ	G'	Slope η^*	T_m (^oC)
tan δ	1.000	-0.680	0.991	0.778
G'	-0.680	1.000	-0.715	-0.522
Slope η^*	0.991	-0.715	1.000	0.840
T_m (^oC)	0.778	-0.522	0.840	1.000

Fig. 7·1 Junction zone models for three algal polysaccharides

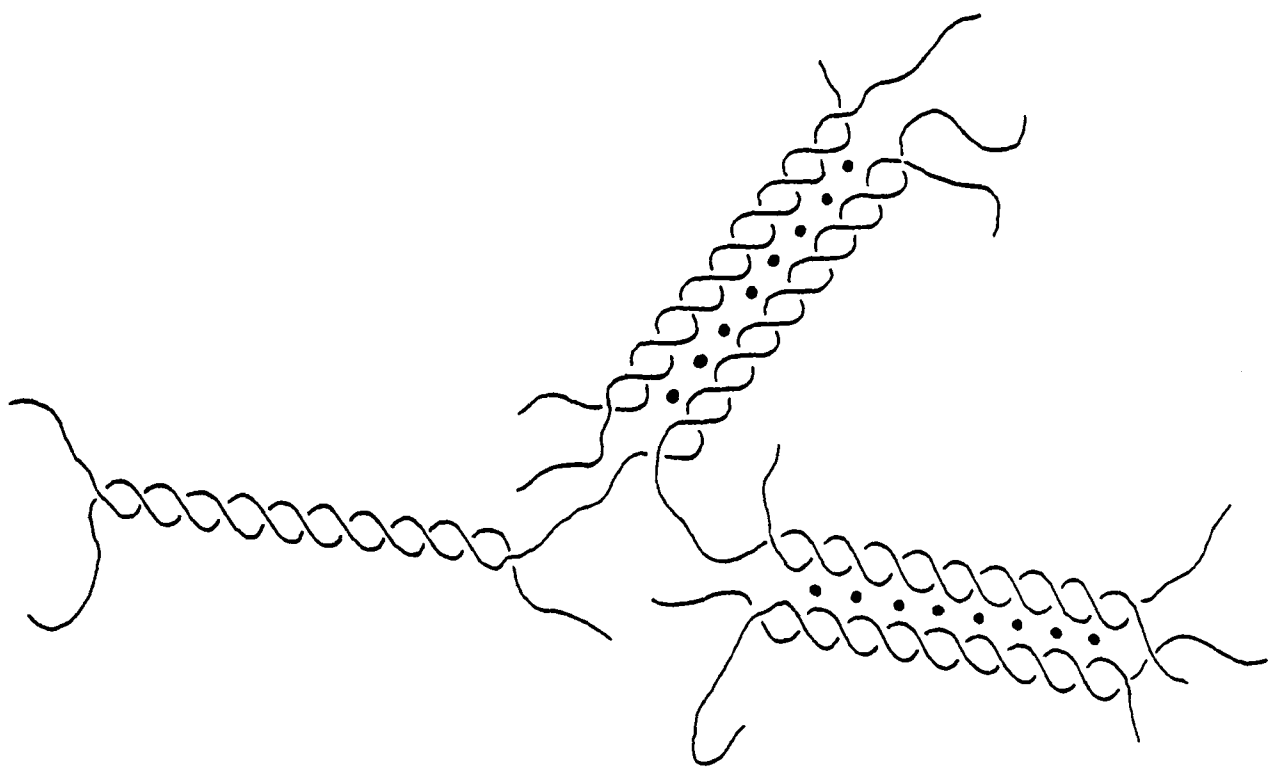

a) Iota-carrageenan: cross links involve double helix formation and limited association of double helices, with possible counterion involvement (Morris et al, 1980).

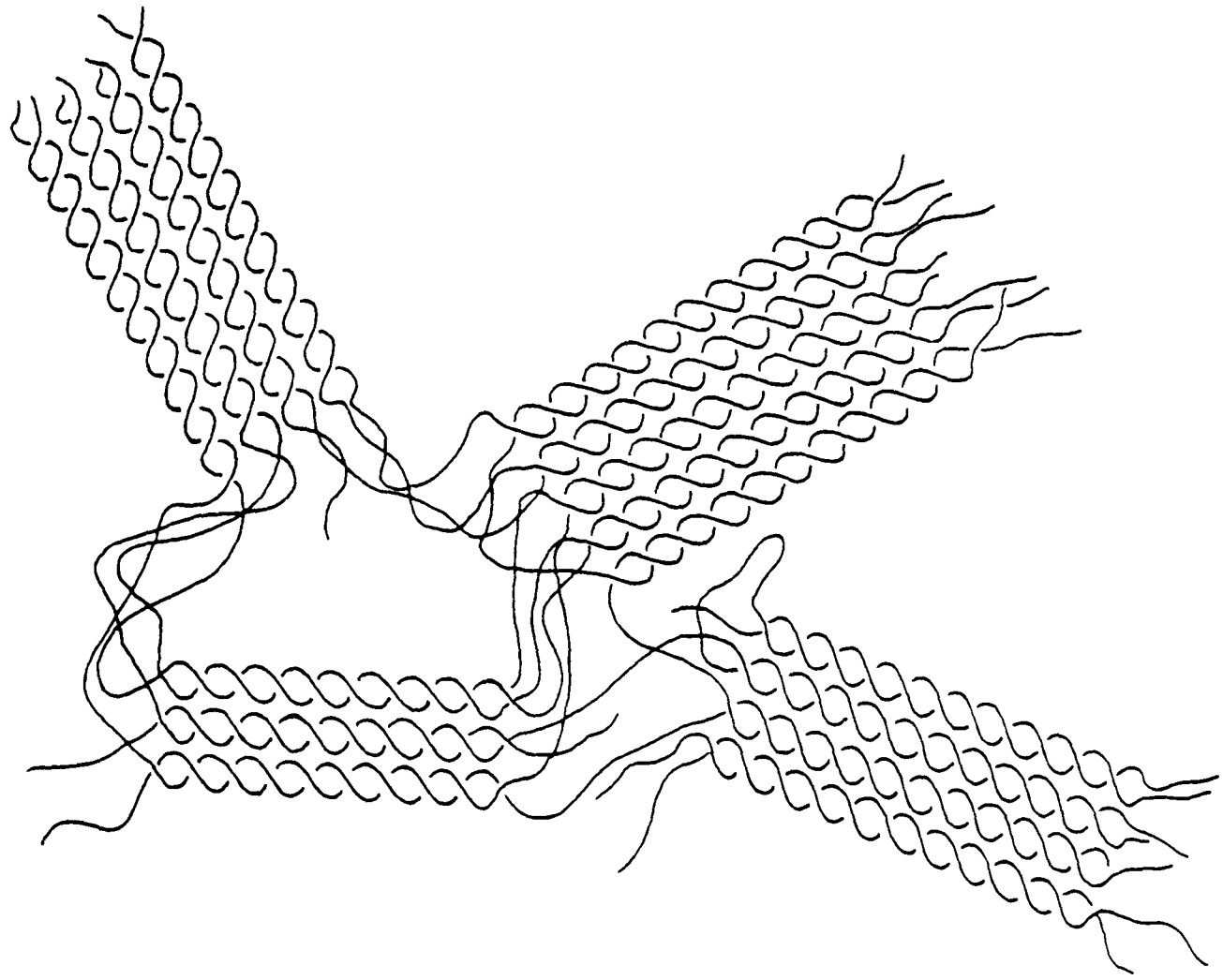

b) Agarose: cross links involve both double helix formation and substantial association of double helices to form microcrystalline junction zones.

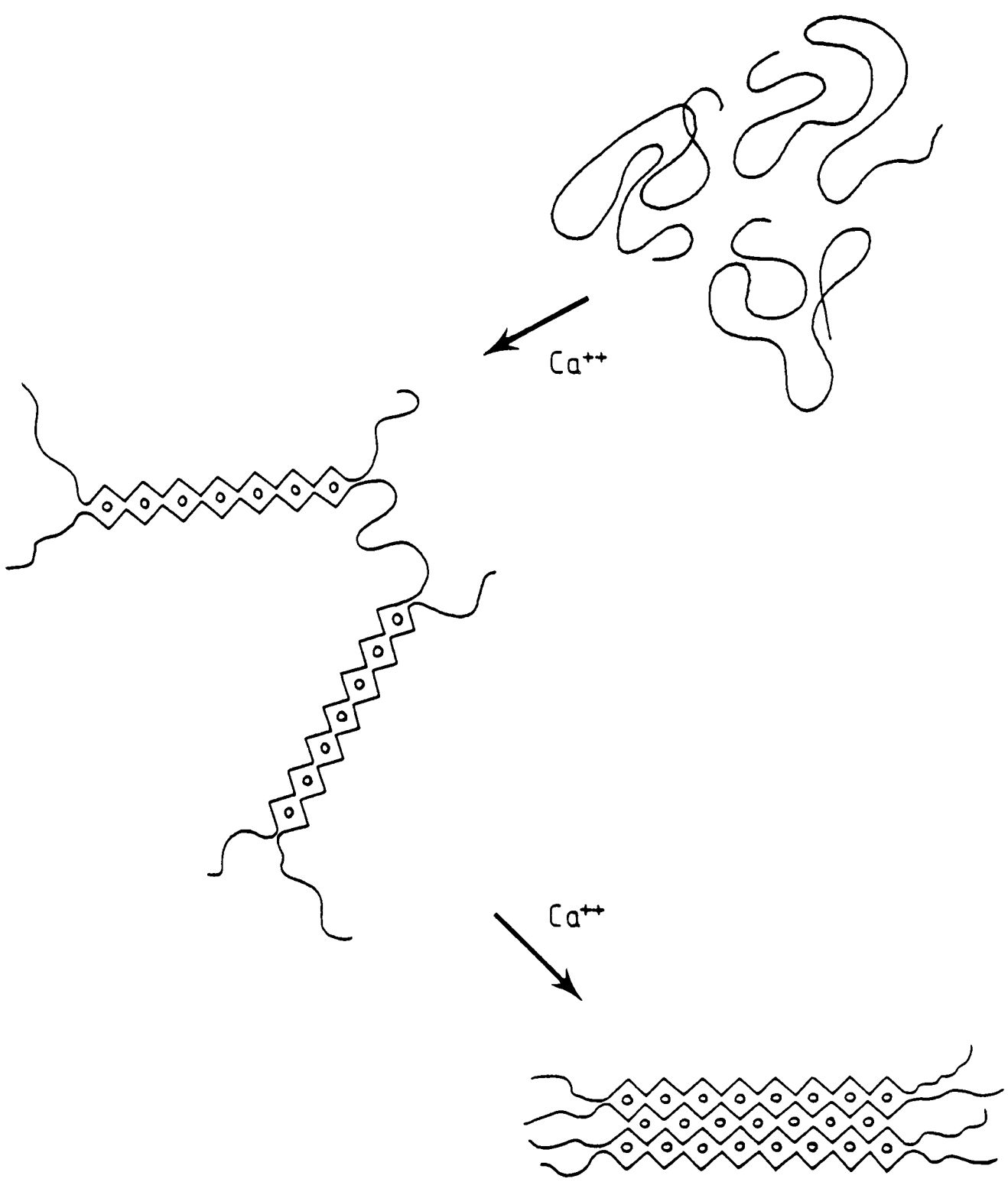

c) Alginate - "egg-box" model: cross links involve lateral association of guluronate sequences to form ordered junction zones. Ca^{++} ions occupy electronegative cavities within the structure.

(a)

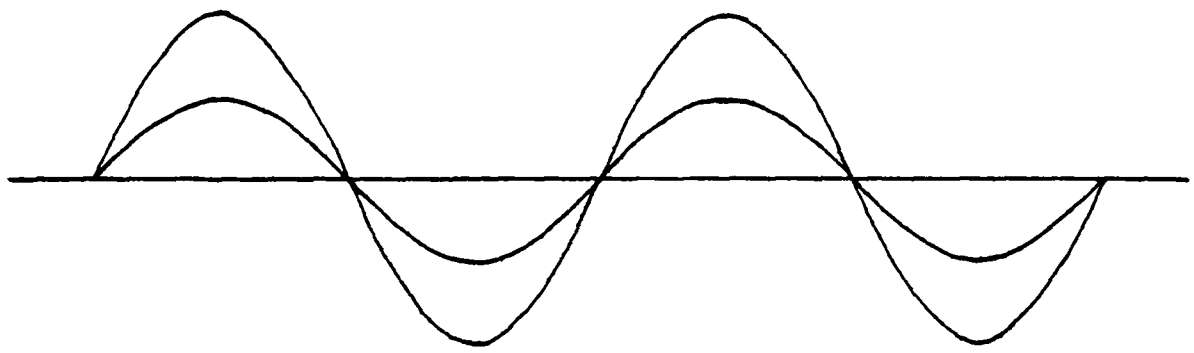

$$G' = \frac{\text{In-phase stress}}{\text{Applied strain}}$$

(b)

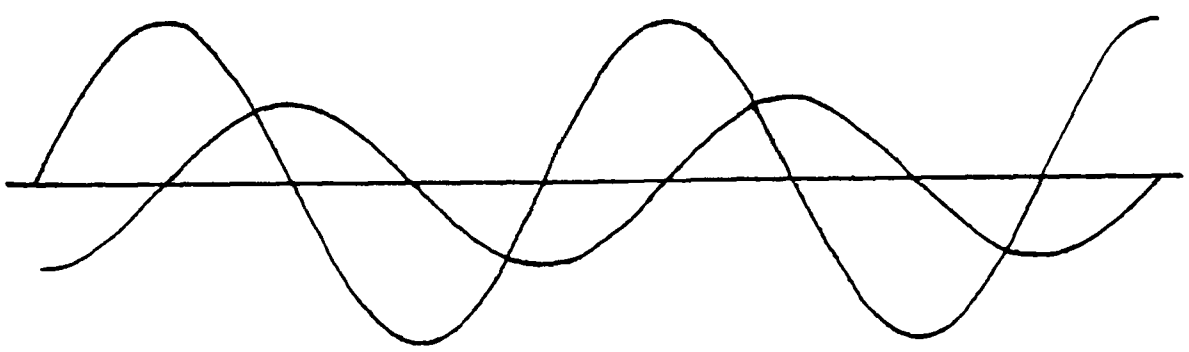

$$G'' = \frac{\text{90° Out-of-phase stress}}{\text{Applied strain}}$$

Fig. 7·2 Applied oscillatory (sinusoidal) strain wave and resultant stress wave for (a) a perfect solid and (b) a Newtonian liquid.

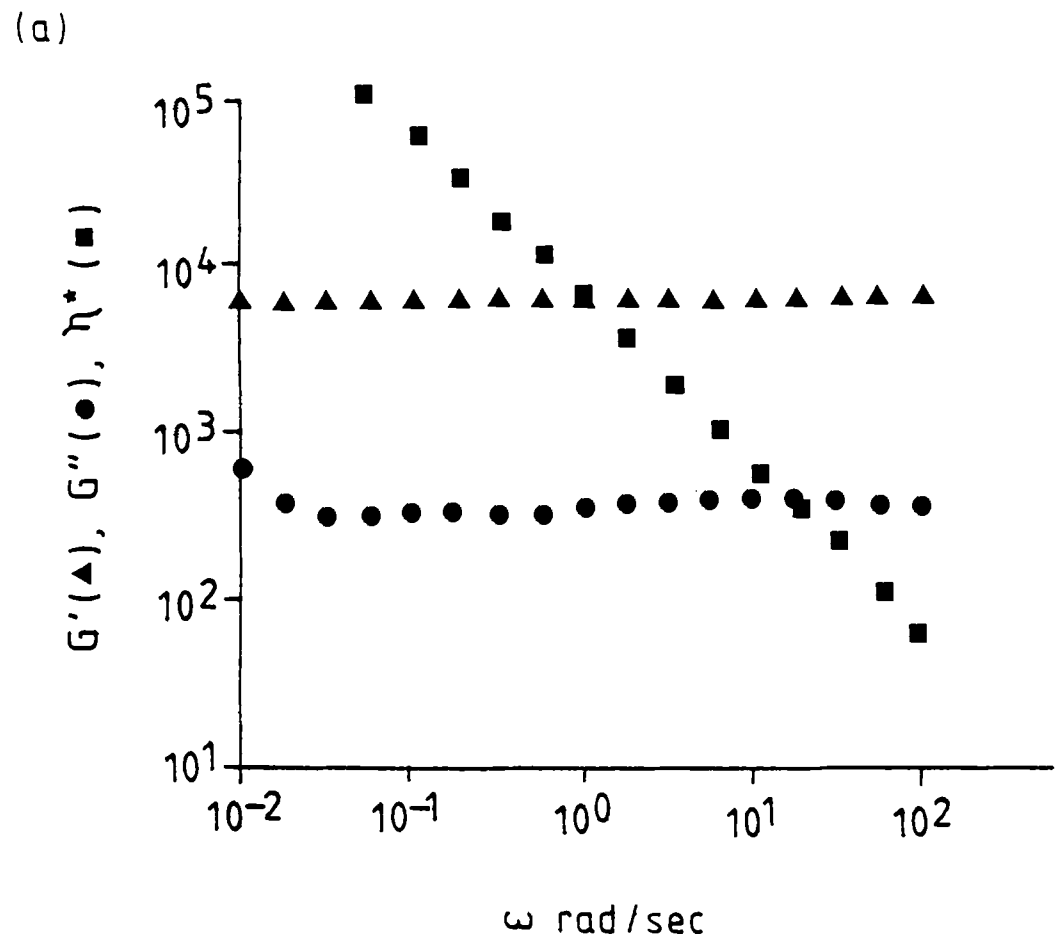

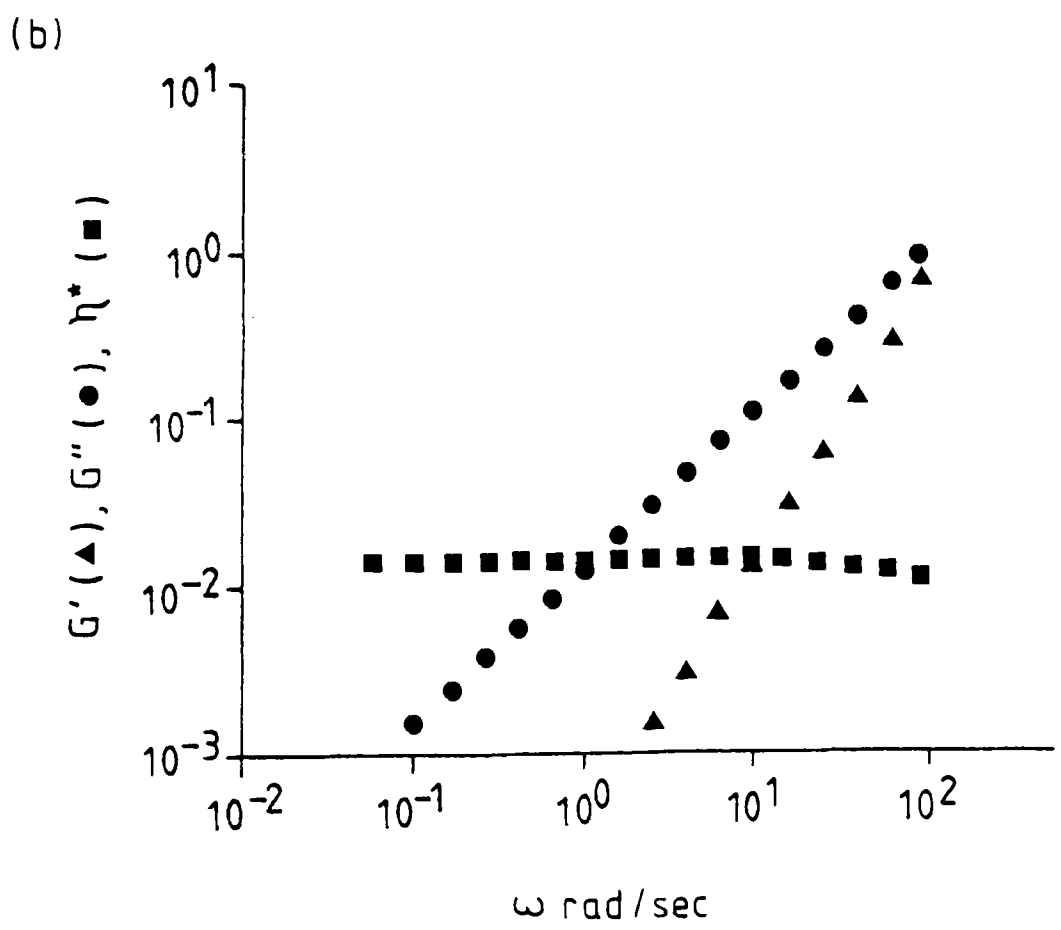

Fig. 7·3 Mechanical spectra for (a) an elastic gel (agarose) and (b) a Newtonian liquid (dextran). Morris and Ross-Murphy, 1981.

Fig. 7·4 Junction zone models for the xanthan - galactomannan interaction.

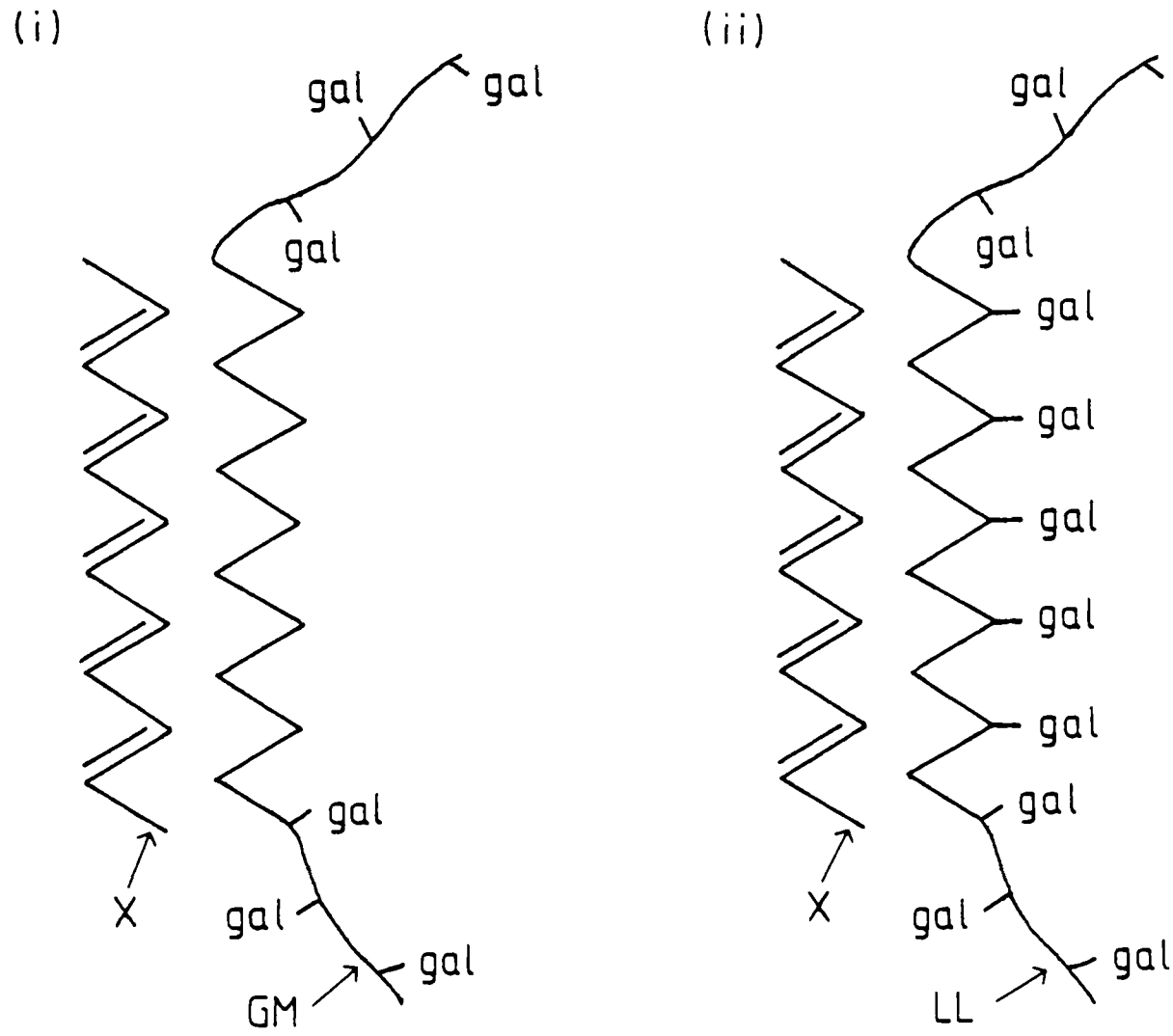

(a) Interaction between the xanthan helix and (i) unsubstituted regions of the galactomannan backbone, (ii) regions of the galactomannan backbone substituted on one side only. (Dea et al, 1977).

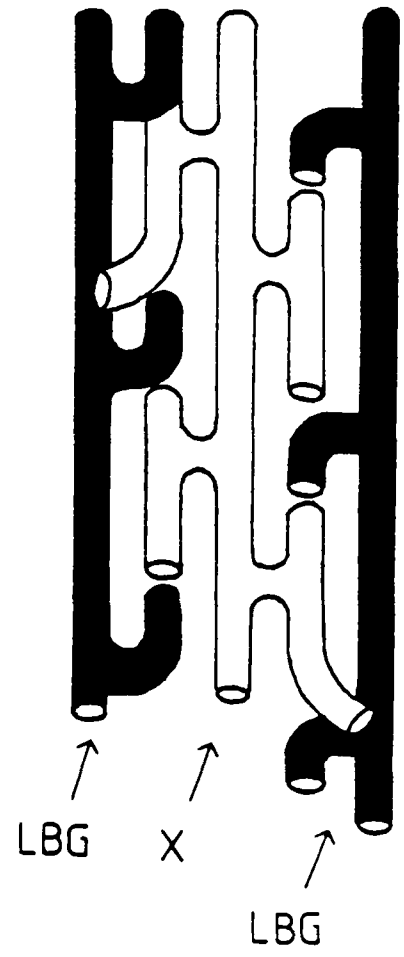

(b) Lock and key model - insertion of the xanthan side-chains into adjacent unsubstituted regions of the galactomannan backbone (Tako et al, 1984)

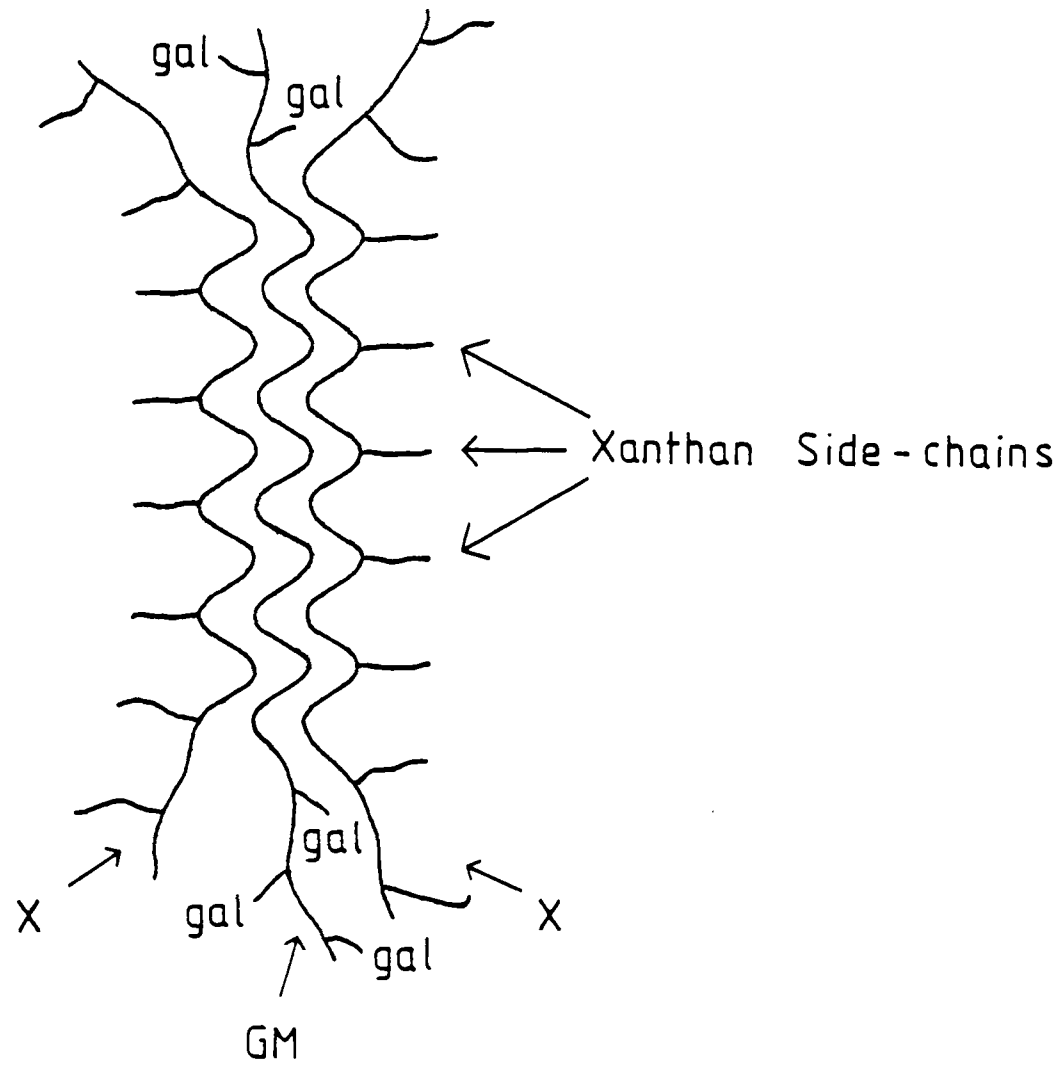

(c) Sandwich structure - bare mannan backbone sandwiched between two xanthan backbones (Cairns et al, 1986a).

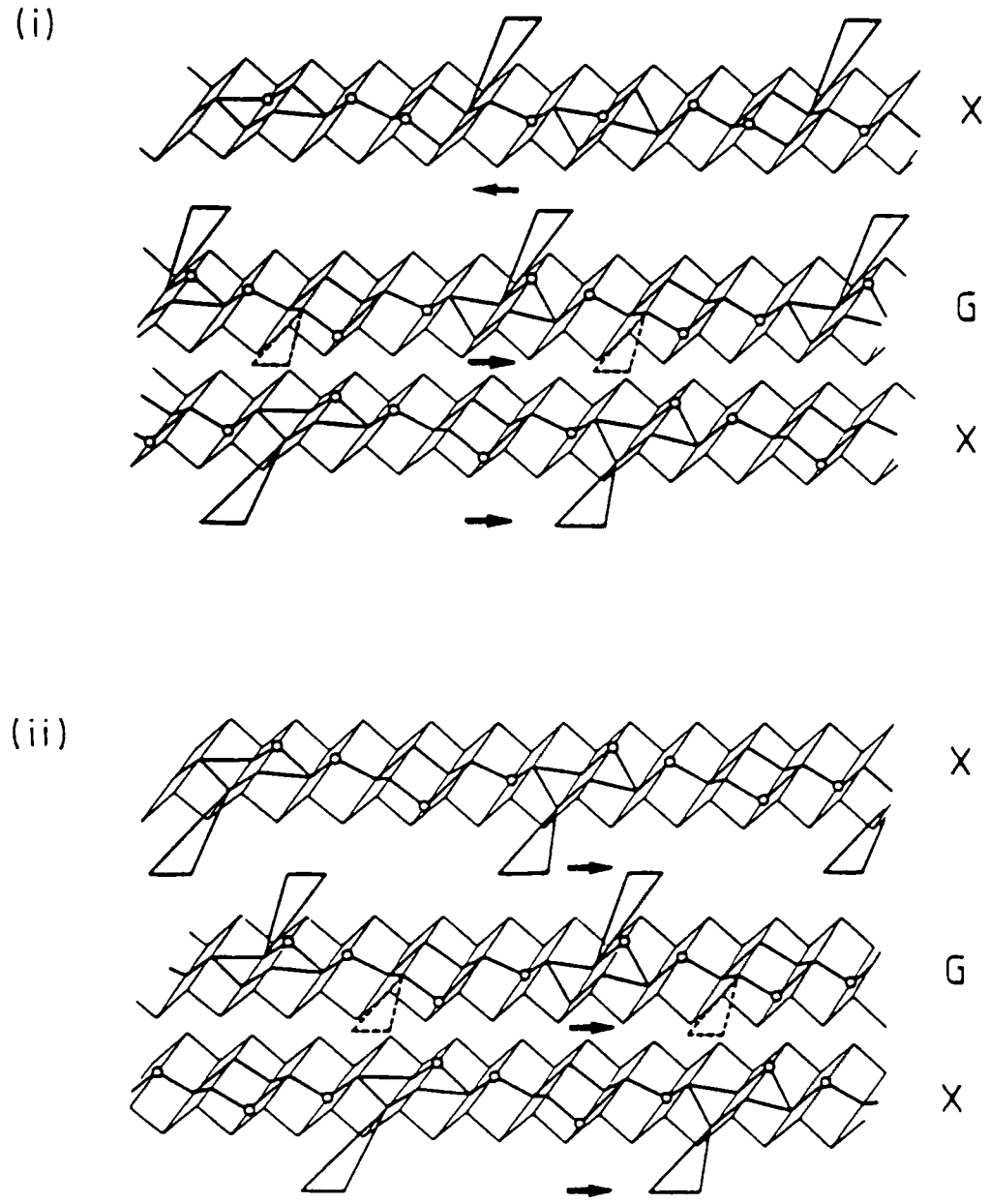

(d) Galactomannan backbone (substituted on one face only) is sandwiched between two xanthan backbones. The chains are in the ribbon conformation and the chain directions are shown by arrows. (i) The xanthan side-chains (triangles) are staggered and are arranged on opposite faces of the two molecules. (ii) The xanthan side-chains remain staggered but are arranged on the same face and could interact with the side-chains on the xanthan molecule below. Full substitution of the galactomannan chain (solid plus dotted triangles) is not accommodated because of steric interactions with the xanthan side-chains (Cheetham and Mashimba, 1988).

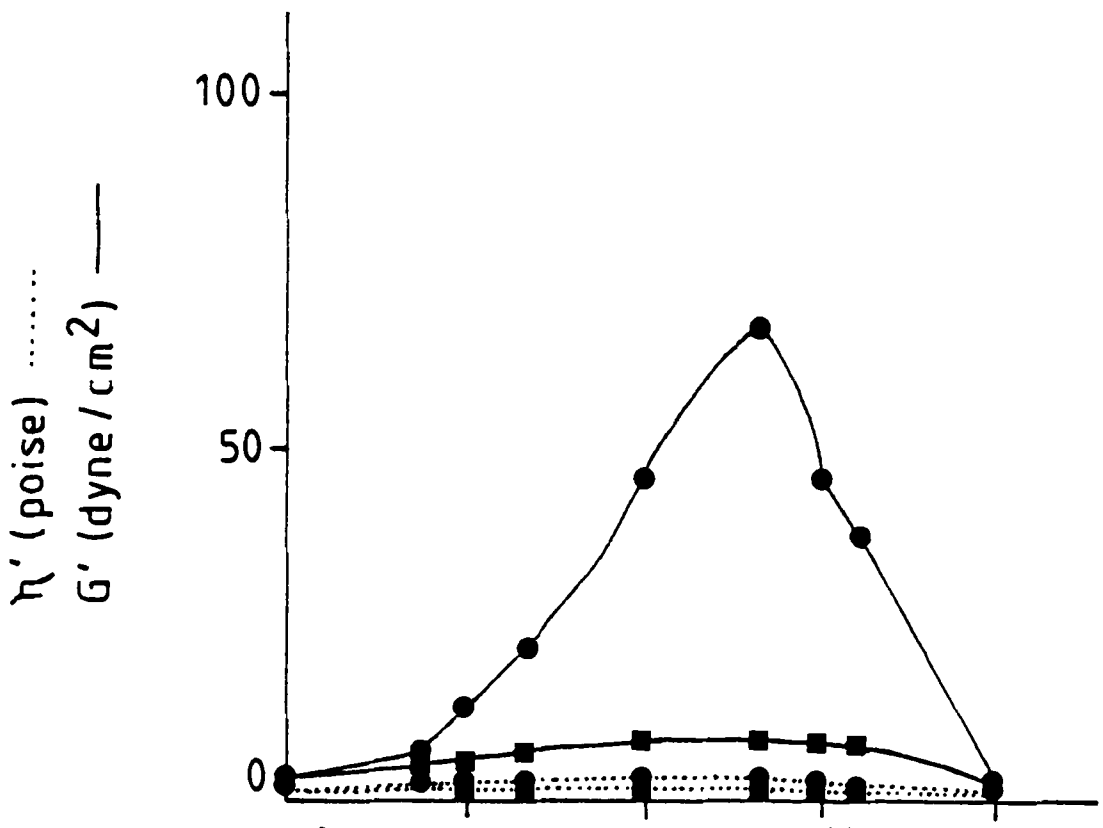

Fig. 7·5 Dynamic viscoelasticity (at 3·768 rad/sec and 25°C) of 0·2% xanthan-guar gum solutions as a function of the ratio of the components: native xanthan (■); deacetylated xanthan (●); (Tako and Nakamura, 1985)

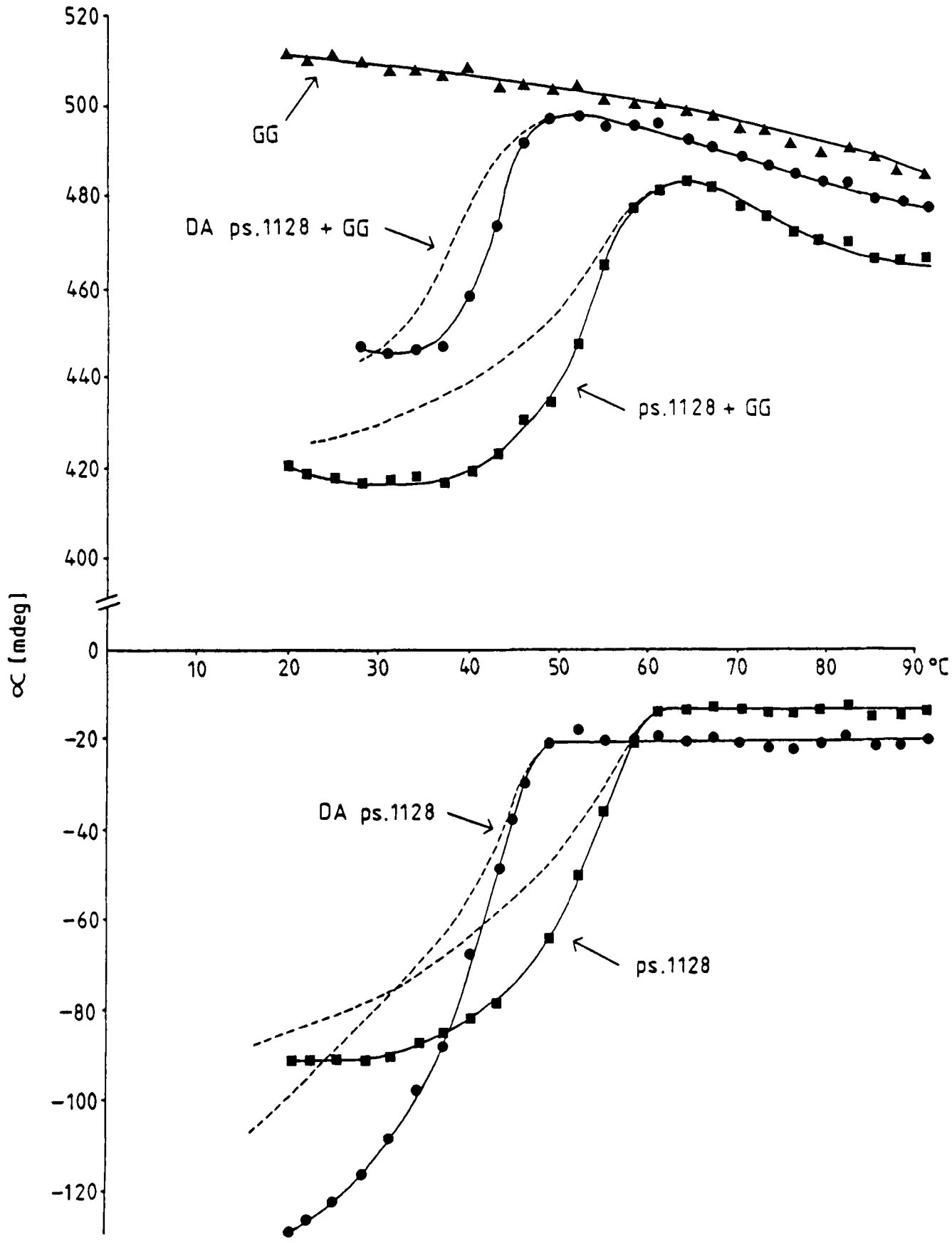

Fig. 7·6 Heating (—) and cooling (---) curves, as monitored by optical rotation, for xanthan (0·2%), guar gum (0·4%) and mixtures of the two.

Fig. 7·7 The Rheometrics Mechanical Spectrometer (RMS - 605)

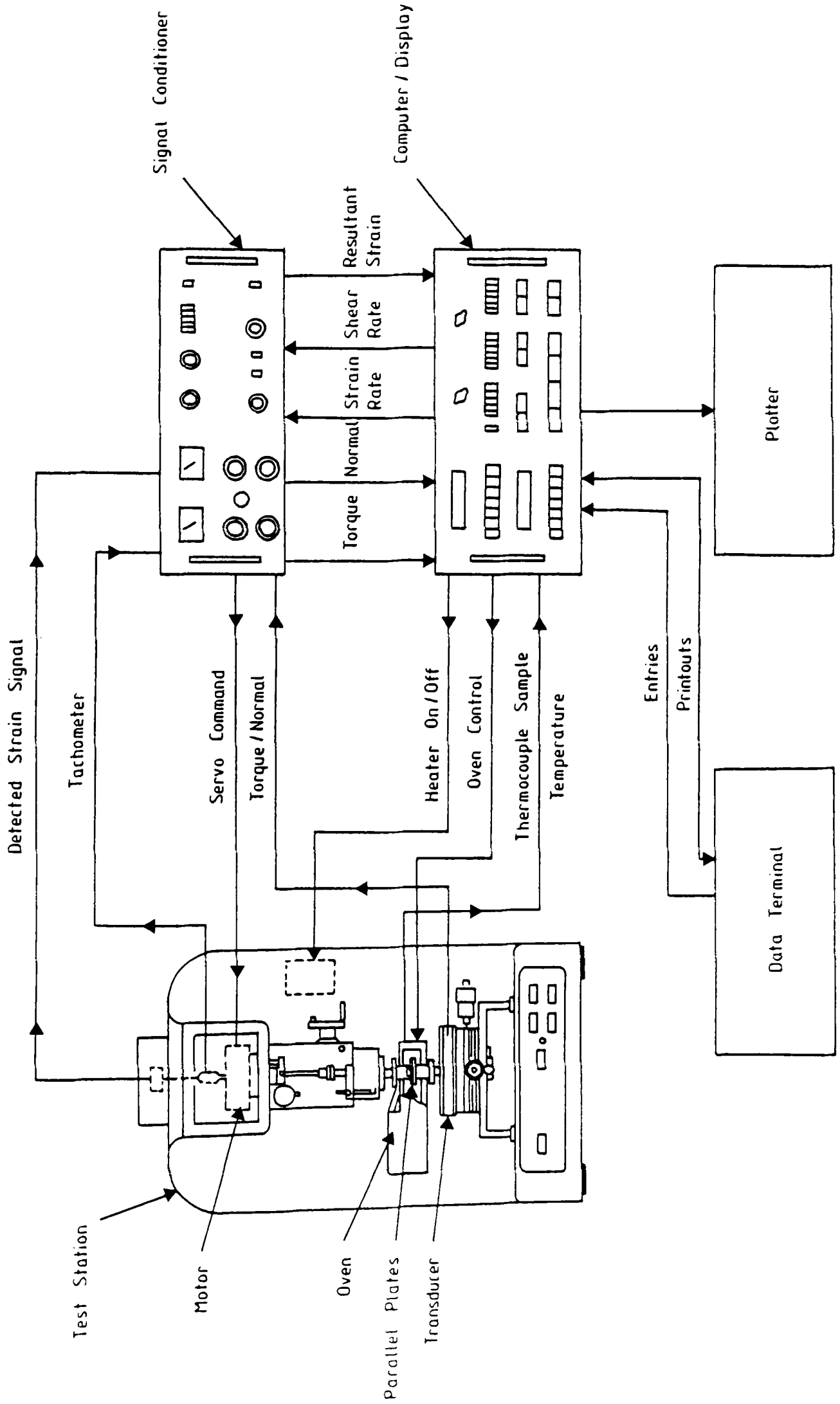

Fig. 7·8 Block diagram of the Rheometrics Mechanical Spectrometer (RMS - 605)

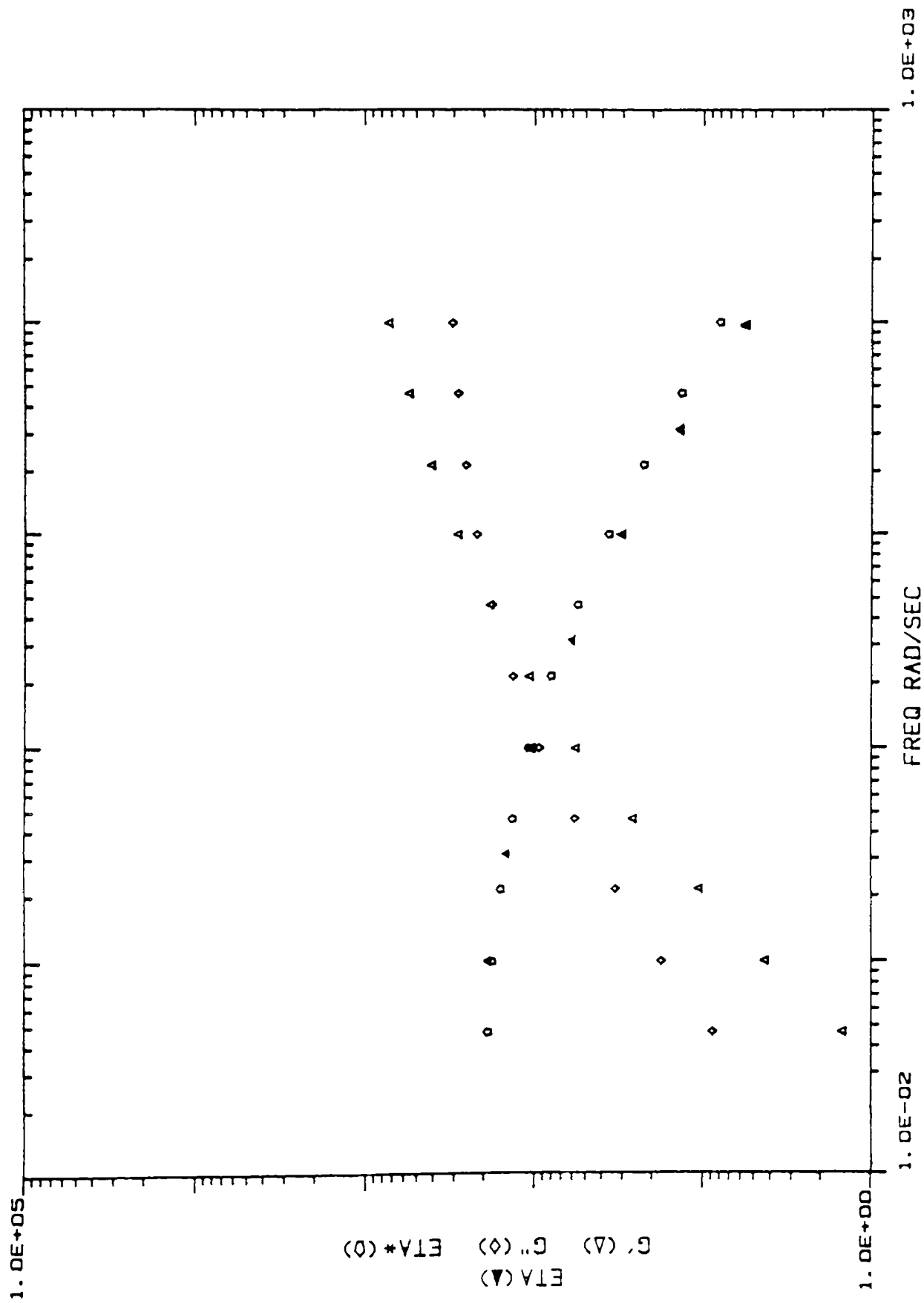

Fig. 7.9 Steady and oscillatory shear measurements for the galacto- and glucomannans.

a) Cox-Merz plot for 1·0% guar gum in deionized water.

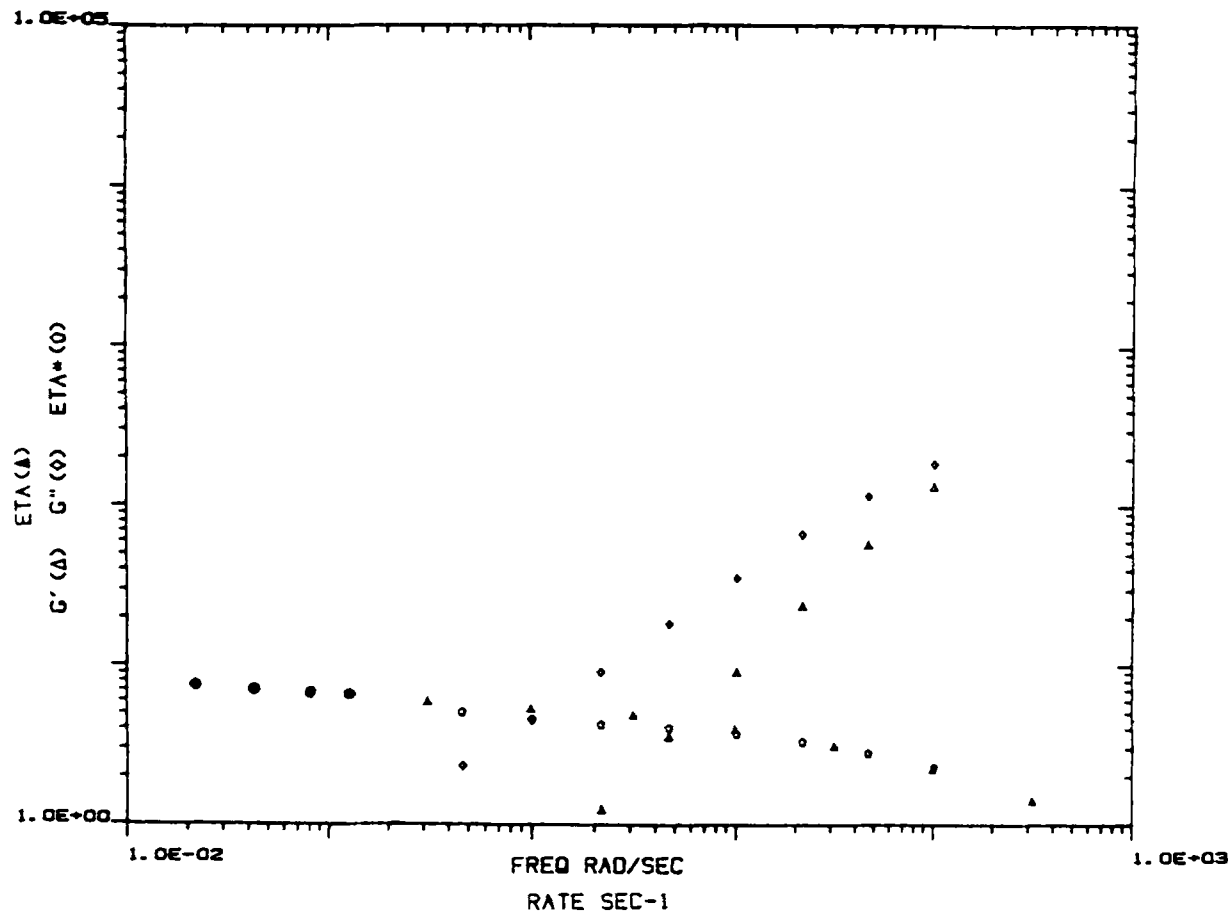

b) Cox - Merz plot for 1·0% locust bean gum in deionized water. Measurements of Eta made using the Contraves LS30 (●).

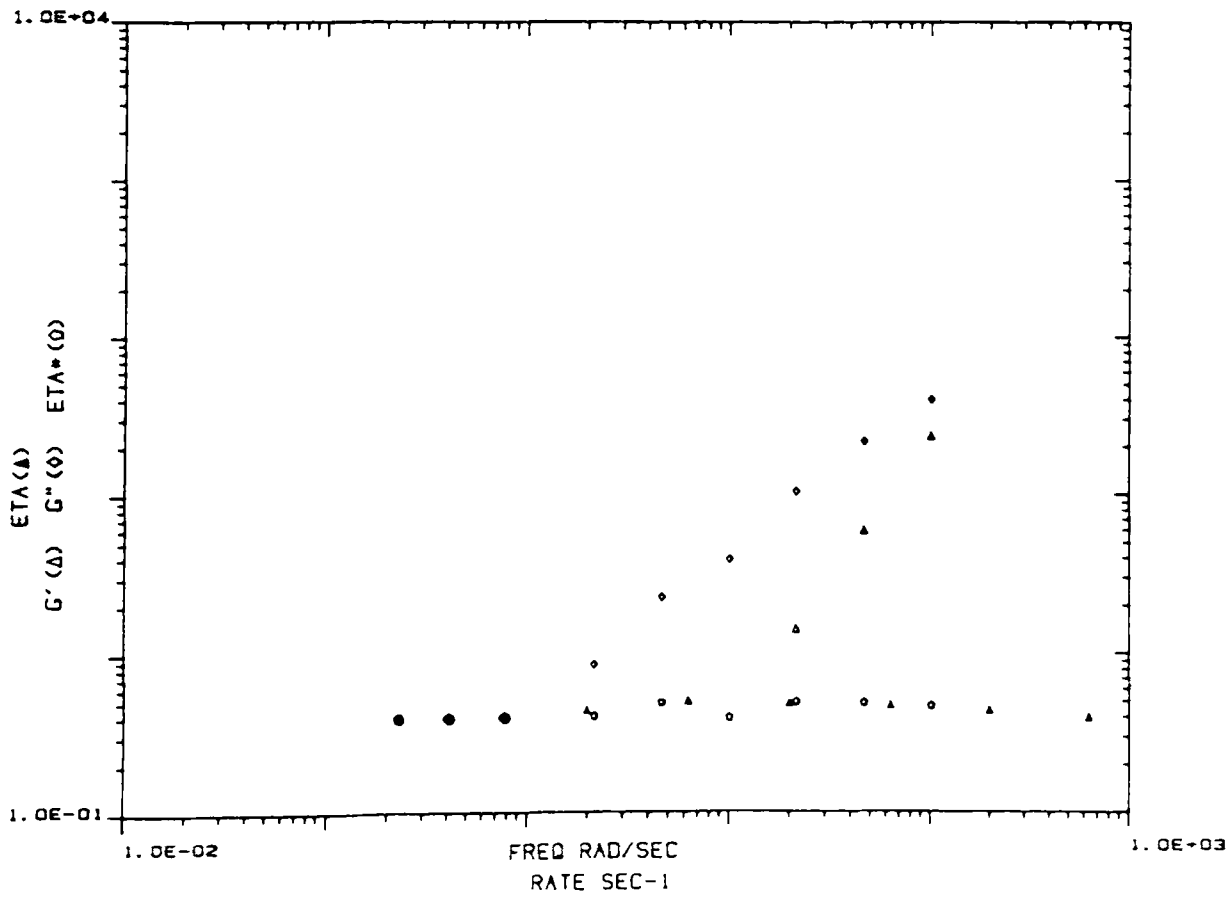

c) Cox - Merz plot for 1·0% konjac mannan in deionized water. Measurements of Eta made using the Contraves LS30 (●).

Fig. 7·10 Steady and oscillatory shear measurements for xanthan.

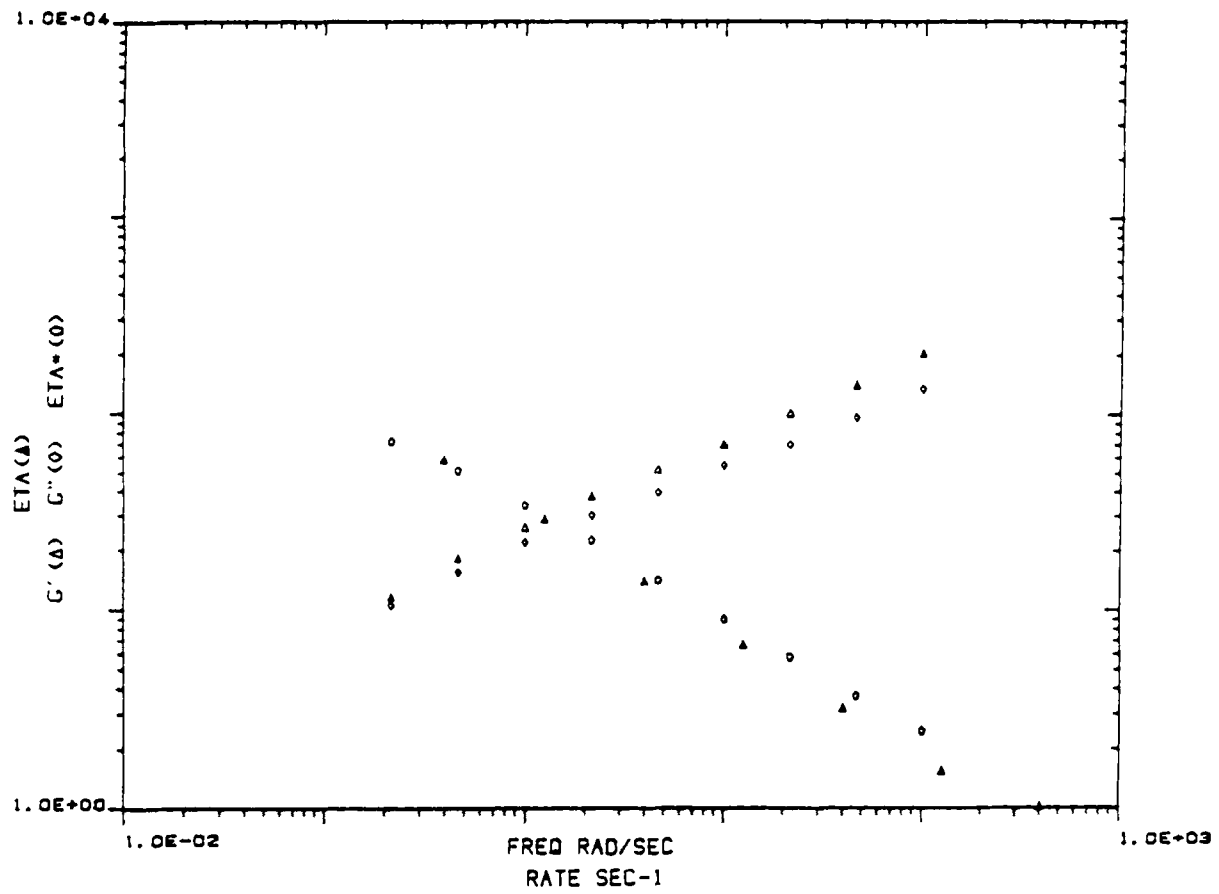

a) Cox - Merz plot for 2·0% ps.646 in deionized water.

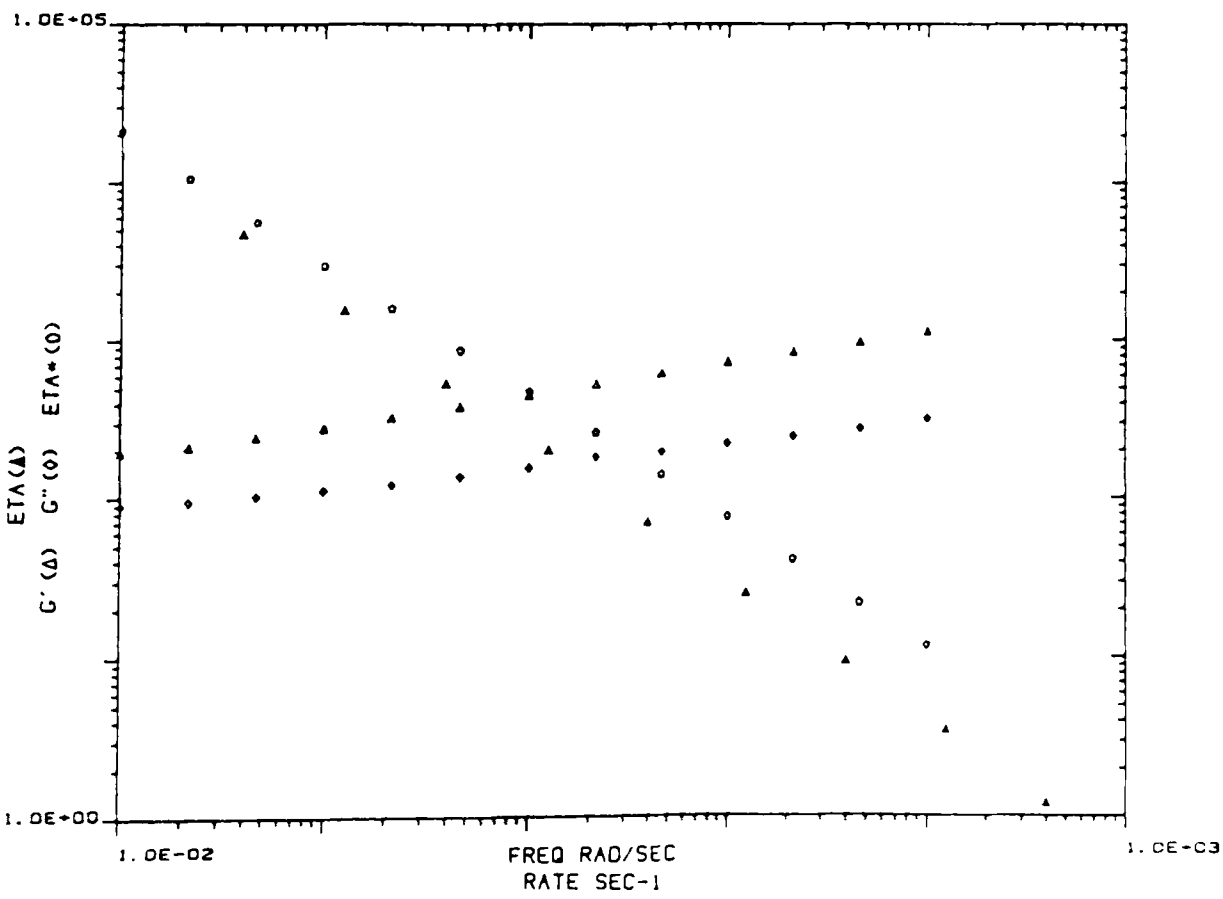

b) Cox - Merz plot for 2·0% ps.646 in 20 mM sodium chloride.

Fig. 7.11 Oscillatory shear measurements for xanthan/locust bean gum mixed systems in deionized water.

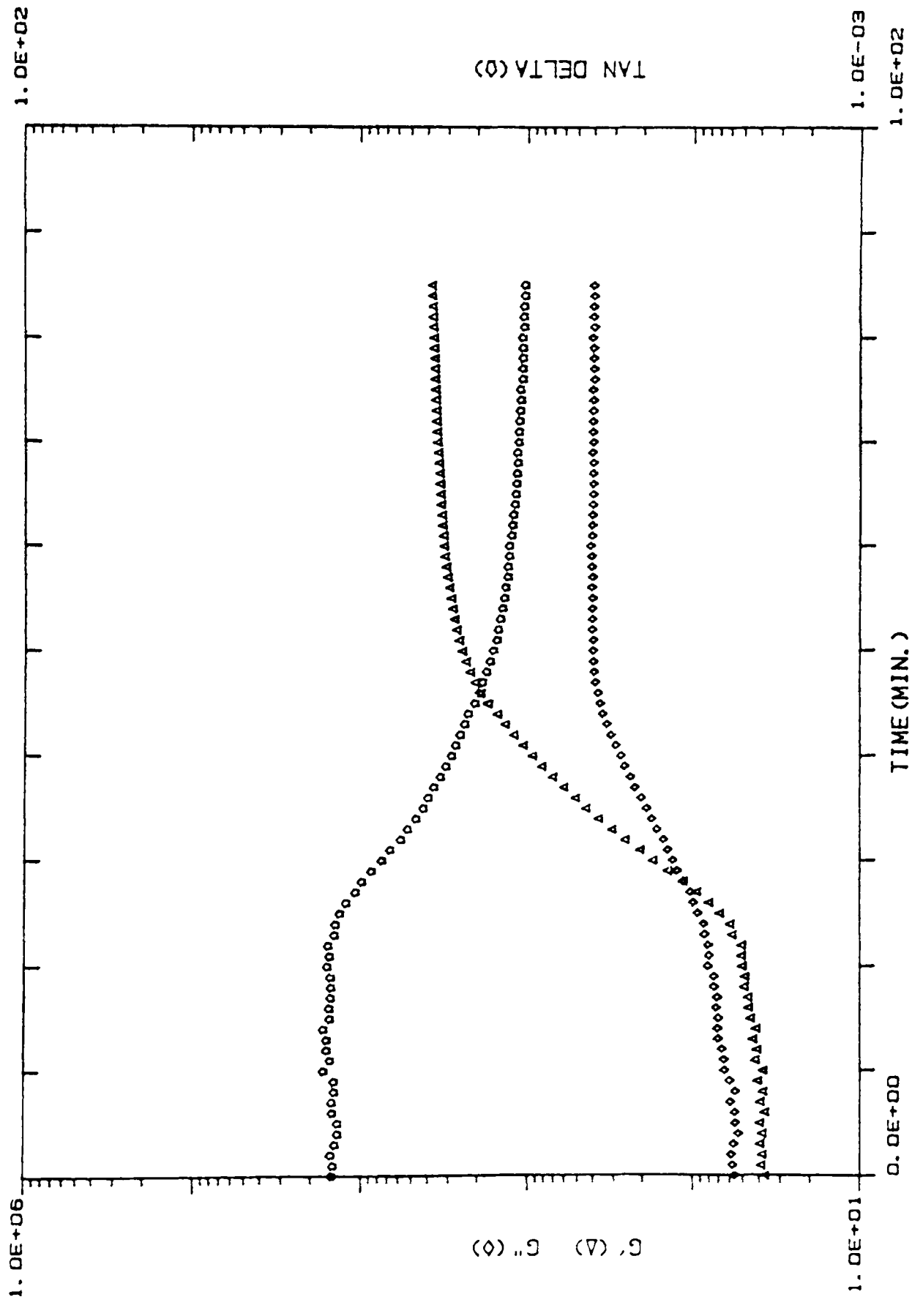

a) Temperature sweep (cooling) for a mixture of 0.5% ps.646 and 1.0% locust bean gum.

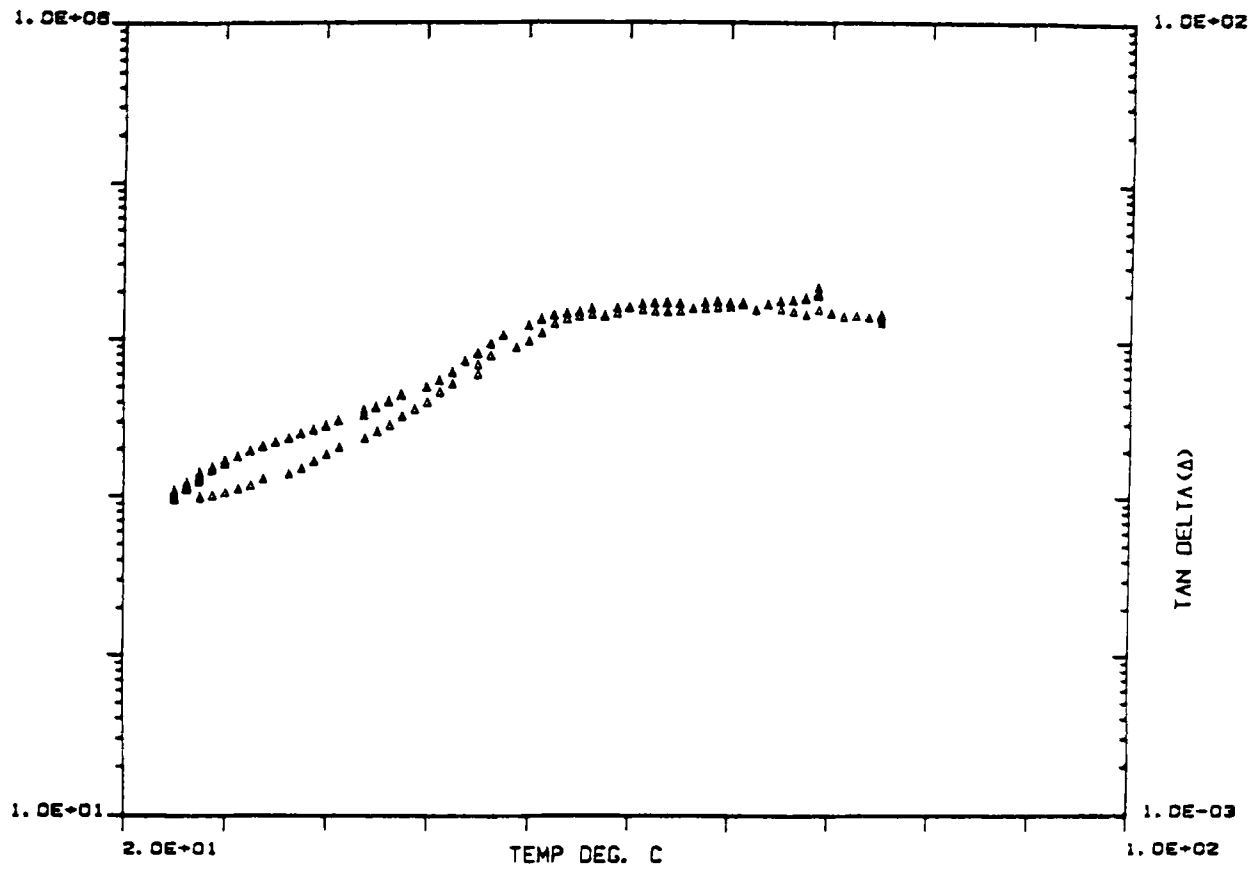

b) Temperature sweep (cooling [▲] and reheating [△]) for a mixture of 0·5% ps.646 and 1·0% locust bean gum.

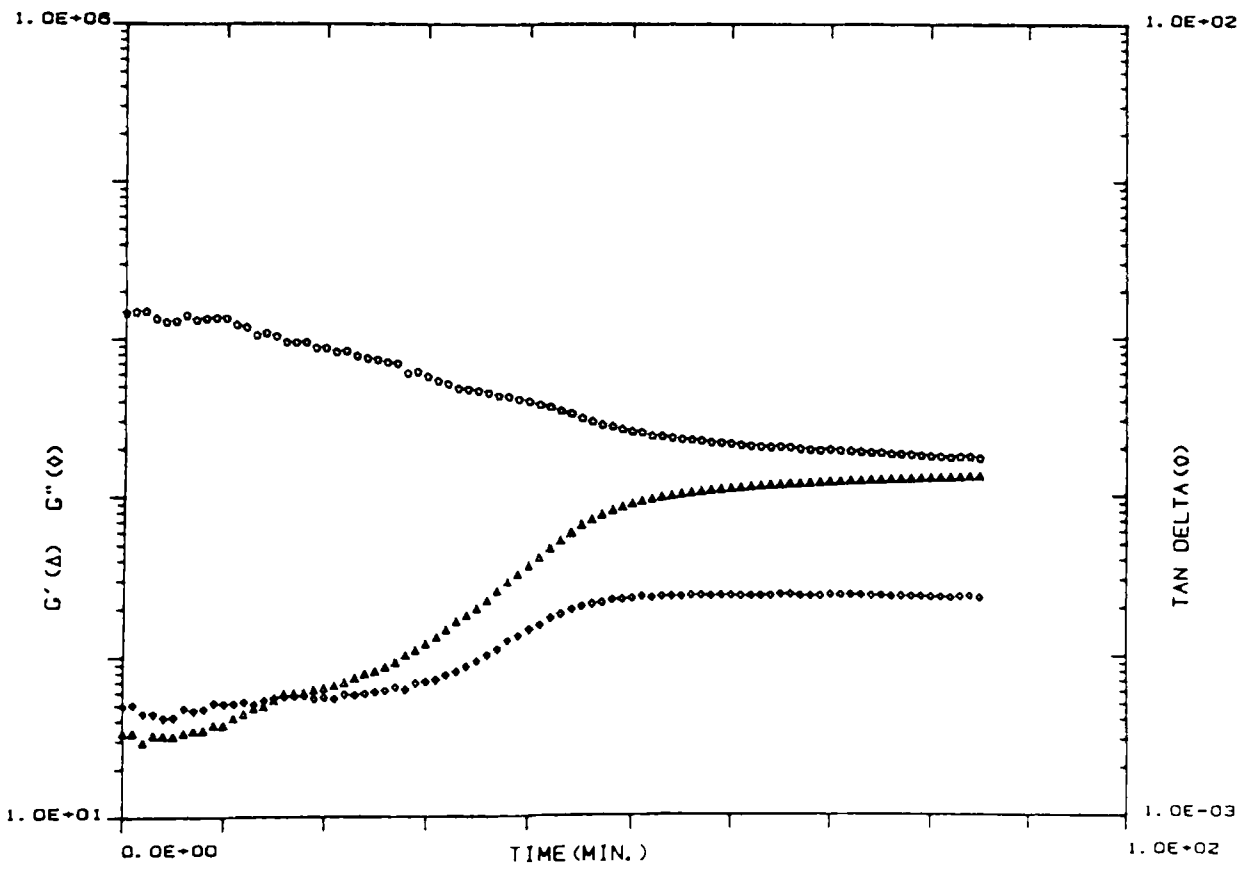

c) Temperature sweep (cooling) for a mixture of 0·5% ps.1128 and 1·0% locust bean gum.

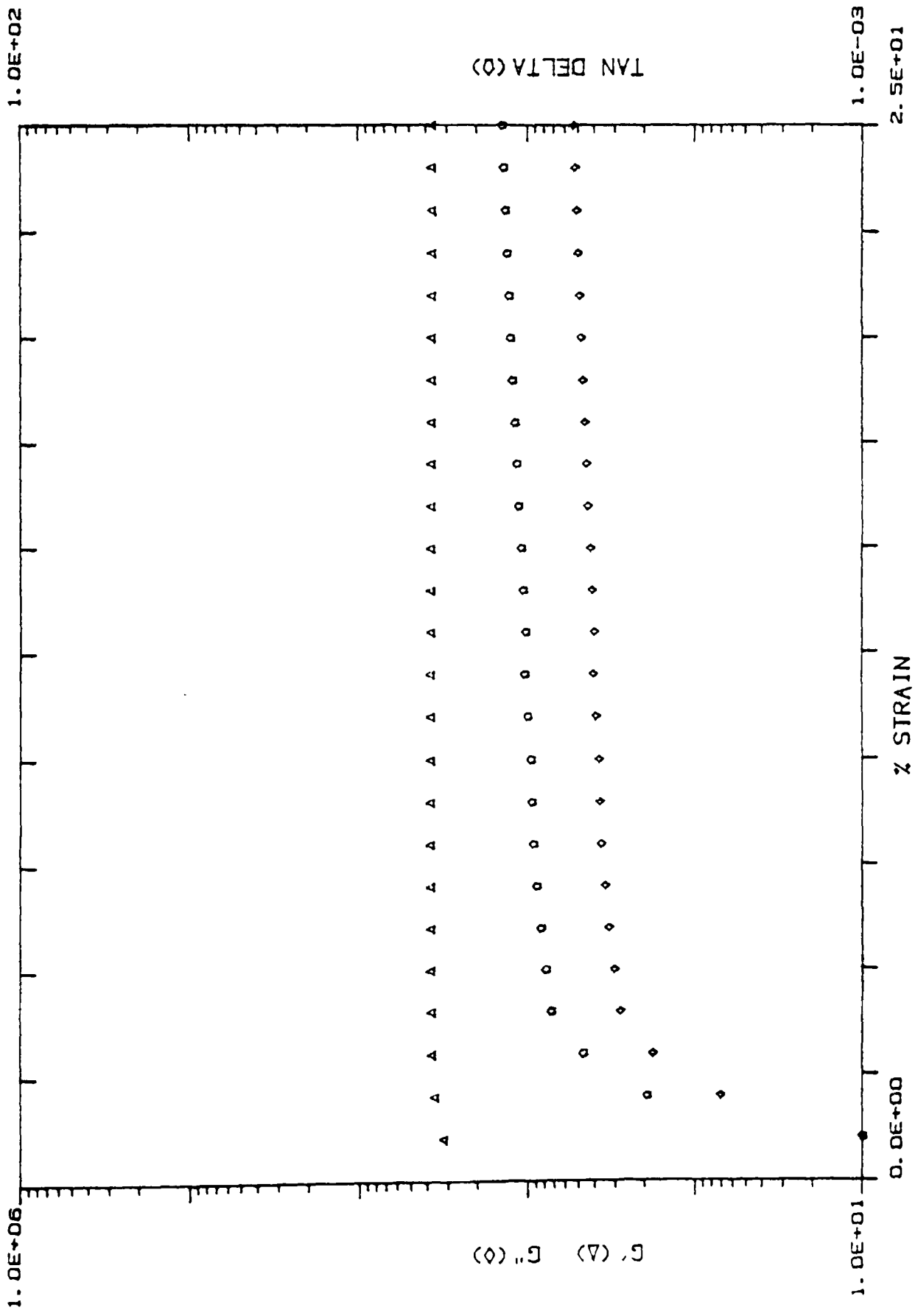

d) Strain sweep for a mixture of 0.5% ps. 646 and 1.0% locust bean gum.

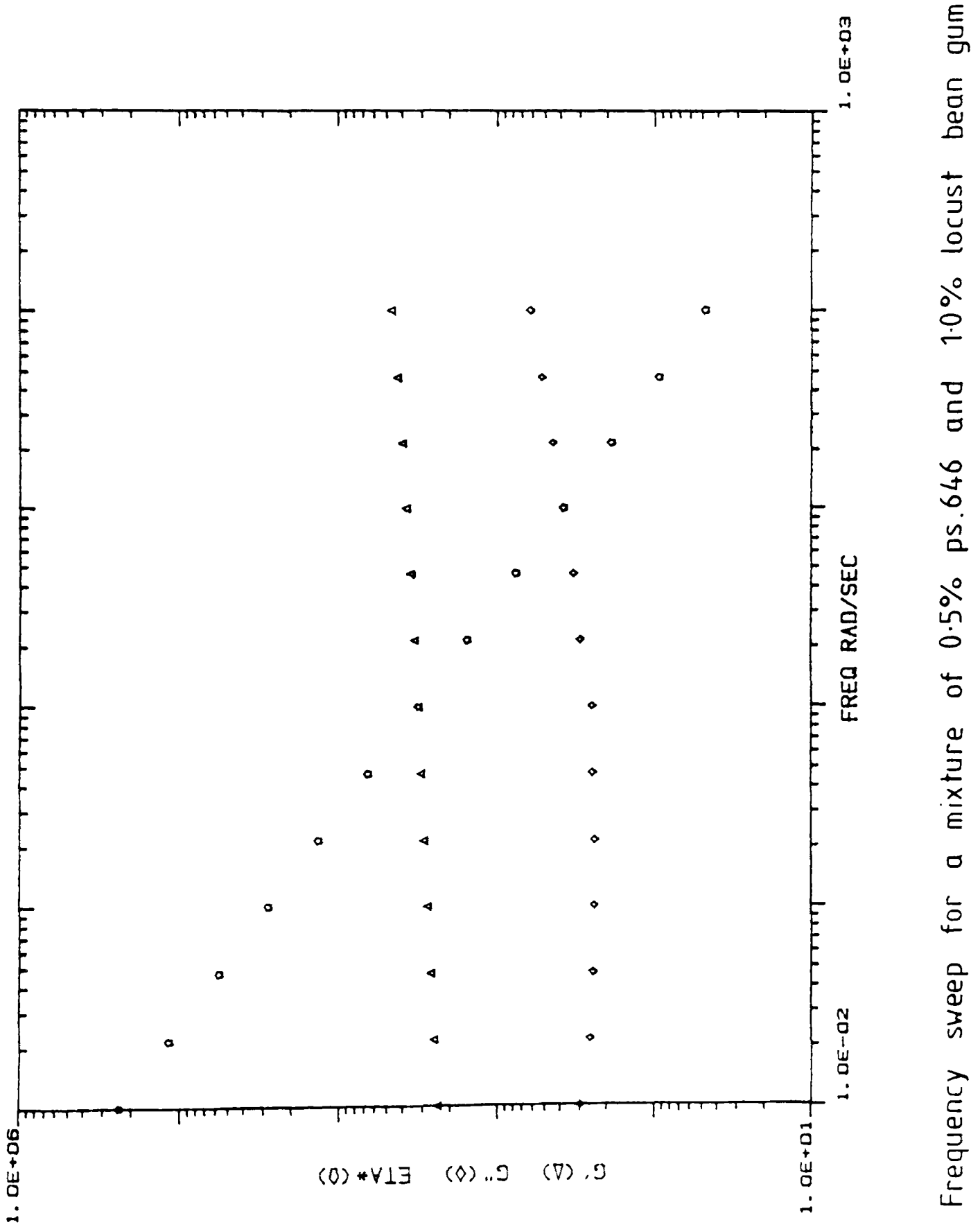

e) Frequency sweep for a mixture of 0·5% ps.646 and 1·0% locust bean gum.

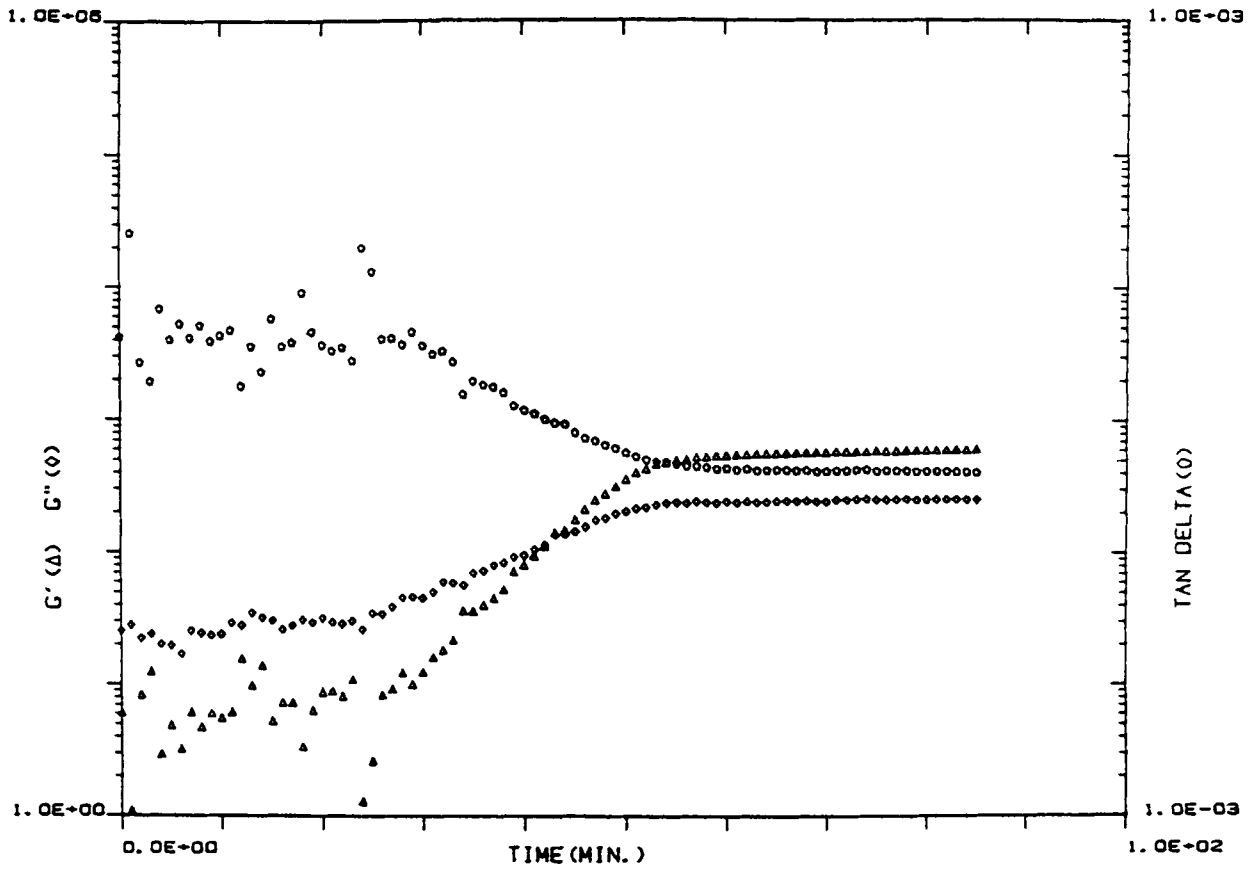

f) Temperature sweep (cooling) for a mixture of 0·5% ps. BD9A and 1·0% locust bean gum.

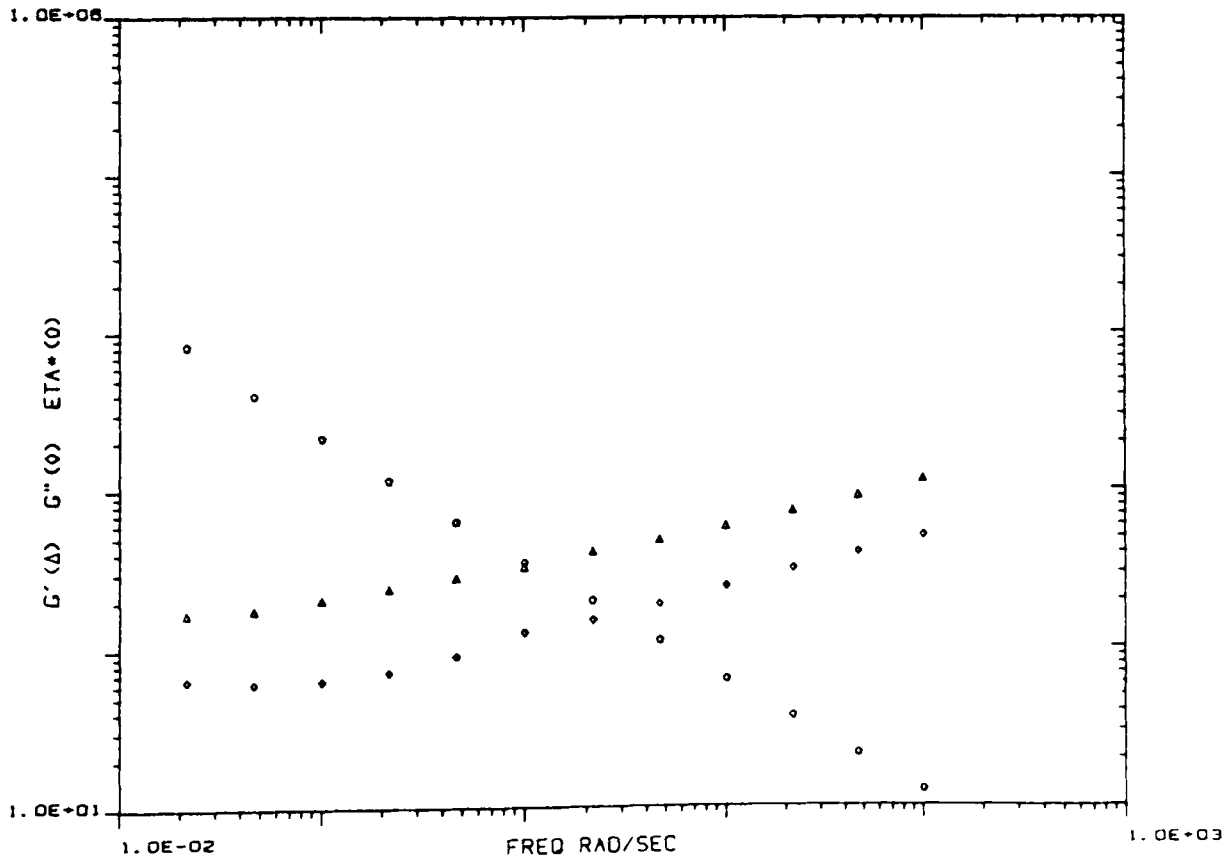

g) Frequency sweep for a mixture of 0·5% ps. BD9A and 1·0% locust bean gum.

Fig. 7·12 Oscillatory shear measurements for xanthan/guar gum mixed systems in deionized water.

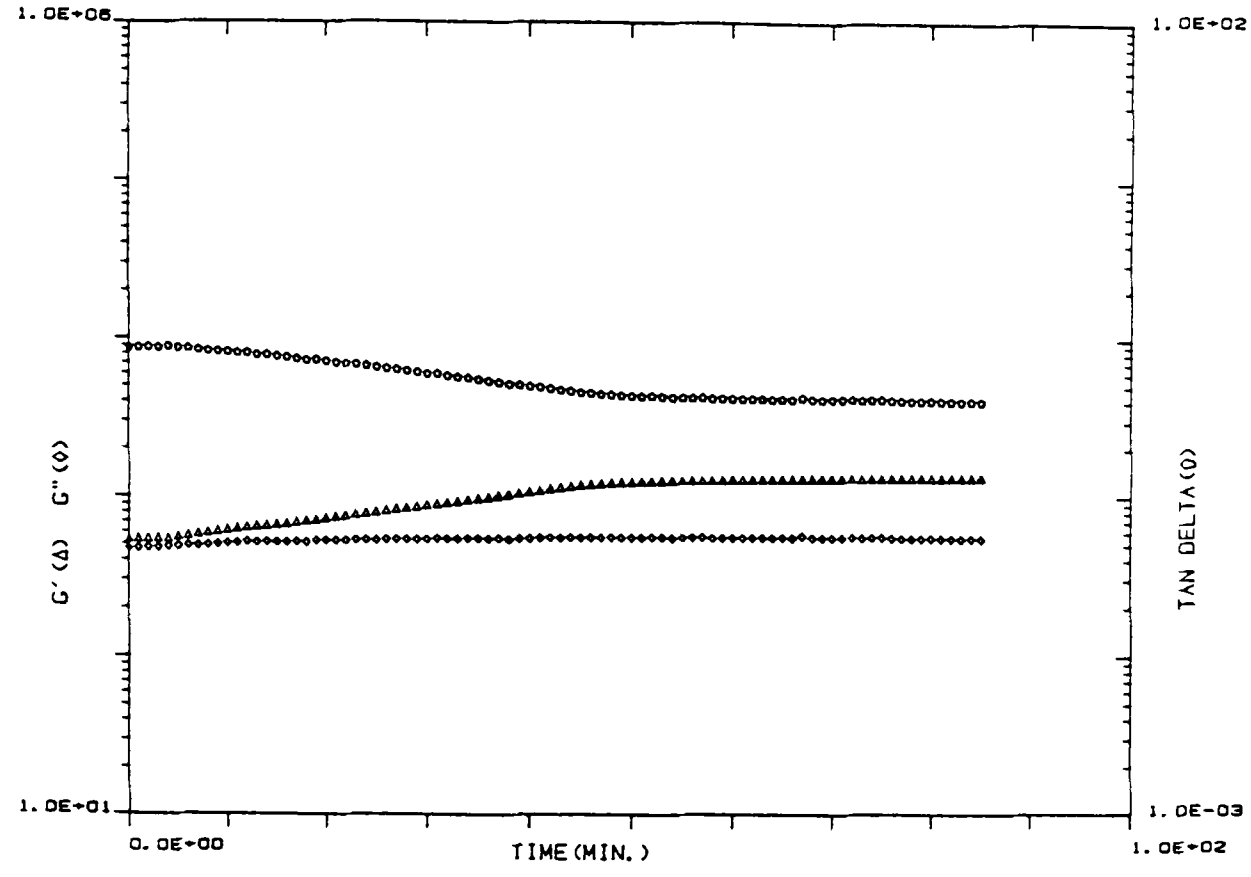

a) Temperature sweep (cooling) for a mixture of 0·5% ps.646 and 1·0 % guar gum.

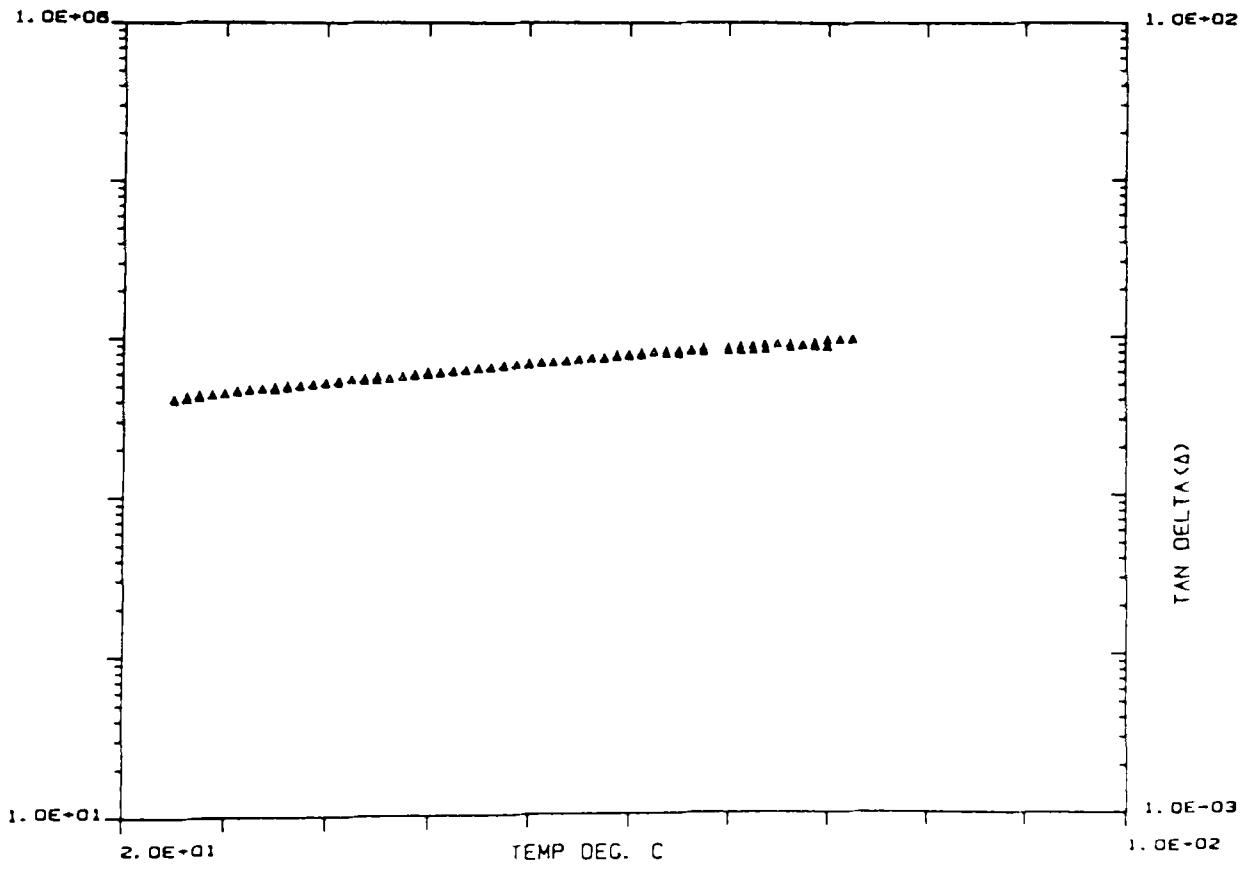

b) Temperature sweep (cooling [▲] and reheating [△]) for a mixture of 0·5% ps.646 and 1·0% guar gum.

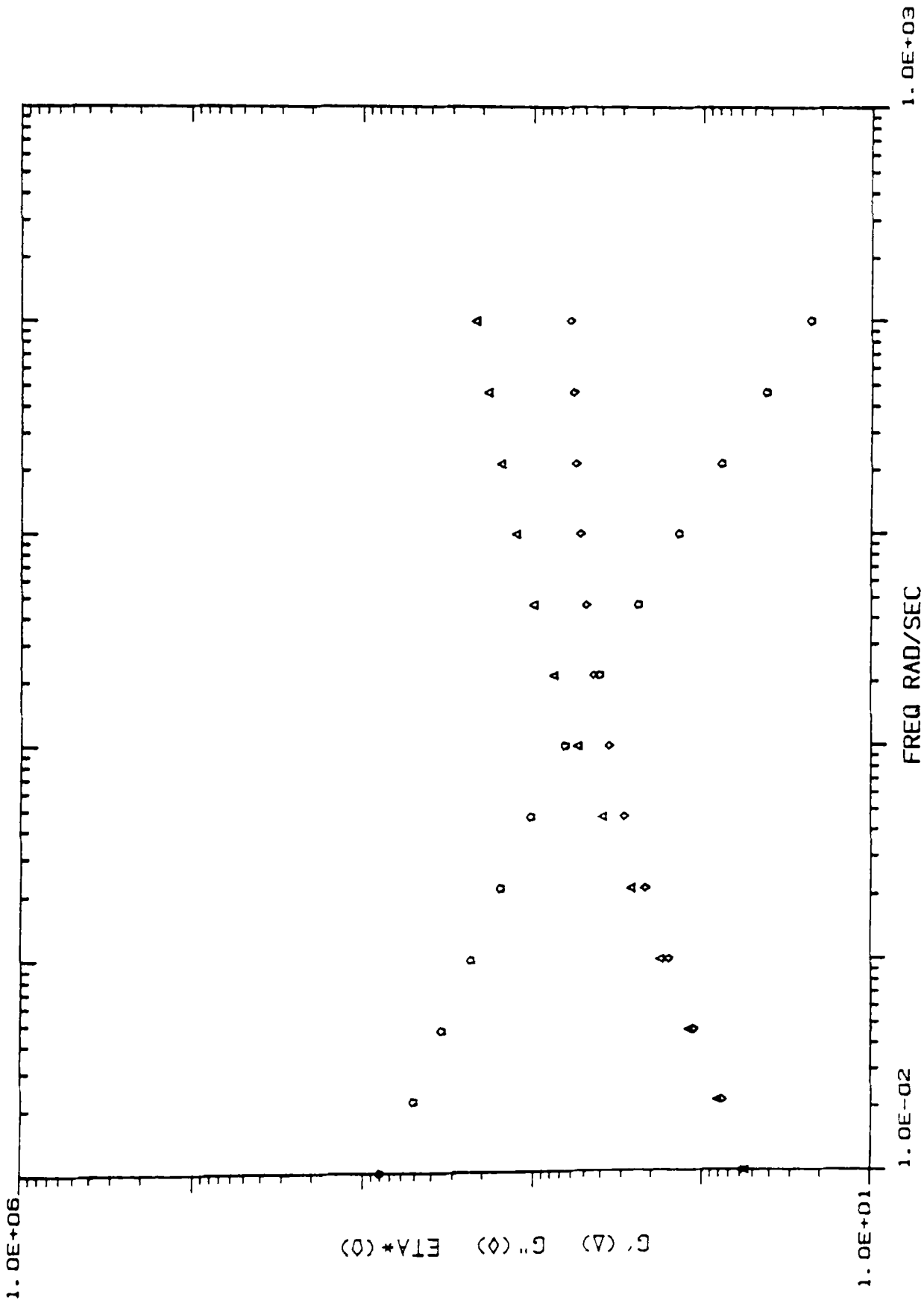

c) Frequency sweep for a mixture of 0·5% ps.646 and 1·0% guar gum.

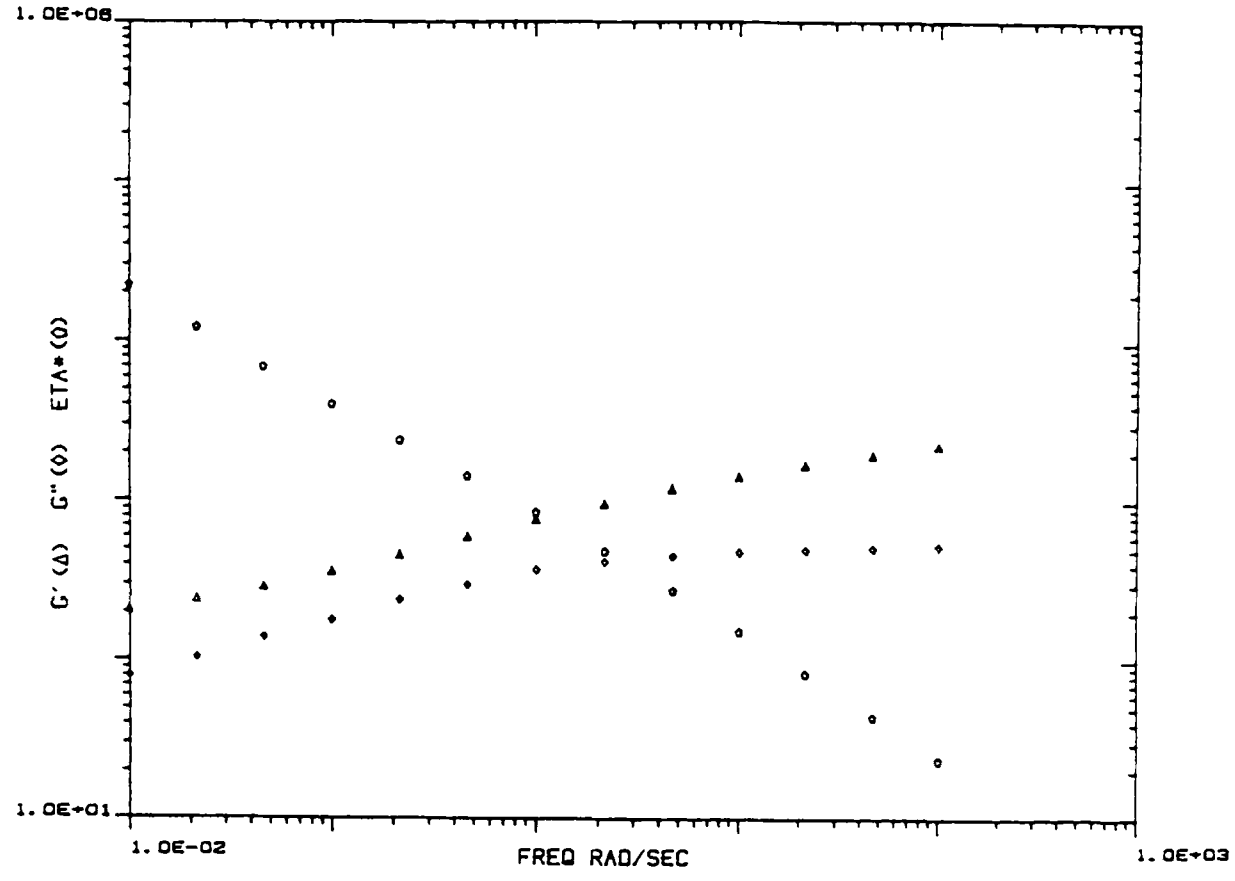

d) Frequency sweep for a mixture of 0·5% ps.556 and 1·0% guar gum.

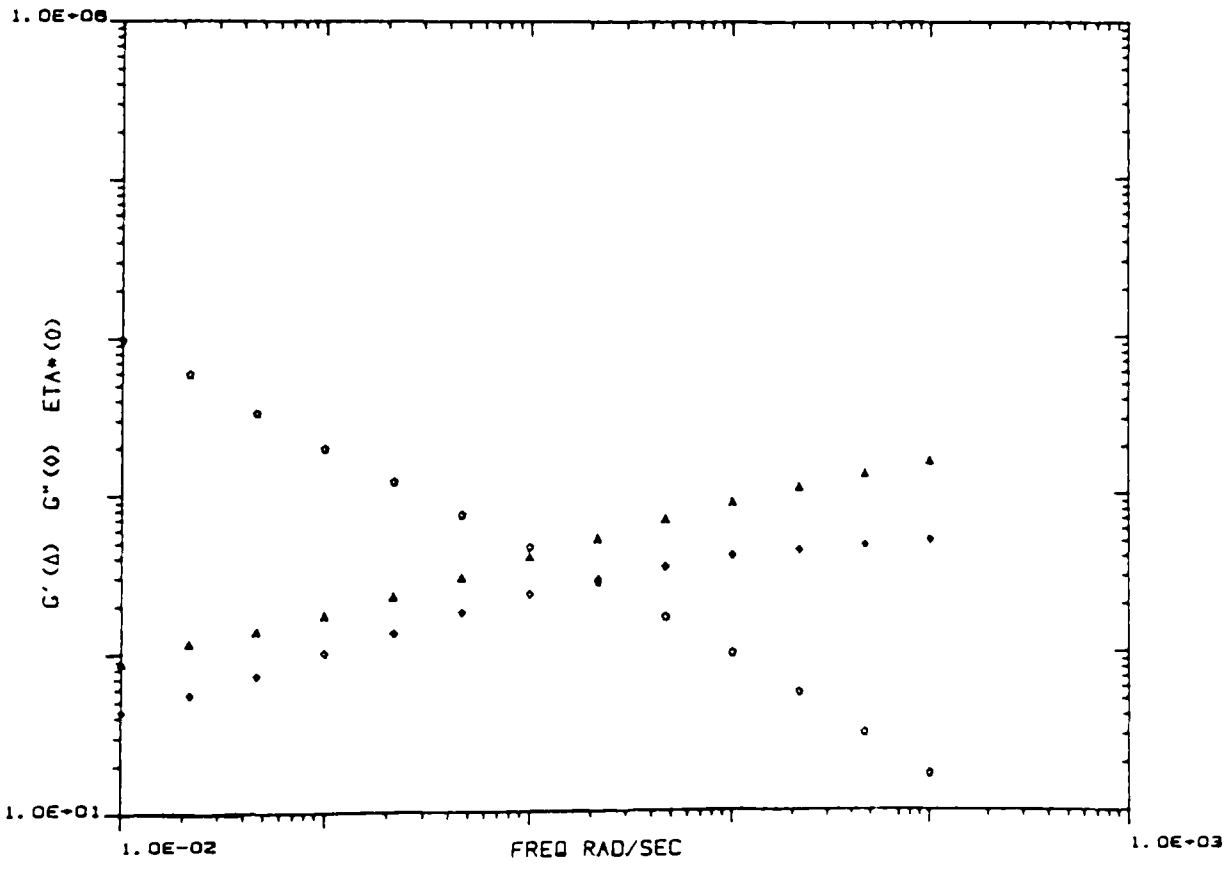

e) Frequency sweep for a mixture of 0·5% deacetylated ps.1128 (batch 2) and 1·0% guar gum.

Fig. 7·13 Oscillatory shear measurements for xanthan/konjac mannan mixed systems in deionized water.

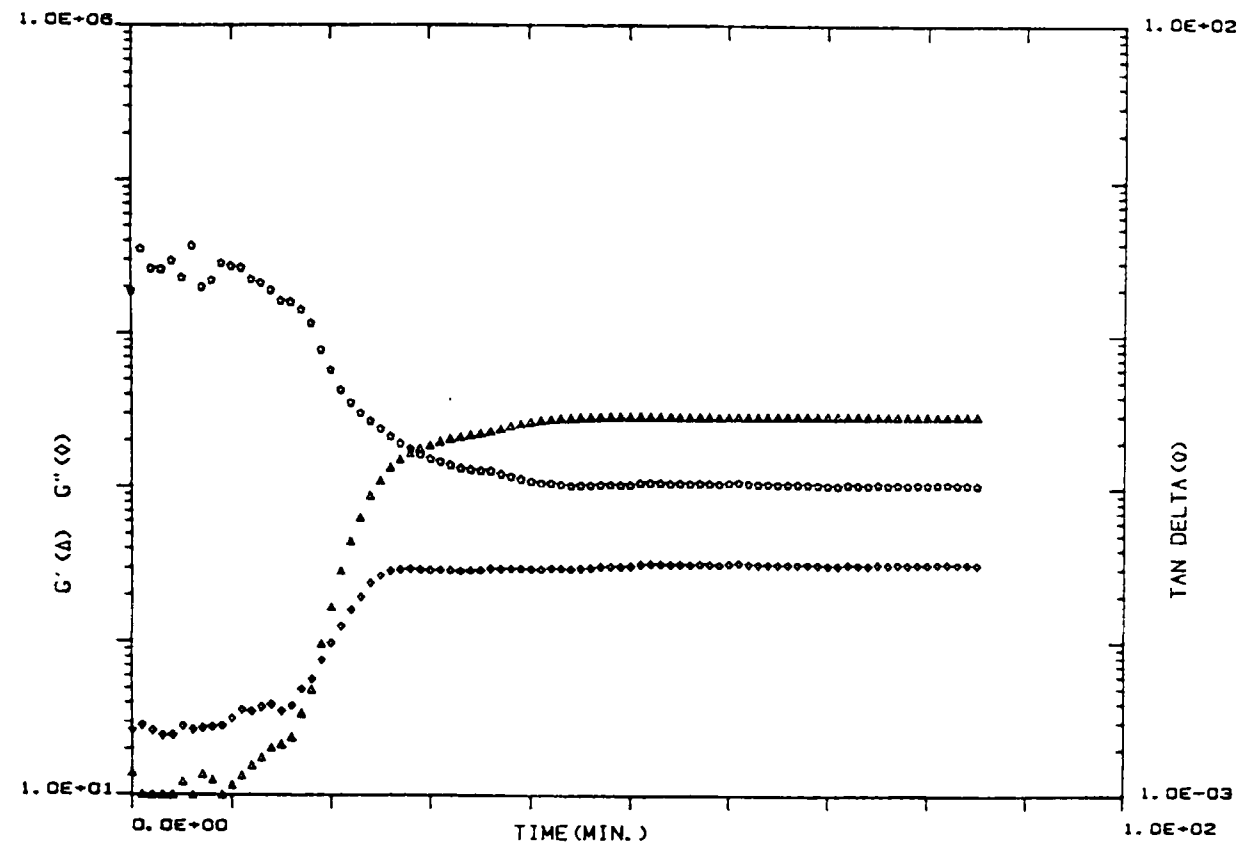

a) Temperature sweep (cooling) for a mixture of 0·5% ps.646 and 1·0% konjac mannan.

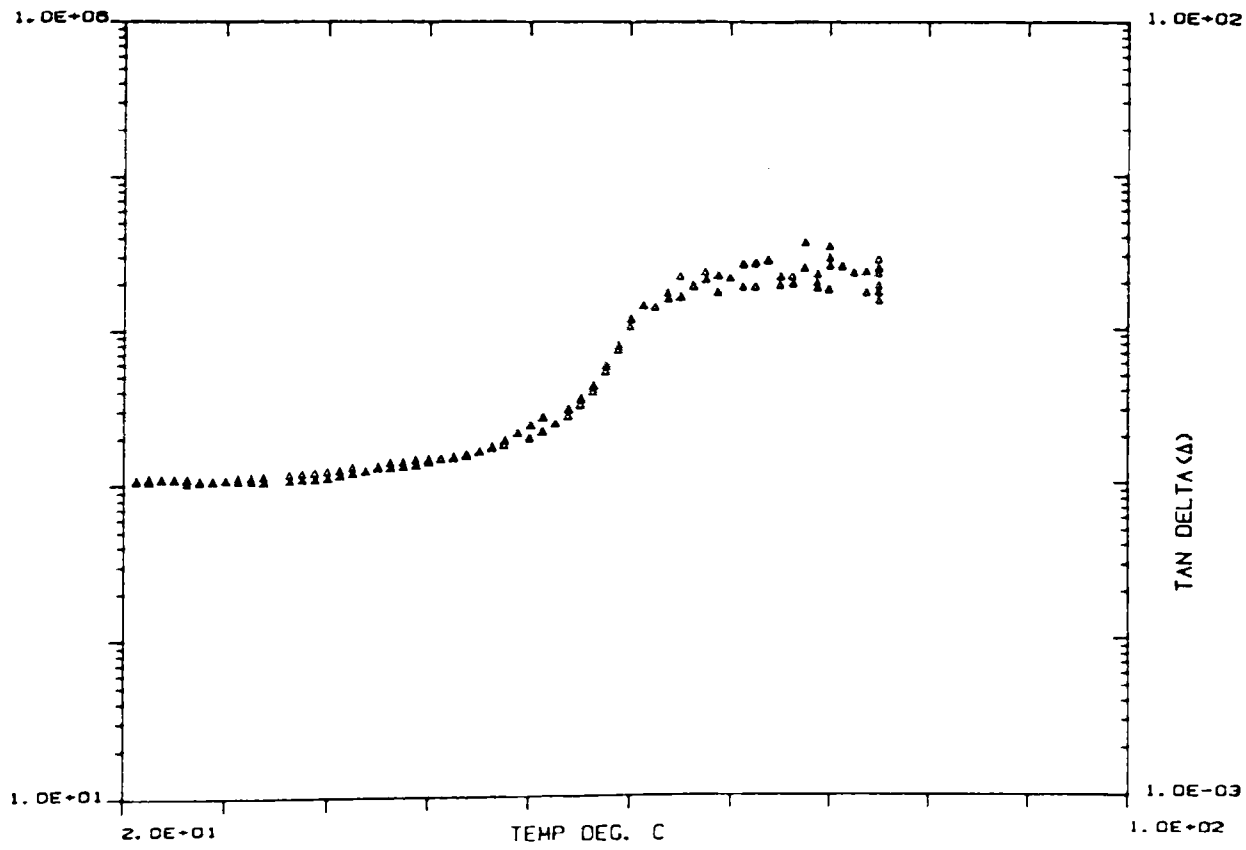

b) Temperature sweep (cooling [▲] and reheating [△]) for a mixture of 0·5% ps.646 and 1·0% konjac mannan.

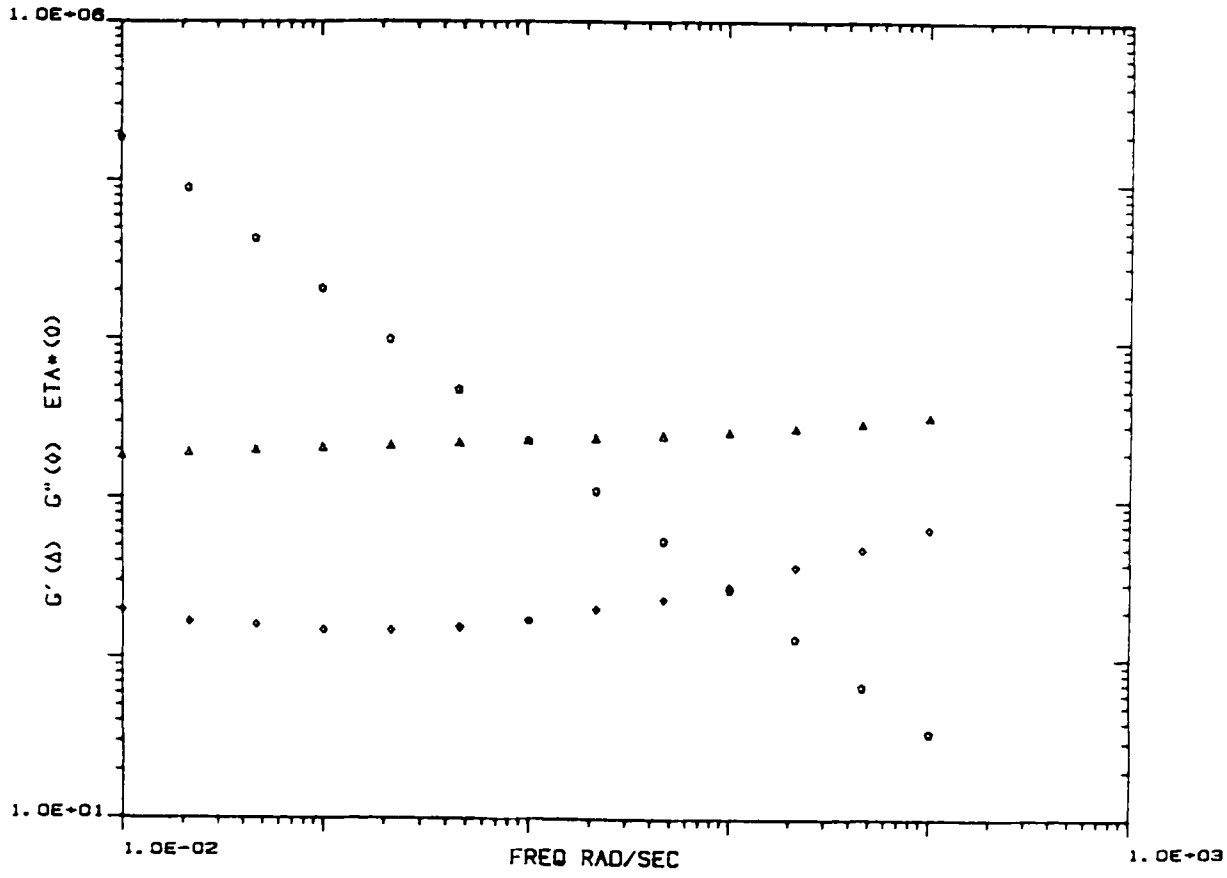

c) Frequency sweep for a mixture of 0·5% ps.646 and 1·0% konjac mannan.

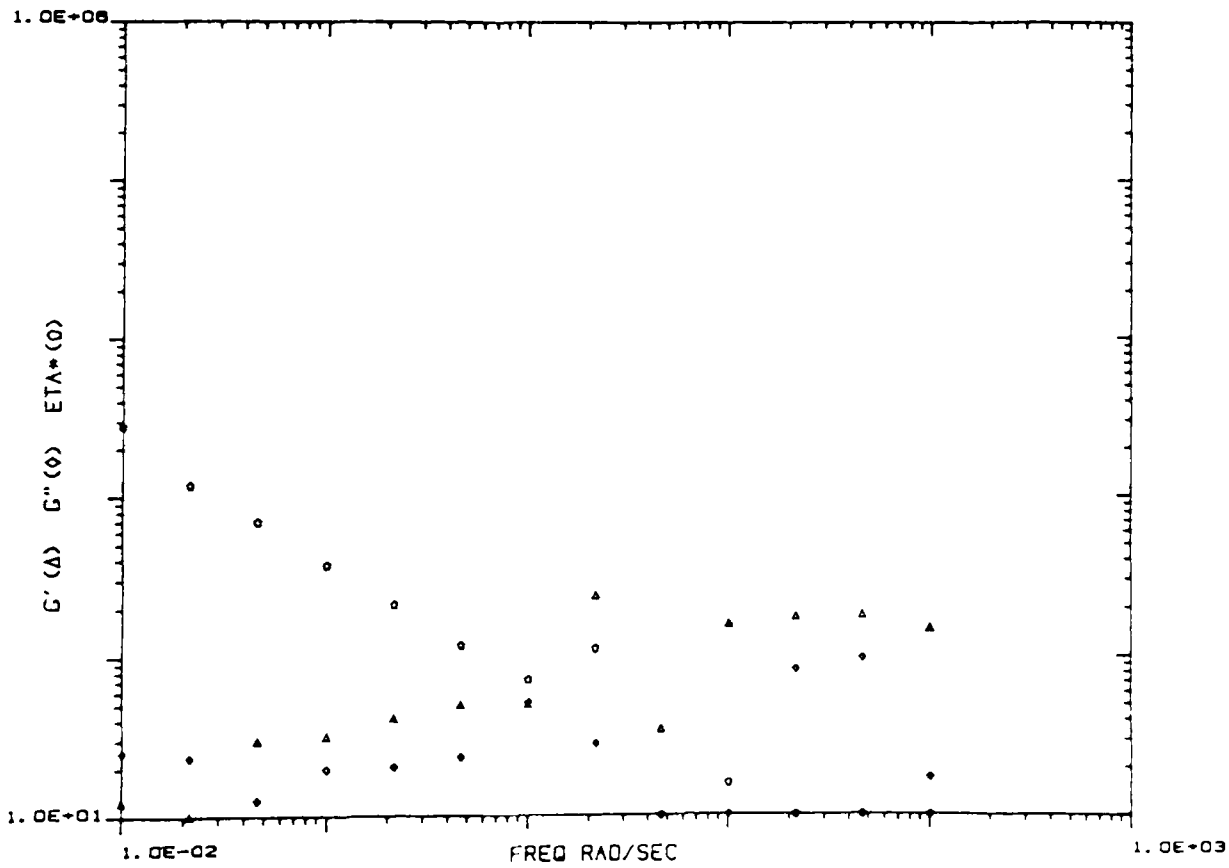

d) Frequency sweep for a mixture of 0·5% ps.1128 and 1·0% konjac mannan.

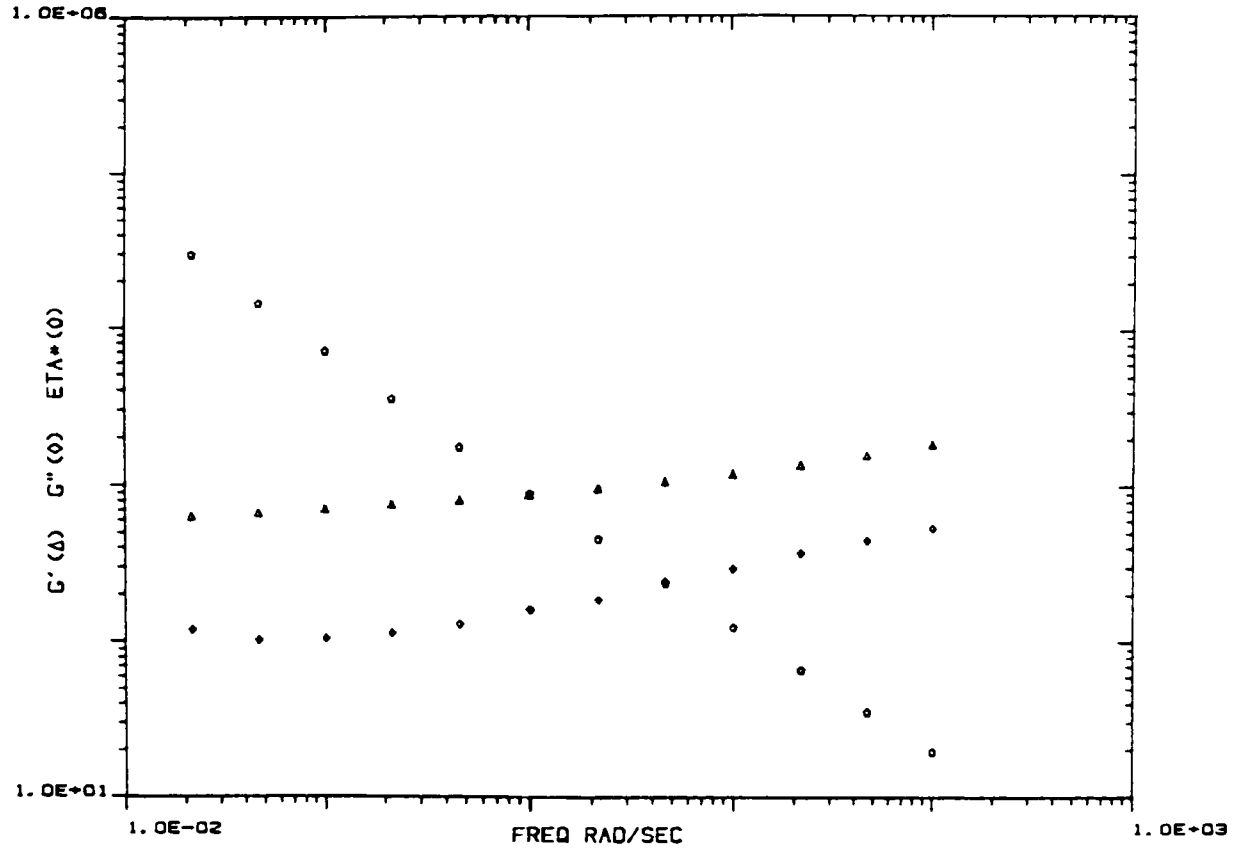

Fig. 7·14 Frequency sweep for a 0·5% ps.646 and 1·0% locust bean gum mixture, mixed cold in the presence of 50 mM sodium chloride.

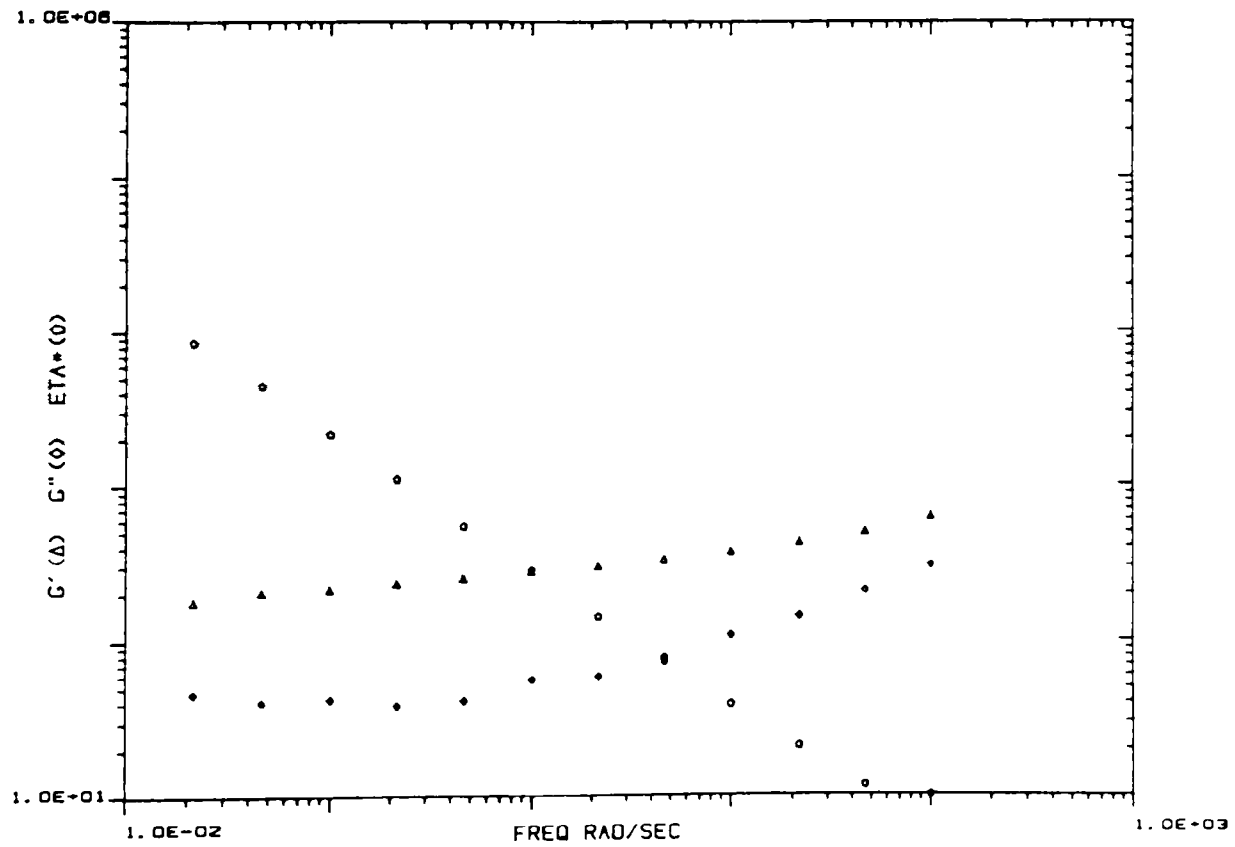

Fig. 7·15 Frequency sweep for a 0·5% ps.646 and 1·0% konjac mannan mixture, mixed cold in the presence of 50mM sodium chloride.

CHAPTER 8
CONCLUDING REMARKS

In the course of this study, a wide range of polysaccharides of the xanthan type were prepared and analysed. These included commercial materials, polymers produced by culturing different bacterial strains and materials modified by chemical deacetylation and/or depyruvylation. Most of the materials had a chemical composition indicative of the normal pentasaccharide repeat unit structure of xanthan and differed only in the levels of acetyl and pyruvate substitution. Two polysaccharides, however, ps.2BD and ps.BD9A, had a reduced mannose content, which seemed to indicate the absence of the terminal mannose residue from all or most of the trisaccharide side-chains. Polymers from the crenated mutants of *X. campestris* had a chemical composition quite different to that of xanthan. Analysis revealed that all of the xanthan-type polysaccharides were extremely pure, and after ion exchange existed predominantly, though not exclusively, in the sodium salt form. The composition of the polymers was not significantly altered by chemical modification but there was some evidence for depolymerisation, particularly as a result of depyruvylation.

OR studies on the helix-coil transition behaviour of a range of xanthans in deionized water confirmed the observation by other authors that acetyl has a stabilizing effect upon the ordered conformation, whilst pyruvate has a destabilizing effect, presumably as a result of intramolecular charge-charge repulsion. Deacetylation was shown to bring about a decrease in the helix-coil transition midpoint whilst depyruvylation resulted in an increase. Furthermore, a strong statistical correlation was found between the melting temperature and the percentage of acyl substituents. The behaviour of ps.PXO_{61} though, was not consistent with this observation. This polymer carried nearly three times the stoichiometric amount of acetyl, but the T_m value was quite low in relation to the acetyl content. Fast atom bombardment spectroscopy studies (Dell and Sutherland - unpublished results) revealed that the internal mannose residue of this polymer was multiply acetylated and the atypical behaviour can therefore be attributed to the unusual acetyl distribution.

Sample ps.BD9A, like normal xanthan, appeared to undergo a conformational change on heating. However, the transition occurred at a very low temperature, indicating that the ordered conformation was weak and readily disrupted by heat. This suggests that the terminal mannose residue has a stabilizing effect upon the ordered helical conformation but that in its absence xanthan is still capable of adopting some degree of conformational order.

The OR curves for all of the polymers, with the possible exception of ps.BD9A (not tested), showed significant thermal hysteresis in deionized water. Storage of the polymers at 10°C, without salt for extended periods resulted in a time-dependent fall in the specific OR. Both phenomena were eliminated in the presence of sufficient sodium chloride. A possible kinetic explanation for these observations has been discussed in section 4.11.

The degree of conformational order and the thermal stability of the xanthan helix were shown to increase in the presence of sodium chloride, presumably as a result of charge shielding. Studies on ps.646, ps.1128, ps.PXO_{61} and ps.556 revealed that the specific OR in the low temperature plateau region of the curve fell as the concentration of sodium chloride increased. The more highly charged the polymer, the greater the fall and the higher the sodium chloride concentration at which the minimum specific OR was reached. The minimum specific OR was much the same for all four materials suggesting that in the presence of sufficient salt the polymers were capable of adopting a similar degree of conformational order. The T_m values for ps.646, ps.1128 and ps.PXO_{61} decreased linearly with the log of the salt concentration. Sample ps.556, however, behaved atypically. The thermal stability of the polymer did increase in the presence of salt, but the OR curve also resolved into two quite separate transition steps. An initial hypothesis that this might be due to the presence of two distinct fractions within the sample, one with a high pyruvate content and the other with very little pyruvic acid, had to be discounted since, although the polymer did separate into two fractions upon ion exchange chromatography, both fractions were shown to contain approximately the same amount of pyruvic acid.

The approximate molecular weights of the xanthan samples were obtained from the intrinsic viscosity measurements in 20mM sodium chloride using the data of Sato *et al* (1984c). Molecular weights within the range 0.96-8.80 x 10^6 were obtained by this method. However, there was some evidence to suggest the formation of high molecular weight aggregates upon freeze drying. This may have increased the intrinsic viscosity value and therefore the molecular weight estimate for some samples. Evidence for the presence of aggregates in solutions of ps.1128 was particularly strong and analysis of some of the data for this sample was complicated as a result. Molecular weight estimates for ps.646, ps.1128, ps,PXO_{61} and ps.556 determined by static light scattering ranged from 0.90-1.60 x 10^6.

S-values, determined from intrinsic viscosity data for four xanthan samples at a range of ionic strengths, served as an indicator of chain flexibility. On the basis of these ps.556 appeared to be the most flexible, followed in turn by ps.646, ps.PXO_{61} and, less reliably as noted above, ps.1128. This seems to agree with the known conformational stability of the polymers ie. the more acetyl and the less pyruvic acid the polymer carries, the greater the stability of the ordered form and the lower its apparent flexibility. However this agreement may be specious, since the Kuhn segment lengths determined in 0.1M potassium chloride using static light scattering, indicated very little difference in the flexibility of the materials under these conditions. An attempt to calculate the persistence lengths of the four polymers from the intrinsic viscosity data using the Smidsrød and Haug B-value method failed, as expected, because of the inherent rigidity of the xanthan molecule.

Comparison of the theoretical mass per unit length with that determined experimentally by light scattering revealed that ps.646, ps.1128 and ps.PXO_{61} in 0.1M potassium chloride exist predominantly in the double-stranded state but that solutions of ps.556 contain a significant number of single strands.

All of the xanthan samples tested showed typical pseudoplastic behaviour. Addition of salt to a 0.2% solution of ps.646, ps.1128, ps.PXO_{61} and ps.556 resulted in an initial sharp fall in viscosity (η_{sp0}) believed to be due to the decrease in hydrodynamic volume resulting from charge shielding. This was followed by a gradual increase in viscosity attributed to the viscosity-enhancing effects of salt-induced macromolecular association. The increase in viscosity occurred not only with ps.646 and ps.556, the pyruvylated polymers, but also with ps.1128 and ps.PXO_{61}, contradicting the conclusions of Smith and coworkers (1981), namely that a minimum critical degree of pyruvic acid substitution is necessary for macromolecular association. Solutions of ps.556 at 0.2% showed an anomalous and unexplained jump in viscosity at concentrations of between 5mM and 10mM sodium chloride.

The majority of the viscosity data collected for ps.556 at a range of polysaccharide concentrations up to 0.3% and at ionic strengths of between 2mM and 20mM sodium chloride, was found to fit a master curve of η_{sp0} versus $c[\eta]$. Data for 0.2% ps.646 and ps.PXO_{61} at various ionic strengths up to 20mM were also found to fit this curve, suggesting that at low ionic strengths the viscosity of xanthan in solution essentially reflects the degree of space occupancy by the molecules. By contrast, data for ps.1128, did not fit this master curve, apparently because of the presence of high molecular weight aggregates which distorted the intrinsic viscosity values upwards.

Steady and oscillatory shear measurements on solutions of xanthan (2%) in 20mM and 50mM sodium chloride revealed the typical weak gel network behaviour expected for xanthan. In deionized water, however, the behaviour was more akin to that of an entanglement system. Under the conditions used in the experiments xanthan, in deionized water, is believed to have existed in predominantly the disordered state. The viscoelastic behaviour of the disordered polymer therefore appears to be governed more by topological entanglements than by intermolecular associations of the type seen in the presence of salt. Solutions of locust bean gum, guar gum and konjac mannan (1%) all showed apparent entanglement behaviour both in deionized water and salt solution.

The majority of the xanthans tested interacted with the locust bean gum and konjac mannan in deionized water to form a strong, thermo-reversible gel network. The xanthan/konjac mannan gels were found to have significantly higher melting and setting temperatures than the xanthan/ locust bean gum gels and the transition from the liquid to the gel state upon cooling was significantly sharper. The xanthan/locust bean gum

systems, on the other hand, formed gels down to a much lower total polysaccharide concentration and the gels, once established, continued to increase in strength (ie. gel modulus) very slowly and over a considerable period of time. Xanthan did not gel with guar gum. Instead the frequency sweep indicated entanglement behaviour which appeared to be a composite of that of the two individual components.

The gel strength for both the locust bean gum and konjac mannan mixed systems appeared to be heavily influenced by the number of acetyl groups carried on the xanthan molecule. Deacetylation generally led to an increase in gel strength and a decrease in the minimum gelling concentration, and the effect was particularly marked in the case of ps.1128. At a total polysaccharide concentration of 1.5% this polymer failed to gel at all with konjac mannan, yet its deacetylated derivative interacted quite strongly with the glucomannan. In addition although xanthan did not form a gel with guar gum, limited data from OR studies and mechanical spectrometry suggested a possible weak interaction between the galactomannan and certain low acetyl polymers. Quite a strong statistical correlation was found between the percentage of acetyl groups and the gel strength for the xanthan/locust bean gum mixed systems, but for the xanthan/konjac mannan gels the correlation was weak and only detectable when the data for ps.PXO_{61} was excluded from the analysis. As with the helix-coil transition studies, the behaviour of ps.PXO_{61} appeared to deviate from the general trend. The interaction of ps.PXO_{61} with both locust bean gum and konjac mannan appeared to be quite strong relative to its high acetyl content, and this may be attributable, once again, to the unusual acetyl distribution. Quite how the acetyl group inhibits the gelling interaction between xanthan and the gluco- and galactomannans is uncertain.

The influence of pyruvic acid on the interactions is even less well understood. Depyruvylation of xanthan often resulted in a slight decrease in gel strength and a slight increase in the minimum gelling concentration but no discernible correlation was found between the pyruvate content and the gel strength in the statistical analysis. Furthermore it is by no means certain that any apparent decrease in gel strength was actually due to loss of the pyruvic acid group and not to the concomitant decrease in molecular weight.

The interaction between ps.BD9A and locust bean gum was far weaker than that of any of the other xanthan-type polysaccharides, indicating that the terminal mannose of the trisaccharide side-chain may play an important role in the interaction between xanthan and the galactomannans.

A strong positive correlation was found between the T_m value and the gel strength for the xanthan/locust bean gum mixed systems but no such relationship existed for the xanthan/konjac mannan gels.

Addition of sodium chloride was shown to bring about a reduction in gel strength and an increase in the minimum gelling concentration for both the xanthan/locust bean gum and xanthan/konjac mannan gels. This may have been the result of enhancement of the xanthan-xanthan interaction in preference to the xanthan-galactomannan or xanthan-glucomannan interaction.

Finally, oscillatory shear measurements on xanthan/locust bean gum and xanthan/konjac mannan systems mixed cold both in deionized water and in 50mM sodium chloride showed apparent gel formation and indicated that, contrary to the assertion of Cairns *et al* (1986a, 1987) and Brownsey *et al* (1988), denaturation of the xanthan helix is unnecessary for the interaction between xanthan and both locust bean gum and konjac mannan. Indeed the evidence presented in this thesis does not preferentially favour any one of the currently available models for the xanthan-galactomannan interaction.

The original aim of this study, as outlined in section 1.6, was to try to gain a better understanding of the role of the trisaccharide side-chain and its acyl substituents in determining the solution and interaction properties of xanthan. This aim was, at least partially, achieved. The acetyl and pyruvic acid groups were shown to be important in modifying the amount of local order and the thermal stability of the polysaccharides. There was also some evidence, albeit equivocal, to suggest that the acyl substituents influence the overall flexibility of the polymer chain. A previous report that pyruvic acid is essential for macromolecular association was found wanting. The apparent inhibition of the gelling interaction between xanthan and locust bean gum by the acetyl group was confirmed and a similar phenomenon was demonstrated for the xanthan-konjac mannan interaction. Limited evidence also indicated a role for the terminal mannose residue, both in stabilizing the ordered helical conformation of the polymer, and in promoting the interaction between xanthan and locust bean gum. However, interpretation of these observations at the molecular level proved problematic. The behaviour of normal wild-type xanthan (eg. Keltrol and ps.646), as defined by Jansson *et al* (1975), is not yet sufficiently well understood to enable the differences in behaviour resulting from minor structural variations to be easily explained. In addition, in many cases, it proved difficult to separate the effects of the more obvious structural dissimilarities from other less apparent and less well-defined differences. The influence of molecular weight is a prime example. For the majority of polymers, the molecular weight was estimated from the intrinsic viscosity value using published data and, as has already been pointed out, in some cases this value may have been distorted upwards by the presence of high molecular weight aggregates. In the absence of a reliable molecular weight estimate for every sample the role of the molecular weight in dictating the solution and interaction properties could not be completely taken into account. A statistical analysis of the helix-coil transition behaviour, and of the strength of the interaction with locust bean gum and konjac mannan,

revealed no correlations with the intrinsic viscosity, but if some of the intrinsic viscosity data were inaccurate, then little would be expected. Problems were also encountered when trying to separate the effects of depyruvylation and, to a lesser extent, deacetylation from any decrease in molecular weight that may have accompanied chemical modification.

The possible effects of fine structural differences between polymers produced by different bacterial strains or under different cultural conditions is another area that would, ideally, have been considered. Slight variations in the proportion of backbone residues substituted with trisaccharide side-chains, or differences in the distribution of the acetyl and pyruvic acid groups, would be undetectable by the type of chemical analyses used in this study but could, nevertheless, have had a marked effect upon the behaviour of the materials. Examination of the polymers for differences in fine structure was not an area of investigation in this study. However, at the outset of this investigation, the possibility of using enzymic degradation in combination with an analytical technique such as HPLC to study the fine structure was considered and would, in the authors opinion, be a useful area for future investigation. Such an approach would be particularly valuable for confirming the proposed structures of ps.2BD and ps.BD9A.

In some respects the choice of polymers used in this study was unfortunate. The majority of the work concentrated on just four materials, ps.646, ps.1128, ps.PXO_{61} and ps.556. These were of similar molecular weight and represented the extremes in terms of the levels of acetyl and pyruvate substitution. They should, therefore, have illustrated quite effectively the influence of the acetyl and pyruvic acid groups on the solution and interaction properties of xanthan. However, as it transpired, two of these materials, ps.1128 and ps.556, showed atypical behaviour which was not necessarily directly attributable to differences in the acyl content. Sample ps.1128 showed a pronounced tendency towards the formation of stable high molecular weight aggregates upon freeze drying and these aggregates interfered with some of the measurements on this sample. Polymer ps.556 showed unusual helix-coil transition behaviour and, to some extent, atypical viscosity behaviour in the presence of salt, neither of which have, to the author's knowledge, been previously reported for other high pyruvate xanthans. Because of this, understanding the role of the acyl substituents was that much more difficult.

In conclusion therefore, whilst the work presented in this thesis should make a significant contribution towards the understanding of the xanthan system and its interaction with the galacto- and glucomannans, there is still a very long way to go before the relationship between the structure of xanthan and its behaviour, both alone and in combination with other polysaccharides, is fully understood.

REFERENCES

Agrios, G.N. (1978) **"Plant Pathology"**, 2nd Ed. Academic Press, London.

Andrew, T.R. (1977) Applications of xanthan gum in foods and related products. In **"American Chemical Society Symposium Series No. 45. Extracellular Microbial Polysaccharides"** (Eds. Sandford, P.A. and Laskin, A.) American Chemical Society, Washington D.C. pp.231-241.

Anon. (1969) CFR 172.695. Xanthan Gum. Federal Register 34, No. 53, 5376-5377.

Anon. (1974) Xanthan gum offers versatility, safety. **Food Technology**, 28, June, 18-21.

Atkins, E.D.T., Attwool, P.T., Miles, M.J., Morris, V.J., O'Neill, M.A. and Sutherland, I.W. (1987) Effect of acetylation on the molecular interactions and gelling properties of a bacterial polysaccharide. **International Journal of Biological Macromolecules**, 9, 115-117.

Baker, C.W. and Whistler, R.L. (1975) Distribution of D-galactosyl groups in guaran and locust bean gum. **Carbohydrate Research**, 45, 237-243.

Barrère, G.C., Barber, C.E. and Daniels, M.J. (1986) Molecular cloning of genes involved in the production of the extracellular polysaccharide xanthan by *Xanthomonas campestris* pv. *campestris*. **International Journal of Biological Macromolecules**, 8, 372-374.

Bayer, M.E. and Thurow, H. (1977) Polysaccharide capsule of *Escherichia coli*: Microscope study of its size, structure and sites of synthesis. **Journal of Bacteriology**, 130, 911-936.

Bewley, J.D. and Reid, J.S.G. (1985) Mannans and glucomannans. In **"Biochemistry of Storage Carbohydrates in Green Plants"** (Eds. Dey, P.M and Dixon, R.A.) Academic Press. pp.289-304.

Bitter, T. and Muir, H.M. (1962) A modified uronic acid carbazole reaction. **Analytical Biochemistry**, 4, 330-334.

Blumenkrantz, N. and Asboe-Hansen, G. (1973) New method for the quantitative determination of uronic acids. **Analytical Biochemistry**, 54, 484-489.

Booth, A.N., Hendrickson, A.P. and DeEds, F. (1963) Physiological effects of three microbial polysaccharides on rats. **Toxicology and Applied Pharmacology**, 5, 478-484.

Bradshaw, I.J., Nisbet, B.A., Kerr, M.H. and Sutherland, I.W. (1983) Modified xanthan - its preparation and viscosity. **Carbohydrate Polymers**, 3, 23-38.

Brivonese, A.C. (1985) Alginate Biosynthesis in *Azotobacter vinelandii*. PhD Thesis. University of Edinburgh.

Brownsey, G.J. and Morris, V.J. (1988) Mixed and filled gels - models for foods. In "**Food Structure - Its Creation and Evaluation**" (Eds. Blanshard, J.M.V. and Mitchell, J.R.) Butterworths. pp.7-23.

Brownsey, G.J., Cairns, P., Miles, M.J. and Morris, V.J. (1988) Evidence for inter-molecular binding between xanthan and the glucomannan konjac mannan. **Carbohydrate Research**, 176, 329-334.

Cadmus, M.C., Rogovin, S.P., Burton, K.A., Pittsley, J.E., Knutson, C.A. and Jeanes, A. (1976) Colonial variation in *Xanthomonas campestris* NRRL B-1459 and characterization of the polysaccharide from a variant strain. **Canadian Journal of Microbiology**, 22, 942-948.

Cadmus, M.C., Knutson, C.A., Lagoda, A.A., Pittsley, J.E. and Burton, K.A. (1978) Synthetic media for production of quality xanthan gum in 20 liter fermentors. **Biotechnology and Bioengineering**, 20, 1003-1014.

Cadmus, M.C., Burton, K.A. and Slodki, M.E. (1982a) Growth-related substituent changes in exopolysaccharides of fast-growing *Rhizobia*. **Applied and Environmental Microbiology**, 44, 242-245.

Cadmus, M.C., Jackson, L.K., Burton, K.A., Plattner, R.D. and Slodki, M.E. (1982b) Biodegradation of xanthan gum by *Bacillus* sp. **Applied and Environmental Microbiology**, 44, 5-11.

Cairns, P., Miles, M.J. and Morris, V.J. (1986a) Intermolecular binding of xanthan gum and carob gum. **Nature**, 322, 89-90.

Cairns, P., Morris, V.J., Miles, M.J. and Brownsey, G.J. (1986b) Synergistic behaviour in kappa carrageenan-tara gum mixed gels. In "**Gums and Stabilisers for the Food Industry 3**" (Eds. Phillips, G.O., Wedlock, D.J. and Williams, P.A.) Elsevier Applied Science. pp.597-604.

Cairns, P., Morris, V.J., Miles, M.J. and Brownsey, G.J. (1986c) Comparative studies of the mechanical properties of mixed gels formed by kappa carrageenan and tara gum or carob gum. **Food Hydrocolloids**, 1, 89-93.

Cairns, P., Miles, M.J. and Morris, V.J. (1986d) X-ray diffraction studies of kappa carrageenan-tara gum mixed gels. **International Journal of Biological Macromolecules**, 8, 124-127.

Cairns, P., Miles, M.J., Morris, V.J. and Brownsey, G.J. (1987) X-ray fibre-diffraction studies of synergistic, binary polysaccharide gels. **Carbohydrate Research**, 160, 411-423.

Cairns, P., Miles, M.J. and Morris, V.J. (1988) X-ray fibre diffraction studies on konjac mannan - kappa carrageenan mixed gels. **Carbohydrate Polymers**, 8, 99-104.

Callet, F., Milas, M. and Rinaudo, M. (1987) Influence of acetyl and pyruvate contents on rheological properties of xanthan in dilute solution. **International Journal of Biological Macromolecules**, 9, 291-293.

Carroll, V., Miles, M.J. and Morris, V.J. (1982) Fibre-diffraction studies of the extracellular polysaccharide from *Pseudomonas elodea*. **International Journal of Biological Macromolecules**, 4, 432-433.

Carroll, V., Miles, M.J. and Morris, V.J. (1984) Synergistic interactions between kappa carrageenan and locust bean gum. In "**Gums and Stabilisers for the Food Industry 2. Application of Hydrocolloids**" (Eds. Phillips, G.O., Wedlock, D.J. and Williams, P.A.) Pergamon Press. pp.501-506.

Charles, M. and Radjai, M.K. (1977) Xanthan gum from acid whey. In "**American Chemical Society Symposium Series No. 45. Extracellular Microbial Polysaccharides**" (Eds. Sandford, P.A. and Laskin, A.) American Chemical Society, Washington D.C. pp.27-39.

Cheetham, N.W.H. and Punruckvong, A. (1985) An HPLC method for the determination of acetyl and pyruvyl groups in polysaccharides. **Carbohydrate Polymers**, 5, 399-406.

Cheetham, N.W.H. and Mashimba, E.N.M. (1988) Conformational aspects of xanthan-galactomannan gelation. **Carbohydrate Polymers**, 9, 195-212.

Chowdhury, T.A., Lindberg, B., Lindquist, U. and Baird, J. (1987) Structural studies of an extracellular polysaccharide, S-657, elaborated by *Xanthomonas* ATCC 53159. **Carbohydrate Research**, 164, 117-122.

Chrisp, J.D. (1967) Galactomannan gum gels for explosive compositions and for textile or paper sizing. US Patent No. 3,301,723. **Chemical Abstracts**, 67, 92485w.

Christianson, D.D., Gardner, H.W., Warner, K., Boundy, B.K. and Inglett, G.E. (1974) Xanthan gum in protein-fortified starch bread. **Food Technology**, 28, June, 23-29.

Clark, A.H., Richardson, R.K., Robinson, G., Ross-Murphy, S.B. and Weaver, A.C. (1982) Structure and mechanical properties of agar/BSA co-gels. In "**Progress in Food and Nutrition Science, Vol. 6. Gums and Stabilisers for the Food Industry. Interactions of Hydrocolloids**" (Eds. Phillips, G.O., Wedlock, D.J. and Williams, P.A.) Pergamon Press. pp.149-160.

Clark, A.H. and Ross-Murphy, S.B. (1987) Structural and mechanical properties of biopolymer gels. **Advances in Polymer Science**, 83, 57-192.

Clark, R.C. (1988) Viscoelastic response of xanthan gum/guar gum blends. In "**Gums and Stabilisers for the Food Industry** 4." (Eds. Phillips, G.O., Wedlock, D.J. and Williams, P.A.) IRL Press, Oxford. pp.165-172.

Corey, R.R and Starr, M.P. (1957) Colony types of *Xanthomonas phaseoli*. **Journal of Bacteriology**, 74, 137-140.

Cottrell, I.W. and Kang, K.S. (1978) Xanthan gum, a unique bacterial polysaccharide for food applications. In "**Developments in Industrial Microbiology**", Vol. 19 (Ed. Underkofler, L.A.) Publication of the Society for Industrial Microbiology, Washington D.C. pp.117-131.

Coviello, T., Kajiwara, K., Burchard, W., Dentini, M. and Crescenzi, V. (1986) Solution properties of xanthan. 1. Dynamic and static light scattering from native and modified xanthans in dilute solutions. **Macromolecules**, 19, 2826-2831.

Cuvelier, G. and Launay, B. (1986) Concentration regimes in xanthan gum solutions deduced from flow and viscoelastic properties. **Carbohydrate Polymers**, 6, 321-333.

Darke, A., Morris, E.R., Rees, D.A. and Welsh, E.J. (1978) Spectroscopic characterisation of order-disorder transitions for extracellular polysaccharides of *Arthrobacter* species. **Carbohydrate Research**, 66, 133-144.

Davidson, I.W. (1978) Production of polysaccharide by *Xanthomonas campestris* in continuous culture. **FEMS Microbiology Letters**, 3, 347-349.

Dea, I.C.M., McKinnon, A.A. and Rees, D.A. (1972) Tertiary and quaternary structure in aqueous polysaccharide systems which model cell wall cohesion: Reversible changes in conformation and association of agarose, carrageenan and galactomannans. **Journal of Molecular Biology**, 68, 153-172.

Dea, I.C.M. and Morrison, A. (1975) Chemistry and interactions of seed galactomannans. In "**Advances in Carbohydrate Chemistry and Biochemistry**, 31" (Eds. Tipson, R.S. and Horton, D.) Academic Press. pp.241-312.

Dea, I.C.M. and Morris, E.R. (1977) Synergistic xanthan gels. In "**American Chemical Society Symposium Series No.**45. **Extracellular Microbial Polysaccharides**" (Eds. Sandford, P.A. and Laskin, A.) American Chemical Society, Washington D.C. pp.174-182.

Dea, I.C.M., Morris, E.R., Rees, D.A., Welsh, E.J., Barnes, H.A. and Price, J. (1977) Associations of like and unlike polysaccharides: Mechanism and specificity in galactomannans, interacting bacterial polysaccharides and related systems. **Carbohydrate Research**, 57, 249-272.

Dea, I.C.M. (1981) Specificity of interactions between polysaccharide helices and β-1,4-linked polysaccharides. In "**American Chemical Society Symposium Series No.** 150. **Solution Properties of Polysaccharides**" (Ed. Brant, D.A.) American Chemical Society, Washington D.C. pp.439-454.

Dea, I.C.M., Clark, A.H. and McCleary, B.V. (1986) Effect of galactose substitution patterns on the interaction properties of galactomannans. **Carbohydrate Research**, 147, 275-294.

Dentini, M., Crescenzi, V. and Blasi, D. (1984) Conformational properties of xanthan derivatives in dilute aqueous solution. **International Journal of Biological Macromolecules**, 6, 93-98.

Dey, P.M. (1978) Biochemistry of plant galactomannans. In "**Advances in Carbohydrate Chemistry and Biochemistry**, 35" (Eds. Tipson, R.S. and Horton, D.) Academic Press Inc. pp.341-376.

Dintzis, F.R., Babcock, G.E. and Tobin, R. (1970) Studies on dilute solutions and dispersions of the polysaccharide from *Xanthomonas campestris* NRRL B-1459. **Carbohydrate Research**, 13, 257-267.

Dubois, M., Gilles, K.A., Hamilton, J.K., Rebers, P.A. and Smith, F. (1956) Colorimetric method for determination of sugars and related substances. **Analytical Chemistry**, 28, 350-356.

Duckworth, M. and Yaphe, W. (1970) Definitive assay for pyruvic acid in agar and other algal polysaccharides. **Chemistry and Industry**, 23, 747-748.

Dye, D.W. and Lelliot, R.A. (1974) In "**Bergey's Manual of Determinative Bacteriology**", 8th Ed. (Eds. Buchanan, R.E. and Gibbons, N.E.) The Williams and Wilkins Company, Baltimore. pp.243-249.

Ellwood, D.C. and Tempest, D.W. (1972) Effects of environment on bacterial wall content and composition. **Advances in Microbial Physiology**, 7, 83-117.

European Economic Community (1974) European Economic Community Emulsifier/ Stabilizer Test, Annex II. EEC, Brussels.

Evans, C.G.T., Yeo, R.G. and Ellwood, D.C. (1979) Continuous culture studies on the production of extracellular polysaccharides by *Xanthomonas juglandis*. In "**Special Publications of the Society for General Microbiology 3. Microbial Polysaccharides and Polysaccharases**" (Eds. Berkeley, R.C.W., Gooday, G.W. and Ellwood, D.C.) Academic Press, London. pp.51-68.

Fett, W.F. and Osman, S.F. (1985) Purification and characterization of *Xanthomonas campestris* pv. *glycines* exopolysaccharide. **Plant Science**, 40, 99-103.

Frangou, S.A., Morris, E.R., Rees, D.A., Richardson, R.K. and Ross-Murphy, S.B. (1982) Molecular origin of xanthan solution rheology: Effect of urea on chain conformation and interactions. **Journal of Polymer Science: Polymer Letters Edition**, 20, 531-538.

Gaisford, S.E., Harding, S.E., Mitchell, J.R. and Bradley, T.D. (1986) A comparison between the hot and cold water soluble fractions of two locust bean gum samples. **Carbohydrate Polymers**, 6, 423-442.

Gabriel, A. (1979) Economic value of biopolymers and their use in enhanced oil recovery. In "**Special Publications of the Society for General Microbiology 3. Microbial Polysaccharides and Polysaccharases**" (Eds. Berkeley, R.C.W., Gooday, G.W. and Ellwood, D.C.) Academic Press, London. pp.191-204.

Garegg, P.J., Jansson, P.-E., Lindberg, B., Lindh, F. and Lönngren, J. (1980) Configuration of the acetal carbon atom of pyruvic acid acetals in some bacterial polysaccharides. **Carbohydrate Research**, 78, 127-132.

Garrett, C.M.E. (1982) Bacterial diseases of food plants - an overview. In "**The Society for Applied Bacteriology Symposium Series No. 10. Bacteria and Plants**" (Eds. Rhodes-Roberts, M.E. and Skinner, F.A.) Academic Press. pp.115-132.

Godet, P. (1973) Fermentation of Polysaccharide gums. **Process Biochemistry**, 8, 33-34.

Gorin, P.A.J. and Spencer, J.F.T. (1961) Structural relationships of extracellular polysaccharides from phytopathogenic *Xanthomonas* spp. Part I. Structure of the extracellular polysaccharide from *Xanthomonas stewartii*. **Canadian Journal of Chemistry**, 39, 2282-2289.

Gorin, P.A.J. and Spencer, J.F.T. (1963) Structural relationships of extracellular polysaccharides from phytopathogenic *Xanthomonas* spp. Part II. *X. hyacinthi*, *X. translucens* and *X. maculofoliigardeniae*. **Canadian Journal of Chemistry**, 41, 2357-2361.

Gorin, P.A.J., Ishikawa, T., Spencer, J.F.T. and Sloneker, J.H. (1967) Configuration of the pyruvic acid ketals, 4,6-O-linked to D-glucose units, in *Xanthomonas campestris* polysaccharide. **Canadian Journal of Chemistry**, 45, 2005-2008.

Grant, G.T., Morris, E.R., Rees, D.A., Smith, P.J.C. and Thom, D. (1973) Biological interactions between polysaccharides and divalent cations: The egg-box model. **FEBS Letters**, 32, 195-198.

Grasdalen, H. and Painter, T. (1980) N.M.R. studies of composition and sequence in legume-seed galactomannans. **Carbohydrate Research**, 81, 59-66.

Gravanis, G., Milas, M., Rinaudo, M. and Tinland, B. (1987) Comparative behaviour of the bacterial polysaccharides xanthan and succinoglycan. **Carbohydrate Research**, 160, 259-265.

Gumbmann, M.R. (1964) Metabolism of C-14 polysaccharide, B-1459, by the rat. United States Department of Agriculture, Western Regional Laboratory. Unpublished Report.

Hacche, L.S., Washington, G.E. and Brant, D.A. (1987) Light-scattering investigation of the temperature-driven conformation change in xanthan. **Macromolecules**, 20, 2179-2187.

Harding, N.E., Cleary, J.M., Cabañas, D.K., Rosen, I.G. and Kang, K.S. (1987) Genetic and physical analyses of a cluster of genes essential for xanthan gum biosynthesis in *Xanthomonas campestris*. **Journal of Bacteriology**, 169, 2854-2861.

Hestrin, S. (1949) The reaction of acetylcholine and other carboxylic acid derivatives with hydroxylamine, and its analytical application. **Journal of Biological Chemistry**, 180, 249-261.

Hjelm Jr., R.P., Thiyagarajan, P. and Johnson, M.E. (1986) CD of gels and suspensions: Apparent CD in the soret region of sickle hemoglobin gels. **Biopolymers**, 25, 1359-1378.

Hoffman, J. and Svensson, S. (1978) Studies of the distribution of the D-galactosyl side-chains in guaran. **Carbohydrate Research**, 65, 65-71.

Holzwarth, G. (1976) Conformation of the extracellular polysaccharide of *Xanthomonas campestris*. **Biochemistry**, 15, 4333-4339.

Holzwarth, G. and Prestridge, E.B. (1977) Multistranded helix of xanthan polysaccharide. **Science**, 197, 757-759.

Holzwarth, G. (1978) Molecular weight of xanthan polysaccharide. **Carbohydrate Research**, 66, 173-186.

Holzwarth, G. and Ogletree, J. (1979) Pyruvate-free xanthan. **Carbohydrate Research**, 76, 277-280.

Holzwarth, G.M. (1981) Is xanthan a wormlike chain or a rigid rod? In **"American Chemical Society Symposium Series No. 150. Solution Properties of Polysaccharides"** (Ed. Brant, D.A.) American Chemical Society, Washington D.C. pp.15-23.

Horton, D., Mols, O., Walaszek, Z. and Wernau, W.C. (1985) Structural and biosynthetic studies on xanthan by ^{13}C-n.m.r. spectroscopy. **Carbohydrate Research**, 141, 340-346.

Humaydan, H.S., Harman, G.E., Nedrow, B.L. and DiNitto, L.V. (1980) Eradication of *Xanthomonas campestris*, the causal agent of black rot, from Brassica seeds with antibiotics and sodium hypochlorite. Phytopathology, 70, Part 1, 127-131.

Ielpi, L., Couso, R. and Dankert, M. (1981a) Lipid-linked intermediates in the biosynthesis of xanthan gum. **FEBS Letters**, 130, 253-256.

Ielpi, L., Couso, R.O. and Dankert, M.A. (1981b) Xanthan gum biosynthesis. Pyruvic acid acetal residues are transferred from phosphoenolpyruvate to the pentasaccharide-P-P-lipid. **Biochemical and Biophysical Research Communications**, 102, 1400-1408.

Ielpi, L., Couso, R.O. and Dankert, M.A. (1983) Xanthan gum biosynthesis. Acetylation occurs at the prenyl-phospo-sugar stage. **Biochemistry International**, 6, 323-333.

Jansson, P.-E., Kenne, L. and Lindberg, B. (1975) Structure of the extracellular polysaccharide from *Xanthomonas campestris*. **Carbohydrate Research**, 45, 275-282.

Janus, J.W. / Flory, P.J. (1974) **Faraday Discussions of the Chemical Society 57. Gels and Gelling Processes**, 279.

Jeanes, A., Pittsley, J.E. and Senti, F.R. (1961) Polysaccharide B-1459: A new hydrocolloid polyelectrolyte produced from glucose by bacterial fermentation. **Journal of Applied Polymer Science**, 5, 519-526.

Jeanes, A.R. and Sloneker, J.H. (1962) Atypical salt-responsive alkali-deacetylated polysaccharides. US Patent No. 3,000,790. **Chemical Abstracts**, 56, 2625d.

Jeanes, A. (1974) Applications of extracellular microbial polysaccharide-polyelectrolytes: Review of the literature, including patents. **Journal of Polymer Science: Symposium No.** 45, 209-227.

Jeanes, A., Rogovin, P., Cadmus, M.C., Silman, R.W. and Knutson, C.A. (1976) Polysaccharide (xanthan) of *Xanthomonas campestris* NRRL B-1459: Procedures for culture maintainance and polysaccharide production, purification and analysis. ARS-NC-51, Agricultural Research Service, North Central Region, US Department of Agriculture, Washington D.C. pp.1-14

Kato, K., Watanabe, T. and Matsuda, K. (1970) Studies on the chemical structure of konjac mannan part II. Isolation and characterization of oligosaccharides from the enzymatic hydrolyzate of the mannan. **Agricultural and Biological Chemistry**, 34, 532-539.

Kato, K. and Matsuda, K. (1973) Isolation of oligosaccharides corresponding to the branching-point of konjac mannan. **Agricultural and Biological Chemistry**, 37, 2045-2051.

Kennedy, J.F., Barker, S.A., Bradshaw, I.J. and Jones, P. (1981a) The isolation of xanthan gum from fermentations of *Xanthomonas campestris* by complexation with quaternary ammonium salts. **Carbohydrate Polymers**, 1, 55-66.

Kennedy, J.F., Barker, S.A., Jones, P. and Bradshaw, I.J. (1981b) Reaction of $PHMBH^{+}Cl^{-}$ with acidic polysaccharides, and its application to the purification of xanthan gum. **Carbohydrate Polymers**, 1, 85-99.

Kennedy, J.F., Jones, P. and Barker, S.A. (1982) Factors affecting microbial growth and polysaccharide production during the fermentation of *Xanthomonas campestris* cultures. **Enzyme and Microbial Technology**, 4, 39-43.

Kennedy, J.F., Stevenson, D.L., White, C.A., Tolley, M.S. and Bradshaw, I.J. (1984) A simple ^{1}H N.m.r. method for the quantitation of O-acetate ester and pyruvic acid acetal content of polymeric xanthan gum and related polysaccharides. **British Polymer Journal**, 16, 5-10.

Kidby, D., Sandford, P., Herman, A. and Cadmus, M. (1977) Maintainance procedures for the curtailment of genetic instability: *Xanthomonas campestris* NRRL B-1459. **Applied and Environmental Microbiology**, 33, 840-845.

Kierulf, C. and Sutherland, I.W. (1988) Thermal stability of xanthan preparations. **Carbohydrate Polymers**, 9, 185-194.

Kishida, N., Okimasu, S. and Kamata, T. (1978) Molecular weight and intrinsic viscosity of konjac gluco-mannan. **Agricultural and Biological Chemistry**, 42, 1645-1650.

Kornfeld, R.H. and Ginsburg, V. (1966) Control of synthesis of guanosine-diphosphate-D-mannose and guanosinediphosphate-L-fucose in bacteria. **Biochimica et Biophysica Acta**, 117, 79-87.

Kovacs, P. (1973) Useful incompatibility of xanthan gum with galacto-mannans. **Food Technology**, 27, March, 26-30.

Kovacs, P. and Kang, K.S. (1977) Xanthan gum. In "**Food Colloids**" (Ed. Graham, H.D.) The Avi Publishing Company, Inc., Westport, Connecticut.

Lambert, F., Milas, M. and Rinaudo, M. (1982) Gel permeation chromatography of the xanthan gum using a light scattering detector. **Polymer Bulletin**, 7, 185-189.

Launay, B., Cuvelier, G. and Martinez-Reyes, S. (1984) Xanthan gum in various solvent conditions: Intrinsic viscosity and flow properties. In "**Gums and Stabilisers for the Food Industry 2. Application of Hydrocolloids**" (Eds. Phillips, G.O., Wedlock, D.J. and Williams, P.A.) Pergamon Press. pp.79-98.

Lawson, C.J. and Symes, K.C. (1977a) Oligosaccharides produced by partial acetolysis of xanthan gum. **Carbohydrate Research**, 58, 433-438.

Lawson, C.J. and Symes, K.C. (1977b) Xanthan gum - acetolysis as a tool for the elucidation of structure. In "**American Chemical Society Symposium Series No. 45. Extracellular Microbial Polysaccharides**" (Eds. Sandford, P.A. and Laskin, A.) American Chemical Society, Washington D.C. pp.183-191.

Leach, J.G., Lilly, V.G., Wilson, H.A. and Purvis Jr., M.R. (1957) Bacterial polysaccharides: The nature and function of the exudate produced by *Xanthomonas phaseoli*. **Phytopathology**, 47, 113-120.

Lecourtier, J., Chauveteau, G. and Muller, G. (1986) Salt-induced extension and dissociation of a native double-stranded xanthan. **International Journal of Biological Macromolecules**, 8, 306-310.

Lehrfeld, J. (1981) Differential gas-liquid chromatography method for determination of uronic acids in carbohydrate mixtures. **Analytical Biochemistry**, 115, 410-418.

Lilly, V.G., Wilson, H.A. and Leach, J.G. (1958) Bacterial polysaccharides II. Laboratory-scale production of polysaccharides by species of *Xanthomonas*. **Applied Microbiology**, 6, 105-108.

Lim, T., Uhl, J.T. and Prud'homme, R.K. (1984) Rheology of self-associating concentrated xanthan solutions. **Journal of Rheology**, 28, 367-379.

Lipps Jr., B.J. (1966) Fermentation of polysaccharides. US Patent No. 3,251,749. **Chemical Abstracts**, 65, 2969g.

Liu, W., Sato, T., Norisuye, T. and Fujita, H. (1987) Thermally induced conformational change of xanthan in 0.01M aqueous sodium chloride. **Carbohydrate Research**, 160, 267-281.

Liu, W. and Norisuye, T. (1988) Thermally induced conformation change of xanthan: Interpretation of viscosity behaviour in 0.01M aqueous sodium chloride. **International Journal of Biological Macromolecules**, 10, 44-49.

Maekaji, K. (1974) The mechanism of gelation of konjac mannan. **Agricultural and Biological Chemistry**, 38, 315-321.

Maret, G., Milas, M. and Rinaudo, M. (1981) Cholesteric order in aqueous solutions of the polysaccharide xanthan. **Polymer Bulletin**, 4, 291-297.

Markovitz, A. (1977) Genetics and regulation of bacterial capsular polysaccharide biosynthesis and radiation sensitivity. In "**Surface Carbohydrates of the Prokaryotic Cell**" (Ed. Sutherland, I.W.) Academic Press, London. pp.415-462.

McCleary, B.V. (1979) Enzymic hydrolysis, fine structure, and gelling interaction of legume-seed D-galacto-D-mannans. **Carbohydrate Research**, 71, 205-230.

McCleary, B.V., Amado, R., Waibel, R. and Neukom, H. (1981) Effect of galactose content on the solution and interaction properties of guar and carob galactomannans. **Carbohydrate Research**, 92, 269-285.

McCleary, B.V., Nurthen, E., Taravel, F.R. and Joseleau, J.-P. (1983) Characterisation of the oligosaccharides produced on hydrolysis of galactomannan with β-D-mannanase. **Carbohydrate Research**, 118, 91-109.

McCleary, B.V., Dea, I.C.M., Windust, J. and Cooke, D. (1984) Interaction properties of D-galactose-depleted guar galactomannan samples. **Carbohydrate Polymers**, 4, 253-270.

McCleary, B.V., Clark, A.H., Dea, I.C.M. and Rees, D.A. (1985) The fine structure of carob and guar galactomannans. **Carbohydrate Research**, 139, 237-260.

McNeely, W.H. and O'Connell, J.J. (1966) Process for producing *Xanthomonas* hydrophilic colloid. US Patent No. 3,232,929. **Chemical Abstracts**, 64, 14878d.

McNeely, W.H. and Kang, K.S. (1973) Xanthan and some other biosynthetic gums. In "**Industrial Gums. Polysaccharides and their Derivatives**" 2nd Ed. (Ed. Whistler, R.L.) Academic Press. pp.473-497.

McNeely, W.H. and Kovacs, P. (1975) The physiological effects of alginates and xanthan gum. In "**American Chemical Society Symposium Series No. 15. Physiological Effects of Food Carbohydrates**" (Eds. Jeanes, A. and Hodge, J.) American Chemical Society, Washington D.C. pp.269-281.

Meier, H. and Reid, J.S.G. (1982) Reserve polysaccharides other than starch in higher plants. In "**Encyclopedia of Plant Physiology 13A**" (Eds. Pirson, A. and Zimmermann, M.H.) Springer-Verlag. pp.418-471.

Melton, L.D., Mindt, L., Rees, D.A. and Sanderson, G.R. (1976) Covalent structure of the extracellular polysaccharide from *Xanthomonas campestris*: Evidence from partial hydrolysis studies. Carbohydrate Research, 46, 245-257.

Midgley, M. and Dawes, E.A. (1973) The regulation of transport of glucose and methylglucoside in *Pseudomonas aeruginosa*. Biochemical Journal, 132, 141-154.

Milas, M. and Rinaudo, M. (1979) Conformational investigation on the bacterial polysaccharide xanthan. Carbohydrate Research, 76, 189-196.

Milas, M. and Rinaudo, M. (1981) Investigation on conformational properties of xanthan in aqueous solutions. In "American Chemical Society **Symposium Series No. 150. Solution Properties of Polysaccharides**" (Ed. Brant, D.A.) American Chemical Society, Washington D.C. pp.25-30.

Milas, M. and Rinaudo, M. (1984) On the existence of two different secondary structures for the xanthan in aqueous solutions. **Polymer Bulletin**, 12, 507-514.

Milas, M. and Rinaudo, M. (1986) Properties of xanthan gum in aqueous solutions: Role of the conformational transition. **Carbohydrate Research**, 158, 191-204.

Miles, M.J., Morris, V.J. and Carroll, V. (1984) Carob gum-χ-carrageenan mixed gels: Mechanical properties and X-ray fiber diffraction studies. **Macromolecules**, 17, 2443-2445.

Moorhouse, R., Walkinshaw, M.D., Winter, W.T. and Arnott, S. (1977a) Solid state conformations and interactions of some branched microbial polysaccharides. In "**American Chemical Society Symposium Series No. 48. Cellulose Chemistry and Technology**" (Ed. Arthur Jr., J.C.) American Chemical Society, Washington D.C. pp.133-152.

Moorhouse, R., Walkinshaw, M.D. and Arnott, S. (1977b) Xanthan gum - molecular conformation and interactions. In "**American Chemical Society Symposium Series No. 45. Extracellular Microbial Polysaccharides**" (Eds. Sandford, P.A. and Laskin, A.) American Chemical Society, Washington D.C. pp.90-102.

Moorhouse, R., Colegrove, G.T., Sandford, P.A., Baird, J.K. and Kang, K.S. (1981) PS-60: A new gel-forming polysaccharide. In "**American Chemical Society Symposium Series No. 150. Solution Properties of Polysaccharides**" (Ed. Brant, D.A.) American Chemical Society, Washington D.C. pp.111-124.

Moraine, R.A. and Rogovin, P. (1966) Kinetics of polysaccharide B-1459 fermentation. **Biotechnology and Bioengineering**, 8, 511-524.

Morris, E.R. (1977) Molecular origin of xanthan solution properties. In "**American Chemical Society Symposium Series No. 45. Extracellular Microbial Polysaccharides**" (Eds. Sandford, P.A. and Laskin, A.) American Chemical Society, Washington D.C. pp.81-89.

Morris, E.R., Rees, D.A., Young, G., Walkinshaw, M.D. and Darke, A. (1977a) Order-disorder transition for a bacterial polysaccharide in solution. A role for polysaccharide conformation in recognition between *Xanthomonas* pathogen and its plant host. Journal of Molecular Biology, 110, 1-16.

Morris, E.R., Rees, D.A., Thom, D. and Welsh, E.J. (1977b) Conformation and intermolecular interactions of carbohydrate chains. **Journal of Supramolecular Structure**, 6, 259-274.

Morris, E.R.,Rees, D.A., Thom, D. and Boyd, J. (1978) Chiroptical and stoichiometric evidence of a specific primary dimerisation process in alginate gelation. **Carbohydrate Research**, 66, 145-154.

Morris, E.R., Rees, D.A. and Robinson, G. (1980) Cation-specific aggregation of carrageenan helices: Domain model of polymer gel structure. **Journal of Molecular Biology**, 138, 349-362.

Morris, E.R., Cutler, A.N., Ross-Murphy, S.B., Rees, D.A. and Price, J. (1981) Concentration and shear rate dependence of viscosity in random coil polysaccharide solutions. **Carbohydrate Polymers**, 1, 5-21.

Morris, E.R. and Frangou, S.A. (1981) Application of circular dichroism and optical rotatory dispersion techniques to carbohydrate systems. **Techniques in Carbohydrate Metabolism**, B308, 1-51.

Morris, E.R. and Ross-Murphy, S.B. (1981) Chain flexibility of polysaccharides and glycoproteins from viscosity measurements. **Techniques in Carbohydrate Metabolism**, B310, 1-46.

Morris, E.R. (1984) Rheology of Hydrocolloids. In "**Gums and Stabilisers for the Food Industry 2. Application of Hydrocolloids**" (Eds. Phillips, G.O., Wedlock, D.J. and Williams, P.A.) Pergamon Press. pp.57-78.

Morris, V.J., Franklin, D. and I'Anson, K. (1983) Rheology and micro-structure of dispersions and solutions of the microbial polysaccharide from *Xanthomonas campestris* (xanthan gum). Carbohydrate Research, 121, 13-30.

Morris, V.J. and Chilvers, G.R. (1984) Cold setting alginate-pectin gels. **Journal of the Science of Food and Agriculture**, 35, 1370-1376.

Morris, V.J. and Miles, M.J. (1986) Effect of natural modifications on the functional properties of extracellular bacterial polysaccharides. **International Journal of Biological Macromolecules**, 8, 342-348.

Muller, G., Lecourtier, J., Chauveteau, G. and Allain, C. (1984) Conformation of the xanthan molecule in an ordered structure. **Makromolekulare Chemie. Rapid Communications**, 5, 203-208.

Muller, G., Anrhourrache, M., Lecourtier, J. and Chauveteau, G. (1986) Salt dependence of the conformation of a single-stranded xanthan. **International Journal of Biological Macromolecules**, 8, 167-172.

Nisbet, B.A., Sutherland, I.W., Bradshaw, I.J., Kerr, M., Morris, E.R. and Shepperson, W.A. (1984) XM-6: A new gel-forming bacterial polysaccharide. **Carbohydrate Polymers**, 4, 377-394.

Norton, I.T., Goodall, D.M., Morris, E.R. and Rees, D.A. (1980) Kinetic evidence for intramolecular conformational ordering of the extracellular polysaccharide (xanthan) from *Xanthomonas campestris*. **Journal of the Chemical Society. Chemical Communications**, 545-547.

Norton, I.T., Goodall, D.M., Frangou, S.A., Morris, E.R. and Rees, D.A. (1984) Mechanism and dynamics of conformational ordering in xanthan polysaccharide. **Journal of Molecular Biology**, 175, 371-394.

Odijk, T. (1977) Polyelectrolytes near the rod limit. **Journal of Polymer Science, Polymer Physics Edition**, 15, 477-483.

Okuyama, K., Arnott, S., Moorhouse, R., Walkinshaw, M.D., Atkins, E.D.T. and Wolf-Ullish, C. (1980) Fiber-diffraction studies of bacterial polysaccharides. In "**American Chemical Society Symposium Series No. 141. Fiber-Diffraction Methods**" (Eds. French, A.D. and Gardner, K.H.) American Chemical Society, Washington D.C. pp.411-427.

O'Neill, M.A., Morris, V.J., Selvendran, R.R., Sutherland, I.W. and Taylor, I.T. (1986) Structure of the extracellular gelling polysaccharide produced by *Enterobacter* (NCIB 11870) species. **Carbohydrate Research**, 148, 63-69.

Orentas, D.G., Sloneker, J.H. and Jeanes, A. (1963) Pyruvic acid content and constituent sugars of exocellular polysaccharides from different species of the genus *Xanthomonas*. **Canadian Journal of Microbiology**, 9, 427-430.

Painter, T.J., González, J.J. and Hemmer, P.C. (1979) The distribution of D-galactosyl groups in guaran and locust bean gum: New evidence from periodate oxidation. **Carbohydrate Research**, 69, 217-226.

Paoletti, S., Cesàro, A. and Delben, F. (1983) Thermally induced conformational transition of xanthan polyelectrolyte. **Carbohydrate Research**, 123, 173-178.

Paradossi, G. and Brant, D.A. (1982) Light scattering study of a series of xanthan fractions in aqueous solution. **Macromolecules**, 15, 874-879.

Parry, R.W.H. (1985) *Xanthomonas* Infections of Rice; The Involvement of Bacterial Extracellular Polysaccharide. PhD Thesis. University of Leeds.

Patton, J.T. and Lindblom, G.P. (1962) Heteropolysaccharide synthesis by bacteria. US Patent No. 3,020,206. **Chemical Abstracts**, 56, 12094d.

Patton, J.T. and Dugar, S.K. (1981) Growth kinetics of *Xanthomonas campestris* B-1459. **Process Biochemistry**, 16, 46-49.

Pérez, S. and Vergelati, C. (1987) Molecular modelling of the xanthan chain conformations. **International Journal of Biological Macromolecules**, 9, 211-218.

Pettitt, J. (1979) Xanthan gum. In "**Polysaccharides in Food**" (Eds. Blanshard, J.M.V. and Mitchell, J.R.) Butterworths. pp.263-282.

Pezron, E., Ricard, A., Lafuma, F. and Audebert, R. (1988a) Reversible gel formation induced by ion complexation. I. Borax-galactomannan interactions. **Macromolecules**, 21, 1121-1125.

Pezron, E., Leibler, L., Ricard, A. and Audebert, R. (1988b) Reversible gel formation induced by ion complexation. 2. Phase diagrams. **Macromolecules**, 21, 1126-1131.

Philips, J.C., Miller, J.W., Wernau, W.C., Tate, B.E. and Auerbachi, M.H. (1982) A new high-pyruvate xanthan for enhanced oil recovery. SPE 10617, Sixth International Symposium on Oilfield and Geometrical Chemistry, Dallas, Texas.

Pippen, E.L., McCready, R.M. and Owens, H.S. (1950) Gelation properties of partially acetylated pectins. **Journal of the American Chemical Society**, 72, 813-816.

Rees, D.A. (1970) Conformational analysis of polysaccharides. Part V. The characterization of linkage conformations (chain conformations) by optical rotation at a single wavelength. Evidence for distortion of cyclohexaamylose in aqueous solution. Optical rotation and the amylose conformation. **Journal of the Chemical Society. Section B. Physical Organic Chemistry**. Part 1, 877-884.

Rees, D.A. (1981) Polysaccharide shapes and their interactions - some recent advances. **Pure and Applied Chemistry**, 53, 1-14.

Reid, J.S.G. (1985) Galactomannans. In "**Biochemistry of Storage Carbohydrates in Green Plants**" (Eds. Dey, P.M. and Dixon, R.A.) Academic Press. pp.265-288.

Richardson, R.K. and Ross-Murphy, S.B. (1981) Mechanical properties of globular protein gels: 1. Incipient gelation behaviour. **International Journal of Biological Macromolecules**, 3, 315-322.

Richardson, R.K. and Ross-Murphy, S.B. (1987a) Non-linear viscoelasticity of polysaccharide solutions. 1: Guar galactomannan solutions. **International Journal of Biological Macromolecules**, 9, 250-256.

Richardson, R.K. and Ross-Murphy, S.B. (1987b) Non-linear viscoelasticity of polysaccharide solutions. 2: Xanthan polysaccharide solutions. **International Journal of Biological Macromolecules**, 9, 257-264.

Rinaudo, M. and Milas, M. (1978) Polyelectrolyte behaviour of a bacterial polysaccharide from *Xanthomonas campestris*: Comparison with carboxymethylcellulose. **Biopolymers**, 17, 2663-2678.

Rinaudo, M., Milas, M., Lambert, F. and Vincendon, M. (1983) ^{1}H and ^{13}C NMR investigation of xanthan gum. **Macromolecules**, 16, 816-819.

Robbins, D.J., Moulton, J.E. and Booth, A.N. (1964) Subacute toxicity study of a microbial polysaccharide fed to dogs. **Food and Cosmetics Toxicology**, 2, 545-550.

Roberts, B.K., Midgley, M. and Dawes, E.A. (1973) The metabolism of 2-oxogluconate by *Pseudomonas aeruginosa*. **Journal of General Microbiology**, 78, 319-329.

Robinson, G., Ross-Murphy, S.B. and Morris, E.R. (1982) Viscosity-molecular weight relationships, intrinsic chain flexibility, and dynamic solution properties of guar galactomannan. **Carbohydrate Research**, 107, 17-32.

Rochefort, W.E. and Middleman, S. (1987) Rheology of xanthan gum: Salt, temperature, and strain effects in oscillatory and steady shear experiments. **Journal of Rheology**, 31, 337-369.

Rocks, J.K. (1971) Xanthan gum. **Food Technology**, 25, May, 476-483.

Rogovin, S.P., Anderson, R.F. and Cadmus, M.C. (1961) Production of polysaccharide with *Xanthomonas campestris*. **Journal of Biochemical and Microbiological Technology and Engineering**, 3, 51-63.

Rogovin, S.P. and Albrecht, W.J. (1964) Recovering microbial polysaccharides from their fermentation broths. US Patent No. 3,119,812. **Chemical Abstracts**, 60, 11348f.

Rogovin, P., Albrecht, W. and Sohns, V. (1965) Production of industrial-grade polysaccharide B-1459. **Biotechnology and Bioengineering**, 7, 161-169.

Ross-Murphy, S.B., Morris, V.J. and Morris E.R. (1983) Molecular viscoelasticity of xanthan polysaccharide. **Faraday Symposium of the Chemical Society**, 18, 115-129.

Ross-Murphy, S.B. (1984) Rheological methods. In "**Critical Reports on Applied Chemistry Vol 5. Biophysical Methods in Food Research**" (Ed. Chan, H.W.-S.) Blackwell Scientific Publications. pp.138-199.

Saier Jr., M.H. (1985) **"Mechanisms and Regulation of Carbohydrate Transport in Bacteria"** Academic Press Inc.

Salamone, J.C., Clough, S.B., Beal Salamone, A., Reid, K.I.G. and Jamison, D.E. (1982) Xanthan gum - a lyotropic, liquid crystalline polymer and its properties as a suspending agent. **Society of Petroleum Engineers Journal**, 22, 555-556.

Sandford, P.A., Pittsley, J.E., Knutson, C.A., Watson, P.R., Cadmus, M.C. and Jeanes, A. (1977) Variation in *Xanthomonas campestris* NRRL B-1459: Characterization of xanthan products of differing pyruvic acid content. In **"American Chemical Society Symposium Series No. 45. Extracellular Microbial Polysaccharides"** (Eds. Sandford, P.A. and Laskin, A.) American Chemical Society, Washington D.C. pp.192-210.

Sandford, P.A., Watson, P.R. and Knutson, C.A. (1978) Separation of xanthan gums of differing pyruvate content by fractional precipitation with alcohol. **Carbohydrate Research**, 63, 253-256.

Sandford, P.A. and Baird, J. (1983) Industrial utilization of polysaccharides. In **"The Polysaccharides"** Vol 2 (Ed. Aspinall, G.O.) Academic Press. pp.411-490.

Sandvik, E.I. and Maerker, J.M. (1977) Application of xanthan gum for enhanced oil recovery. In **"American Chemical Society Symposium Series No. 45. Extracellular Microbial Polysaccharides"** (Eds. Sandford, P.A. and Laskin, A.) American Chemical Society, Washington D.C. pp.242-264.

SAS Users Guide: Statistics. Version 5 Edition (1985) SAS Institute Inc., Cary, North Carolina, USA.

Sato, T., Norisuye, T. and Fujita, H. (1984a) Double-stranded helix of xanthan: Dimensional and hydrodynamic properties in 0.1M aqueous sodium chloride. **Macromolecules**, 17, 2696-2700

Sato, T., Norisuye, T. and Fujita, H. (1984b) Double-stranded helix of xanthan in dilute solution: Evidence from light scattering. **Polymer Journal**, 16, 341-350.

Sato, T., Kojima, S., Norisuye, T. and Fujita, H. (1984c) Double-stranded helix of xanthan in dilute solution: Further evidence. **Polymer Journal**, 16, 423-429.

Sawardeker, J.S., Sloneker, J.H. and Jeanes, A. (1965) Quantitative determination of monosaccharides as their alditol acetates by gas liquid chromatography. **Analytical Chemistry**, 37, 1602-1604.

Schaad, N.W. and Dianese, J.C. (1981) Cruciferous weeds as sources of inoculum of *Xanthomonas campestris* in black rot of crucifers. **Phytopathology**, 71, 1215-1220.

Schweiger, R.G. (1962) Acetylation of alginic acid. I. Preparation and viscosities of algin acetates. **Journal of Organic Chemistry**, 27, 1786-1789.

Shimahara, H., Suzuki, H., Sugiyama, N. and Nisizawa, K. (1975a) Isolation and characterization of oligosaccharides from an enzymic hydrolysate of konjac glucomannan. **Agricultural and Biological Chemistry**, 39, 293-299.

Shimahara, H., Suzuki, H., Sugiyama, N. and Nisizawa, K. (1975b) Partial purification of β-mannanases from the konjac tubers and their substrate specificity in relation to the structure of konjac glucomannan. **Agricultural and Biological Chemistry**, 39, 301-312.

Sho, T., Sato, T. and Norisuye, T. (1986) Viscosity behaviour and persistence length of sodium xanthan in aqueous sodium chloride. **Biophysical Chemistry**, 25, 307-313.

Siddiqui, I.R. (1967) An extracellular polysaccharide from *Xanthomonas campestris*. **Carbohydrate Research**, 4, 284-291.

Silman, R.W. and Rogovin, P. (1970) Continuous fermentation to produce xanthan biopolymer: Laboratory investigation. **Biotechnology and Bioengineering**, 12, 75-83.

Silman, R.W. and Rogovin, P. (1972) Continuous fermentation to produce xanthan biopolymer: Effect of dilution rate. **Biotechnology and Bioengineering**, 14, 23-31.

Skjak-Braek, G., Larsen, B. and Grasdalen, H. (1985) The role of O-acetyl groups in the biosynthesis of alginate by *Azotobacter vinelandii*. **Carbohydrate Research**, 145, 169-174.

Skolnick, J. and Fixman, M. (1977) Electrostatic persistence length of a wormlike polyelectrolyte. **Macromolecules**, 10, 944-948.

Sloneker, J.H. and Jeanes, A. (1962) Exocellular bacterial polysaccharide from *Xanthomonas campestris* NRRL B-1459. Part I: Constitution. **Canadian Journal of Chemistry**, 40, 2066-2071.

Sloneker, J.H. and Orentas, D.G. (1962a) Pyruvic acid, a unique component of an exocellular bacterial polysaccharide. **Nature**, 194, 478-479.

Sloneker, J.H. and Orentas, D.G. (1962b) Exocellular bacterial polysaccharide from *Xanthomonas campestris* NRRL B-1459. Part II: Linkage of the pyruvic acid. **Canadian Journal of Chemistry**, 40, 2188-2189.

Sloneker, J.H., Orentas, D.G. and Jeanes, A. (1964) Exocellular bacterial polysaccharide from *Xanthomonas campestris* NRRL B-1459. Part III: Structure. **Canadian Journal of Chemistry**, 42, 1261-1269.

Smidsrød, O. and Haug, A. (1971) Estimation of the relative stiffness of the molecular chain in polyelectrolytes from measurements of viscosity at different ionic strengths. **Biopolymers**, 10, 1213-1227.

Smidsrød, O. (1974) Molecular basis for some physical properties of alginates in the gel state. **Faraday Discussions of the Chemical Society, 57. Gels and Gelling Processes**, 263-274.

Smith, F. and Srivastava, H.C. (1959) Constitutional studies on the glucomannan of konjak flour. **Journal of the American Chemical Society**, 81, 1715-1718.

Smith, I.H., Symes, K.C., Lawson, C.J. and Morris, E.R. (1981) Influence of the pyruvate content of xanthan on macromolecular association in solution. **International Journal of Biological Macromolecules**, 3, 129-134.

Smith, I.H., Symes, K.C., Lawson, C.J. and Morris, E.R. (1984) The effect of pyruvate on xanthan solution properties. **Carbohydrate Polymers**, 4, 153-157.

Southwick, J.G., McDonnell, M.E., Jamieson, A.M. and Blackwell, J. (1979) Solution studies of xanthan gum employing quasielastic light scattering. **Macromolecules**, 12, 305-311.

Southwick, J.G., Lee, H., Jamieson, M. and Blackwell, J. (1980) Self-association of xanthan in aqueous solvent-systems. **Carbohydrate Research**, 84, 287-295.

Southwick, J.G., Jamieson, A.M. and Blackwell, J. (1981a) Quasi-elastic light scattering studies of semidilute xanthan solutions. **Macromolecules**, 14, 1728-1732.

Southwick, J.G., Jamieson, A.M. and Blackwell, J. (1981b) Quasielastic light-scattering studies of xanthan in solution. In "**American Chemical Society Symposium Series No. 150. Solution Properties of Polysaccharides**" (Ed. Brant, D.A.) American Chemical Society, Washington D.C. pp.1-13.

Souw, P. and Demain, A.L. (1979) Nutritional studies on xanthan production by *Xanthomonas campestris* NRRL B-1459. **Applied and Environmental Microbiology**, 37, 1186-1192.

Starr, M.P. (1946) The nutrition of phytopathogenic bacteria I. Minimal nutritive requirements of the genus *Xanthomonas*. **Journal of Bacteriology**, 51, 131-143.

Stinson, M.W., Cohen, M.A. and Merrick, J.M. (1977) Purification and properties of the periplasmic glucose-binding protein of *Pseudomonas aeruginosa*. **Journal of Bacteriology**, 131, 672-681.

Stokke, B.T., Elgsaeter, A. and Smidsrød, O. (1986) Electron microscopic study of single- and double-stranded xanthan. **International Journal of Biological Macromolecules**, 8, 217-225.

Sugiyama, N., Shimahara, H., Andoh, T., Takemoto, M. and Kamata, T. (1972) Molecular weights of konjac mannans of various sources. **Agricultural and Biological Chemistry**, 36, 1381-1387.

Sutherland, I.W. (1977) Microbial exopolysaccharide synthesis. In **"American Chemical Society Symposium Series No. 45. Extracellular Microbial Polysaccharides"** (Eds. Sandford, P.A. and Laskin, A.) American Chemical Society, Washington D.C. pp.40-57.

Sutherland, I.W. (1981a) *Xanthomonas* polysaccharides - improved methods for their comparison. **Carbohydrate Polymers**, 1, 107-115.

Sutherland, I.W. (1981b) Affinity column for separation of pyruvylated and non-pyruvylated polysaccharides. **Journal of Chromatography**, 213, 301-306.

Sutherland, I.W. (1984) Hydrolysis of unordered xanthan in solution by fungal cellulases. **Carbohydrate Research**, 131, 93-104.

Sutherland, I.W. and Kennedy, A.F.D. (1986) Comparison of bacterial lipopolysaccharides by high-performance liquid chromatography. **Applied and Environmental Microbiology**, 52, 948-950.

Sutton, J.C. and Williams, P.H. (1970a) Relation of xylem plugging to black rot lesion development in cabbage. **Canadian Journal of Botany**, 48, 391-401.

Sutton, J.C. and Williams, P.H. (1970b) Comparison of extracellular polysaccharide of *Xanthomonas campestris* from culture and from infected cabbage leaves. **Canadian Journal of Botany**, 48, 645-651.

Symes, K.C. (1980) The relationship between the covalent structure of the *Xanthomonas* polysaccharide (xanthan) and its function as a thickening, suspending and gelling agent. **Food Chemistry**, 6, 63-76.

Tait, M.I. (1984) Exopolysaccharide Production by *Xanthomonas campestris*. PhD Thesis. University of Edinburgh.

Tait, M.I., Sutherland, I.W. and Clarke-Sturman, A.J. (1986) Effect of growth conditions on the production, composition and viscosity of *Xanthomonas campestris* exopolysaccharide. **Journal of General Microbiology**, 132, 1483-1492.

Tako, M. and Nakamura, S. (1984) Rheological properties of deacetylated xanthan in aqueous media. **Agricultural and Biological Chemistry**, 48, 2987-2993.

Tako, M., Asato, A. and Nakamura, S. (1984) Rheological aspects of the intermolecular interaction between xanthan and locust bean gum in aqueous media. **Agricultural and Biological Chemistry**, 48, 2995-3000.

Tako, M. and Nakamura, S. (1985) Synergistic interaction between xanthan and guar gum. **Carbohydrate Research**, 138, 207-213.

Thom, D., Dea, I.C.M., Morris, E.R. and Powell, D.A. (1982) Interchain associations of alginate and pectins. In "**Progress in Food and Nutrition Science, Vol. 6. Gums and Stabilisers for the Food Industry. Interactions of Hydrocolloids**" (Eds. Phillips, G.O., Wedlock, D.J. and Williams, P.A.) Pergamon Press, Oxford. pp. 97-108.

Towle, G.A. (1977) Xanthan Recovery Process. US Patent No. 4,051,317. **Chemical Abstracts** 87, 186390b.

Trevelyan, W.E., Proctor, D.P. and Harrison, J.S. (1950) Detection of sugars on paper chromatograms. **Nature**, 166, 444-445.

Turner, S.H. and Cherniak, R. (1981) Total characterization of polysaccharides by gas-liquid chromatography. **Carbohydrate Research**, 95, 137-144.

Wernham, C.C. (1948) The species value of pathogenicity in the genus *Xanthomonas*. **Phytopathology**, 38, 283-291.

Whitcomb, P.J. and Macosko, C.W. (1978) Rheology of xanthan gum. **Journal of Rheology**, 22, 493-505.

Whitfield, C. (1979) Exopolysaccharide Biosynthesis in *Xanthomonas* sp. PhD Thesis. University of Edinburgh.

Whitfield, C., Sutherland, I.W. and Cripps, R.E. (1981) Surface polysaccharides in mutants of *Xanthomonas campestris*. **Journal of General Microbiology**, 124, 385-392.

Whitfield, C., Sutherland, I.W. and Cripps, R.E. (1982) Glucose metabolism in *Xanthomonas campestris*. **Journal of General Microbiology**, 128, 981-985.

Whiting, P.H., Midgley, M. and Dawes, E.A. (1976) The role of glucose limitation in the regulation of the transport of glucose, gluconate and 2-oxogluconate, and of glucose metabolism in *Pseudomonas aeruginosa*. **Journal of General Microbiology**, 92, 304-310.

Williams, P.H. (1980) Black rot: A continuing threat to world crucifers. **Plant Disease**, 64, Part 2, 736-742.

Woodard, G., Woodard, M.W., McNeely, W.H., Kovacs, P. and Cronin, M.T.I. (1973) Xanthan gum: Safety evaluation by two-year feeding studies in rats and dogs and a three-generation reproduction study in rats. Toxicology and **Applied Pharmacology**, 24, 30-36.

Zaar, K. (1979) Visualization of pores (export sites) correlated with cellulose production in the envelope of the gram-negative bacterium *Acetobacter xylinum*. **Journal of Cell Biology**, 80, 773-777.

Zagallo, A.C. and Wang, C.H. (1967) Comparative glucose catabolism of *Xanthomonas* species. **Journal of Bacteriology**, 93, 970-975.

Zatz, J.L. and Knapp, S. (1984) Viscosity of xanthan gum solutions at low shear rates. **Journal of Pharmaceutical Sciences**, 73, 468-471.

APPENDICES

APPENDIX 1

Calculation of the Sugar Composition for Polysaccharides

The sugar ratios were determined from the HPLC and colorimetric data obtained as described in Chapter 2 and section 3.5. The relative amounts of hexoses were established from the HPLC peak heights. The equivalent glucose concentration for the peak height was read from a calibration curve, and this was then multiplied by a factor which corrected for the difference in the refractive index monitored for each sugar. The percentage glucuronic acid was determined by the carbazole assay and was related to the hexose content as outlined below:

Correction Factors:

D-glucose	1.00
D-mannose	1.11
D-galactose	1.25
D-rhamnose	1.14

Example: Deacetylated ps.1128 (see figure 3.4a).

Data: Peak Heights: D-glucose = 5.6 cm
D-mannose = 5.3 cm

Percentage D-glucuronic acid = 23.4

Calculation:

Sugar	Peak Height (cm)	Glucose Content from Calibration Curve (μg)	Correction Factor	Quantity of Sugar in Sample (μg)
D-glc	5.6	278	1.00	278
D-man	5.3	262	1.11	291

% GlcA = 23.4

The remaining 76.6% consists of 278 μg D-glc + 291 μg D-man.

Therefore Weight GlcA = $\frac{23.4}{76.6}$ x (278 + 291) = 174 μg

and total sugar = $\frac{100}{76.6}$ x (278 + 291) = 743 μg

Sugar	Percentage Composition
D-glc	37.4
D-man	39.2
D-glcA	23.4

The molar ratios were calculated by dividing the weight of the sugar by the appropriate molecular weight, viz. 180 for D-glc and D-man, and 194 for D-glcA.

Sugar	Molar Sugar Ratio
D-glc	2.00
D-man	2.10
D-glcA	1.17

APPENDIX 2

Intrinsic Viscosity Data: Correction for Concentration

Xanthan	%C
100% Ac, 0% Pyr	43.24
0% Ac, 100% Pyr	42.22
0% Ac, 0% Pyr	42.55

$$\%C_{THEO} = \frac{(\%Ac \times 43.24) + (\%Pyr \times 42.22) + (100 - [\%Ac + \%Pyr] \times 42.55)}{100}$$

$\%C_{EXP}$ = Percentage carbon determined experimentally by elemental analysis (see table 3.9).

$CONC_{NOM}$ = Nominal concentration (0.1% for xanthan and 0.2% for the gluco- and galactomannans).

$CONC_{DW}$ = Concentration determined from the dry weight after lyophilization.

$CONC_{TRUE}$ = True concentration.

$[\eta]_{APP}$ = Apparent intrinsic viscosity determined using the nominal concentration.

$[\eta]_{TRUE}$ = Actual intrinsic viscosity corrected for concentration.

Calculation:

$$\frac{\%C_{EXP}}{\%C_{THEO}} = CORRECTION$$

$$CONC_{TRUE} = CORRECTION \times CONC_{DW}$$

$$\frac{CONC_{TRUE}}{CONC_{NOM}} = FACTOR$$

$$[\eta]_{TRUE} = \frac{[\eta]_{APP}}{FACTOR}$$

Example: ps.556 in 20mM sodium chloride

Data:

%Ac	=	1.6	
%Pyr	=	6.0	
$\%C_{EXP}$	=	39.03	
$\%CONC_{NOM}$	=	0.1	
$\%CONC_{DW}$	=	0.1048	
$[\eta]_{APP}$	=	48.286 dl/g	(Huggins extrapolation)
	=	49.373 dl/g	(Kraemer extrapolation)

NB. The viscosity data used to determine the intrinsic viscosity is given in table 5.2, whilst the Huggins and Kraemer extrapolations are shown in figure 5.8.

$$\%C_{THEO} = \frac{(1.6 \times 43.24) + (6.0 \times 42.22) + (100 - [1.6 + 6.0] \times 42.55)}{100}$$

$$= 42.54124$$

$$\frac{39.03}{42.54124} = 0.91746$$

$$CONC_{TRUE} = 0.91746 \times 0.1048$$

$$= 0.09615$$

$$\frac{0.09615}{0.1} = 0.9615$$

$$[\eta]_{TRUE} = \frac{48.286}{0.9615} = 50.2 \text{ dl/g (Huggins extrapolation)}$$

$$= \frac{49.373}{0.9615} = 51.3 \text{ dl/g (Kraemer extrapolation)}$$